Dissertation
submitted to the
Combined Faculties for the Natural Sciences and for Mathematics
of the Ruperto-Carola University of Heidelberg, Germany
for the degree of
Doctor of Natural Sciences

presented by

M.Sc. Dario Lucas Frey
born in Heilbronn-Neckargartach

Oral Examination: 16th September 2021

Association of airway inflammation, microbiome structure and clinical parameters within the airways in cystic fibrosis and other chronic obstructive lung diseases

Referees: Dr. Rainer Pepperkok
Prof. Dr. Marcus Mall

Table of contents

Abbreviations ..... **V**

List of figures ..... **IX**

List of tables ..... **XI**

Abstract ..... **XIII**

Zusammenfassung ..... **XV**

1 Introduction **1**

1.1 Cystic fibrosis 1

1.1.1 Airway inflammation and bacterial colonization in CF 2

1.1.2 *Pseudomonas aeruginosa* is the key pathogen in CF lung disease 4

1.2 Chronic obstructive pulmonary disease 4

1.3 Neutrophilic airway inflammation 5

1.3.1 Granules of neutrophils 7

1.3.2 Neutrophil elastase 7

1.3.3 The NSPs: Proteinase 3, cathepsin G and neutrophil serine proteinase 4 9

1.3.4 NSP interactions with cytokines, chemokines and growth factors 10

1.3.5 Matrix metalloproteinases 11

1.3.6 Endogenous anti-proteases 12

1.4 NE measurement techniques 13

1.4.1 Measurement of free NE activity 14

1.4.2 Measurement of membrane associated NE 14

1.4.3 Synthetic NE inhibitor sivelestat 15

1.5 Objectives 15

2 Material and methods **17**

2.1 Study conception 17

2.1.1 Investigation of the relationship between airway inflammation, microbiome composition and clinical parameters in CF patients 17

2.1.2 Investigation of membrane associated NE activity in healthy controls, CF and COPD patients 17

2.2 Human sample acquisition 17

2.2.1 Sputum sample preparation 18
2.2.2 Blood sample preperation 18
2.3 Measurement of free NE activity 19
2.3.1 Measurement of free NE activity using N-Methoxysuccinyl-Ala-Ala-Pro-Val *p*-nitro-anilide 19
2.3.2 Measurement of free NE activity using the Förster-resonance electron transfer probe NEmo-1 19
2.4 Measurement of membrane associated NE activity 20
2.4.1 Transfer of probes manufacturing process to industry 20
2.4.2 Measurement of membrane associated NE activity by confocal microscopy 21
2.4.3 Measurement of membrane associated NE activity by flow cytometry 23
2.4.4 Evaluation of NEmo-2E target specificity by flow cytometry 25
2.5 Enzyme-linked immunosorbent assay 25
2.6 Cytometric bead array 26
2.7 Western blot 26
2.8 Differential cell counts 27
2.9 Cell culture 27
2.10 Clinical data 27
2.11 Microbiology 28
2.11.1 Sample preparation 28
2.11.2 DNA extraction 28
2.11.3 Quantitative polymerase chain reaction 28
2.11.4 Next generation sequencing library preparation 29
2.11.5 Sequence analysis 29
2.12 Secretomics 30
2.12.1 Sample preparation 30
2.12.2 LC-MS/MS analysis and protein identification 30
2.12.3 Gene ontology enrichment and protein analysis 31
2.13 Statistics 31
2.13.1 Comparisons of individual parameters between groups and clusters 31

2.13.2 Microbiological analysis – Cross-sectional study 31
2.13.3 Microbiological analysis – Longitudinal study 32
2.13.4 Microbiological analysis – CF/COPD/healthy comparison 33
2.13.5 Secretomics 33
3 Results 35
3.1 Association of inflammatory markers with dysbiosis of airway microbiota and lung function in CF 35
3.1.1 Cross-sectional study 35
3.1.2 Longitudinal study 41
3.2 Assay refinement to measure membrane associated NE 51
3.2.1 Characterization of the NEmo-2 variants 51
3.2.2 Change in technology, transferring the assay from microscopy to flow cytometry 52
3.2.3 Evaluation of NEmo-2E specificity by flow cytometry 57
3.2.4 In depth characterization of the airway secretions of CF, COPD patients and controls 60
3.2.5 Validation of enzyme quantities by western blot and mass spectroscopy . 70
4 Discussion 73
4.1 Association of inflammatory markers with airway dysbiosis and lung function in patients with CF 73
4.1.1 Identification of interdependencies of airway dysbiosis, inflammation and lung function utilizing a cross-sectional study design 73
4.1.2 Longitudinal changes and dependencies of inflammatory markers with airway dysbiosis and lung function on an individual CF patient basis 76
4.2 Small molecule FRET flow cytometry 79
4.2.1 The redefined methodology allows a faster and more robust quantification of membrane associated NE activity 80
4.2.2 Characterization of airway secretions of CF and COPD patients alongside with healthy controls 81
4.2.3 Potential applications for NE activity evaluation 87
4.2.4 NE quantity can be measured by multiple assay formats, while NEmo reporters can provide further information regarding NE activity 88

4.2.5 Is it enough to monitor NE activity alone or are there probes for NSPs available? 88

5 Conclusions and further perspectives 91

6 References 93

Publications, Talks and Posters during PhD studies 119

Statement on copyright and self-plagiarism 121

Acknowledgements 123

Appendix 125

Abbreviations

+	with
7-AAD	7-amino-actinomycin D
A1AT	α-1-antitrypsin (protein)
ABS	absorbance
Achro	cluster dominated by *Achromobacter* species
ACT	α-1-antichymotrypsin
AF	Alexa Fluor
ANAKIN	a study to evaluate safety and efficacy of subcutaneous administration of anakinra in patients with CF
ARDS	acute respiratory distress syndrome
ARG1	arginase 1 (gene)
Arg1	arginase 1 (protein)
ASL	airway surface liquid
ASV	amplicon sequence variants
BALf	bronchoalveolar lavage fluid
BH	Benjamini-Hochberg
BMI	body mass index
BV	Brilliant Violet
CBA	Cytometric Bead Array
CD	cluster of differentiation
CF	cystic fibrosis
CFTR	cystic fibrosis transmembrane conductance regulator
Cl^-	chloride ion
COPD	chronic obstructive lung disease
COVID-19	coronavirus disease
CRP	C-reactive protein
CTSG	cathepsin G
Cxcl1	chemokine ligand 1
CXCR1	CXC chemokine receptor type 1 (CD181)
Cy	cyanine
D/A ratio	donor/acceptor ratio
dd	double distilled
DNase	deoxyribonuclease
DRAQ5	1, 5-bis{[2-(di-methylamino) ethyl] amino}-4, 8-dihydroxyanthracene-9, 10-dione, nuclear stain
ELANE	neutrophil elastase (gene)
ELISA	enzyme-linked immunosorbent assay
ENaC	epithelial sodium channel
ECP	eosinophilic cationic protein (gene: *RNASE3*)

EtOH	ethanol
F508del	deletion of a phenylalanine at residue 508
FBS	fetal bovine serum
FEV_1	forced-expiratory volume in one second
FEV_1 % predicted	forced-expiratory volume in one second in percent predicted
fg	femtogram
FITC	fluorescein isothiocyanate
fMLP	N-formyl-methionyl-leucyl-phenylalanine
FRC_{pleth} % predicted	functional residual capacity determined by body plethysmography in percent predicted
FRET	Förster resonance energy transfer
FSC	forward scatter
g	gravitational force equivalent
GLMMs	generalized linear mixed models
GO	gene ontology
GOLD	global initiative for chronic obstructive lung disease
GPD	granulomatosis with polyangiitis
GRIM	granule releasing, immunomodulatory and metabolically active
HC	hierarchical clusters
HPLC	high performance liquid chromatography
HRP	horseradish peroxidase
IFN-γ	Interferon γ
IgG	immunoglobulin G
IL	interleukin
IL-10	interleukin 10 / human cytokine synthesis inhibitory factor (CSIF)
IL-1α	interleukin 1α / hematopoietin 1
IL-1β	interleukin 1β / leukocytic pyrogen
IL-1Ra	interleukin 1 receptor antagonist
IL-5	interleukin 5 / eosinophil differentiation factor
IL-6	interleukin 6 / Interferon β-2
IL-8	interleukin 8 / granulocyte chemotactic protein 1
IQR	inter quartile range
kDa	kilo Dalton
LCI	lung clearance index
LFQ	label-free quantitation
LMMs	linear mixed effect models
LOD	limit of detection
LPS	lipopolysaccharides
LTA	lipoteichoic acid

LTB_4	leukotriene B_4
LTF	lactoferrin
MCC	mucociliary clearance
MFI	mean fluorescent intensities
MMP	matrix metalloproteinase
MMP12	matrix metalloproteinase 12 / macrophage elastase
MMP2	matrix metalloproteinase 2 / gelatinase A
MMP3	matrix metalloproteinase 3 / stromelysin-1
MMP7	matrix metalloproteinase 7 / matrilysin
MMP8	matrix metalloproteinase 8 / neutrophil collagenase
MMP9	matrix metalloproteinase 9 / gelatinase B
MPO	myeloperoxidase
MRI	magnetic resonance imaging
MS	mass spectroscopy
MUC5AC	mucin 5AC
MUC5B	mucin 5B
Na^+	sodium ion
NaCl	sodium chloride
NE	neutrophil elastase (protein)
NETs	neutrophil extracellular traps
NF-κB	nuclear factor kappa-light-chain-enhancer of activated B cells
NSG	next generation sequencing
NSP	neutrophil serine protease
NSP4	neutrophil serine protease 4 / serine protease 57 (protein)
OF	oropharynx-like flora
Orkambi	combination of Lumacaftor and Ivacaftor
P. aeruginosa	*Pseudomonas aeruginosa*
PAMP	pathogen-associated molecular pattern
PANTHER	protein analysis through evolutionary relationships
PBS	phosphate buffered saline
PCA	principal component analysis
PCoA	principal coordinate analysis
PDL-1	programmed dead-cell ligand 1 / CD274
PE	phycoerythrin
PEG	polyethylene glycol
PerCP	peridinin-chlorophyll-protein complex
pg	picogram
PGP	proline-glycine-proline
PI	protease inhibitor cocktail

PM	propidium monoazide
PMA	phorbol 12-myristse 13-acetate
PMN	polymorphonuclear
*p*NA	N-methoxysuccinyl-Ala-Ala-Pro-Val *p*-nitroanilide
PR3	proteinase 3 (protein)
PRSS57	neutrophil serine protease 4 / serine protease 57 (gene)
PRTN3	proteinase 3 (gene)
Psae	cluster dominated by *Pseudomonas aeruginosa*
qPCR	quantitative polymerase chain reaction
RFU	relative fluorescent unit
RSV	ribosomal sequence variants
S. aureus	*Staphylococcus aureus*
SERPINA1	α-1-Antitrypsin (gene)
SLPI	secretory leukocyte peptidase inhibitor
sm	small molecule
sp.	particular species
spp.	several species
SSC	side scatter
Staph	cluster dominated by *Staphylococcus* species
Symdeko	combination of Tezacaftor/Ivacaftor and Ivacaftor
t_0	time point 0
TCEP	tris(2-carboxyethyl) phosphine hydrochloride
TEAB	tri-ethylammonium bicarbonate buffer
TGF-β1	transforming growth factor β1
TIMP	tissue inhibitor of metalloproteinases
TIMP1	tissue inhibitor of metalloproteinases 1
TLR	toll-like receptor
TLR4	toll-like receptor 4
TNF-α	tumor necrosis factor
Trikafta	combination of Ivacaftor, Tezacaftor and Elexacaftor (every 24h) and Ivacaftor (12h later)
t_x	time point x
v/v	volume per volume
VX-445	Elexacaftor
VX-661	Tezacaftor
VX-770	KALYDECO (Ivacaftor)
VX-809	Lumacaftor
w/o	with out
w/v	weight per volume
ZIGMMs	zero-inflated Gaussian mixed effect models

List of figures

Figure 1: Establishment of a chronic bacterial lung infection. 3

Figure 2: Neutrophilic inflammation in the lung. 6

Figure 3: Chemical structure of FRET reporters NEmo-1 and NEmo-2E. 14

Figure 4: Intact and cleaved structure of FRET reporter NEmo-1. 20

Figure 5: Chemical structure of FRET reporters NEmo-2E and NEmo-2G 21

Figure 6: Intact and cleaved structure of FRET reporter NEmo-2E. 22

Figure 7: Gating strategy for the detection of neutrophils by flow cytometry. 24

Figure 8: Correlation matrix of sputum microbiota parameters, inflammation markers and lung function of CF patients. 37

Figure 9: Clustering of CF patient sputum microbiota based on their inter-individual variability. 39

Figure 10: Box plots of most relevant parameters of microbiome diversity, inflammatory markers and lung function. 40

Figure 11: Distribution of visits for each patient. 42

Figure 12: Network of the rates of change between parameters of the microbiome, pro-inflammatory factors, anti-proteases, clinical parameters and general factors. 47

Figure 13: Network of the distance between t_x and t_0 of the samples between parameters of the microbiome, pro-inflammatory factors, anti-proteases, clinical parameters and general factors. 48

Figure 14: Network of the relationship of the variability between parameters of the microbiome, pro-inflammatory factors, anti-proteases, clinical parameters and general factors. 49

Figure 15: Network of the relationship of the rate of change over time including initial conditions between parameters of the microbiome, pro-inflammatory factors, anti-proteases, clinical parameters and general factors. 50

Figure 16: Characterization of NEmo-2 variants. 52

Figure 17: Control plots of donor and acceptor MFI intensities. 53

Figure 18: Fluorescence minus one staining’s for the antibody panel used for neutrophil gating. 53

Figure 19: Quantification of membrane associated NE activity using FRET reporter NEmo-2E by flow cytometry in comparison to quantification by confocal microscopy. 55

Figure 20: Correlation of the surface marker CD16 with normalized fold change measured by flow cytometry as well as MFIs of different surface markers. 56

Figure 21: Surface markers and membrane associated NE activity of stimulated blood neutrophils. 57

Figure 22: Evaluation of FRET probe selectivity 58

Figure 23: Comparison of inhibitory capacity of several relevant inhibitors after 10 min of inhibition, measured on neutrophils isolated from one COPD and three CF patients. 59

Figure 24: Assessment of cell type percentages, cell numbers and cell recruitment factor LTB_4 in CF and COPD patients and healthy controls 61

Figure 25: Principal Coordinate Analysis based on Unifrac weighted distances with kmean clustering 62

Figure 26: Comparison of microbiome parameters based on kmean clustering. 62

Figure 27: Comparison of significantly different inflammatory markers of the PCoA clusters. 63

Figure 28: Comparison of free and membrane associated NE activity, as well as relevant endogenous anti-protease levels of all cluster. 64

Figure 29: Comparison of surface-markers CD16. CF63 and CD66b of the clusters. 65

Figure 30: Comparison of clinical markers from the PCoA 66

Figure 31: Hierarchical clustering of the correlation between microbiome indices or individual ASVs and all other markers analyzed. 67

Figure 32: PCA of the Log_2 LFQ intensities of identified proteins, and volcano plots of the secretome comparisons between CF and COPD as well as the corresponding GO analysis 69

Figure 33: Western blot of MMP9, ELANE and CTSG. 70

Figure 34: Comparison of the slope of the activity, quantification via western blot as well as the LFQ values measured by mass spectroscopy of NE 71

Figure 35: Comparison of the RSV abundance of the three pairwise comparisons between healthy, COPD and CF. 85

List of tables

Table 1: Antibody master mix for the detection of neutrophils by flow cytometry 23

Table 2: Compensation matrix of the flow cytometry assay. 24

Table 3: Inhibitors utilized for assessment of target specificity of NEmo-2E by flow cytometry 25

Table 4: Antibodies used for Western Blot experiments. 27

Table 5: Clinical characteristics of the cross-sectional study CF cohort. 36

Table 6: Effect of antibiotic treatment, CFTR modulator therapy, genotype and exacerbations. 36

Table 7: Clinical characteristics of CF patients of the longitudinal study. 41

Table 8: Pancreatic status and CFTR genotypes of CF patients of the longitudinal study 42

Table 9: Overview of relationships of all factors of the longitudinal study with time 44

Table 10: Summary of p-values of the correlations of the most common phyla to clinical and inflammatory measures. 45

Table 11: Clinical characteristics of CF, COPD patients and healthy controls 60

Abstract

Cystic fibrosis (CF) and chronic obstructive pulmonary disease (COPD) are characterized by a severe inflammation and infiltration of neutrophiles which secrete neutrophil elastase (NE), which leads to lung parenchyma destruction and disease progression. In CF, disease severity has been linked with airway dysbiosis. As the relationship of dysbiosis, respiratory tract inflammation and impaired lung function is not fully understood this study aimed to assess this interplay.

In an initial cross-sectional study, the inflammatory profile of spontaneous sputum samples of CF patients was analyzed. Cytokines were measured by Cytometric Bead Array, anti-proteases levels by enzyme-linked immunosorbent assay and free NE activity via Förster resonance energy transfer (FRET) probe NEmo-1 in the supernatant fraction. The interplay of those parameters together with lung function were evaluated in a multiparameter analysis.

The increase in the inflammatory markers NE, IL-1β, IL-8 and TNF-α correlated negatively with the lung function parameter forced expiratory volume in one second percent (FEV_1 %) predicted and α-diversity of the airway microbiome. Based on the microbiome composition, patients were grouped in 7 clusters. One cluster had a diverse microbiome, which was rich in species of the oropharynx-like flora and had a high evenness. These patients had the highest FEV_1 % predicted and the lowest inflammatory load. In contrast, the dominance of a particular pathogen in other clusters was associated with higher levels of inflammation and lower lung function; this was most pronounced in the cluster dominated by *Pseudomonas aeruginosa*. The time-resolved interdependencies of the parameters was evaluated in a longitudinal follow-up study. Repeated sampling over a year revealed a strong decrease of the microbiome diversity while inflammatory markers were rather volatile. However, during a 3-year study, inflammatory markers continuously increased, and FEV_1 % predicted declined. Moreover, the patients' initial condition and disease stage had an important effect on the disease progression. Thus, the combined investigation of microbial clusters, inflammation parameters and lung function may provide information about disease severity and allow a more directed therapeutic treatment.

Previous studies considered only free NE activity, though recent evidence suggests importance in pathogenesis of its membrane associated fraction. As a rapid and sensitive quantification method to measure membrane bound NE is missing, a flow cytometric approach based on the FRET probe NEmo-2E was established. With the new method it was shown that, a saturation of the membrane NE was detected in CF and COPD, whereas free NE activity was substantially elevated in CF sputum samples. This indicates that NE first associates to the membrane before excess NE is detectable in the supernatant fraction. Thus, membrane associated NE activity could be a potential early inflammation marker for both, COPD and CF.

Zusammenfassung

Obstruktive Lungenerkrankungen wie zystische Fibrose (CF) und chronisch obstruktive Lungenerkrankung (COPD) sind durch eine schwere Entzündung und eine erhöhte Infiltration von Neutrophilen gekennzeichnet, die neutrophile Elastase (NE) sekretieren. Das daraus resultierende Ungleichgewicht von Proteasen und Antiproteasen führt zur Zerstörung des Lungenparenchyms und zum Fortschreiten der Erkrankung. Bei CF wurde der Schweregrad der Lungenerkrankung mit einem dysbiotischen Mikrobiom der Atemwege in Verbindung gebracht. Die Beziehung zwischen Dysbiose, Inflammation und einer beeinträchtigter Lungenfunktion sind dennoch nicht vollständig verstanden. Ziel dieser Arbeit war es deshalb, den Zusammenhang dieser Parameter zu untersuchen.

In einer ersten Querschnittsstudie wurden spontane Sputumproben von CF-Patienten hinsichtlich ihrer Entzündungsmarker analysiert. Zytokine wurden mittels Cytometric Bead Array, Antiproteasenkonzentrationen mittels Enzyme-linked Immunosorbent Assay und freie NE-Aktivität mittels Förster-Resonanz-Energie-Transfer (FRET)-Reporter NEmo-1 im Überstand gemessen. Das Zusammenspiel dieser Parameter und der Lungenfunktion wurde in einer Multiparameteranalyse eingehender untersucht.

Der Anstieg inflammatorischer Marker wie NE, IL-1β, TNF-α und IL-8 korrelierte invers mit dem Lungenfunktionsparameter der Einsekundenkapazität (FEV_1 %) und der α-Diversität des Atemwegmikrobioms. Basierend auf der Zusammensetzung des Mikrobioms konnten die Patienten in 7 Cluster eingeteilt werden. Eines dieser Cluster war durch ein diverses, ausgeglichenes Mikrobiom, reich an Spezies der Oropharyngealen Flora, gekennzeichnet. Diese Patienten hatten das höchsten FEV_1 und die geringste Inflammation. Im Gegensatz dazu war die Dominanz eines bestimmten Erregers in anderen Clustern mit höheren Entzündungswerten und einer niedrigeren Lungenfunktion verbunden, dies war in dem von *Pseudomonas aeruginosa* dominierten Cluster am ausgeprägtesten. Die zeitlichen Abhängigkeiten der Parameter wurden in einer longitudinalen Folgestudie untersucht. Wiederholte Probenahmen über ein Jahr zeigten eine starke Abnahme der Mikrobiomdiversität, während die Entzündungsmarker äußerst volatil waren. Während einer 3-jährigen Studie stiegen die Entzündungsmarker jedoch kontinuierlich an, während die Lungenfunktion abnahm. Darüber hinaus hatten der Ausgangszustand und das Krankheitsstadium der Patienten einen wichtigen Einfluss auf die Pathogenese. Somit kann die kombinierte Untersuchung von mikrobiellen Clustern, inflammatorischen Parametern und der Lungenfunktion Informationen über den Schweregrad der Erkrankung liefern und eine gezieltere therapeutische Behandlung ermöglichen.

Vorausgegangene Studien betrachteten nur die freie NE-Aktivität, obwohl neuere Ergebnisse, darauf hindeuten, dass die membrangebundene NE Fraktion eine bedeutende Rolle bei der Pathogenese inflammatorischer Lungenerkrankungen spielt. Da es keine schnelle und sensitive Quantifizierungsmethode zur Messung der membrangebundenen NE Aktivität gibt, wurde ein durchflusszytometrischer Ansatz mittels der FRET-Sonde NEmo-2E etabliert. Mit der neuen Methode konnte gezeigt werden, dass bei CF und COPD zu einer Sättigung der membrangebundenen NE kommt, während die Aktivität der freien NE in CF-Sputumproben deutlich erhöht war. Dies deutet darauf hin, dass NE zunächst an die Membran bindet, bevor überschüssige NE im Überstand nachweisbar ist. Somit könnte die membrangebundene NE-Aktivität ein potenzieller Marker für die ersten Anzeichen einer Inflammation sowohl für COPD als auch für CF sein.

1 Introduction

1.1 Cystic fibrosis

Cystic fibrosis (CF) is the most frequent life threatening autosomal recessive disease in Caucasian population (Ramsey 1996). CF disease is caused by mutations in the cystic fibrosis transmembrane conductance regulator (CFTR) gene, situated on chromosome 7 in humans (Rosenfeld et al. 1992). To date more than 2 000 mutations are known to cause CF. Of these the deletion of a phenylalanine at residue 508 (F508del) is the most common mutation (Boeck 2020). Even though CF is a complex disease that leads to a malfunction of many organ systems, morbidity and mortality is predominantly caused by chronic obstructive lung disease caused by mucus plugging in the small airways already in early childhood. With increasing disease severity a persistent neutrophilic airway inflammation as well as chronic bacterial infection follows (Mall und Hartl 2014; Voynow et al. 2008).

The CFTR a multi-domain transmembrane chloride channel is situated in the apical membrane (Schwiebert et al. 1999; Smith und Welsh 1992). The malfunction of CFTR results in a decreased transport of chloride (Cl^-) into the extracellular space which leads to augmented sodium (Na^+) influx into the cell via the epithelial sodium channel (ENaC) (Saint-Criq und Gray 2017; Anderson et al. 1991). Along with this, increased water influx results in a dehydration of the airway surface liquid (ASL) (Mall et al. 2004; Hobbs et al. 2013). The resulting increased concentrations of sticky mucus in the airways of CF patients favors excessive persistent bacterial colonization. In early life primarily with the acquisition of *Haemophilus influenzae* and *Staphylococcus aureus* (*S. aureus*) has been described, whereas in later disease stages *Pseudomonas aeruginosa* (*P. aeruginosa*) becomes dominant (Ramsey 1996; Heijerman 2005). These chronic airway infections with pathogens trigger an inflammation and structural lung damage which promotes further disease progression, especially in later stages (Mall und Hartl 2014; Sly et al. 2013). A main driver of the inflammatory reaction is Interleukin (IL) 8 (Birrer et al. 1994). It is related to tremendous numbers of infiltrating neutrophils and triggers the release of neutrophil elastase (NE) into the ASL (Birrer et al. 1994). The arising final destruction of the lung architecture provokes bronchiectasis and emphysema that lead to a decline in lung function (Voynow et al. 2008; Sly et al. 2013). Previous studies showed, that disease severity can be directly linked to neutrophil counts, increased levels of NE as well as IL-8 (Mayer-Hamblett et al. 2007; Dittrich et al. 2018). NE has been identified as one of the key modulators of CF lung disease and is directly associated to the pathogenesis as well as progression of the disease (Dittrich et al. 2018; Margaroli et al. 2019; Sly et al. 2013; Sagel et al. 2012; Sly et al. 2009).

Until recently, CF patients received a symptomatic treatment such as pancreatic enzymes, mucolytics and antibiotics, which can contain low dose macrolides or other anti-inflammatory agents. The underlying genetic defect cannot be cured with gene therapy yet. However, there are several CFTR modulators available that improve the CF treatment substantially by increasing the expression and function of CFTR. Those modulator therapeutics include CFTR correctors such as: Lumacaftor (VX-809), Tezacaftor (VX-661) and since lately Elexacaftor (VX-445) as well such as potentiators as: Ivacaftor (VX-770). With Orkambi a combination of Ivacaftor and Lumacaftor, CF patients with 2 copies of the F508del-CFTR mutation can be treated starting from the second year of life (Vertex Pharmaceuticals (Europe) Ltd. 2018a). Symdeko a combination of Tezacaftor with Ivacaftor, is available for patients homozygous for F508del or carrying a single F508del variant combined with certain other residual function variants responsive to Ivacaftor (Vertex Pharmaceuticals (Europe) Ltd. 2018b; Somayaji et al. 2020). Since August 2020, the triple combination of Ivacaftor/Tezacaftor/ Elexacaftor (Trikafta) can be prescribed to ~90 % of the CF patients that are either homozygous for F508del or heterozygous for F508del with an additional minimal function mutation (Heijerman et al. 2019; Bell et al. 2020; Bear 2020; Middleton et al. 2019).

1.1.1 Airway inflammation and bacterial colonization in CF

CF patients acquire a chronic polymicrobial airway infection during life. Whole genome metagenomics studies in neonates have shown that the airway microbiomes of CF and healthy newborns are similar at birth (Al Alam D. et al. 2020). The defective mucociliary clearance (MCC) and antimicrobial defense of CF patients are most likely the reason for the characteristic atypical microbial colonization in comparison to healthy adults (Boutin und Dalpke 2017).

An appropriate concept to describe the evolution of the lung microbiome is the island model (Dickson et al. 2016), which described the upper airways as mainland and origin of most microbes invading the lungs. The lower airways are described as islands, rarely colonized by microbes in the beginning. In this model, different parts of the lung or different islands develop independently to local microenvironments (Figure 1). Consistent with this concept, studies have shown that the common route of colonization is micro-aspiration from the upper airways (Boutin et al. 2015; Madan et al. 2012; Charlson et al. 2011). In early life, there is an equilibrium between immigration and elimination, whereas later on the regional growth of microbes is determines the colonization (Boutin und Dalpke 2017). The dysbiosis of the nasal cavity of CF patients creates the basis for an altered airway microbiome (Boutin und Dalpke 2017). One reason for the dysbiosis is the defective immune response as well as altered mucus composition (Boutin und Dalpke 2017). The

altered mucus structure is beneficial for the colonization by *Staphylococcaceae* peculiarly *S. aureus*, which favors an increased aspiration and initial colonization of *S. aureus* in the lower airways, qualifying the airways for a secondary infection (e.g. by *P. aeruginosa*) (Folkesson et al. 2012; Lyczak et al. 2000; Rosenfeld et al. 2012). The beneficial effect of *S. aureus* for the growth and establishment of an *P. aeruginosa* infection has been described in several studies (Armbruster et al. 2016; Pernet et al. 2014; Limoli et al. 2016). The throat microbiota is rather affected by the oropharyngeal microbiota than the nose microbiota (Boutin et al. 2015; Segata et al. 2012; Charlson et al. 2011). Typical genera found in the throat microbiota of CF patients are *Streptococcus*, *Veillonella* and *Prevotella*. This also applies to the microbiota of healthy adults (Boutin et al. 2015; Segata et al. 2012; Charlson et al. 2011; Madan et al. 2012). Characteristic for the lung microbiota is a transient colonization from the upper airways rather than a stable growth of commensals (Dickson et al. 2015). In early life there seem to be several cycles of aspiration, colonization and removal of bacteria from the throat, until one pathogen like *Bordetella*, *Burkholderia, Haemophilus, S. aureus* or *P. aeruginosa* becomes dominant enough to establish a chronic infection (Boutin und Dalpke 2017). A strong driver of selective pressure is the antibiotic-resistance of bacteria due to intensive use of antibiotics for the treatment of CF patients (Worlitzsch et al. 2009; Sherrard et al. 2013). Probiotic supplementation of the diet of children with CF has demonstrated beneficial effects regarding their lung microbiota and a decrease in pulmonary exacerbation over time (Bruzzese et al. 2007; Bruzzese et al. 2014).

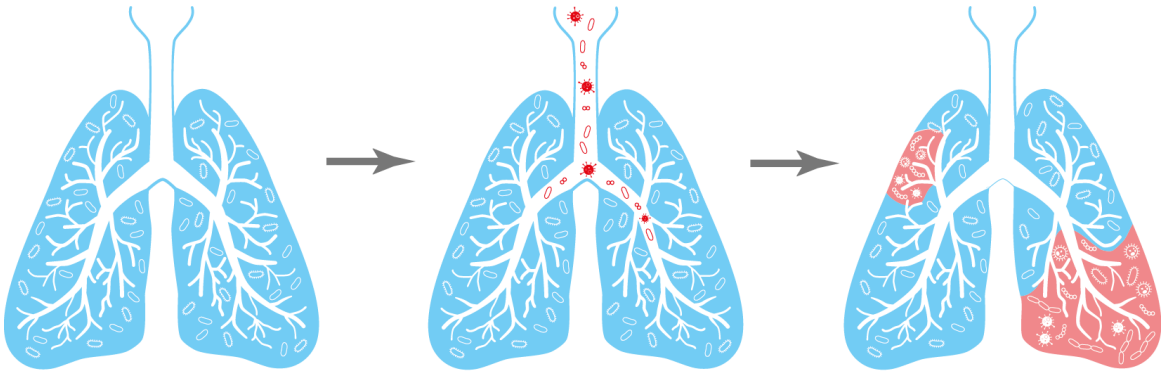

Figure 1: Establishment of a chronic bacterial lung infection. The healthy lung (**left**) is populated by commensal bacteria throughout. Pathogens, can be aspirated or migrate from the nasal or oral cavity migrate into the lung (**center**). Due to the impaired mucociliary clearance in the lung of chronic infected (**right**) patients those pathogens settle and induce a chronic inflammation (red areas).

Important characteristics to describe the microbiome structure are the richness of a species, mirrors how many different species are present, the evenness indicates how homogenous they are, whereas the dominance defines how distinct the presence of the most frequently identified species is (Shannon 1948). Using these parameters, the

Shannon index or α-diversity can be calculated (Shannon 1948). A higher α-diversity indicates a divers microbiome structure, whereas a rather low α-diversity suggest the dominance of a specific pathogen (Shannon 1948). The microbiota of CF patients is less diverse than the microbiota of healthy people (Zemanick et al. 2017; Erb-Downward et al. 2011). The reduction in richness and diversity and the increased dominance of an individual pathogen has been linked to age, quantity of antibiotic use, decline in lung function and disease progression (Zhao et al. 2012; Muhlebach et al. 2018a; Carmody et al. 2018; Coburn et al. 2015). Besides, Tunney and colleagues revealed a positive link of the prevalence of anaerobes with pancreatic sufficiency, better lung function and nutrition (Tunney et al. 2011).

1.1.2 *Pseudomonas aeruginosa* is the key pathogen in CF lung disease

Patients with chronic respiratory diseases, such as CF, are limited in their capabilities to clear pathogens from their lung efficiently, which makes them susceptible for chronic airway infections (Welp und Bomberger 2020). In case of CF airway disease, certain bacteria are closely associated with disease progression, and are therefore of particularly interest. Those are: *P. aeruginosa*, *S. aureus*, *Burkholderia cepacia* complex, *Haemophilus influenzae*, *Stenotrophomonas maltophilia* and *Achromobacter xylosoxidans* (Marshall et al. 2018; Cuthbertson et al. 2020). Most often, CF patients suffer from *P. aeruginosa* infections which are difficult to eradicate and besides foster a reduction of the lung function (Malhotra et al. 2019).

P. aeruginosa is a common Gram-negative bacterium in human and can be cleared by host defense mechanism in healthy people. Due to their impaired MCC, CF patients often fail to eradicate the pathogen, which results in infections, that once established, can result in an acute pneumonia or even infections of the bloodstream (Faure et al. 2018). *P. aeruginosa* has several strategies to adapt to the inflammatory milieu in the lungs and thereby promote its persistence (Faure et al. 2018). It can not only live in a planktonic state, but also switch to an adherent biofilm growth state. Many intrinsic immune responses are less efficient against *P. aeruginosa* as they form biofilms that limit the effectiveness of certain antibiotic treatment regimens (Malhotra et al. 2019).

1.2 Chronic obstructive pulmonary disease

Chronic obstructive pulmonary disease (COPD) is a respiratory disease with a severely increasing prevalence word wide (Trivedi und Barve 2020). Already now, COPD is the third most fatal disease, a scenario that the World Health Organization had predicted to happen in 2030 (Trivedi und Barve 2020). Currently, it is expected to be the most lethal disease in 15 years (Quaderi und Hurst 2018). Two third of the COPD cases are caused by cigarette smoke. Alternatively, it can evolve either from repeated exposure to harmful

environmental stimuli as dust, fumes, vapors and gases or from genetic factors as A1AT shortage or MMP12 single nucleotide polymorphisms (Centers for Disease Control and Prevention (CDC) 2008; Balmes et al. 2003). The committee of the Global Initiative for chronic obstructive lung disease (GOLD) claims the disease as treatable but not curable (Singh et al. 2019). COPD goes along with a not completely reversible airflow limitation with associated inflammatory response; usually it has a progressive course with extrapulmonary effects (World Health Organization 2017). The classification of the disease stage (GOLD stages) is based on the severity of the airflow limitation on basis of defined cut-offs (Global Initiative for Chronic Obstructive Lung Disease, Inc. 2020). Patients with a ratio of forced expiratory volume in one second (FEV_1) divided by the forced vital capacity < 0.7 are categorized into four stages (Global Initiative for Chronic Obstructive Lung Disease, Inc. 2020): GOLD I, mild (FEV_1 in percent predicted [FEV_1 % predicted] ≥ 80), GOLD II, moderate (50 ≤ FEV_1 % predicted < 80), GOLD III, severe (30 ≤ FEV_1 % predicted < 50) and GOLD IV, very severe (FEV_1 % predicted < 30) (Global Initiative for Chronic Obstructive Lung Disease, Inc. 2020). Those stages are further subcategorized into A, B, C and D by symptoms and number of exacerbations within the last year, with D being the most severe subcategory (Global Initiative for Chronic Obstructive Lung Disease, Inc. 2020). As COPD is acquired and not inherited as CF, it is a more diverse disease as it (Eisner et al. 2010). However, there are certain parallels to CF such as the excessive production of sputum, obstructions of the airflow, symptoms as cough, vulnerability for exacerbations, infections and prolonged as well as increased infiltration of neutrophils (Trivedi und Barve 2020). As CF, COPD is a pulmonary disorder propelled by an protease-antiprotease disequilibrium (Senior et al. 1977). Several proteases have been linked to COPD including matrix metallo-proteinase (MMP) 8, MMP9 and MMP12 as well as the serine protease NE (Hou et al. 2018; Lowrey et al. 2008; Pinto-Plata et al. 2007). Recently, Genschmer et al. showed that exosomes, important mediators of intercellular crosstalk, from activated neutrophils of COPD patients contain active NE on their surface (Genschmer et al. 2019). This strengthens the importance to monitor NE activity in various inflammatory lung diseases, given the inaccessibly of membrane associated NE for alpha-1-antitrypsin (A1AT), one of the main inhibitors of NE (Genschmer et al. 2019).

1.3 Neutrophilic airway inflammation

Polymorphonuclear neutrophils are the first line of defense and, therefore, one of the key immune cells involved in the inflammatory response observed in lungs of patients with chronic airway diseases. In the epithelial lining fluid of a healthy individuals roughly 1 % of the inflammatory cell population consist of neutrophils, whereas in the lung of a CF and COPD patient the percentage rises to more than 70 % (Singh et al. 2010; Downey et al. 2009; Kelly et al. 2008). Neutrophils are recruited from the bone marrow to the site of

inflammation by primary chemoattractants such as IL-6 and IL-8 or secondary attractants for example Leukotriene B_4 (LTB_4). During inflammation, the level of IL-8, expressed by epithelial cells of the lung, is highly increased which leads to elevated numbers of infiltrating neutrophils and further amplifies their level of activation (Conese et al. 2003; Baggiolini et al. 1993). When primed neutrophils are activated, they start to degranulate and thereby release several neutrophil serine proteases (NSPs), but also other molecules such as Myeloperoxidase (MPO) and reactive oxygen species, to fight the bacterial infection. As a consequence, the healthy surrounding tissue is destroyed by the excessive inflammatory response and the amount of released enzymes (Figure 2) (Downey et al. 2009). Further, during a process called NETosis, neutrophil fight pathogens by secretion of extracellular traps (NETs), which are web-like structures consisting of DNA filaments (Khan et al. 2017; Brinkmann und Zychlinsky 2007). The NETs are supposed to enmesh pathogens, to further deteriorate the mucus dehydration which promotes mucus plugging and clogging of the airway and, thereby, worsen the situation by creating a perfect environment for further bacterial infections (Branzk und Papayannopoulos 2013; Rahman und Gadjeva 2014). During the described infectious and inflammatory conditions neutrophils have a prolonged life time caused by delayed apoptosis (Lay et al. 2011).

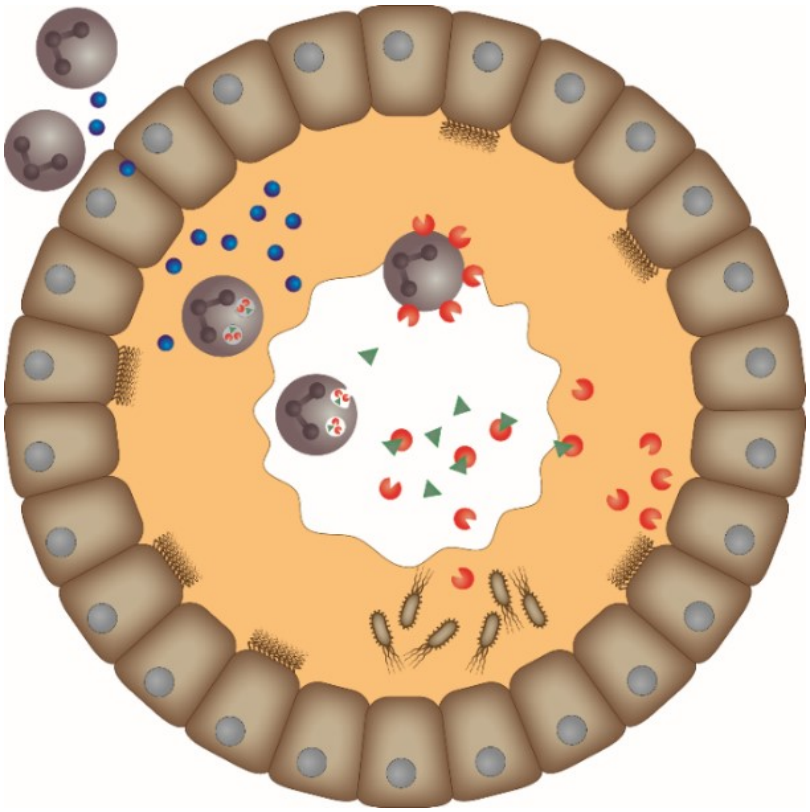

Figure 2: Neutrophilic inflammation in the lung. Neutrophils (gray) are recruited by pro-inflammatory cytokines (blue). Neutrophil serine proteases (red) are released via degranulation at the site of inflammation. Anti-proteases (green) counteract the released proteases. In the thick and sticky mucus (light brown) combined with decreases mucociliary clearance pathogens (dark brown) get trapped.

1.3.1 Granules of neutrophils

Neutrophils store preformed molecules in different intracellular granules, to be ready to combat the inflammatory conditions at the site of inflammation right after arrival. These consist of, primary (azurophilic), secondary (specific), tertiary (gelatinase) granules as well as secretory vesicles and endocytic multivesicular bodies (Rørvig et al. 2013; Uriarte et al. 2008; Cieutat et al. 1998). In azurophilic granules, the NSPs; neutrophil elastase (NE), proteinase 3 (PR3), cathepsin G (CTSG) as well as neutrophil serine proteinase 4 (NSP4) are found (Korkmaz et al. 2010). They are involved in a variety of processes like orchestration of the inflammatory response or processing of the extracellular matrix, chemokines, cytokines and cell surface receptors (Korkmaz et al. 2010). Thereby, NSPs have pro- and anti-inflammatory activities, shaping the immune response at the site of inflammation. The NSPs, NE, PR3 and CTSG share a common three dimensional structure consisting of a C-terminal α-helix and two homologous β-barrels (Bode et al. 1986). The active center comprises the catalytic triad (histidine, serine and aspartate) (Korkmaz et al. 2010). Due to their positively charged residues all three are highly cationic proteases with the S1 pocket defining their substrate specificity (Korkmaz et al. 2010). For NSPs activation, signal peptidase removes the amino-terminal peptide, followed by the truncation of an amino terminal dipeptide by cathepsin C (Korkmaz et al. 2010; Perera et al. 2012). Specific granules for example, contain Lactoferrin (LTF), whereas MMP9 can be found in tertiary granules (Adlerova et al. 2008; Chakrabarti und Patel 2005). The intracytoplasmic granules either fuse with the phagolysosomes to digest phagocytized microbes or fuse with the plasma membrane to expel their granular content into the extracellular space, whereby some of the molecules remain on the cell membrane (Kettritz 2016; Campbell et al. 2000). In diseases like CF, the enormous numbers of recruited and activated neutrophils cause an massive release of NSPs, which overwhelms the capacity of endogenous anti-proteases and mediates matrix destruction, tissue damage and inflammation (Korkmaz et al. 2010). Additionally, recruited neutrophils are less efficiently phagocytized by macrophages and augmented amounts of necrotic neutrophils boost the inflammation further which results in a constant vicious cycle (Haslett 1999; Watt et al. 2005).

1.3.2 Neutrophil elastase

Neutrophil expressed NE is encoded on chromosome 19 by the gene *ELANE* and has a size of 29 kDa (Zimmer et al. 1992). For CF patients, micromolar concentrations of NE have been reported in bronchoalveolar lavage fluid (BALf) (Konstan et al. 1994), and blood neutrophils of CF patients have been shown to secrete higher amounts of NE than neutrophils from heathy controls (Taggart et al. 2000). Though the complete underlying mechanism of increased NE concentrations in CF airways is not completely understood, several consequences of the elevated NE levels are known. Those include, airway

remodeling, impaired MCC, proinflammatory activity and impairment of the adaptive as well as the innate immune response (Twigg et al. 2015). The main factors of airway clogging of CF patients are mucins, highly glycosylated proteins secreted by epithelial cells (Kreda et al. 2012). It is known that NE interferes with the expression of the mucins Mucin 5AC (MUC5AC) and Mucin 5B (MUC5B) by upregulating either the epithelial growth factor receptor or the protein kinase pathway (Shao und Nadel 2005; Park et al. 2005). Moreover, NE reduces the ciliary beat frequency by degrading the cilia, which further impairs MCC and therefore increases mucus plugging, facilitating a chronic colonization of bacteria and other pathogens (Mall 2008). Further, NE has the ability to directly activate MMPs such as MMP3 and MMP9, and can antagonize the inhibitor of MMP9: the Tissue inhibitor of MMPs 1 (TIMP1) (Ferry et al. 1997; Jackson et al. 2010). Additionally, NE exhibits an antimicrobial effect as it can cleave protein A of the outer membrane of Gram-negative bacteria (Belaaouaj et al. 2000). One fate of neutrophils in the CF airways has been described as granule releasing, immunomodulatory and metabolically active (GRIM) (Tirouvanziam et al. 2008; Forrest et al. 2018; Mitchell 2018). Airway neutrophils in CF lose the surface phagocytic receptor cluster of differentiation (CD) 16 and have a modify expression of arginase-1 (Arg1) and programmed death-cell ligand-1 (PDL-1) to alter inhibitory molecules of T-cells, leading to inhibited bacterial killing (Forrest et al. 2018; Tirouvanziam et al. 2008; Ingersoll et al. 2015).

NE is not only stored in primary granules, but can be also found within the nuclear envelope (Clark et al. 1980). Hence, NE translocated to the nucleus degrades histones and mediates chromatin decondensation, a process highly important for NETosis. Further, MPO, another enzyme has been shown to be highly involved in this process (Papayannopoulos et al. 2010). Moreover, NE has the ability to reduce the uptake of apoptotic cells through macrophages, by cleaving the macrophage apoptotic cell receptors such as CD36 (Vandivier et al. 2002), and to cleave T-cell receptors including, CD2, CD4, CD8 and CD14(Döring et al. 1995; Le-Barillec et al. 1999). This leads to impaired monocyte activation and prevents dendritic cells to fully maturate and present their antigens, to antagonize the adaptive immune response (Döring et al. 1995; Le-Barillec et al. 1999). Lastly, the mucus found in CF patient lungs is full of DNA which a significant proportion is made up by NETs, that increases mucus viscosity and therefore further promotes mucus plugging (Brinkmann und Zychlinsky 2007; Fahy und Dickey 2010). Those NETs not only contain NE but also other NSPs as CTSG and PR3 that are stored together in azurophilic granules of neutrophils (Korkmaz et al. 2010; Guerra et al. 2020).

1.3.3 The NSPs: Proteinase 3, cathepsin G and neutrophil serine proteinase 4

PR3, a serine protease with a size of 29 kDa, is encoded by the *PRTN3* gene (Sturrock et al. 1993). PR3 and NE are closely related and share many similarities in regard to their biological effect (Goldschmeding et al. 1989). In contrast to NE, PR3 can truncate IL-8 to increase the potency of neutrophil chemoattractants, by boosting the interplay between IL-8 and its corresponding receptor CXC motif chemokine receptor 1 (van den Steen et al. 2000). Additionally, PR3 has antimicrobial properties against both, Gram-positive and Gram-negative bacteria as well as fungi (Korkmaz et al. 2010). Lastly, PR3 is not only found in primary granules but can also be located in secretory vesicles (Witko-Sarsat et al. 1999).

The mature form of CTSG has a size of 28.5 kDa and is slightly smaller than NE and PR3 (Salvesen und Enghild 1991). Besides, it has only one glycosylation site whereas NSP4 and PR3 have two and NE has three (Perera et al. 2012). Roughly one-fifth of the primary granular content is made up by CTSG (Ute Bank und Siegfried Ansorge 2001). Although CTSG is, as NE and PR3, a serine protease, it is a member of a larger protease family the cysteine cathepsins (Turk et al. 2012). Upon neutrophil activation, CTSG is released in high concentrations mediates degradation of structural components of the extra cellular matrix (Korkmaz et al. 2008b). Furthermore, CTSG prevents the removal of apoptotic cells by macrophages and elevated numbers of necrotic neutrophils enhance the exocytosis of NSPs into the airways (Korkmaz et al. 2008b). In BALf of CF patients, CTSG has been shown to have the highest degradation efficiency against surfactant protein A, which endorses clearance of pathogens by macrophages and prompts bacterial survival (Rubio et al. 2004). Secreted CTSG and NE can degrade flagellin, an important bacterial pathogen associated molecular pattern (PAMP) and cleave leukotoxin from Gram-negative bacteria, a neutrophil inhibitor (López-Boado et al. 2004; Tsai et al. 1979). The NSPs degrade the complement receptors C3bi, CR1 and C5, the clearance of pathogens can be hampered, and phagocytosis can be reduced (Tosi et al. 1990). The degradation of antimicrobial peptides such as LTF and β-defensins by NE impedes the efficient bacterial killing (Rogan et al. 2004; Griffin et al. 2003). Lately, there is a particular interest of the role of membrane associated NSPs that make up a significant fraction of the exocytosed enzymes during inflammatory response (Owen 1995; Brinkmann und Zychlinsky 2007).

Recently, NSP4 was discovered, wherefore only little is known so far about it (Perera et al. 2012). In comparison to NE, PR3 and CTSG, the concentration of NSP4 in primary granules is with ~5 % of the CTSG amount comparably low (Perera et al. 2012). NSP4 is

encoded by the gene *PRSS57* on chromosome 19 (Perera et al. 2012). In contrast to the other NSPs, NSP4 functions as a trypsin-like protease and requires an arginine at position 1 due to its occluded pocket (Lin et al. 2014). Moreover, NSP4 shows closer similarity to mast cell chymase than the other NSPs (Perera et al. 2012). Inhibitors of NSP4 are A1AT, C1 inhibitor and most effectively antithrombin-heparin, whereas elafin and SLPI show no inhibitory effect (Perera et al. 2012).

1.3.4 NSP interactions with cytokines, chemokines and growth factors

Several factors are associated to inflammation response and/or infection in CF; these incorporate cytokines such as IL-1β, IL-6. IL-8, LTB_4, tumor necrosis factor alpha (TNF-α) and granulocyte-macrophage colony-stimulating factor (Greally et al. 1993; Kube et al. 2001). *In vitro* experiments with immortalized human CF bronchial epithelial cells have shown that mutated CFTR activity is elevated and the localization of the ion channel within the cell membrane is enhanced after exposure to TNF-α (Chhuon et al. 2016). Further, TNF-α as well as IL-1β are both inflammatory cytokines, which need to be activated by MMPs or NSPs first (Black et al. 1997). IL-1α and IL-1β belong to the IL-1 family and are crucial cytokines that orchestrate the innate as well as the acquired immune response (Korkmaz et al. 2010). Higher levels of IL-1α and IL-1β, together with elevated proportions of necrotic cells, have been described as one reason for a worsening of the inflammatory cascade after a viral infection (Montgomery et al. 2020). These are driven by NOD-, LRR- and pyrin domain-containing protein 3 activation in a cell culture model for CF (Montgomery et al. 2020). Besides, supernatants rich in IL-1α and IL-1β have been described to interfere with the expression of MUC5AC and MUC5B via the IL-1 receptor (Abdullah et al. 2018). Rhinovirus infections are common in children suffering from CF (Montgomery et al. 2020). A key chemokine essential for the recruitment, migration and degranulation of neutrophils to the site of inflammation is IL-8 (Baggiolini et al. 1993). Sources of IL-8 are endothelial cells, fibroblasts as well as monocytes reacting to inflammatory stimuli. Pro-IL-8 can be cleaved to a highly active and less active form by PR3 and MMP9, respectively (Padrines et al. 1994). Toll-like receptor 4 (TLR4) and epidermal growth factor receptor of lung epithelial cells can be directly been upregulated by NE, therefore, promote the overproduction of pro-IL-8 which boosts the neutrophilic infiltration (Devaney et al. 2003). Elevated levels of transforming growth factor β1 (TGF-β1) have been linked to a more severe progression of lung fibrosis, associated with decreased lung function and elevated influx of neutrophils (Arkwright et al. 2000; William T. Harris et al. 2009). Major source of TGF-β1 are hematopoietic endothelial cells as well as cells of the connective tissue (Blobe et al. 2000).

1.3.5 Matrix metalloproteinases

MMPs are a subfamily of the superfamily of metzincins also known as metalloendo-peptidases (Stöcker und Bode 1995). The most relevant MMPs in the context of CF lung disease are MMP2, MMP7, MMP8, MMP9 and MMP12 (Dunsmore et al. 1998). Most frequently, they are expressed by macrophages (Dunsmore et al. 1998). Contrary to NSPs, MMPs are stored and secreted in an inactive form, called zymogens and need to be truncated to get enzymatically active (McElvaney et al. 2019). There are several mechanisms leading to activation of MMPs (Gaggar et al. 2011). Those include protease mediated activation, either by another protease or by the active form of the same MMP, as well as matrix mediated or oxidant mediated activation (Gaggar et al. 2011). During inflammatory conditions, the expression and activation of MMPs is elevated (Stamenkovic 2003). Several biological functions have been associated to MMPs, like remodeling of tissues, degradation of matrix components, release of growth factors, cytokines and chemokines as well as the modulation of cell migration and mobility (Sternlicht und Werb 2001).

MMP2 can to disrupt Cl^- currants, MMP7 is important during the reepithelization of the airways and may activate TNF-α by truncating its pro-form, whereas MMP8 and MMP9 are capable of modifying CXC chemokines and compose collagens (Chen et al. 2009; McElvaney et al. 2019; Parks et al. 2004). In BALf from the lower airways of CF patients, the amount and activity of MMP9 was shown to be elevated (Gaggar et al. 2007; Ratjen et al. 2002). In one study a correlation between the lung function, measured as FEV_1, and MMP9 concentrations has been described (Roderfeld et al. 2009). Furthermore, MMP8 and MMP9 are not only released by macrophages but also highly expressed by neutrophils (Greenlee et al. 2007). In sputum of CF patients MMP8 is a crucial enzyme for the generation of proline-glycine-proline, which is a novel neutrophil (Gaggar et al. 2008). Further, MMP9 is involved in enhancing the potency of IL-8 and has been associated with matrix destruction repair (van den Steen et al. 2000; McCawley et al. 1998). MMP12 released from macrophages upon mucus dehydration results in emphysema formation and, therefore, disease progression (Trojanek et al. 2014). Further, especially the membrane associated MMP12 activity was elevated compared to the soluble fraction (Trojanek et al. 2014). Primary target of MMP12 is elastin which might further activate airway macrophages that mediate tissue damage (McElvaney et al. 2019; Trojanek et al. 2014).

The prominent unspecific inhibitor of MMPs is α-2-macroglobulin, whereas TIMP1 is the most specific (McElvaney et al. 2019). TIMPs can be degraded by NE, or by MMP12 if present in enormous concentrations, resulting in inactivation of their inhibitory capacity

against MMPs (Jackson et al. 2010; Shapiro et al. 2003). The pathogenesis of several disease like COPD, asthma and CF has been linked to a disequilibrium between TIMPs and MMPs (Finlay et al. 1997; Tanaka et al. 2000; Gaggar et al. 2011).

1.3.6 Endogenous anti-proteases

Anti-proteases antagonize NSPs to regulate their proteolytic activity and can be categorized in three major groups: the serpins, chelonianins and macroglobulins (Groutas et al. 2011). Secreted anti-proteases have the overall aim to protect the connective tissue from enzymatic degradation by NSPs (Janoff 1985). In diseases like CF, this balance between NSPs and anti-proteases is disturbed and the tissue is exposed to excessive amounts of highly active NSPs that disrupt the connective tissue. Further, anti-proteases exhibit immune modulatory capacity along with anti-microbial actions (Greene und McElvaney 2009), and clinical studies have shown that defects of the inhibitor expression results in structural lung damage (Taggart et al. 2017).

Alpha-1-antitrypsin (A1AT) is a single-chain glycoprotein. It is the most frequent serpin, and is synthesized by the liver and transported via the blood stream to the lung where it exhibits its main function: the protection of lung tissue from NSPs (Janciauskiene 2001; McElvaney et al. 2019). Primarily, A1AT inhibits irreversibly NE, both its free and membrane associated form, however A1AT also shows inhibitory effects towards PR3 and CTSG by incorporating them irreversible to a soluble complex (Korkmaz et al. 2005a; Korkmaz et al. 2005b). Further, A1AT can be enzymatically cleaved by several proteases, including MMP7, MMP8, MMP9,the cathepsin L and by the bacterial proteases secreted by *S. aureus* and *P. aeruginosa* (Knäuper et al. 1990; Zhang et al. 1994; Rapala-Kozik et al. 1999; Morihara et al. 1984; Michaelis et al. 1990; Desrochers et al. 1992). This shredding of serpins by MMPs is further fueling the destruction caused by NSPs (Rodríguez et al. 2010; Dean und Overall 2007).

The cationic serine protease inhibitor, secretory leukocyte protease inhibitor (SLPI) is one of the best characterized endogenous anti-proteinases and is crucial for lung homeostasis (Twigg et al. 2015). SLPI is secreted locally by several cell types including neutrophils, macrophages and non-ciliated bronchial epithelial cells (Böhm et al. 1992; Jin et al. 1997; van Wetering et al. 2000). Those cells express SLPI as response to NE, but also several cytokines and bacterial lipopolysaccharides (LPS) (van Wetering et al. 2000; Saitoh et al. 2001). Further, the activation of toll-like receptors (TLR) and the nuclear factor kappa-light-chain-enhancer of activated B cells (NF-κB) is prevented by hampering the expression of pro-inflammatory molecules due to the ability to bind LPS and lipoteichoic (LTA) (Taggart et al. 2005; Lentsch et al. 1999; Taggart et al. 2002). Besides, SLPI can inhibit NE, CTSG, trypsin and chymotrypsin (Eisenberg et al. 1990). In patients with CF, who encounter a

P. aeruginosa infection, SLPI levels are decreased, as a consequence of excessive NE levels (Weldon et al. 2009). Besides, the by NE truncated form of SLPI losses its ability to bind LPS (Twigg et al. 2015).

Elafin or the preform trappin-2, share 40 % of structural analogy with SLPI and are expressed by neutrophils and macrophages (Scott et al. 2011). As SLPI, elafin has the ability to inhibit NE, trypsin and chymotrypsin (Sallenave 2000). Elafin can additionally inhibit PR3 but not CTSG (Sallenave 2000; Wiedow et al. 1990). The monocyte mediated NF-κB activation can be inhibited by elafin, which reduce the expression of inflammatory molecules (Butler et al. 2006). If NE is present in excess, it can cleave elafin (Guyot et al. 2008) without changing its antimicrobial property, however, the inhibitory capacity against NE is lost (Guyot et al. 2010).

α-1-antichymotrypsin (ACT) produced from hepatocytes, can inhibit only CTSG among the NSPs (Travis et al. 1978). But has an inhibitory effect against pancreatic chymotrypsin, mast cell chymase and kallikrein 2 and 3, which are both enzymes of the prostate (Poller et al. 1993; Frenette et al. 1997). NE, MMP8 and proteases with bacterial origin cannot be inhibited by ACT but can truncate it (Kress 1983; Desrochers et al. 1992). During acute inflammation phases ATC levels are dramatically increased (Aronsen et al. 1972). In contrast to other members of the serpin family it has the particular ability to bind DNA (Naidoo et al. 1995). Further, milder cases of CF have been associated with ACT deficiency (Mahadeva et al. 2001).

1.4 NE measurement techniques

For clinical diagnosis, ELISA based detection of the NE protein amount is still the most commonly used technique, though it has several limitations: it is time consuming and laborious and can only determine the total enzyme concentration but not the enzyme activity (Liu et al. 2020). To measure NE activity, specific probes that change their characteristics when cleaved by NE, are used (Gehrig et al. 2012). These include either, chemical probes, based on peptides (Gehrig et al. 2012; Schulz-Fincke et al. 2018a; Schulenburg et al. 2016), synthetic probes, based on small molecules (Schulz-Fincke et al. 2018b; Ruivo et al. 2016; Sun et al. 2013). To quantify the amount of cleaved probes, they are linked to Förster resonance energy transfer (FRET), where energy is transferred between a donor and acceptor or quencher moiety (Hamano et al. 2016; Yuan et al. 2013). Compared to chromogenic substances, FRET reporters are more sensitive and can be set up in a way to be ratiometric, FRET reporters are more sensitive and can be ratiometric, which makes them independent of local probe concentration variations (Korkmaz et al. 2008a; Gehrig et al. 2012). The latest developed probes are based on quantum dots, which have a limit of detection (LOD) in the lower picomolar range, show a good photostability and biocompatibility (Liu et al. 2020).

1.4.1 Measurement of free NE activity

In most cases, NE activity measurements focus on the free NE fraction in the supernatant (Sly et al. 2013; Sagel et al. 2012; Ratjen et al. 2016). Therefore, the chromophoric substrate Methoxysuccinyl-Ala-Ala-Pro-Val *p*-nitroanilide (*p*NA) or its fluorescent variants (Nakajima et al. 1979; Castillo et al. 1979) are predominantly used. The handling of *p*NA is easy but it is rather insensitive (Korkmaz et al. 2008a). The LOD of *p*NA is in the nanomolar range, wherefore it's are often not sensitive enough to detect NE activity in samples of CF children or BALf (Sly et al. 2009).

With NEmo-1 (Figure 3a), a novel FRET based NE probe has been described recently. It consists of the target sequence QPMAVVQSVPQ flanked by a polyethylene glycol (PEG) spacer on both sides, the fluorophore methoxy coumarin on the N terminus and a lysin residue as well as coumarin343 on the C terminus (Gehrig et al. 2012). As the *p*NA substrate, NEmo-1 can be read out using a plate reader or any kind of equipment that allows fluorescence detection. As long as NEmo-1 is intact, it shows highly effective donor quenching. Enzymatic segregation of the donor and acceptor moiety leads to a strong gain in the donor signal whereas the acceptor signal faintly increases (Gehrig et al. 2012). NEmo-1 is ratiometric and allows the detection of NE activity in the picomolar range with a LOD ~20 pM for human NE (Gehrig et al. 2012; Dittrich et al. 2018).

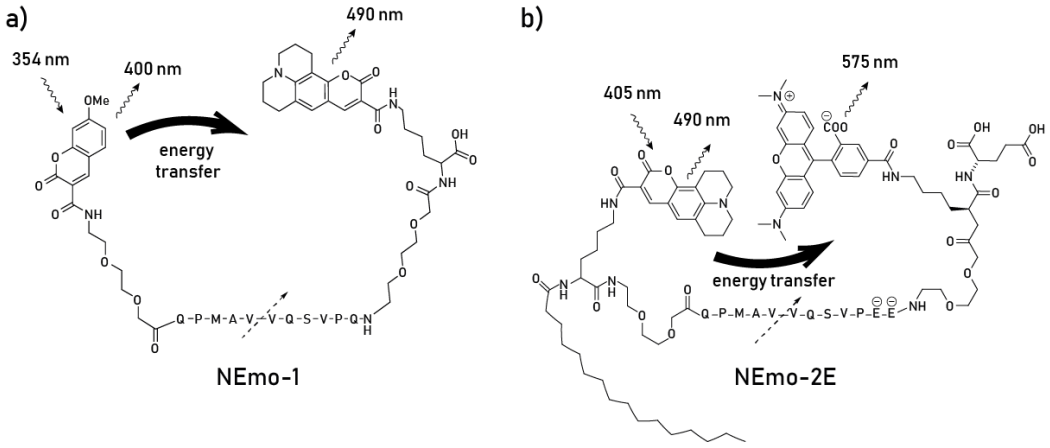

Figure 3: Chemical structure of FRET reporters NEmo-1 and NEmo-2E. A) probe for free NE measurements (NEmo-1). **B)** NEmo-2E probe for membrane associated NE quantification. The NE-specific peptide target sequence is given by amino acids with single-letter codes. Dashed arrows indicate the cleavage site. Excitation and emission wavelength (indicated by waved arrows) in nm are given accordingly. Adapted from Gehrig et al. 2012.

1.4.2 Measurement of membrane associated NE

NE is a highly cationic enzyme that, when released from granules upon exocytosis, attaches to the neutrophil membrane via electrostatic interactions (Campbell und Owen 2007; Owen et al. 1997). This membrane associated fraction of NE is particularly difficult to access for inhibitors since they cannot surpass the microenvironment surrounding the infiltrating neutrophils or reach the active site of the enzyme (Sly et al. 2009; Bartoli et al.

2009; Khan et al. 1995). Membrane associated NE is, therefore, by far more dangerous for the lung epithelium than free NE (Boxio et al. 2016). It can be measured with NEmo-2E (Figure 3b) which has the same target sequence (QPMAVVQSVP) as NEmo-1 used for free NE assessment. However, its structure was slightly modified to perfectly suit the measurement of membrane associated NE. Accordingly, NEmo-2E contains a lipid anchor palmitic acid to direct it to the plasma membrane, and the glutamine at the C-terminal end of the flaking region was replaced by two glutamic acid residues to prevent phagocytosis of the reporter due to negative charge (Gehrig et al. 2012). Moreover, the off target glutamic acid residue was introduced after the PEG linker to increase coupling efficiency of the fluorophore during synthesis a red-shifted fluorophore pair, which consisted of coumarin343 and 5-carboxytetra-methylrhodamin (TAMRA) was selected.

1.4.3 Synthetic NE inhibitor sivelestat

Sivelestat is a synthetic small molecule inhibitor and is specific for NE. It retains neutrophil deformability and enhances the pulmonary microcirculation in animals and humans (Fujii und Bessho 2019; Kawabata et al. 1991). In Japan, sivelestat is commonly used to treat patients suffering from acute respiratory distress syndrome which is often provoked by pneumonia (Kishimoto et al. 2017). Sivelestat is important for assays aiming to measure the NE activity as it is specific towards NE, therefore it is often used for *in vitro* experiments (Gehrig et al. 2014; Dittrich et al. 2018).

1.5 Objectives

Cystic fibrosis (CF) and chronic obstructive pulmonary disease (COPD) are characterized by a severe inflammation and infiltration of neutrophiles which secrete neutrophil elastase (NE), which leads to lung parenchyma destruction and disease progression.

To better characterize the relation between airway inflammation, sputum microbiome and lung function of mostly clinically stable patients with CF, a prospective cross-sectional study was performed. Therefore, the relationship between i) a broad panel of inflammatory markers including IL-1β, IL-6, IL-8, TNF-α and NE, ii) endogenous anti-proteases such as SLPI, A1AT, NE/A1AT and TIMP1, ii) microbiome structure and cluster type and iv) the lung function parameter FEV_1 % predicted was assessed. The hypotheses of the cross-sectional study regarding the identified links between airway dysbiosis, inflammation and lung function were followed-up in longitudinal study which allowed to identify the parameters association with temporal resolution on the basis of individual patients over a short (during one-year) and long-term (over a period of 3 years) period.

NE is not only present in the soluble fraction, but also on the surface of neutrophils (Dittrich et al. 2018). This membrane associated fraction of NE activity has been inherently difficult to measure but can be detected utilizing confocal microscopy. While this procedure allows spatial resolution, it is too laborious for clinical diagnostics and requires expensive equipment. To overcome these limitations, the second part of this study focused on the establishment of an advanced novel method based on flow cytometry using FRET probe NEmo-2E. In the next step this study aimed to access the applicability of the new approach to address clinical questions. Therefore, the novel method for membrane associated NE activity measurement, together with established inflammatory markers, anti-proteases, clinical parameters, microbiome structure and in-depth analysis of their airway secretome were investigated in a cross-sectional study comprised of CF and COPD patients together with healthy controls.

2 Material and methods

2.1 Study conception

In this study, sputum samples from adolescent and adult CF and adult COPD patients, that were able to spontaneously expectorate sputum were investigated. CF was diagnosed and verified by established criteria (Boeck et al. 2011).

2.1.1 Investigation of the relationship between airway inflammation, microbiome composition and clinical parameters in CF patients

To gain a better understanding of the relationships between airway inflammation, microbiome and various clinical parameters these factors were evaluated in a cross-sectional study of a representative cohort of 106 adolescent and adult patients with CF. To test, whether the relations found in the cross-sectional study are also valid on an individual patient basis, a longitudinal follow-up study of a sub-cohort was performed to characterize CF derived samples within a multi-parameter analysis. In order to better understand the interdependencies of the parameters studied, three or more samples were collected within one year or at least one sample per year for at least three consecutive years. By dividing the study population into a short- and long-term study arm, the effect and progression of inflammatory markers as well as parameters of the microbiome structure on the short- and long-term development of the disease course could be observed.

2.1.2 Investigation of membrane associated NE activity in healthy controls, CF and COPD patients

To assess if membrane associated NE activity can be used as an applicable marker for inflammatory airway diseases, samples from CF and COPD patients as well as healthy controls were compared in a cross-sectional study. COPD patients were in advanced disease stage (GOLD III-IV) and the control cohort was age matched to the CF cohort and had no history of lung diseases. From these samples, inflammatory markers, lung function and the microbiome structure were examined.

2.2 Human sample acquisition

From patients spontaneous expectorated sputum samples were collected. Therefore, from all subjects or their parents/legal guardians an informed written consent (CF: S-370/2011; COPD: S-041/2018 and healthy controls S-046/2009) was obtained, and the study was approved by the ethics committee of the University of Heidelberg (Heidelberg, Germany). Spontaneously expectorated sputum was collected from CF or COPD patients during their ambulant or stationary visits to the CF Center Heidelberg (Heidelberg, Germany) and used

if it contained more than one million viable cells. To obtain sputum samples from healthy controls, sputum was induced by first inhaling 200 µg of the β-2-receptor-antagonist salbutamol. Subsequently, the sputum induction procedure was started by inhaling nebulized hypertonic (6 %) saline solution for about 15 min. If blood from healthy controls were obtained, this was withdrawn before sputum induction.

2.2.1 Sputum sample preparation

Samples of the airways, spontaneous and induced sputum were processed to separate cells and the soluble fraction. First, saliva and mucus particles were separated using a pipet tip. The mucus clumps were weighted and treated with 4 parts v/w of 10 % Sputolysin (Merck, Darmstadt) for 15min at ambient temperature on a rocking shaker, allowing the mucus to dissolve. The reaction was stopped by adding an equal volume of 4 °C cold phosphate buffered saline (PBS) (Gibco, Karlsruhe, Germany). The mixture was pipetted up and down several times to get a homogenous solution and filtered through a 100 µm and 40 µm Nylon cell strainer (Corning Inc., Corning, NY, USA) sequentially. Afterwards the mixture was centrifuged for 10 min at 300 x *g.* The supernatant fraction was separated from the cell pellet aliquoted into smaller portions, aliquots for cytokine measurements were supplemented with cOmplete Protease Inhibitor Cocktail (Roche, Basel, Switzerland) and aliquots for enzyme assays were stored at -80 °C directly. The cell pellet was recovered in cold PBS and the cells were counted using trypan blue staining to be able to discriminate live and dead cells.

2.2.2 Blood sample preperation

Blood samples were collected using S-Monovette 5 ml, Citrat 3.2 % (1:10), (Sarstedt AG & Co. KG, Nümbrecht, Germany) and stored at 4 °C immediately after. They were purified using MACSxpress Whole Blood Neutrophil Isolation Kit (Miltenyi Biotec, Bergisch Gladbach, Germany) according to the manufacturers protocol. Brief, two parts of blood were mixed with one part of MACSxpress Whole Blood Neutrophil Isolation Cocktail mixture for 5 min on a tube rotator and afterwards placed in the magnet for 15 min at ambient temperature. The liquid fraction including the neutrophils was separated from the unwanted magnetized other cells, and centrifuged for 10 min at 300 x *g*. Afterwards the supernatant was sucked of and the pellet resuspended in 500 µL of cold PBS. 5 mL of 1x RBC lysis buffer were added and the solution incubated for 5 min at ambient temperature, the reaction was stopped by adding 5 mL of cold PBS and the mixture was centrifuged again for 10 min at 300 x *g*. The supernatant fraction was discarded and the cell pellet resuspended and the cell number determined by performing a trypan blue based cell count.

2.3 Measurement of free NE activity

Free NE activity was measured using two different approaches activities in supernatant fraction of sputum samples. The first and so far, gold standard procedure uses a chromogenic substrate N-Methoxysuccinyl-Ala-Ala-Pro-Val-*p*-nitroanilide (Sigma-Aldrich, St. Louis, MO, USA). The second is based on the more recently developed FRET based reporter NEmo-1 (Sirius Fine Chemicals, Bremen, Germany) see Figure 3.

2.3.1 Measurement of free NE activity using N-Methoxysuccinyl-Ala-Ala-Pro-Val *p*-nitro-anilide

Absorbance based assay of free NE was measured using chromogenic substrate N-Methoxysuccinyl-Ala-Ala-Pro-Val *p*-nitroanilide (*p*NA) (Sigma-Aldrich, St. Louis, MO, USA). CF and COPD supernatant samples were diluted 1:20, samples from healthy controls 1:10 with PBS. 25 µL of diluted sample were pipetted in duplicates using white half area flat bottom µCLEAR microplates (Greiner Bio-One, Frickenhausen, Germany). Immediately after addition of 25 µL of master mix (containing 10 mM TRIS-HCl, 500 mM NaCl, pH 7.5 and 600 µM of *p*NA) absorbance was recorded at 410 nm for 100 cycles each 45 s. Besides the samples a 1:2 dilution series of known Human Sputum Leucocyte Elastase (Elastin Products Company, Owensville, Missouri, USA) concentrations starting from 8 µg/mL to 0.125 µg/mL was run as standard curve in parallel. After the run the slopes of each absorbance curve were plotted over time and the slope of the linear area was calculated. Unknown samples were fitted to the slope of the standard curve and afterwards multiplied by the dilution factor to calculate the enzyme concentration.

2.3.2 Measurement of free NE activity using the Förster-resonance electron transfer probe NEmo-1

Fluorescent based quantification of free NE was performed using FRET reporter NEmo-1 (Sirius Fine Chemicals, Bremen, Germany). CF and COPD supernatants were diluted 1:500 with PBS, supernatants of healthy controls were diluted 1:10 with PBS. 40 µL of prediluted samples were prepared in duplicates using black flat bottom 96 well half area plate (Corning Life Science, Kennebunk, Maine, USA). Direct after addition of 10 µL of master mix (containing 10 mM TRIS-HCl, 500 mM NaCl, pH 7.5 and 1 µM of NEmo-1 (Sirius Fine Chemicals, Bremen, Germany) the assay read out was immediately recorded. FRET reporter was excited at 354 nm and fluorescence was read at 400 nm_{Donor} and 490 $nm_{Acceptor}$ for 50 cycles each 60 s. Additionally duplicates of a 1:2 dilution series of Human Sputum Leucocyte Elastase (Elastin Products Company, Owensville, Missouri, USA) reaching from 0.5 µg/mL to 0.008 µg/mL this was used as standard curve and recorded in parallel. After the run the donor/acceptor (D/A) ratios for the individual

time points were calculated by dividing the RFU at 400 nm_{Donor} by the RFUs at 490 $nm_{Acceptor}$ those were plotted over time. The slope of the linear area of the curve was calculated, criteria for a successful run were to have at least 5 time points within this range, samples and standard that did not fulfill this criterion were excluded from further analysis. The average slopes of the duplicates of the standards were plotted against the known concentration of the enzyme to generate a standard curve were used to interpolate the average of the slopes of the sample-duplicates to calculate their enzyme concentration. Afterwards the calculated concentrations were multiplied by the dilution factor to get the final concentration.

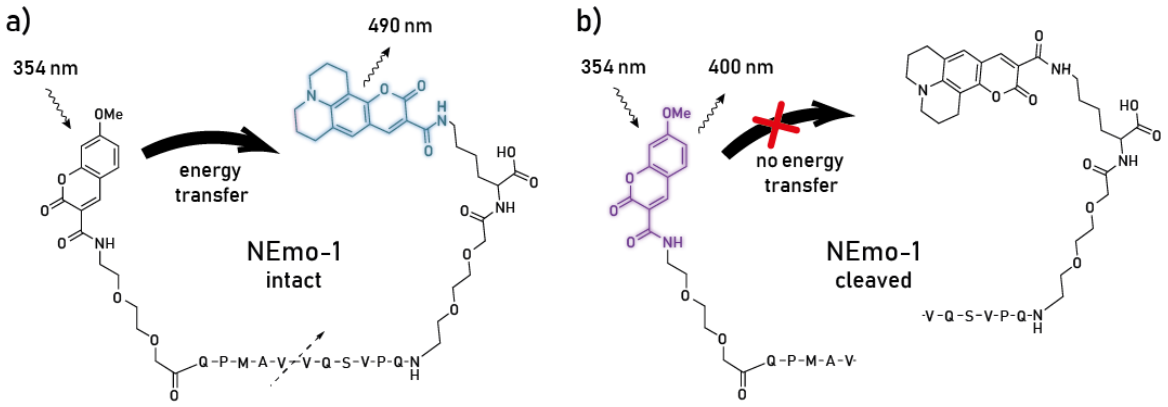

Figure 4: Intact and cleaved structure of FRET reporter NEmo-1. A) Intact probe for free NE measurements (NEmo-1). **B)** NEmo-1 probe after enzymatic cleavage. Energy transfer is no longer possible. The emitting fluorophore is shown colorized. The NE-specific peptide target sequence is given by amino acids with single-letter codes. The dashed arrow indicates the cleavage site. Structure adapted from Gehrig et al. 2012.

2.4 Measurement of membrane associated NE activity

The membrane associated NE activity was quantified applying two different techniques. At the beginning membrane associated NE activity was initially quantified based on confocal microscopy allowing spatial resolution. Based on these studies, a novel approach utilizing flow cytometry could be validated, allowing additional gating of the desired cell type.

2.4.1 Transfer of probes manufacturing process to industry

The synthesis of the NEmo reporter was transferred from the EMBL to Sirius Fine Chemicals in Bremen. To increase the coupling efficiency's during reporter synthesis, small off target modifications have been introduced, by either including a glutamic acid (in case of NEmo-2E) or a glycine (in case of NEmo-2G) residue (Figure 5).

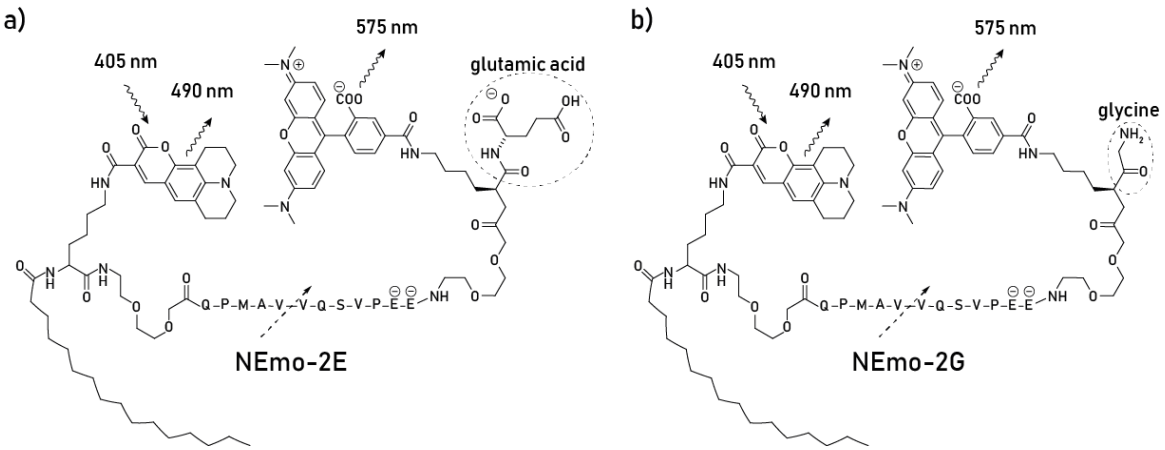

Figure 5: Chemical structure of FRET reporters NEmo-2E and NEmo-2G, A and **B** respectively, for membrane associated NE quantification. The NE-specific peptide target sequence is given by amino acids with single-letter codes. Dashed arrows indicate the cleavage site. Both NEmo-2 variants have different off target side groups highlighted with dashed lines. Excitation and emission wavelength (indicated by wavy arrows) in nm are given accordingly.

2.4.2 Measurement of membrane associated NE activity by confocal microscopy

For quantification of membrane associated NE activity the lipidated FRET reporter NEmo-2E (Figure 6, Sirius Fine Chemicals, Bremen, Germany) at a final concentration of 2 µM was used as previously described (Gehrig et al. 2012; Dittrich et al. 2018). In brief, aliquots of 30 000 cells per tube were prepared in 1.5 mL safe-lock microcentrifuge tubes (Eppendorf AG, Hamburg, Germany). For each of the three conditions, 0 min (negative control) 10 min and 10 min spiked with NE (positive control) duplicates with a volume of 50 µL were prepared after the given incubation times. The positive control samples were supplemented with 1 µL of NE (Elastin Products Company, Owensville, Missouri, USA) with a final concentration of 340 nM. NE inhibitor sivelestat (Cayman Chemical Ann Arbor, MI, USA) was added to the negative control to reach a final concentration of 100 µM and incubated at ambient temperature for 10 min. 50 µl of master mix (containing 10 mM TRIS-HCl, 500 mM NaCl, pH 7.5, 1:1000 DRAQ5 (BioStatus Limited, Shepshed, UK) and 2 µM NEmo-2E (Sirius Fine Chemicals, Bremen, Germany)) was added to all aliquots and the reaction was carried out for 10 min. Immediately after all aliquots were put on ice and 100 µl of stop solution (containing 100 µM of sivelestat in PBS) was added to the 10 min and positive control aliquots, negative control aliquots were supplemented with 100 µL of PBS. Afterwards cells were spun on coverslips (Thermo Fisher Scientific, Waltham, MA, USA) at 300 x *g* for 5 min using a Cytospin 4 (Thermo Fisher Scientific, Waltham, MA, USA). Slips were air dried in the dark and mounted on SuperFrost Plus Adhesion slides (Thermo Fisher Scientific, Waltham, MA, USA) using ROTI Histokitt (Carl Roth GmbH + Co. KG, Karlsruhe, Germany). Slides were dried in the dark at room temperature and stored at 4 °C till they were imaged.

Slides were imaged using a Leica SP8 confocal microscope (Leica Microsystems GmbH, Wetzlar, Germany) equipped with an HC PL APO CS2 40x/1.3 oil objective. Cells were imaged sequentially starting with the nuclear straining (DRAQ5), followed by the donor and acceptor FRET channel combined with a bright field image and finally a DIC image was recorded. The nuclear stain DRAQ5 was excited at 633 nm using a HeNe laser, emission was recorded with a PMT between 650 and 710 nm. The pinhole was set to 3 AU. FRET reporter was excited at 458 nm with an Argon laser, emission was recorded using Hybrid detectors between 470 and 510 nm for the donor and 480 to 610 nm for the acceptor. Simultaneously a bright field picture was recorded with the PMT trans detector the pinhole was set to 5 AU. Finally, a DIC image was recorded using the Argon laser at 458 nm excitation, emission was recorded by PMT trans detector. Recorded images were analyzed using Fiji (Schindelin et al. 2012) with the FluoQ plugin (Stein et al. 2013) to calculate the D/A ratio per cell and condition. For each slide at least 100 cells were analyzed. D/A ratios were background corrected and calculated per pixel and per cell. D/A ratios of the 10 min time point and the positive control were normalized to the negative control. Measurements were excluded if the D/A ratio of the negative control was ≥ 1.6.

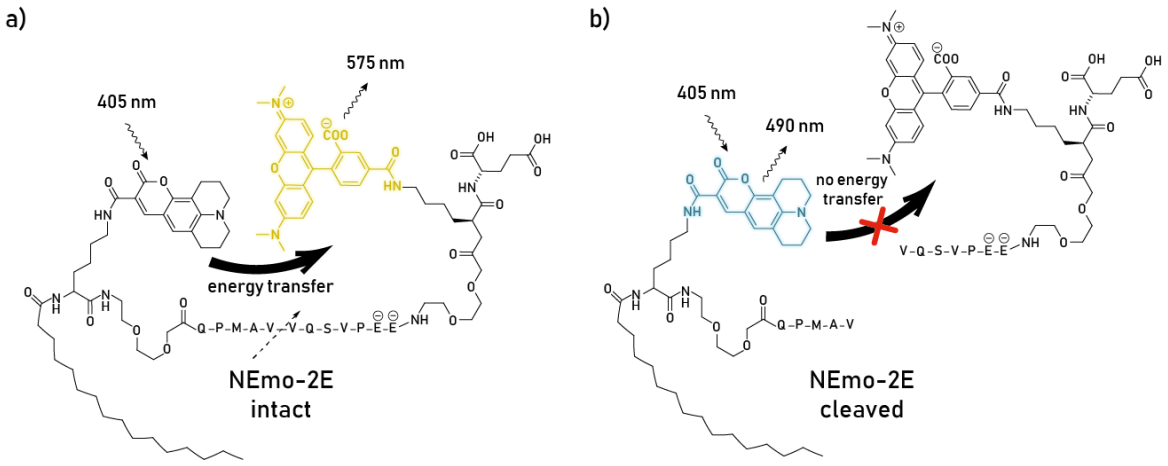

Figure 6: Intact and cleaved structure of FRET reporter NEmo-2E.A) Probe for membrane associated NE activity (NEmo-2E) intact **B)** cleaved NEmo-2E probe, cleaved fragment diffuses away, energy transfer is no longer possible. The NE-specific peptide target sequence is given by amino acids with single-letter codes. Two negative charges were introduced in NEmo-2E in comparison to NEmo-1 to prevent internalization from the cell membrane as well as a lipid anchor to facilitate a localization of the probe to the cell surface. The emitting fluorophore is shown colorized. The dashed arrow indicates the NE cleavage site.

2.4.3 Measurement of membrane associated NE activity by flow cytometry

2 µL FcBlock (BD Biosciences, Heidelberg, Germany) was added to the 5 ml polystyrene round-bottom tube (BD Biosciences, Heidelberg, Germany) with a volume of 100 µl cold PBS containing 1 million cells and incubated for 5 min at room temperature. The antibody master mix specified in Table 1 was added and incubated for 25 min at 4 °C in the dark.

Table 1: Antibody master mix for the detection of neutrophils by flow cytometry

Antibody	Clone	Fluorophore	Supplier	Dilution
CD14	M5E2	Peridinin-chlorophyll-protein complex -Cyanine (Cy) 7	BD Biosciences	1:50
CD16	3G8	Alexa Fluor (AF) 700	BD Biosciences	1:50
CD45	2D1	Allophycocyanin (APC)-Cy 7	BD Biosciences	1:33
CD63	H5C6	AF 647	BioLegend	1:50
CD66b	G10F5	Phycoerythrin (PE)/Dazzle 594	BioLegend	1:50

Cells were washed with 2 mL PBS, centrifuged for 5 min at 300 x *g* (Heraeus Megafuge 16R, Thermo Fisher Scientific, Waltham, MA, USA), supernatant was discarded and the cells were resuspended in 200 µL of cold PBS. 100 µL were pipetted in a separate round-bottom tube and 5 µL of viability staining solution (BioLegend, San Diego, CA, USA) was added to both tubes. To one tube 5 µL of sivelestat (Cayman Chemical Ann Arbor, MI, USA) at a final concentration of 225 µM and 20 µL of proteinase cOmplete inhibitor (Roche, Basel, Switzerland) was added additionally, and incubated for 10 min at ambient temperature in the dark, tube without inhibitors was incubated at 4 °C in the dark. Flow cytometry was performed on a BD LSRFortessa cell analyzer (BD Biosciences, Heidelberg, Germany) direct after addition of 0.8 µL of NEmo-2E (Sirius Fine Chemicals, Bremen, Germany) at a final concentration of 4 µM cellular staining with exclusion of debris, dead cells and cell doublets. Donor intensities were recorded between 425 and 475 nm (450/50 nm filter), acceptor intensities were recorded between 564 and 606 nm (585/42 nm filter) of the violet laser line. Data were analyzed with FACSDiva software (v8.0.1; BD Biosciences, Heidelberg, Germany) or Flow Jo software (v10; TreeStar, Ashland, OR, USA) using the gating strategy shown in Figure 7.

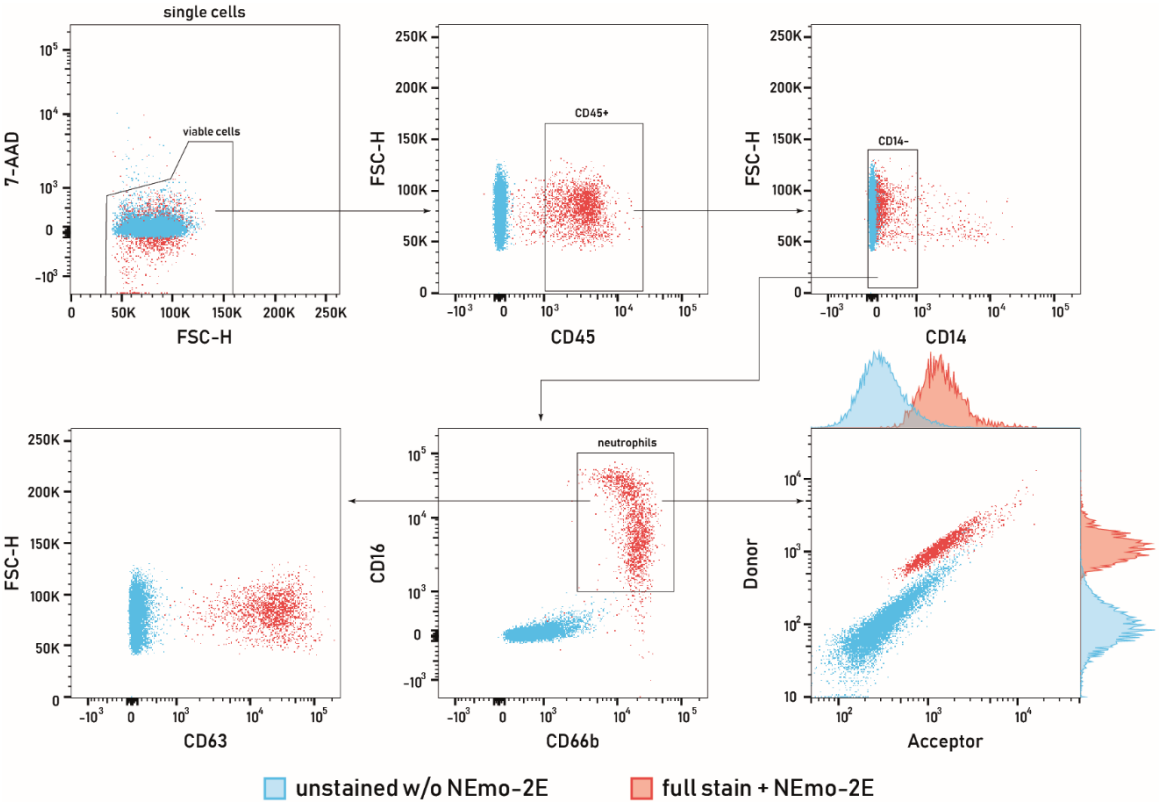

Figure 7: Gating strategy for the detection of neutrophils by flow cytometry. Single cell suspension was prepared and stained according to the protocol described above. Neutrophils were gated as single 7-AAD$^-$, CD45$^+$ CD14$^-$, CD66b$^+$ and CD16$^+$ cells. Cells that were gated as neutrophils were analyzed for their D/A ratio of the FRET reporter NEmo-2E to evaluate the membrane associated NE activity as well as their intensity of the phenotypic marker CD63. Unstained cells are shown in blue, stained cells with FRET reporter NEmo-2E are shown in red. All values are given as mean fluorescent intensities (MFI). $^+$: positive cells; $^-$: negative cells.

Spectral compensations (Table 2) was applied for all antibodies and live dead marker 7-AAD to prevent a false positive signal.

Table 2: Compensation matrix of the flow cytometry assay.

%	CD66b	7-AAD	CD14	CD63	CD16	CD45
	PE-Dazzle594	PerCP	PE-Cy7	AF647	AF700	APC-Cy7
	610/20 Blue	695/40 Blue	780/60 Blue	670/14 Red	730/45 Red	780/60 Red
610/20 Blue	100	53.05	4.53	0.00	0.01	0.00
695/40 Blue	15.73	100	0.99	0.70	0.69	0.04
780/60 Blue	0.87	9.84	100	0.07	0.10	0.40
670/14 Red	0.13	7.15	0.12	100	1.95	7.70
730/45 Red	0.06	7.20	3.80	44.05	100	12.08
780/60 Red	0.00	2.07	48.48	9.32	18.06	100

2.4.4 Evaluation of NEmo-2E target specificity by flow cytometry

To evaluate the target specificity of the FRET reporter NEmo-2E, several relevant inhibitors were added to the cells (Table 3). For this purpose, the protocol described in the section above for the inhibition with sivelestat and protease inhibitor cocktail (PI) was utilized. Inhibitors and final concentrations are given in Table 3. For A1AT, elafin and SLPI a low and high concentration were used. Sivelestat and PI were used in combination with the same concentrations as for the negative control described above, and were used additionally on their own.

Table 3: Inhibitors utilized for assessment of target specificity of NEmo-2E by flow cytometry

	Concentration			
Inhibitor	**Low**	**High**	**IC_{50}**	**Supplier**
A1AT, from human plasma	0.50 µM	5.08 µM	5 nM	Athens Research & Technology, Inc., Athens, GA, USA
rhSLPI	0.32 µM	2.98 µM	4 nM	R&D Systems, Minneapolis, MN, USA
rhTrappin-2/elafin	0.16 µM	1.55 µM	50 nM	R&D Systems, Minneapolis, MN, USA
Sivelestat	0.43 mM	-	44 mM	Cayman Chemical Ann Arbor, MI, USA
proteinase cOmplete inhibitor	7.5-fold	-	-	Roche, Basel, Switzerland

2.5 Enzyme-linked immunosorbent assay

Endogenous inhibitors and chemoattractant were quantified using commercially available ELISA assays. Free Alpha-1-Antitrypsin (A1AT) was quantified using SERPINA1 (Human) ELISA Kit (Abnova, Taipei, Taiwan) and the complex of NE and Alpha-1-Antitrypsin (NE/A1AT complex) was quantified using PMN (Neutrophil) Elastase Human ELISA Kit (Invitrogen, Carlsbad, CA, USA). Secretory leukocyte peptidase inhibitor (SLPI) was measured using Quantakine ELISA Human SLPI Immunoassay (R&D Systems, Minneapolis, MN, USA). Tissue inhibitor of metalloproteinases 1 (TIMP1) an inhibitory molecule of MMPs was quantified via Quantakine ELISA Human TIMP1 Immunoassay (R&D Systems, Minneapolis, MN, USA). Leukotriene B4 (LTB_4) a leukocyte attractant was measured using LTB_4 Parameter Assay Kit (R&D Systems, Minneapolis, MN, USA). Dilutions of the samples were adjusted for the individual assays and kept consistent during the course of measurements. All ELISA read outs were performed in duplicates. Calculation of the standard curves was done in accordance to the manufacturers' information.

2.6 Cytometric bead array

Cytokines and chemokines were quantified by Cytometric Bead Array a flow cytometer-based application allowing the simultaneous analysis of several molecules at once in the pico to femto gram range. For the CBA measurements the supernatants supplemented with proteinase cOmplete inhibitor (Roche, Basel, Switzerland) were used to prevent enzymatic degradation of the molecules of interest. CF and COPD samples were diluted for the standard set (IL-1α, IL-1β and IL-8) 1:50 and 1:10 with PBS respectively. Enhanced sensitivity flex sets (IL-5, IL-6, IL-10, TNF-α and IFN-γ) and single plex (TGF-β1) sets were measured undiluted, healthy control samples were always measured undiluted. Calculation of the standard curves was done according to the manufacturers' guidelines.

2.7 Western blot

All reagents and instruments in this chapter were bought from Bio-Rad Laboratories GmbH, Feldkirchen, Germany except otherwise noted. For Western Blot analysis, 10 µg of protein were mixed 1:4 with 4x Laemmli sample buffer containing 2-Mercaptoethanol (Sigma-Aldrich, St. Louis, MO, USA) in a volume of 20 µL, boiled for 5 min at 95 °C (Thermomixer compact, Eppendorf AG, Hamburg, Germany) and centrifuged (Centrifuge 5418R, Eppendorf AG, Hamburg, Germany). Soluble fraction was loaded along with 5 µL Precision Plus Protein Standards into the wells of Any kD Mini-PROTEAN TGX Stain-Free Protein Gels. Gels were in vertical electrophoresis cells run at 50 V for 5 min afterwards voltage was increased to 150 V for 45 min using 1x Running buffer. Stain free gels were imaged for 1 s after 2.5 min activation using ChemiDoc MP. Gels were Blotted using Transfer Pack PVDF membranes and a Trans-Blot Turbo system for 45 min at 25 V. Gels were after the run imaged again first without further activation afterwards with additional activation to proof complete transfer of all proteins. Membranes were blocked for 1 h at ambient temperature on an orbital shaker (RS-OS 5, Phoenix Instrument, Garbsen, Germany) with Tris Buffered Saline buffer containing 0.1 % Tween20 and 5 % milk powder. Primary antibodies were diluted in 8 ml of blocking buffer at a dilution mentioned in Table 4 and incubated over night at 4 °C on an orbital shaker. Followed by 3 washes for 5 min each in blocking buffer, corresponding secondary antibodies mixed with 0.1 µl per mL StrepTactin-HRP Conjugate were added and membranes were incubated for 1 h at ambient temperature on an orbital shaker. After 3 more washes with blocking buffer, the membrane was developed using SuperSignal West Pico PLUS Chemiluminescent Substrate (Thermo Fisher Scientific, Waltham, MA, USA) for 15 min at ambient temperature on an orbital shaker in the dark. Chemiluminescence was recorded for 15 – 45 sec depending on the antibody used but kept consistent for all of the same kind. Band intensity was analyzed using Image Lab Software.

Table 4: Antibodies used for Western Blot experiments.

Antibody	Clone	Host	Supplier	Dilution
Anti-MMP9	5G3	Mouse	Abcam	1:1 000
Anti-ELANE	950317	Mouse	R&D systems	1:10 000
Anti-CTSG	12H15L69	Rabbit	Invitrogen	1:1 000
Anti-rabbit IgG, HRP-linked		Goat	CellSignaling	1:2 500
Anti-mouse IgG, HRP-linked		Donkey	R&D systems	1:25 000

2.8 Differential cell counts

200 µL PBS containing 30 000 cells were spun on SuperFrost Plus Adhesion slides (Thermo Fisher Scientific, Waltham, MA, USA) using a Cytospin 4 (Thermo Fisher Scientific, Waltham, MA, USA) for 5 min at 300 x *g*. Slides were air dried and stained for 3 min in May-Grünwald's eosin-methylene blue solution (Merck, Darmstadt, Germany) and 7 min in Giemsa's azure eosin methylene blue solution (Merck, Darmstadt, Germany). Afterwards they were fixed for 2 min with Xylene (Carl Roth GmbH + Co. KG, Karlsruhe, Germany). Dried slides were mounted with ROTI Histokitt (Carl Roth GmbH + Co. KG, Karlsruhe, Germany). Four times 100 cells from different areas were counted and the percentage of the different cell types were calculated from the mean of the quadruplicates.

2.9 Cell culture

The promyeloblast cell line HL-60 (ATCC CCL-240) (American Type Culture Collection, Manassas, VA, USA) were cultured in T-75 cell culture flasks (TPP Techno Plastic Products AG, Trasadingen, Switzerland) in RPMI 1640 (Gibco, Karlsruhe, Germany) media supplemented with 10 % (v/v) heat inactivated fetal bovine serum (Gibco, Karlsruhe, Germany) and 0.01 mg/mL Primocin (InvivoGen, San Diego, CA, USA). The media was changed three times a week, cells were passaged if they reached a certain density.

2.10 Clinical data

Different clinical parameters were taken from the database, these included, patient age, gender, body mass index (BMI), CFTR genotype, Pancreatic sufficiency status as well as lung function parameters like forced expiratory volume in one second percent predicted (FEV_1 % predicted) and status regarding clinical stability. Functional residual capacity was determined by body plethysmography percent predicted (FRC_{pleth} % predicted) according to European Respiratory society/ American Thoracic Society guidelines (Wanger et al. 2005; Miller et al. 2005) and calculated based on the equations proposed by the global lung initiative (Quanjer et al. 2012).

2.11 Microbiology

All microbiology related experiments were performed in close collaboration with Prof. Dr. Dalpke and Dr. Boutin of the Department of Infectious Diseases, Medical Microbiology and Hygiene, University of Heidelberg, Heidelberg, Germany according to published protocols (Boutin et al. 2015; Frey et al. 2021a).

2.11.1 Sample preparation

Specimens were conducted as previously described (Boutin et al. 2015). 50 µL of Propidium Monoazide (PM) dye (Biotium Inc., Hayward, CA, USA) was added to the 200 µL aliquot and incubated for 5 min in the dark. DNA from dead cells is crosslinked with PM and therefore subsequent amplification by PCR is prevented. Coupling of the PM with the DNA is achieved by exposure of the sample mixture to light (650 Watt, with 20 cm distance) on ice while shaking at 100 rpm for 5 min. Viable cells were pelleted by centrifugation at 5000 x *g* for 10 min. Supernatant fraction was removed and cell pellet was resuspended in 200 µL of sterile PBS. Resuspended cells were immediately frozen and stored at -20 °C until the DNA was extracted.

2.11.2 DNA extraction

After gentle thawing DNA extraction was performed with the QIAamp Mini Kit (QIAGEN, Hilden, Germany) according to the manufacturer's instruction. 200 µL of Buffer AL and protease solution (7.2 mAU) were added to the sample and vortexed for 15 sec. Followed by a 10 min incubation at 56 °C and purification as mentioned in the protocol of the Kit. 100 µL of AE buffer were added and incubated for 1 min, followed by a centrifugation step at 6000 x *g* for 1 min to elute the DNA from the column. As negative control steps were performed as mentioned without adding any clinical sample.

2.11.3 Quantitative polymerase chain reaction

To evaluate the bacterial biomass within the samples the 16S ribosomal RNA gene copy numbers were quantified by quantitative polymerase chain reaction (qPCR) using universal 16S primers (forward: 5′-TGG AGC ATG TGG TTT AAT TCG A-3′; reverse: 5′-TGC GGG ACT TAA CCC AAC A-3′). qPCR reactions were performed in 15 µL volumes of 1x Sybr-green master mix (Life technology, Darmstadt, Germany) containing 2 µL of DNA (or plasmid DNA standard) and 50 pM of each primer. Denaturation step was performed at 95 °C for 20 sec, followed by 40 amplification cycles (95 °C for 3 sec, 60 °C for 30 sec) and two final steps at 95 °C for 15 sec and 60 °C for 1 min with a subsequent melt curve. For quantification of the 16S number of copies, an in-house cloned plasmid DNA standard curve quantified by spectrophotometry, was used. All samples and controls were run in duplicates in a 7900HT Fast Real-time PCR system (Applied Biosystems, Foster City, CA, USA) (Nonnenmacher et al. 2004).

2.11.4 Next generation sequencing library preparation

Amplification of DNA was achieved using universal bacterial primers flanking the V6 region (v6L and v6R according to (Gloor et al. 2010)). Primers were tagged with individual barcodes to assign the sequences to the samples. PCR reactions were performed in 25 µL volumes consisting of 1x FastStart Master mix (Roche Diagnostics Deutschland GmbH, Mannheim, Germany), 2 µL of DNA and 50 pM of each primer. The thermal cycler (Primus 25, Peqlab Biotechnologie GmbH, Germany or FlexCycler², Analytik Jena AG, Germany) was set to 94 °C for 5 min for a first denaturation step, followed by 32 amplification cycles (94 °C for 45 sec, 52 °C for 1 min and 72 °C for 1 min 30 sec) and a final extension at 72 °C for 10 min. PCR products were evaluated by agarose gel (2 %) and concentrations were determined by intensity comparison to the standards analyzed in parallel. Purification of Amplicons was enforced using QIAquick PCR purification kit (QIAGEN, Hilden, Germany). Quality and quantity of the purified products was determined using a ND-1000 Nanodrop instrument (Nanodrop, Wilmington, USA) and Bioanalyser (Agilent Technologies Inc., Böblingen, Germany). An equimolar mix of all PCR products was sent to GATC biotech (Konstanz, Germany) for ligation of the sequencing adapters to the library and paired-end sequencing on an Illumina MiSeq sequencing system with 250 cycles.

2.11.5 Sequence analysis

Evaluation of raw fastq files was done with R package DADA2 (Callahan et al. 2016). Filtering and trimming were done according to the following criterion: no ambiguity, one error maximum allowed per read and truncation at the first instance of a quality score less than 2. Reads were merged to contigs and checked for chimera with the default parameters. The Silva database (version 132) was used to assign ASVs to taxonomy. ASV assigned to archaea, eukaryotes or chloroplast as well as ASV found in the negative control were removed from further analysis. For the cross-sectional study (3.1.1) 4,701,972 clean and non-chimeric reads were used. In total 1831 ASVs were found. All 22 ASVs found in the mock community are a perfect match of the sequences of the mock community. Between the 10 mock communities the mean weighted Unifrac distance is 0.07. In the pooled negative control 10 ASVs were found. Of those, only 4 belonging to the genera *Anaerococcus, Corynebacterium, Cutibacterium* and *Methylobacterium* that were also found in either the mock community or the samples. The ASV belonging to the genus *Cutibacterium* was expected in the mock community and reached a maximal relative abundance of 0.0015 in one sample. 12 samples were affected by potential contamination with relative abundances below 0.0005. Nevertheless, we decided to remove the 10 ASVs as potential contaminants from the analysis of the samples (Frey et al. 2021a). For the longitudinal study (3.1.2) 4,556,760 reads remained after filtering. In total 614 ASVs were identified. For each sample rarefaction curves were produces using the ‘rarecurve’ function in the r package vegan (v. 2.5-6) (Oksanen J et al.).

2.12 Secretomics

All proteomic experiments were conducted in close collaboration with the group of Prof. Dr. Klingmüller of the German Cancer Research Center (DKFZ).

2.12.1 Sample preparation

To perform the proteome analysis, stored samples were thawed at room temperature, centrifuged at 12 000 × *g* for 2 min at 4 °C and total protein concentration was assessed by the Protein A280 application using the DeNovix DS-11 spectrophotometer (DeNovix Inc., Wilmington, DE, USA). The single-pot, solid-phase-enhanced sample-preparation (SP3) protocol was carried out manually as previously described (Hughes et al. 2019). Briefly, 20 µg of total protein per sample was suspended in a total volume of 60 µL lysis buffer (5 % SDS, 50 mM tri-ethylammonium bicarbonate buffer [TEAB]). The disulfide bonds of proteins were reduced with 40 mM Tris(2-carboxyethyl) phosphine hydrochloride (TCEP) and alkylated with 160 mM chloroacetamide at 95 °C temperature for 5 min. Magnetic beads were prepared by combining 20 µL of both, Sera-Mag Speed Beads A and B (Fisher Scientific, Germany), washed, and re-suspend in 18 µL ddH2O for a final working concentration of 100 µg/µL. In total, 2 µL of pre-washed beads and 102 µL 100 % ethanol (EtOH) were added to each sample to reach a final concentration of 50 % EtOH. Samples were incubated for 15 min at room temperature and 1000 rpm to allow protein-beads binding. After incubation in a magnetic rack, the supernatant was removed, and beads were washed three times with 80 % EtOH. For tryptic protein digestion, beads were re-suspended in 75 µL of 50 mM TEAB containing trypsin, in an enzyme:protein ratio of 1:25, and incubated overnight at 37 °C and 1000 rpm. Beads were then immobilized on a magnetic rack, and the digested samples were dried down by vacuum centrifugation (1300 rpm. at 45 °C).

2.12.2 LC-MS/MS analysis and protein identification

The nano-flow LC-MS/MS analysis was performed by coupling an EASY-nLC 1200 (Thermo Scientific, Bremen, Germany) to an Orbitrap Exploris 480 MS (Thermo Scientific, Bremen, Germany). Samples were dissolved in 15 µl loading buffer (0.1 % formic acid, 2 % acetonitrile in High Performance Liquid Chromatography (HPLC) grade water) and 2.5 µL were injected for each analysis. Peptides were delivered to an analytical column (100 µm × 30 cm, packed in-house with Reprosil-Pur 120 C18-AQ, 1.9 µm resin, Dr. Maisch, Ammerbuch, Germany) at a flow rate of 3 µL/min in 100 % buffer a (0.1 % formic acid in HPLC grade water). After loading, peptides were separated using an 84 min gradient from 2 % to 98 % of solvent B (0.1 % FA, 80 % acetonitrile in HPLC grade water; solvent A: 0.1 % formic acid in HPLC grade water) at 350 nL/min flow rate. The Orbitrap Exploris 480 was operated in data-dependent mode, automatically switching between MS

and MS2. Full scan MS spectra were acquired in the Orbitrap at 60,000 resolution after accumulation to a target value of 3,000,000 (300 %). Tandem mass spectra were generated for up to 20 peptide precursors in the Orbitrap (isolation window 1.0 m/z) for fragmentation using higher-energy collisional dissociation at a normalized collision energy of 30 % and a resolution of 15,000 with a target value of 100,000 (100 %) charges after accumulation for a maximum of 22 ms. Raw MS spectra were processed by MaxQuant (version 1.6.3.3) for peak detection and quantification. MS/MS spectra were searched against the Uniprot human reference proteome database by Andromeda search engine enabling contaminant detection and the detection of reversed versions of all sequences with the following search parameters: Carbamidomethylation of cysteine residues as fixed modification and acetyl (Protein N-term), oxidation (M) as variable modifications. Trypsin/P was specified as the proteolytic enzyme with up to three missed cleavages allowed. The mass accuracy of the precursor ions was determined by the time-dependent recalibration algorithm of MaxQuant. The maximum false discovery rate for proteins and peptides was 0.01 and a minimum peptide length of eight amino acids was required.

2.12.3 Gene ontology enrichment and protein analysis

For the gene ontology (GO) enrichment analysis the online tool in combination with the protein analysis through evolutionary relationships (PANTHER) classification system was utilized (Carbon und Mungall 2018). The PANTHER analysis was bases on a Fisher exact test with a p-value < 0.05 regarding the false discovery rate. They are depicted as balloon plot ordered by their p-value, using R software (R version 3.6.1) and the package ggraph (version 2.04) (Pedersen 2020)

2.13 Statistics

2.13.1 Comparisons of individual parameters between groups and clusters

Statistical analysis to compare individual parameters between groups and clusters were performed with D'Agostino-Pearson omnibus test to check if data was normal distributed afterwards, one-way ANOVA with Tukey's post hoc test, Kruskal-Wallis ANOVA with Dunn's post hoc test, unpaired t-test with Brown-Forsythe test and Welch ANOVA test with Tamhane's T2 correction for multiple comparison when appropriate using R software (version 3.6.1 (R Core Team 2017)) and GraphPad Prism 8.0.1 (GraphPad Software, San Diego, CA, USA) if not stated otherwise.

2.13.2 Microbiological analysis – Cross-sectional study

Microbiota data and clinical parameters were correlated with a Spearman correlation adjusted for multiple comparison by the Benjamini-Hochberg (BH) correction. To correlate the relative abundance of all ASVs with the inflammation markers and clinical data the same procedure was applied. A group-wise comparison of between the microbial clusters

was performed with pairwise Wilcoxon rank sum Test adjusted for multiple comparisons BH correction. Statistical analysis was performed using R software (version 3.6.1. (Team 2017)) and the packages microbiome (Lahti et al. 2012-2017) and phyloseq (McMurdie und Holmes 2012). Important characteristics to describe the structure are the richness of a species, describing how many different species are found, the evenness describes how homogenous they are, whereas the dominance describes how distinct the presence of the most frequently identified species is (Shannon 1948). The Shannon index or α-diversity is calculated including the parameters before, the higher the value indicate the more divers is the microbiome structure (Shannon 1948).To assess the microbiome structure in detail, indices as α-diversity (Shannon index), dominance (relative abundance of the most dominant ASV) and richness (number of ASV observed) and were calculated. To investigate the difference between the samples based on Unifrac weighted distance (Lozupone und Knight 2005) the β-diversity was calculated. Based on s hierarchical clustering from a tree based on the weighted Unifrac distance matrix the individual microbiota profiles were clustered applying Ward's hierarchical agglomerative clustering method (Murtagh und Legendre 2014). The best possible number of clusters was assessed using Gap statistics applying the criterion proposed by Tibshirani et al. (Tibshirani et al. 2001).

2.13.3 Microbiological analysis – Longitudinal study

Statistical analysis were performed using R software (version 3.6.1 (R Core Team 2017)) and the packages vegan (version 2.5-6) (Oksanen J et al.), phangorn (version 2.5.5) (Schliep 2011), phytools package (Revell 2012), package phyloseq (version 1.28.0) (McMurdie und Holmes 2012), package lme4 (version 1.1-21) (Bates et al. 2015), lmerTest (version 3.1-1) (Kuznetsova et al. 2017), glmmTMB (version 1.0.2.1) (Brooks et al. 2017), package NBZIMM (version 1.0) (Xinyan Zhang und Nengjun Yi 2020), package psych (version 1.9.12.31) (Revelle W 2019), packages ggraph (version 2.04) (Pedersen 2020) and igraph (version 1.7.4.2) (Csardi G und Nepusz T 2006).Microbiome parameters as α-diversity (utilizing Hill numbers when q=0 and q=1), β-diversity (measured as weighted UniFrac distance between samples) and dominance (relative abundance of the most common ASV of a sample) were calculated to characterize the bacterial communities per sample. Differences of the microbiome composition between the patients were assessed by a PERMANOVA test. Linear mixed effect models (LMMs), zero-inflated Gaussian mixed effect models (ZIGMMs) or generalized linear mixed models (GLMMS) with a beta distribution, in accordance to the distribution of the parameter of interest were used to examine the relationship between time and each parameter of the microbiome, inflammation or clinical parameter assessed, as well as with the most abundant genera and phyla. A detailed assessment of the associations between the relative abundance of

the phyla and inflammatory as well as clinical parameters was performed by LMMs with a BH correction to control the false discovery rate. Relationships between microbiome indices, inflammatory markers and clinical parameters over time were examined in more detail by calculating Spearman rank correlation coefficients between: I) the slope (regression coefficients) of the variables per patients; II) the variability of the parameters, defined as the mean pairwise distance between all samples within a patients; III) the distance between time x (t_x) and the first stable time point (t_0) for several variables (t_x-t_0); and IV) the value of α-diversity and FEV_1 % predicted at t_0 with the slope of the parameters as well as with the stability of α- and β-diversity.

2.13.4 Microbiological analysis – CF/COPD/healthy comparison

The optimal number of clusters are based on clustering using kmeans method on the principal coordinate analysis (Morisita-horn index). The algorithm was performed for clusters ranging from 1 to 25 potential groups with 1000 permutations and optimal number of groups was calculated based on the Gap statistics and the first SEmax criteria (Figure S1) developed by Tibshirani et al. In 2001 (Tibshirani et al. 2001).

2.13.5 Secretomics

The MaxLFQ algorithm for label-free quantitation (LFQ) (Cox et al. 2014) implemented into MaxQuant was used and normalized intensities were obtained and used for the differential expression analysis. Statistical significance was assessed using the R limma package (moderated t-statistic) (Gordon et al. 2017) implemented in an in-house build MSpypeline for the analysis of proteomics data. Prior to groups comparison, it was determined whether a protein can be compared between two different groups and dynamic thresholds were stablished on the number of samples in given group. The acquired p-values (significance $p< 0.05$) were plotted against the log2 fold-change and depicted in volcano plots. Measured intensities of unique proteins are indicated at the sides of the volcano plot for each group.

3 Results

The result part of the thesis is split into two major parts. The first section investigates the association between inflammatory markers and dysbiosis of the airway microbiota in CF patients. This correlation was first examined in a cross-sectional study, which was then followed-up in a longitudinal study. The second section focuses on the development of an advanced method to quantify membrane associated NE activity for diagnostics and its applicability on samples of CF and COPD patient sputum samples in comparison to healthy controls.

3.1 Association of inflammatory markers with dysbiosis of airway microbiota and lung function in CF

To better characterize the still not fully understood interdependencies of airway infection, inflammation and lung function, the relationship between i) microbiome structure and cluster type, ii) pro-inflammatory cytokines (IL-1β, IL-6, IL-8 and TNF-α), iii) NE activity, iii) levels of anti-proteases (SLPI, NE/A1AT complex and TIMP1), iv) neutrophil counts in sputum, and v) lung function (forced expiratory volume in one second [FEV1], % predicted) in patients with CF, were investigated in this work. Therefore, a two-step approach, to evaluate spontaneous expectorated sputum of mostly stable CF patients, was chosen. In the first step a cross-sectional study of a representative cohort of CF patients was conducted to unveil the basic interdependencies. In the second step, the key findings were followed-up in a longitudinal study of a sub cohort to evaluate the relations on a time-resolved individual patient basis, during a one and/or 3-year observation period of iterative sampling. Since, most studies focused on changes in the microbiome during exacerbations (Cox et al. 2010; Boutin et al. 2017a; Cuthbertson et al. 2016; Fodor et al. 2012), this work aimed to provide a more detailed understanding of clinically stable CF patients by correlating more factors and by including a larger cohort.

3.1.1 Cross-sectional study

In the cross-sectional study, 106 CF patients, with a median age of 28 years (range 12-72) were enrolled to assess lung function, sputum microbiome and pro-inflammatory cytokines. 95 patients were pancreatic insufficient, 54 homozygous for F508del, 41 heterozygous for the F508del CFTR mutation and 38 % were female. Demographics and clinical characteristics are summarized in Table 5. PERMANOVA and two-way ANOVA tests were performed to assess the effect of antibiotic treatment regimes, CFTR modulator therapy as well as the impact of genotype and exacerbations concerning the microbial cluster, α- and β-diversity, inflammatory cytokines or lung function. With exception of the exacerbation status of the patients, which had a significant effect on the lung function and IL-8 (p-values=0.016), none of the parameters showed a significant impact (Table 6).

Table 5: Clinical characteristics of the cross-sectional study CF cohort. Adapted from Frey et al. 2021a.

Patients	n	106
Sex	n, females/males	40/66
Age (years)	median (range)	28 (12-72)
BMI (kg/m²)	median (range)	20.14 (14.88-30.69)
Clinical status		
stable	n (percent)	96 (90.6 %)
exacerbated	n (percent)	10 (9.4 %)
Pancreatic insufficiency	n (percent)	95 (89.6 %)
FEV_1 % predicted	median (range)	52.79 (17.41-110.9)
FRC_{pleth} % predicted *	median (range)	127.4 (71-297.3)
CFTR genotype		
F508del/F508del	n (percent)	54 (50.9 %)
F508del/other	n (percent)	41 (38.7 %)
other/other	n (percent)	11 (10.4 %)
CFTR modulator		
Ivacaftor/Lumacaftor	n (percent)	11 (10.4 %)
Tezacaftor/Ivacaftor	n (percent)	2 (1.9 %)
Ivacaftor	n (percent)	1 (0.9 %)

*FRC_{pleth} % predicted are only available from 76 of 106 patients

Table 6: Effect of antibiotic treatment, CFTR modulator therapy, genotype and exacerbations. Tested by two-way ANOVA and PERMANOVA.

		CFTR modulator	**genotype**	**exacerbation**
Cluster*	R^2 / p-value	0.021 / 0.058	0.012 / 0.817	0.011 / 0.329
α-diversity	F / p-value	0.003 / 0.958	0.517 / 0.672	1.080 / 0.301
FEV_1 % predicted	F / p-value	0.364 / 0.548	0.280 / 0.840	6.075 / 0.0155
IL-8	F / p-value	1.376 / 0.244	0.192 / 0.902	5.981 / 0.016
IL-6	F / p-value	0.179 / 0.673	0.570 / 0.636	0.29 / 0.591
IL-1β	F / p-value	0.417 / 0.520	0.260 / 0.854	0 / 0.997
TNF-α	F / p-value	0.599 / 0.441	0.913 / 0.438	1.104 / 0.296
Free NE	F / p-value	0.780 / 0.379	0.558 / 0.644	0.168 / 0.683
SLPI	F / p-value	0.009 / 0.924	0.611 / 0.609	0.703 / 0.404
NE/A1AT complex	F / p-value	2.374 / 0.127	0.782 / 0.507	0.243 / 0.624
Neutrophils %	F / p-value	0.143 / 0.706	0.348 / 0.791	0.028 / 0.868
Neutrophils absolute	F / p-value	3.012 / 0.087	0.454 / 0.715	3.841 / 0.054

*effect of microbiome cluster was tested by PERMANOVA

Investigation of the relationship between microbiota diversity, airway inflammation and lung function in CF sputum samples

Microbiome parameters, inflammatory markers and lung function were evaluated regarding their dependencies via Spearman correlation. Significant inverse correlations between α-diversity in sputum samples of CF patients and the pro-inflammatory cytokines IL-1β, IL-8 and TNF-α as well as free NE activity were found (Figure 8). The evenness and dominance of the microbiome showed significant correlations to inflammatory markers and NE activity, which was in contrast to the raw richness (Figure 8). Unexpectedly, a higher inflammation did not correlate to increased biomass (Figure 8). To investigate the composition of the microbiome, bacterial DNA sequences have been classified according their taxonomic level using Amplicon Sequence Variants (ASVs). This revealed that individual bacterial species could be corelated to inflammation. An elevated abundance of *P. aeruginosa* (ASV16) was related to elevated IL-8 levels, whereas the abundance of *Veillonella* sp. (ASV648) correlated with lower levels of NE activity and TNF-α.

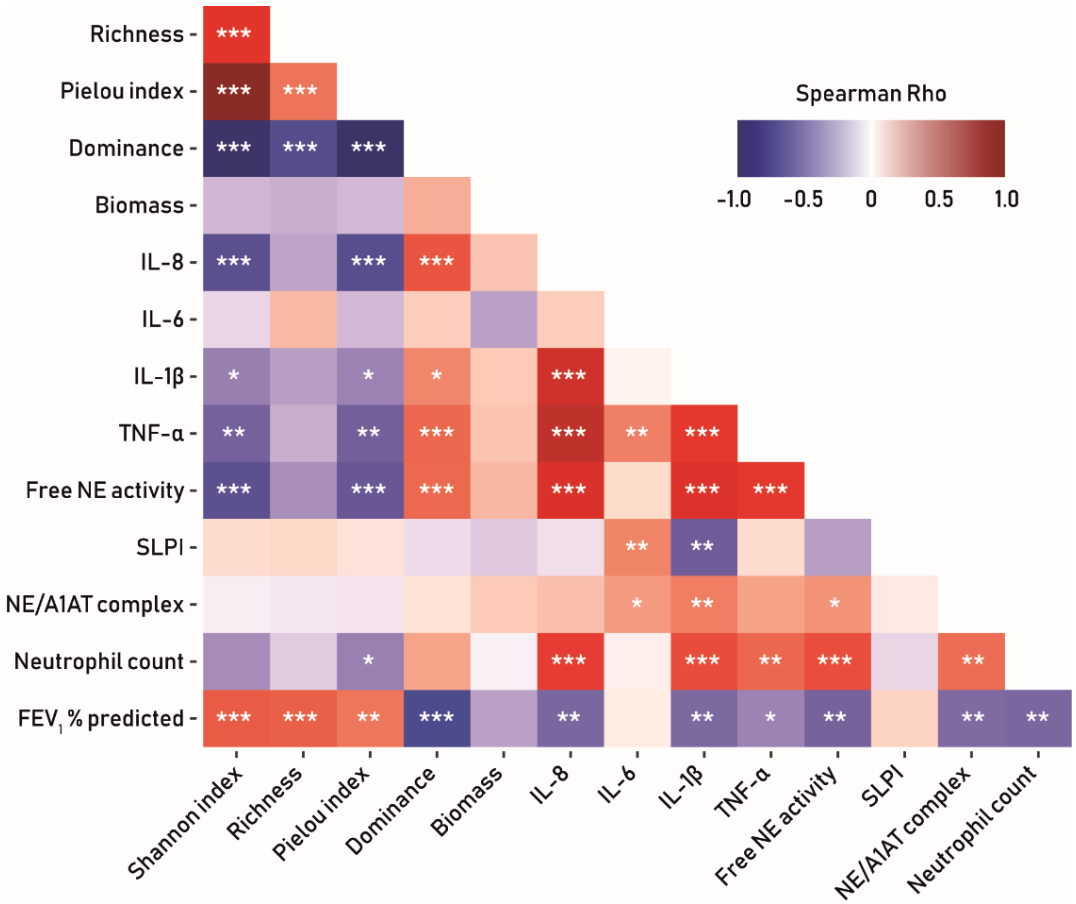

Figure 8: Correlation matrix of sputum microbiota parameters, inflammation markers and lung function of CF patients. Sputum microbiome parameters α-diversity (Shannon index), richness, evenness (Pielou index), dominance and biomass were correlated to quantitative measures of airway inflammation (IL-8, IL-6, IL-1β, TNF-α, free NE activity and endogenous anti-proteases [SLPI and NE/A1AT complex]) as well as the neutrophil count and the lung function (FEV_1 % predicted). All correlations were performed with a Spearman correlation, corrected for multiple comparison by Benjamini-Hochberg correction. P-values are indicated with asterisk as: *: p <0.05, **: p <0.01 and ***: p <0.001. Adapted from Frey et al. 2021a.

In addition, α-diversity was positively associated with FEV_1 % predicted (Figure 8). The abundance of *P. aeruginosa* (ASV16) (Rho=-0.35, p<0.05) correlated negatively with FEV_1 % predicted. In contrast, *Veillonella* sp. (ASV648) (Rho=0.35, p<0.05) were positively related to FEV_1 % predicted. Further, all inflammatory markers, including free NE activity but not IL-6, and the neutrophil percentage of the sputum samples was inversely correlated to FEV_1 % predicted (Figure 8). Thus, these data suggest that, microbiome diversity can be associated with lung inflammation and lung function in CF lung disease (Figure 8).

Clustering of CF sputum samples according to relative abundances

Besides the microbiome indices, a hierarchical clustering based on the weighted Unifrac distance, was performed to better characterize the structure of the microbiome in sputum samples. Seven clusters were found in the highly heterogenic cohort (Figure 9A). The first and largest cluster was characterized by a diverse microbiome structure that has been previously (Muhlebach et al. 2018b; Dickson et al. 2015) described as “healthy” oropharynx-like flora (OF), rich in aerobic commensals, especially of the genera *Neisseria* and *Streptococci*, and in anaerobe commensals, especially of the genera *Veillonella* and *Prevotella* (Figure 9B). The following three cluster were highly dominated by typical CF pathogens such as *P. aeruginosa* (Psae, n=42), *Achromobacter* sp. (Achro, n=5) and *Staphylococcus* sp. (Staph; n=4). The remaining hierarchical clusters (HC5-7) contained only one or two samples and were due to power limitations, excluded from the subsequential analysis. Taken together, these data show a clear separation of the different cluster on the PCoA, of which the first two axis could explain more than 50 % of the spread between the samples. The OF and pathogen dominated clusters (Psae, Achro and Staph) were separated along axis 1. Axis 2 clearly separated Staph form the other clusters, whereas the Achro cluster was separated from the Psae cluster along axis 3.

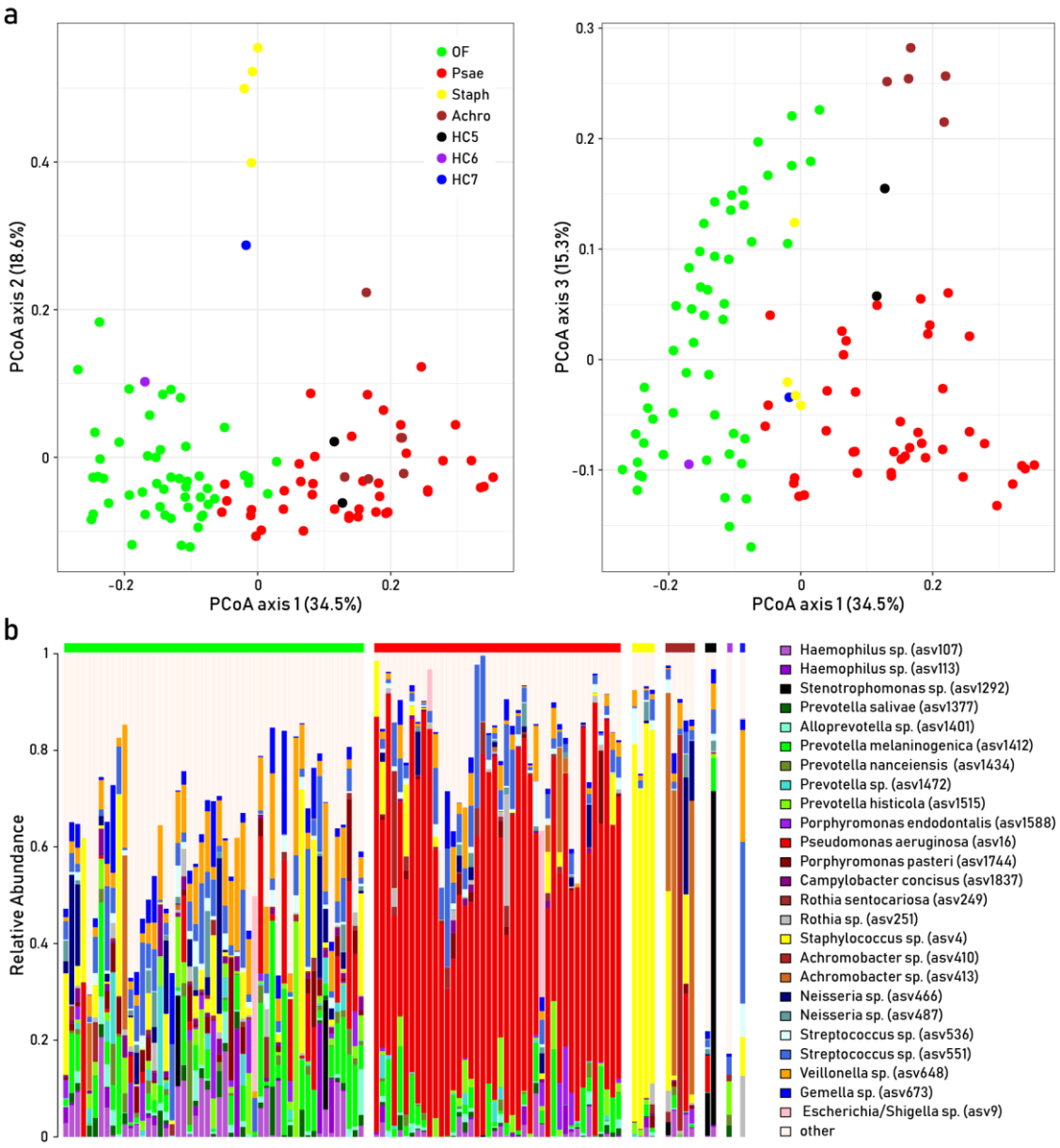

Figure 9: Clustering of CF patient sputum microbiota based on their inter-individual variability. A) The upper panel shows a principal coordinate analysis (PCoA) based on a Unifrac weighted distance matrix. On the left axis 1 and 2, whereas on the right axis 1 and 3 of the PCoA are depicted. The clusters were defined on the same distance matrix using hierarchical clustering. **B)** Abundance of the 25 most common ASVs are shown, the 106 patients are classified in their respective clusters (shown by colored bars at the top). Adapted from Frey et al. 2021a

Microbial clusters reflect different status of inflammation and lung function of CF patients

To identify similarities and differences among the four largest clusters revealed by the PCoA, they were further characterized with regard to the microbiome indices as α-diversity and biomass, inflammatory parameters and lung function in the next step. In comparison to the clusters Psae, Staph and Achro, the OF cluster showed a strongly increased α-diversity due to the dominance of either *P. aeruginosa, Staphylococcus* sp. or *Achromobacter* sp. in the other clusters (Figure 10A). The Psae cluster showed

significantly elevated biomass, measured as number of 16S gene copies per µl of sputum, compared to the other clusters, which was not the case for the Staph and Achro cluster (Figure 10B). The inflammatory cytokines IL-8, IL-1β and TNF-α were significantly increased in samples of the Psae cluster compared to the OF cluster, which displayed the lowest levels of all clusters (Figure 10C-E). Free NE activity was significantly increased in samples of the Psae and Staph cluster (Figure 10F). OF cluster patients exhibited a significant increased FEV_1 % predicted in comparison to those grouped in to the Psae cluster (Figure 10G).

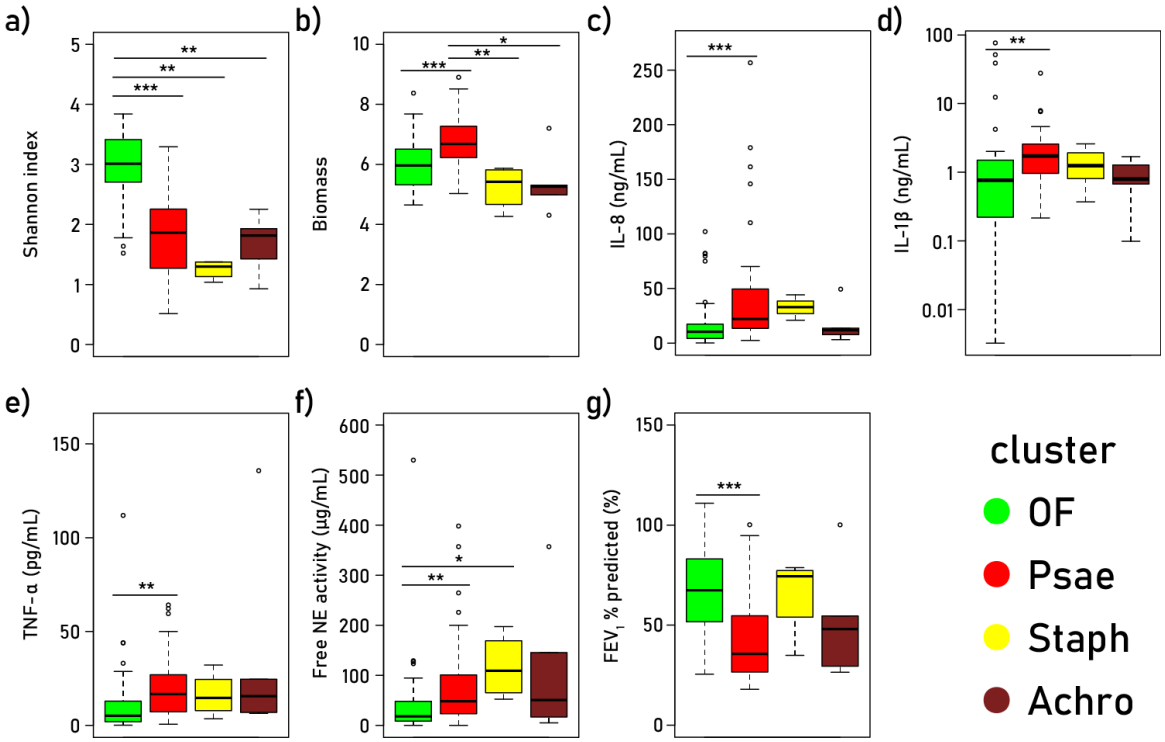

Figure 10: Box plots of most relevant parameters of microbiome diversity, inflammatory markers and lung function. The 4 most abundant microbiota clusters were compared for the different parameters, applying a pairwise Wilcoxon test corrected for multiple comparison by Holm correction. **A)** α-diversity, **B)** biomass, **C)** IL-8, **D)** IL-1β (log scale), **E)** TNF-α, **F)** free NE activity and **G)** FEV_1 % predicted. P-values are indicated with asterisk as: *: p <0.05, **: p <0.01 and ***: p <0.001, ○: outliers. Adapted from Frey et al. 2021a.

In summary, α-diversity declined with the increasing dominance of a specific pathogen, independent of the species. In contrast, the biomass was only elevated in the Psae cluster. Inflammatory parameters tended to be elevated in pathogen dominated clusters, and were associated with a decline in FEV_1 % predicted, with exception of the Achro cluster. However, the here conducted cross-sectional study has limitations since the revealed different clusters regarding the microbiome structure as well as inflammatory markers cannot show the exact time course of these factors in individual patients and only speculation can be made about their relation. Thus, to answer the hypothesis if this association can be shown on an individual patient level, a longitudinal follow-up study was conducted.

3.1.2 Longitudinal study

Since only presumptions could be made about the exact temporal course of inflammatory markers, microbiome structure and lung function in individual patients a sub-cohort of the cross-sectional study was used to elaborate more details regarding the disease progression on an individual patient basis. This follow-up longitudinal study consisted of 27 patients and was split in two sub-analyses, one comprised of patients with at least 3 visits during a one-year interval called short-term (n=18) and a second one which lasted for a period of ≥ 3 years with at least one visit/year/patient termed long-term (n=19). The distribution of the cohort into two sub-studies allowed to identify driving factors during a short-term and long-term observation period. Further, the variability as well as the difference to the baseline of the evaluated parameters was examined. The cohort characteristics of the two sub-studies are listed in Table 7 and Table 8. The distribution of the visits over time is illustrated in Figure 11.

Table 7: Clinical characteristics of CF patients of the longitudinal study.

		Short-term	**Long-term**
Number of subjects	*n*	18	19
Number of visits	*n* (mean)	62[#] (3.44)	96[#] (5.05)
Age (years)*	Median (range)	29 (18-61)	23 (18-72)
Sex	*n*, females/males	4/14	5/14
BMI (kg/m²)*	Median (range)	21.52 (15.41-30.32)	20.16 (17.27-28.02)
FEV_1 % predicted*	Median (range)	50.99 (17.49-89.67)	48.81 (17.41-108.9)
CFTR genotype			
F508del/F508del	*n* (percentage)	10 (55 %)	7 (37 %)
F508del/other	*n* (percentage)	5 (28 %)	9 (47 %)
Other/other	*n* (percentage)	3 (17 %)	3 (16 %)
Pancreatic insufficiency	*n* (percentage)	16 (89 %)	17 (89 %)
Patients receiving IV treatment	n (percentage)	6 (33 %)	8 (42 %)

* at baseline visit; [#] 35 visits are shared

Investigation of the microbiome composition of sputum samples of CF patients

Investigation of the microbiome using ASVs revealed that most common phyla within all samples, independent of the study-arm, were the Bacteroidetes, Firmicutes and Proteobacteria, which in sum represented 89 % of all reads. On the genus level, *Pseudomonas* was dominated followed by *Veillonella*, *Prevotella*_7, *Staphylococcus*, *Streptococcus* and *Haemophilus*, with more than 5 % each. The 10 most frequent ASV covered more than half of the reads. Of those, *Rothia*, *Prevotella*_7, *Streptococcus* and *Veillonella* were the most common and had a high prevalence and low abundance whereas

Pseudomonas was the most abundant genera was present in only 58 % of the samples. The microbiotas structure of two consecutive samples of the same patients were more similar (67 % similarity) to each other than samples from two different patients.

Table 8: Pancreatic status and CFTR genotypes of CF patients of the longitudinal study.

Pancreatic insufficient		Pancreatic sufficient	
***CFTR* genotype**	**subjects (n)**	***CFTR* genotype**	**subjects (n)**
F508del / F508del	11	1717-1G>A / R764X	1
F508del / 1811+17T>G	1	G542X / X	1
F508del / 3905insT	1	I336K / c.3964-7A>G	1
F508del / 711+ 3A>G	1		
F508del / c.3468+2dupT	1		
F508del / CFTRdel17 (2.5Kb)	1		
F508del / E403D	1		
F508del / G551D	1		
F508del / I507del	1		
F508del / Q220X	1		
F508del / R347P	1		
F508del / T1299I	1		
F508del / W1282X	1		
174delA / R347P	1		

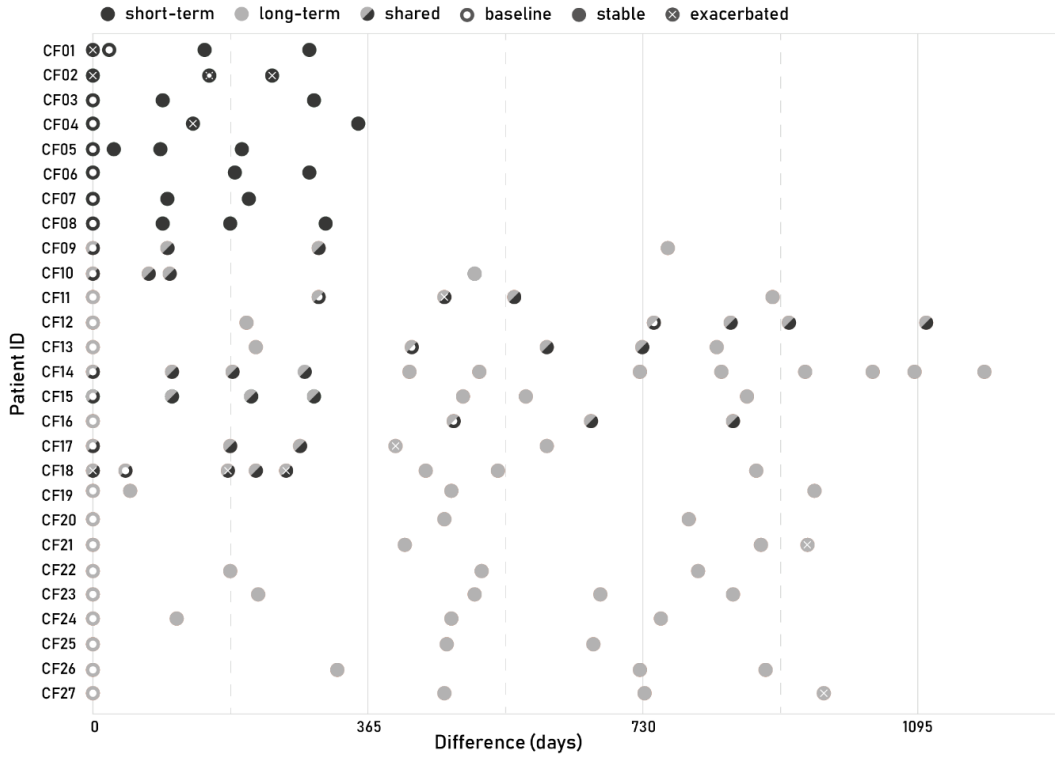

Figure 11: Distribution of visits for each patient. Visits are color-coded according to the study arm they were assigned to, black: short-term, light grey: long-term. Baseline visits are indicated with a white dot, stable visits are solid dots and exacerbated visits are indicated with a white X. If several factors are true, they are plotted over each other.

Relationship between changes in microbiota diversity, airway inflammation and lung function over time in CF sputum samples

The relationship with time of the individual factors regarding diversity, lung function and inflammation were evaluated first utilizing a linear mixed effect model. Within the short-term study, α-diversity significantly declined with time, for Hill numbers q=1 and q=0. The diversity order q of the Hill numbers regulates the sensitivity of the measures to the relative abundances of the species (Hsieh et al. 2016). For samples with an α-diversity of order q=1, diversity in effective species number is calculated by Shannon diversity, by raising the abundances to 1 (Shannon 1948). In the context of q=0 all species are assigned a 0 regarding the abundance, thus, the diversity is equivalent to species richness, which is the case for highly diverse microbiomes (Shannon 1948). In contrast, dominance and β-diversity showed the opposite effect and temporally increased significantly, see Table 9. In both sub-studies, biomass did not correlate with time.

Meanwhile, in both longitudinal sub-studies significant correlation over time were only found with α-diversity when q=0. Further, biomass did not correlate with time in both sub-studies. The FEV_1 % predicted decreased significantly with time in the long-term data. Inflammatory parameters and anti-proteases showed the most significant correlations in the long-term study with an increase of IL-1β and NE and decreasing levels SLPI and TIMP1 over time. Further, the protein amount, NE/A1AT complex and TNF-α showed a positive trend. Whereas in the short-time analysis TNF-α was the only inflammatory parameter reaching significance. Regarding parameters of the microbiome a significant decline in Firmicutes, Bacteroidetes and Fusobacteria as well as an increase in Proteobacteria was observed in the short-term. Which is reflected on the genera level by significant increase in relative abundance of *Pseudomonas* whereas genera as *Alloprevotella*, *Veillonella* and *Streptococcus* diminished. In the long-term neither on level of the phyla nor the genera significant correlation with time were found. Taken together, these data show a significant linear change in several diversity indices in the short-term caused by a decrease in commensals together with an increase in Proteobacteria abundance. In contrast, inflammatory parameters are more variable in the short-term but show continuously change in the long therm.

Table 9: Overview of relationships of all factors of the longitudinal study with time using a linear mixed model. Effect size, standard error and p-value are given for all factors included. Significant correlations are highlighted in bold. The effect sizes (relative abundance) of the taxonomic factors are given per month instead of days.

	Short-Term		Long-Term	
Factor	Effect Size (Standard Error)	p-value	Effect Size (Standard Error)	p-value
Diversity				
α-diversity (q=0)	**-0.076 (0.021)**	**0.001**	**-0.03 (0.006)**	**<0.001**
α-diversity (q=1)	**-0.002 (0.0005)**	**<0.001**	-0.0003 (0.002)	0.127
β-diversity	**0.002 (0.0007)**	**0.012**	-0.00002 (0.0002)	0.936
Dominance	**0.003 (0.0007)**	**<0.001**	0.0001 (0.0002)	0.659
Biomass	0.0006 (0.002)	0.769	0.00006 (0.0005)	0.919
Clinical Parameters				
FEV_1 % predicted	-0.005 (0.006)	0.480	**-0.008 (0.002)**	**<0.001**
Inflammation				
Protein content°	0.002 (0.002)	0.240	0.005 (0.003)	0.056
IL-1β*	-0.0001 (0.002)	0.941	**0.002 (0.0004)**	**<0.001**
IL-6*	0.002 (0.001)	0.088	-0.0006 (0.0003)	0.132
IL-8°	0.0003 (0.001)	0.822	0.003 (0.003)	0.108
NE/A1AT complex*	-0.0007 (0.001)	0.525	**-0.0008 (0.0003)**	**0.004**
Free NE°	-0.002 (0.003)	0.638	**0.001 (0.0004)**	**0.011**
SLPI*	-0.002 (0.001)	0.092	**-0.002 (0.0004)**	**<0.001**
TIMP1°	-0.11 (0.08)	0.163	**-0.005 (0.0009)**	**<0.001**
TNF-α°	**0.003 (0.001)**	**0.017**	0.0007 (0.0004)	0.053
Phyla				
Proteobacteria	**0.087 (0.026)**	**0.004**	0.02 (0.009)	0.100
Bacteroidetes	**-0.043 (0.02)**	**0.047**	-0.017 (0.007)	0.081
Firmicutes	**-0.057 (0.02)**	**0.041**	0.003 (0.007)	0.734
Actinobacteria	-0.052 (0.032)	0.127	-0.002 (0.008)	0.799
Fusobacteria	**-0.007 (0.003)**	**0.026**	-0.002 (0.0009)	0.100
Tenericutes	-0.0006 (0.0006)	0.350	-0.0005 (0.0005)	0.465
Genera				
Pseudomonas	**0.017 (0.005)**	**0.013**	0.002 (0.002)	0.406
Prevotella_7	-0.002 (0.004)	0.809	-0.017 (0.008)	0.406
Veillonella	**-0.003 (0.0009)**	**0.013**	-0.011 (0.008)	0.406
Streptococcus	**-0.002 (0.001)**	**0.048**	0.017 (0.009)	0.406
Haemophilus	-0.003 (0.005)	0.751	0.002 (0.002)	0.520
Staphylococcus	-0.00009 (0.004)	0.980	0.001 (0.001)	0.419
Prevotella	-0.005 (0.003)	0.390	-0.012 (0.008)	0.406
Neisseria	-0.006 (0.005)	0.553	-0.0007 (0.001)	0.721
Rothia	-0.001 (0.001)	0.553	-0.003 (0.008)	0.730
Porphyromonas	-0.003 (0.003)	0.556	-0.001 (0.001)	0.406
Alloprevotella	**-0.007 (0.002)**	**0.043**	-0.001 (0.0009)	0.406
Gemella	0.0002 (0.003)	0.980	-0.0003 (0.0008)	0.730
Stenotrophomonas	0.0004 (0.003)	0.980	-0.0006 (0.0005)	0.406

* log transformed data; ° cube root transformed data

Other factors did only show temporal dependencies in either long- or short-term studies. In the short-term analysis, TNF-α was the only inflammatory parameter that positively correlated to time. Regarding the microbiome a significant decline in Firmicutes, Bacteroidetes and Fusobacteria as well as an increase in Proteobacteria was observed. On the genera level this is reflected by a significant increase in relative abundance of *Pseudomonas* whereas genera as *Alloprevotella*, *Veillonella* and *Streptococcus* diminished. In the long-term study positive time correlations were seen for inflammatory parameters such as IL-1β and NE whereas for anti-proteases such as SLPI, TIMP1 and NE/A1AT complex and FEV_1 % negative correlation predicted a was observed. Concerning the microbiome, neither on level of the phyla nor the genera significant correlation with time were found. Taken together, the time resolved dependencies of the microbiome were more profound in the short-term study, whereas inflammatory markers and lung function were more profound in the long-term study.

Relationship between changes in phyla abundance and clinical & inflammation parameters over time in CF sputum samples

Next, the microbiome phyla were correlated either with inflammation markers or lung function. In the short-term analysis, no significant correlation was found. In contrast, in the long-term study microbiomes rich in commensals such as Bacteroidetes negatively correlated with the amount of protein, the inflammatory markers IL-1β and TNF-α but positively to FEV_1 % predicted. Contrarily, microbiomes with a high abundance of specific pathogens such as Proteobacteria showed a positive correlation to IL-1β, IL-8, and TNF-α and a negative to FEV_1 % predicted. Other pathogens such as Tenericutes were only positively linked to IL-6 whereas for others (Firmicutes, Fusobacteria and Actinobacteria) no significant relation to individual parameters could be observed (Table 10). Thus, a relation between a change in phyla to inflammatory markers and lung function could only be detected in the long-term study.

Table 10: Summary of p-values of the correlations of the most common phyla to clinical and inflammatory measures.

	Variable	Proteo-bacteria	Bactero-idetes	Firmi-cutes	Actino-bacteria	Fuso-bacteria	Teneri-cutes
Short-Term	FEV_1 % predicted	0.232 (-)	0.578 (+)	0.370 (+)	0.284 (+)	0.284 (+)	0.232 (+)
	BMI	0.912 (-)	0.912 (+)	0.912 (-)	0.912 (+)	0.912 (-)	0.912 (+)
	Protein content	0.073 (+)	0.135 (-)	0.595 (-)	0.135 (-)	0.923 (-)	0.923 (+)
	IL-1β	0.255 (+)	0.173 (-)	0.898 (+)	0.446 (-)	0.898 (-)	0.898 (-)
	IL-6	0.861 (-)	0.666 (+)	0.666 (-)	0.861 (+)	0.666 (+)	0.666 (+)
	IL-8	0.139 (+)	0.353 (-)	0.405 (-)	0.353 (-)	0.680 (-)	0.754 (-)
	NE/A1AT complex	0.855 (+)	0.855 (-)	0.855 (+)	0.855 (-)	0.855 (+)	0.855 (-)
	Free NE	0.096 (+)	0.239 (-)	0.239 (-)	0.209 (-)	0.854 (-)	0.423 (-)
	SLPI	0.919 (-)	0.451 (+)	0.451 (-)	0.653 (+)	0.653 (+)	0.451 (+)
	TIMP1	0.946 (+)	0.946 (-)	0.946 (+)	0.946 (-)	0.946 (+)	0.946 (+)
	TNF-α	0.096 (+)	0.096 (-)	0.767 (-)	0.767 (-)	0.529 (-)	0.962 (-)

Long-Term	FEV_1 % predicted	**0.044 (-)**	**0.021 (+)**	0.965 (+)	0.213 (+)	0.330 (+)	0.330 (-)
	BMI	0.606 (-)	0.746 (+)	0.872 (+)	0.606 (+)	0.748 (+)	0.748 (+)
	Protein content	0.080 (+)	**0.046 (-)**	0.438 (+)	0.438 (-)	0.199 (-)	0.438 (-)
	IL-1β	**0.012 (+)**	**0.005 (-)**	0.863 (+)	0.202 (-)	0.287 (-)	0.862 (-)
	IL-6	0.781 (+)	0.781 (+)	0.171 (-)	0.781 (-)	0.781 (+)	**<0.001 (+)**
	IL-8	**0.006 (+)**	0.196 (-)	0.663 (-)	0.378 (-)	0.689 (-)	0.689 (-)
	NE/A1AT complex	0.961 (-)	0.837 (-)	0.837 (+)	0.837 (-)	0.837 (+)	0.837 (+)
	Free NE	0.219 (+)	0.053 (-)	0.720 (+)	0.533 (-)	0.229 (-)	0.922 (+)
	SLPI	0.368 (-)	0.281 (+)	0.368 (-)	0.368 (+)	0.510 (+)	0.735 (+)
	TIMP1	0.973 (-)	0.973 (-)	0.973 (+)	0.973 (+)	0.973 (+)	0.973 (+)
	TNF-α	**<0.001 (+)**	**<0.001 (-)**	0.401 (-)	0.388 (-)	0.076 (-)	0.388 (+)

Relationship between slopes of the microbiome with lung function and inflammation in CF sputum samples

To associate all three parameters to each other, their slops were correlated in the succeeding step. In the short-term study, the slope of dominance and α-diversity was inversely associated (Figure 12). Thus, for patients with a decline in α-diversity individual pathogens become more pronounced. Further, the slope of protein content, IL-1β and IL-8 were positively correlated amongst each other. Significant links between the slopes of microbiome parameters, inflammatory markers, anti-proteases or clinical parameters were not found. In the long-term data, the negative link between the slope of α-diversity and dominance was confirmed. In addition, the slope of the dominance of individual microbes was positively linked to a decline in FEV_1 % predicted, and the slope of the biomass was inversely associated with the slope of the BMI. In summary, patients which acquired a pathogen of the Proteobacteria phylum, showed a decreased α-diversity caused by a diminished abundance of commensals this led to a more rapid decline in lung function, in the long term.

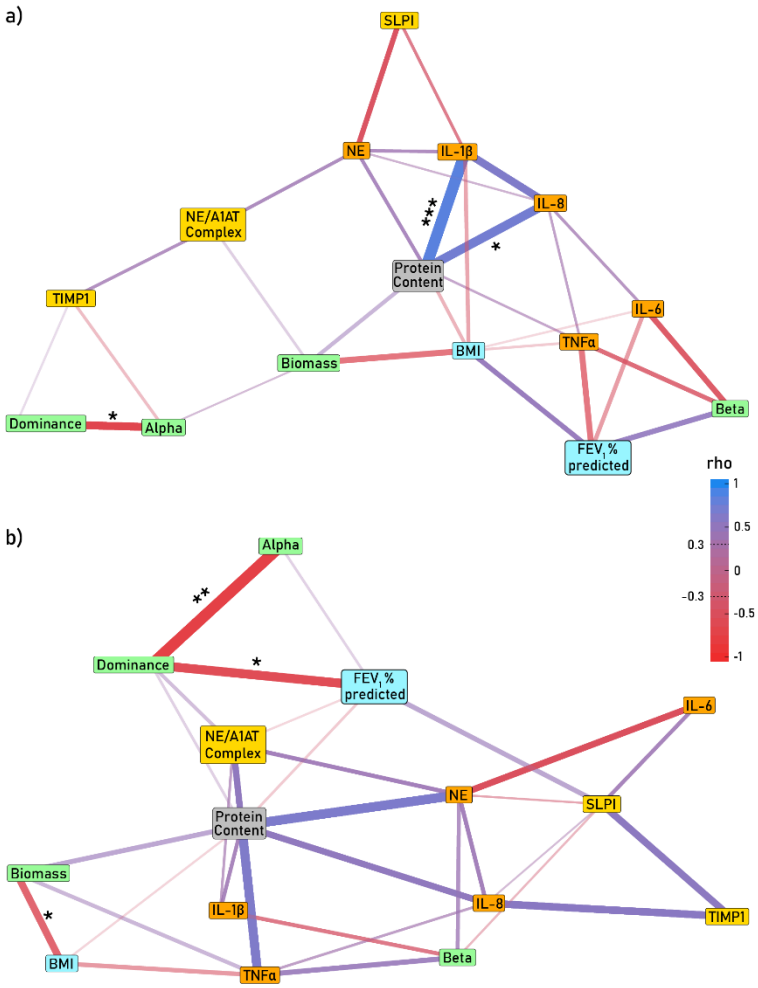

Figure 12: Network of the rates of change between parameters of the microbiome, pro-inflammatory factors, anti-proteases, clinical parameters and general factors. Links of the short-term and long-term are given in **A** and **B** respectively. Nodes of parameters which belong together are given in the same color. The strength of the correlations (rho) is indicated by the width of the connections and the direction by color. Only correlation with a coefficient <0.3 or >0.3 are shown. Significant correlations are indicated with asterisks according to their p-value: *: p <0.05, **: p <0.01 and ***: p <0.001.

Relationship between t_x-t_0 distances and between intra-patient variability of the microbiome with lung function and inflammation in CF sputum samples

The influence of the baseline condition was assessed, by relating the different time points (t_x) to baseline time point 0 (t_0). Strong positive associations were found between dominance and β-diversity as well as among TNF-α and IL-8, which are part of a cluster of significant correlations between several inflammatory markers. Besides, TNF-α correlated significantly with IL-6 and IL-8. Further, IL-8 correlated with NE as well as IL-1β (Figure 13), which was in accordance to the relationship of the variability (Figure 14). Further, of the clinical parameters, BMI was associated to FEV_1 % predicted and α-diversity to the distance between t_x and t_0 of TIMP1 which was the only significant negative correlation within the short-term analysis. This was also the case for the variability network (Figure 14) and further the only significant link of factors from different groups. In the short-term, no association with time were found. In contrast, in the long-term data

differences of TIMP1 were significantly but weakly correlated with time. Overall, there were more and stronger associations found in the long-term, besides the factors are in closer proximity to each other indicating a higher interdependency. The densest cluster was found among dominance, β-diversity, IL-8 and TNF-α which were all significantly interconnected, those factors also show significant associations regarding their variability (Figure 14). IL-8 and TNF-α were further associated to IL-1β. BMI and α-diversity were weak but significantly associated with IL-6 as well as among each other. Further, BMI was inversely correlated with biomass. Strong positive associations were found between TIMP1 and SLPI, which was further significant related to β-diversity and IL-6. Additionally, an association was found between FEV_1 % predicted and the β-diversity. Of note, free NE and NE/A1AT complex clustered apart from the other factors.

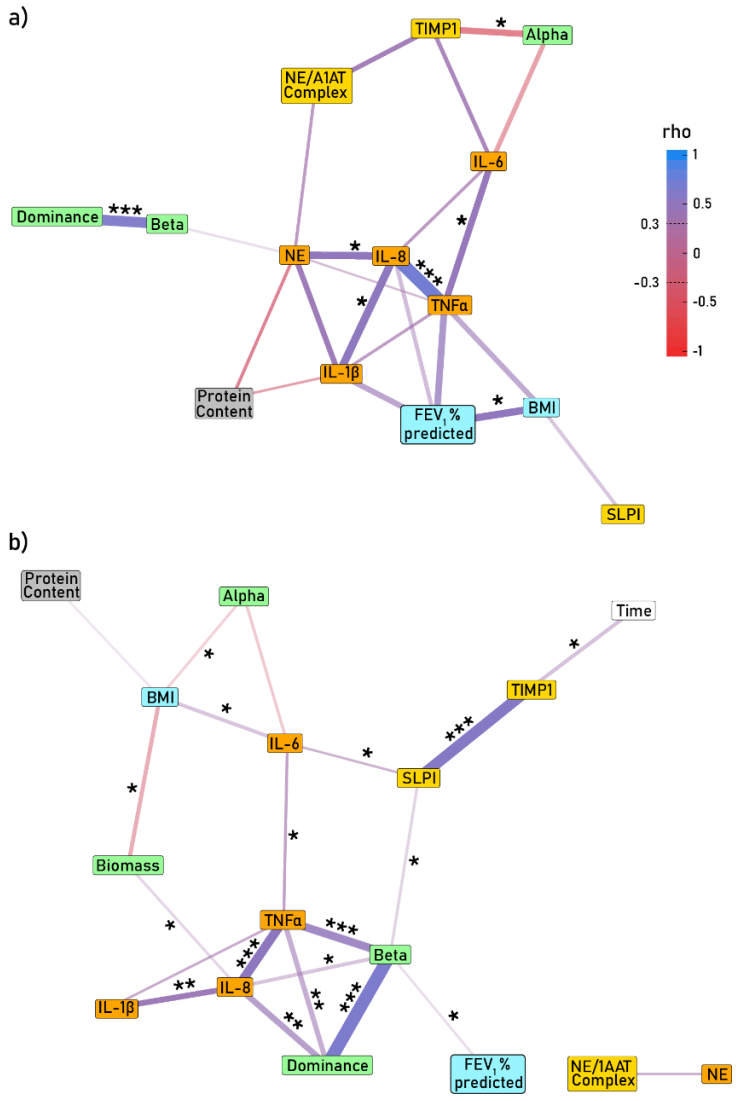

Figure 13: Network of the distance between t_x and t_0 of the samples between parameters of the microbiome, pro-inflammatory factors, anti-proteases, clinical parameters and general factors. Correlations of the short-term and long-term are given in **A** and **B** respectively. Nodes of parameters which belong together are given in the same color. The strength of the correlations (rho) is indicated by the width of the connections and the direction by color. Only correlation with a coefficient <0.3 or >0.3 are shown. P-values of significant correlations are indicated as asterisks: *: p <0.05, **: p <0.01 and ***: p <0.001.

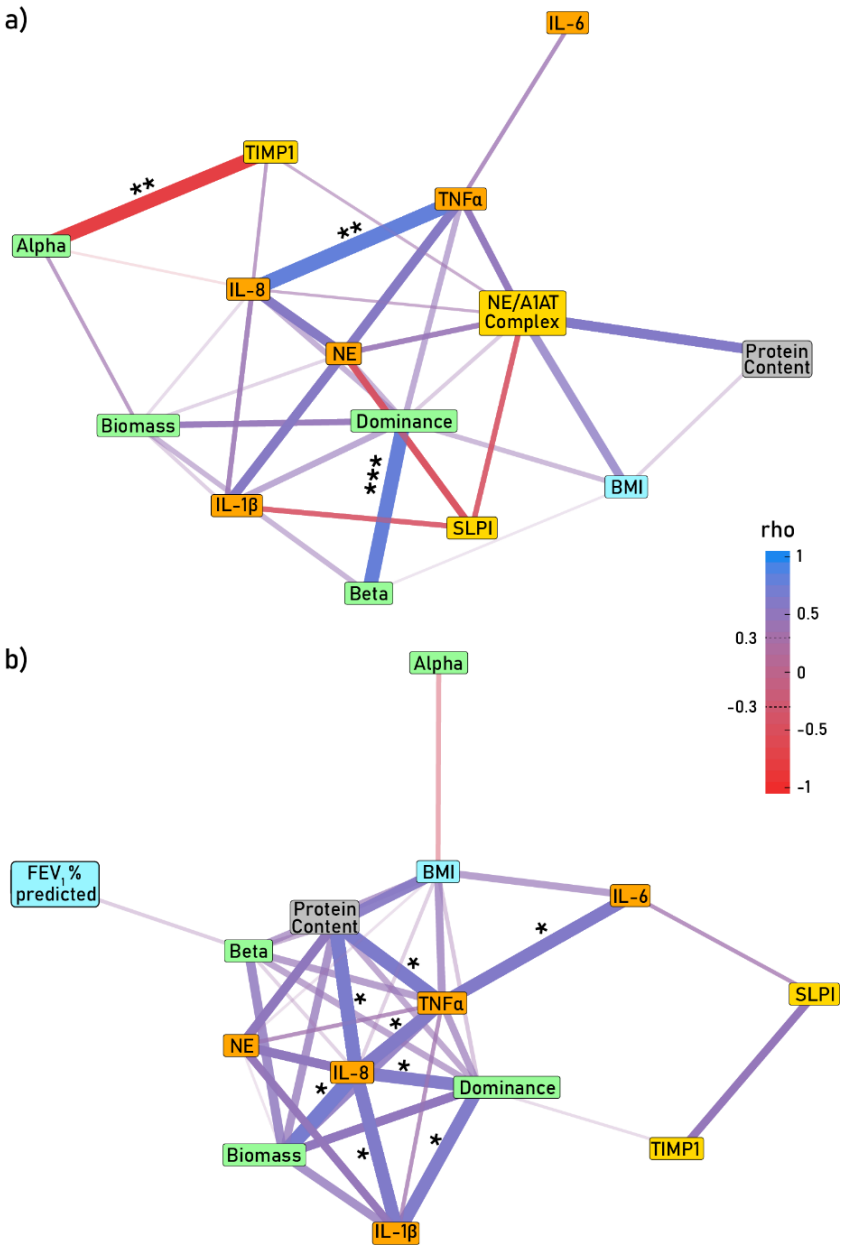

Figure 14: Network of the relationship of the variability between parameters of the microbiome, pro-inflammatory factors, anti-proteases, clinical parameters and general factors. Links of the short-term and long-term are given in A and B respectively. The strength of the correlations (rho) is indicated by the width of the connections and the direction by color. Correlation with a coefficient <0.3 or >0.3 are shown. Significant correlations are indicated with asterisks for their p-value: *: p <0.05, **: p <0.01 and ***: p <0.001.

Relationship with initial condition between the microbiome with lung function and inflammation in CF sputum samples

The initial time point of the α-diversity was linked to the decline of α-diversity over time within the short-term analysis (Figure 15a). Nevertheless, no association was found to β-diversity and dominance with initial α-diversity. However, dominance was linked to the initial FEV_1 % predicted. In contrast, within the long-term study the initial FEV_1 % predicted were not linked to parameters of the microbiome (Figure 15b). Further, the association of initial α-diversity and slope of α-diversity over time could not be observed, even though the stability of the α-diversity was linked to the initial α-diversity.

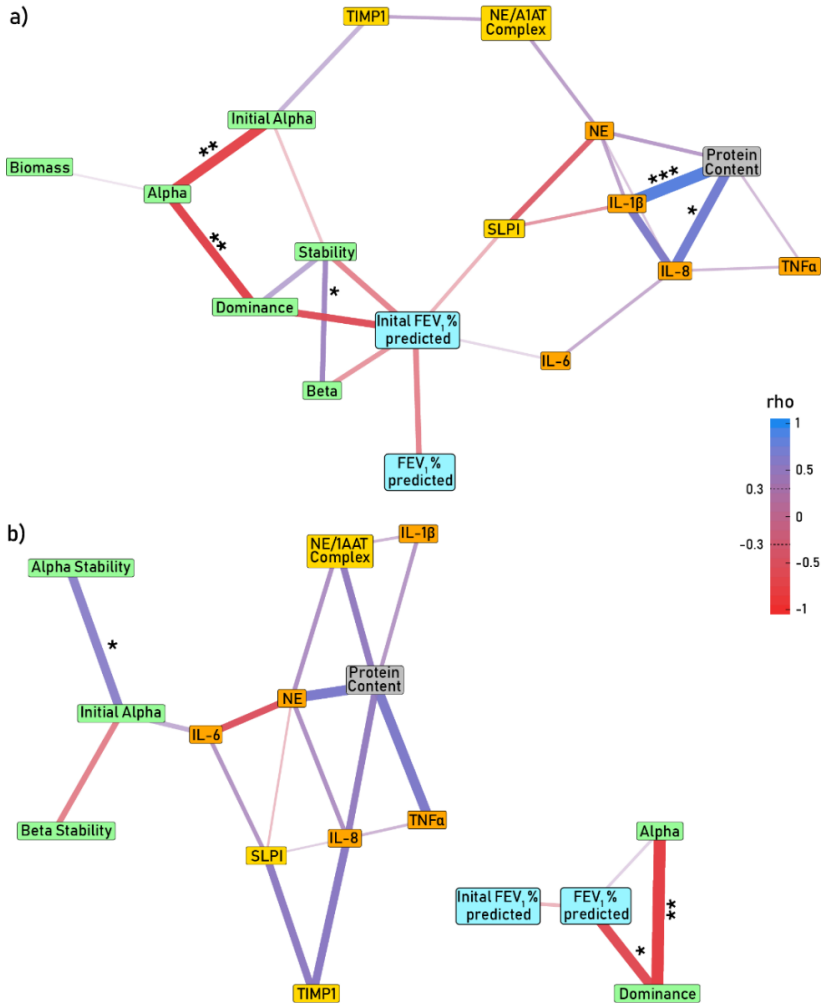

Figure 15: Network of the relationship of the rate of change over time including initial conditions between parameters of the microbiome, pro-inflammatory factors, anti-proteases, clinical parameters and general factors. Links of the short-term and long-term are given in **A** and **B** respectively. The strength of the correlations (rho) is indicated by the width of the connections and the direction by color. Correlation with a coefficient <0.3 or >0.3 are shown. Significant correlations are indicated with asterisks for their p-value: *: p <0.05, **: p <0.01 and ***: p <0.001.

Investigation of effects of exacerbation and antibiotic use on changes in microbiota diversity, airway inflammation and lung function over time in CF sputum samples

Lastly, the effect of antibiotic treatment as well as exacerbations on the other parameters was evaluated. A significant contribution of antibiotic treatment to levels of protein content (LMM: Effect=1.91, p=0.035), free NE activity (LMM: Effect=1.64, p=0.009) and NE/A1AT complex (LMM: Effect=1.18, p=0.007), as well as a significant negative effect of exacerbations on NE activity (LMM: Effect=-1.80, p=0.026) within the short-term study was found. In the long-term study, the relative abundance of *Neisseria* was significantly impacted by exacerbations (ZIGMM: Effect=0.280, p=0.026). Further, levels of NE/A1AT complex (LMM: Effect=1.91, p<0.001) and protein content (LMM: Effect=1.61, p=0.024) were affected by antibiotic treatment regimes. Taken together, antibiotic treatment regimens had a significant impact on NE/A1AT complex and protein content in both sub-studies, whereas exacerbation interferes with different parameters.

3.2 Assay refinement to measure membrane associated NE

Increased secretion of NE in airways is a major hallmark for the onset and progression of structural lung damage and decline in lung-function of patients suffering from CF (Sly et al. 2009; Sly et al. 2013; Sagel et al. 2012; Chalmers et al. 2017). Accordingly, quantification of NE activity in sputum is a promising biomarker of airway inflammation in CF (Sly et al. 2013; Mayer-Hamblett et al. 2007; McKelvey et al. 2019). Until recently, most studies quantified free NE activity which can be monitored as soon as the endogenous anti-proteases shield can no longer cope with the tremendous amounts of released NE (McKelvey et al. 2019). However, recent studies suggest that long before free NE activity becomes detectable, membrane associated NE activity is present on CF sputum neutrophils from early childhood (Montgomery et al. 2017; Balázs und Mall 2019). For the quantification of free NE activity multiple assay systems are available (Sly et al. 2009; Sly et al. 2013; Chalmers et al. 2017; Korkmaz et al. 2008a; McElvaney et al. 2018), but membrane bound NE can only be assessed directly with confocal microscopy (Gehrig et al. 2012; Dittrich et al. 2018). However, confocal microscopy is not well suited to evaluate large numbers of cells or for sequential sampling. Thus, an assay suitable for diagnostic laboratories is desperately needed, wherefore a highly flexible flow cytometry-based approach was developed within this work.

3.2.1 Characterization of the NEmo-2 variants

To allow large scale NEmo probe synthesis, its manufacturing was transferred to industry recently. To increase the coupling efficiency of fluorophores to the reporter backbone, two different slight off target modifications were introduced to gain NEmo-2E and NEmo-2G reporters, respectively. To exclude changes in specificity and target selectivity of NEmo variants, introduced by the off target modification, NEmo-2 probe variants were characterized. Therefore, NEmo-2 cleavage was assessed by addition of known NE concentrations via plate reader experiments. As NEmo-2, is designed to integrate into cell membranes, HL-60 cells that do not express intrinsic NE, were used as carrier. The profiles of the two NEmo-2 versions were mostly comparable, with a slight shift of the NEmo-2G version, which tended to have a steeper slope of D/A ration increase (Figure 16a). To evaluate the reporter performance on target samples, they were tested in context of sputum samples via confocal microscopy. These experiments showed a diminished sensitivity regarding NEmo-2G. Representative images of neutrophils isolated from the same patient that were analyzed with NEmo-2E and NEmo-2G in parallel are shown in Figure 16b. Taken together, NEmo-2G showed a slightly better performance regarding the evaluation via plate reader experiments. However, NEmo-2E showed a higher resolution on patient derived neutrophils and was, therefore, used for subsequent experiments.

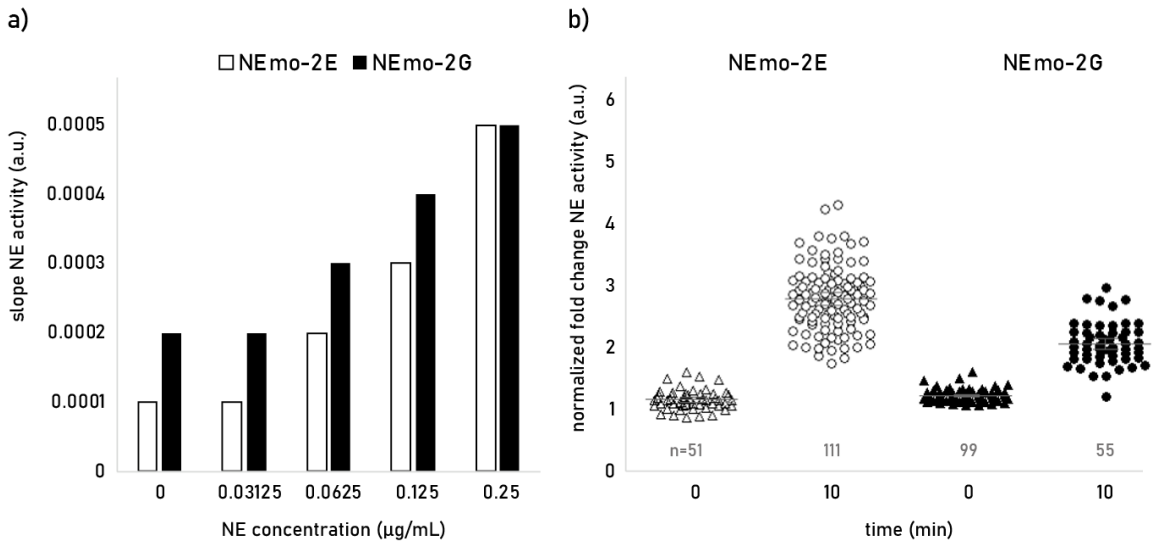

Figure 16: Characterization of NEmo-2 variants. A) Via plate reader experiments using HL-60 cells and known NE concentrations and **B)** via confocal microscopy using primary patient neutrophils natively releasing NE. Results for NEmo-2E are shown in white and for NEmo-2G in black. Mean and standard error of the mean are indicated in grey.

3.2.2 Change in technology, transferring the assay from microscopy to flow cytometry

In the next step the readout of the selected NEmo-2E probe was transferred from confocal microscopy to flow cytometry, as it is available in most diagnostic laboratories, has a higher dynamic range, is more robust, faster and belongs rather to standard laboratory equipment than confocal microscopy.

Design of a specific antibody panel for flow cytometry to gate viable neutrophils

Since sputum samples contain a mixed cell population, viable neutrophils had to be identified by selective gating. Therefore, a panel of multiple fluorochrome-conjugated antibodies was designed that consisted of anti-CD14 (monocytes), anti-CD16 (neutrophils), anti-CD45 (leukocytes) and anti-CD66d (granulocytes) (Table 1) and neutrophils were gated as 7-AAD$^-$/CD45$^+$/CD14$^-$/CD16$^+$ and CD66b$^+$ events. Additionally, a staining for CD63, a phenotypic marker for primary granule exocytosis, was included in the panel. To prevent spectral overlap, only two of the three available laser lines (red and blue) were used for the detection of the antibodies and the live/dead marker. The third, violet laser line was utilized for the FRET reporter exclusively, to prevent bleed through from or to the channels used for the anti-body panel. Control plots of the donor and acceptor channel acquired at 450/50 nm and 585/42 nm respectively and excited with the violet laser are shown in Figure 17. Fluorescence minus one (FMO) controls (Figure 18) were performed for all antibodies as well as the live dead marker 7-AAD to ensure specific binding.

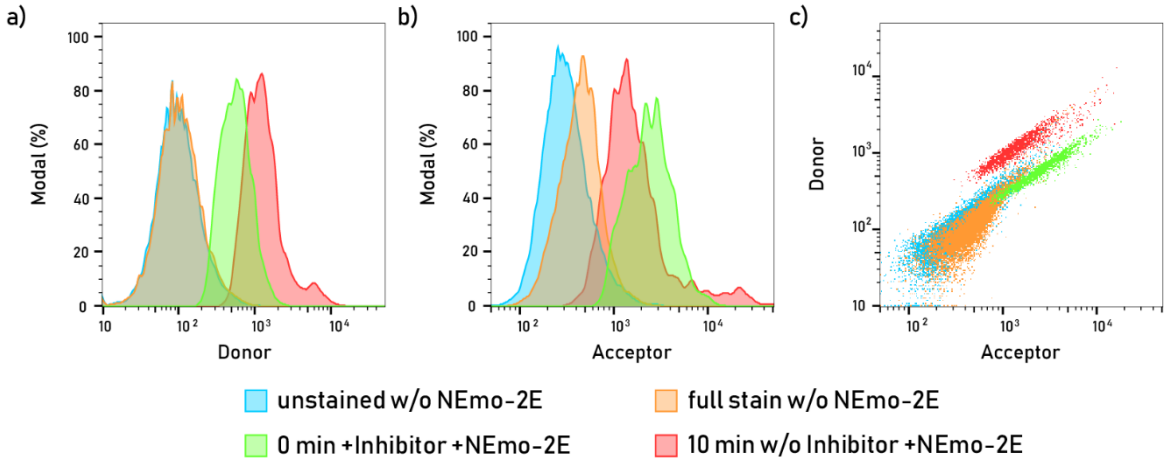

Figure 17: Control plots of donor and acceptor MFI intensities. A) Donor intensity histograms, MFI shown as % modal. **B)** Acceptor intensity histograms, MFI depicted as % modal. **C)** Donor and acceptor MFIs plotted against each other. Each dot represents a cell.

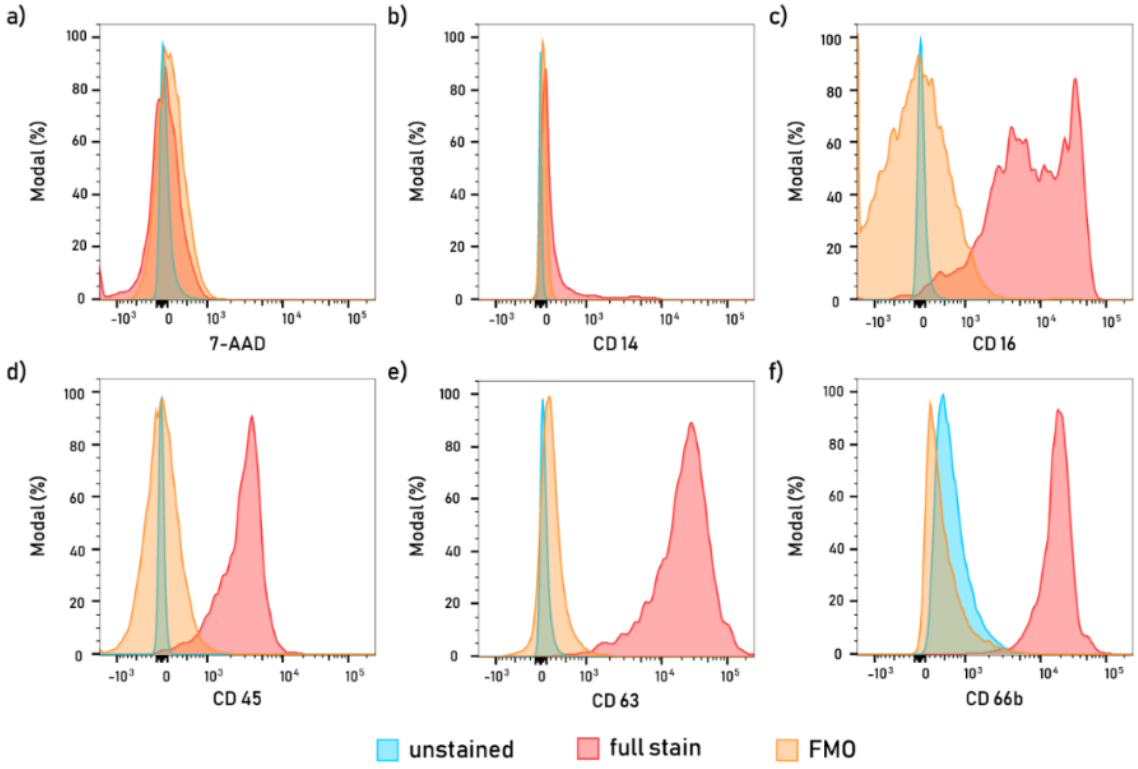

Figure 18: Fluorescence minus one staining's for the antibody panel used for neutrophil gating. FMOs of a representative CF patient are given. All histograms are shown in modal share (%) of the gated events. **A)** 7-AAD; **B)** CD14; **C)** CD16; **D)** CD45; **E)** CD63 and **F)** CD66b.

Comparison of membrane associated NE activity analysis of sputum samples of CF patients and healthy controls by flow cytometry and confocal microscopy.

As proof of concept, the confocal microscopy and flow cytometry-based techniques were compared by applying both setups to neutrophils isolated from sputum of 12 CF patients and 5 healthy controls. Analyses were based on single cell measurements and data were reported as mean of all cells analyzed from the same individual. Representative images

of cells analyzed by microscopy are shown in Figure 19a, representative histograms of the analysis via flow cytometry are depicted in Figure 19b. By measuring the D/A ratio over time using flow cytometry (Figure 19c), a rapid increase was observed over the first 10 min, before ratios reached a plateau. To ensure that membrane associated NE activity measurements detect the maximum change in D/A ratios, analyzes were based on the 10 min time point and normalized to the 0 min time point of the negative control (with inhibitor). A strong correlation between membrane associated NE activity quantified by confocal microscopy or flow cytometry was observed (Figure 19d). Besides, FEV_1 % predicted of patients with CF correlated with the membrane associated NE activity measured by flow cytometry (Figure 19e), which was not observed for membrane associated NE activity quantified by confocal microscopy. This observation can be explained, by the increased dynamic range and higher number of analyzed cells with the flow cytometry-based method, which results in a decreased variability within a sputum sample of a specific patient. This becomes particularly obvious with regard to the observed spread of healthy controls (Figure 19f-g).

Relationship between neutrophil activation and membrane associated NE activity in sputum samples of CF patients and healthy controls

To investigate associations of neutrophil activation and membrane associated NE activity, neutrophil surface markers including CD16, CD63 and CD66b were measured. CD16, also known as low affinity immunoglobulin gamma Fc region receptor III, a marker for mature granulocytes involved in degranulation (Cossarizza et al. 2019). The CD16 expression decreases during the lifespan of a neutrophil (Makam et al. 2009). Accordingly, $CD16^{low}$ neutrophils are activated, non-functional and apoptotic (Moulding et al. 1999). Assessment of CD16 expression revealed an inverse correlation to the normalized fold change (Figure 20a). Further, the level of CD16 expression of CF patient derived neutrophils, of an extended cohort, was significantly lower compared to neutrophils of healthy controls (Figure 20b). Thus, the more NE is released by the neutrophils, the more prone they are to apoptosis.

CD63 and CD66b are both markers for neutrophilic granule release. While, CD66b, is a marker for secondary granule release (Ingersoll et al. 2015), CD63 is a marker for exocytosis of primary granules, in which NE is stored (Ingersoll et al. 2015), and is besides part of the tetraspanin family (Naegelen et al. 2015). Levels of CD66b were comparable among the CF patients and healthy controls (Figure 20c). MFI mean values of CD63 were significantly lower in healthy controls compared to CF patients (Figure 20d). This suggests, that release of primary granules and apoptosis is increased in CF derived sputum neutrophils, whereas level of secondary granule release are comparable to the healthy controls.

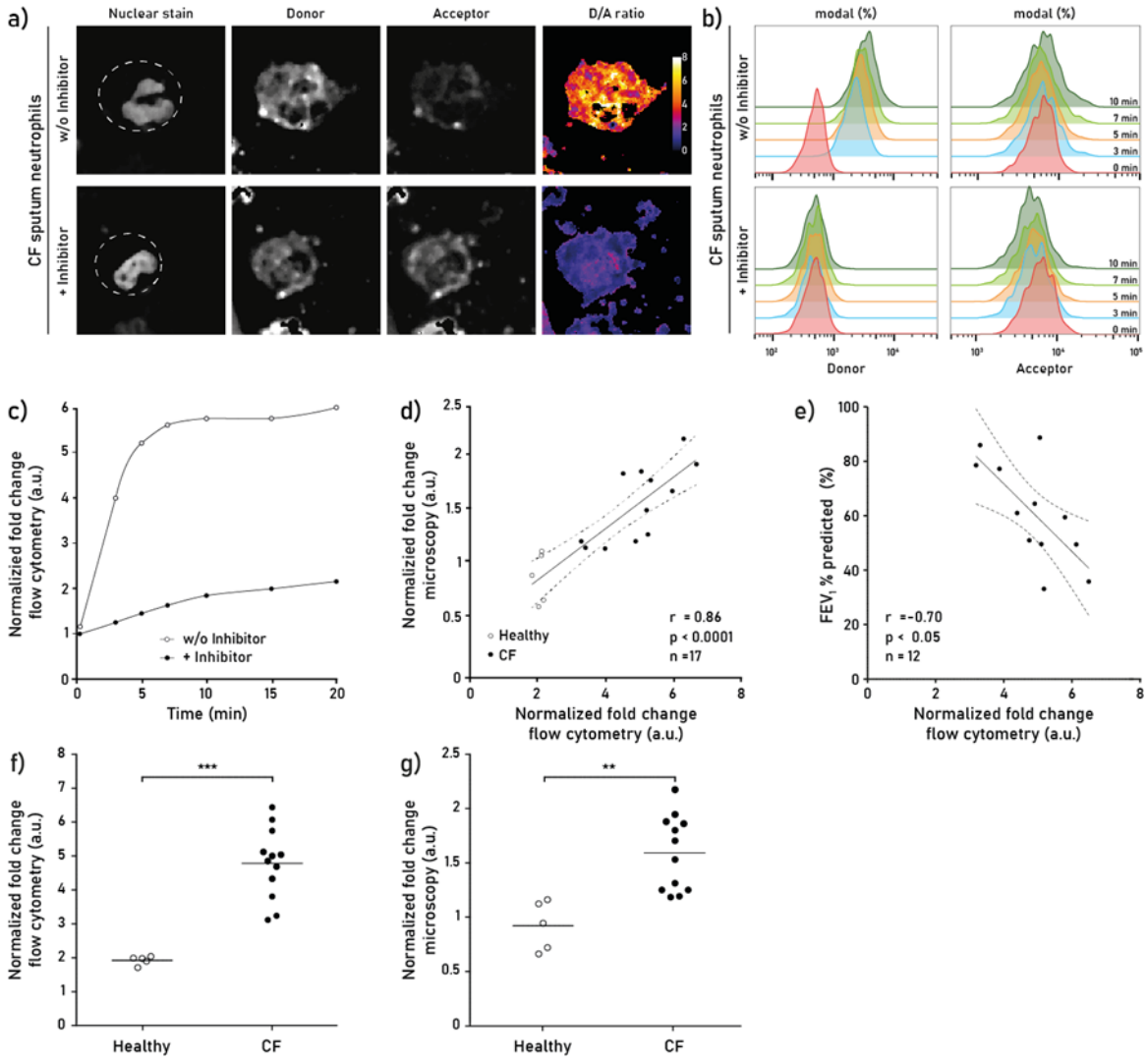

Figure 19: Quantification of membrane associated NE activity using FRET reporter NEmo-2E by flow cytometry in comparison to quantification by confocal microscopy. A) Representative images of CF sputum neutrophils show nuclear staining (DRAQ5) as well as donor and acceptor intensities after 10 min of incubation with NEmo-2E with (+) and without (w/o) the specific NE inhibitor sivelestat. Analyzed region of interest is indicated with a dashed line. **B)** Mean fluorescent intensities (MFI) of NEmo-2E measured in presence an absence of sivelestat and PI inhibitor cocktail by flow cytometry on ~1000 CF sputum neutrophils at different time points, indicated by color. **C)** Calculated donor/acceptor (D/A) ratio over a period of 20 min. MFI were derived from ~1000 CF sputum neutrophils in presence (●) and absence (○) of inhibitor by flow cytometry. D/A ratios were normalized to the 0 min time point with inhibitor (negative control). **D)** Correlation between the measurements performed by microscopy versus flow cytometry after 10 min on sputum neutrophils of 12 CF patients (●) and 5 healthy controls (○). **E)** Correlation between the membrane associated NE activity measured with flow cytometry and the FEV_1 % predicted of 12 CF patients. Correlation analyses were performed using the Spearman rank order method. **F-G)** Comparison of normalized fold change measured by flow cytometry (**F**) and confocal microscopy (**G**) of 5 healthy controls (○) and 12 CF patients (●). Mean and significance level of unpaired nonparametric t-test are given: **: p <0.01 and ***: p <0.001 Panels

A-E, adapted from Hagner et al. 2020.

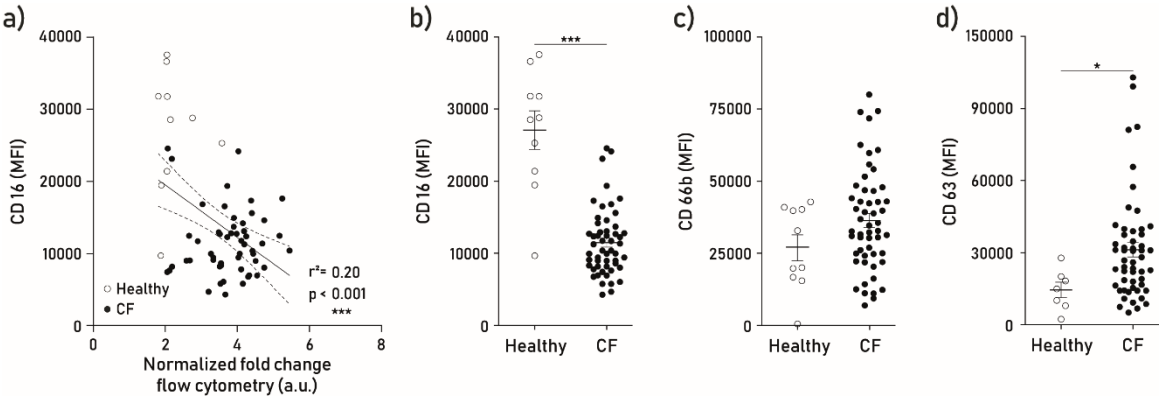

Figure 20: Correlation of the surface marker CD16 with normalized fold change measured by flow cytometry as well as MFIs of different surface markers. A) Correlation of CD16 expression, which is a marker for neutrophil degranulation, and normalized fold change of the NE activity at the flow cytometer for a cohort of CF patients (n=53) and healthy controls (n=10). Expression levels of specific neutrophil surface markers: **B)** CD16 of CF patients (n=53) and healthy controls (n=10), **C)** CD66b of CF patients (n=53) and healthy controls (n=10) and **D)** CD63 of CF patients (n=53) and healthy controls (n=7). Streaks show mean, error bars indicate standard error of the mean. Stars depict the significance level of unpaired nonparametric t-test, given as: *: p <0.05 and ***: p <0.001.

Effects of priming and activation of naïve neutrophils on surface markers and NE release in blood samples of healthy controls

The effects of priming and activation of naïve neutrophils on surface markers and NE release was investigated, by stimulation of primary blood neutrophils of a healthy control, in a sub-study. Therefore, blood was withdrawn, neutrophils were isolated and primed with cytochalasin B for 5 min and afterwards triggered with N-formyl-methionyl-leucyl-phenylalanine (fMLP) for 30 min at 37 °C to release the granular contend as previously published (Saeki et al. 2001). Stimulated neutrophils showed a dose- and time-depended increase of CD66b and decrease of CD16 minutes after stimulation together with an increase in the D/A ratio (Figure 21). These results indicate, that an increase in membrane associated NE activity is accompanied by an increase or decrease of known activation markers, which further supports the validity of the flow cytometer-based technique. The possibility to measure NE activity and expression of phenotypic markers in parallel, allows a multi parameter assessment in one single experiment.

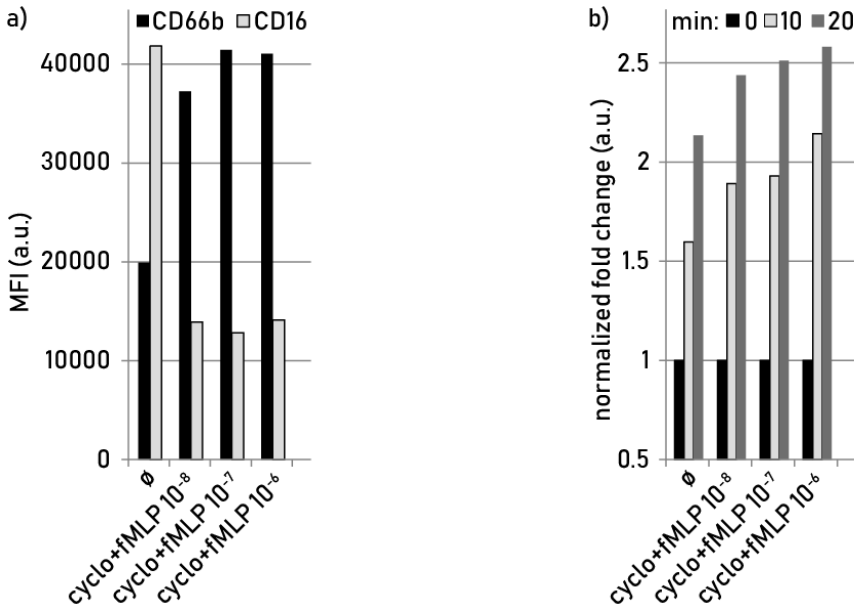

Figure 21: Surface markers and membrane associated NE activity of stimulated blood neutrophils. Cells were primed with 5 µg/mL cytochalasin B for 5 min and subsequently stimulated with the indicated molar concentration of fMLP for 30 min. **A)** MFIs of surface markers CD66b and CD16 of gated neutrophils measured immediately after stimulation and **B)** membrane associated NE activity of the same cells measured in parallel to the cell surface markers, immediately after reporter addition (0 min) aa well as after 10 and 20 min.

3.2.3 Evaluation of NEmo-2E specificity by flow cytometry

To prove target specificity of NEmo-2E, the NE inhibitors sivelestat, A1AT, SLPI and elafin and the protease inhibitor (PI), a cocktail of inhibitors targeting various serine, cysteine and matrix metalloproteinases (Roche Diagnostics 2020) were added to the sm FRET flow assay on neutrophils isolated from CF patient sputum.

Samples from the same patient were supplemented with either a specific inhibitor, at previously described concentrations (Campbell et al. 2000) or the inhibitor cocktail in (Figure 22). The most efficient inhibition was reached with sivelestat (0.427 mM) alone, followed by sivelestat in combination with PI. Of the endogenous anti-proteases, elafin at the high concentration (1.55 µM) showed the most efficient inhibition of the endogenous anti-proteases, followed by the high concentration of A1AT (5.08 µM). PI alone (7.5-fold concentration of the recommended final concentration (Roche Diagnostics 2020)) and the low concentrated A1AT (0.5 µM) only achieved a slight inhibition. Both, SLPI concentrations (0.32 µM and 2.98 µM) as well as the low concentrated elafin (0.16 µM) could not obtain inhibition (Figure 22j).

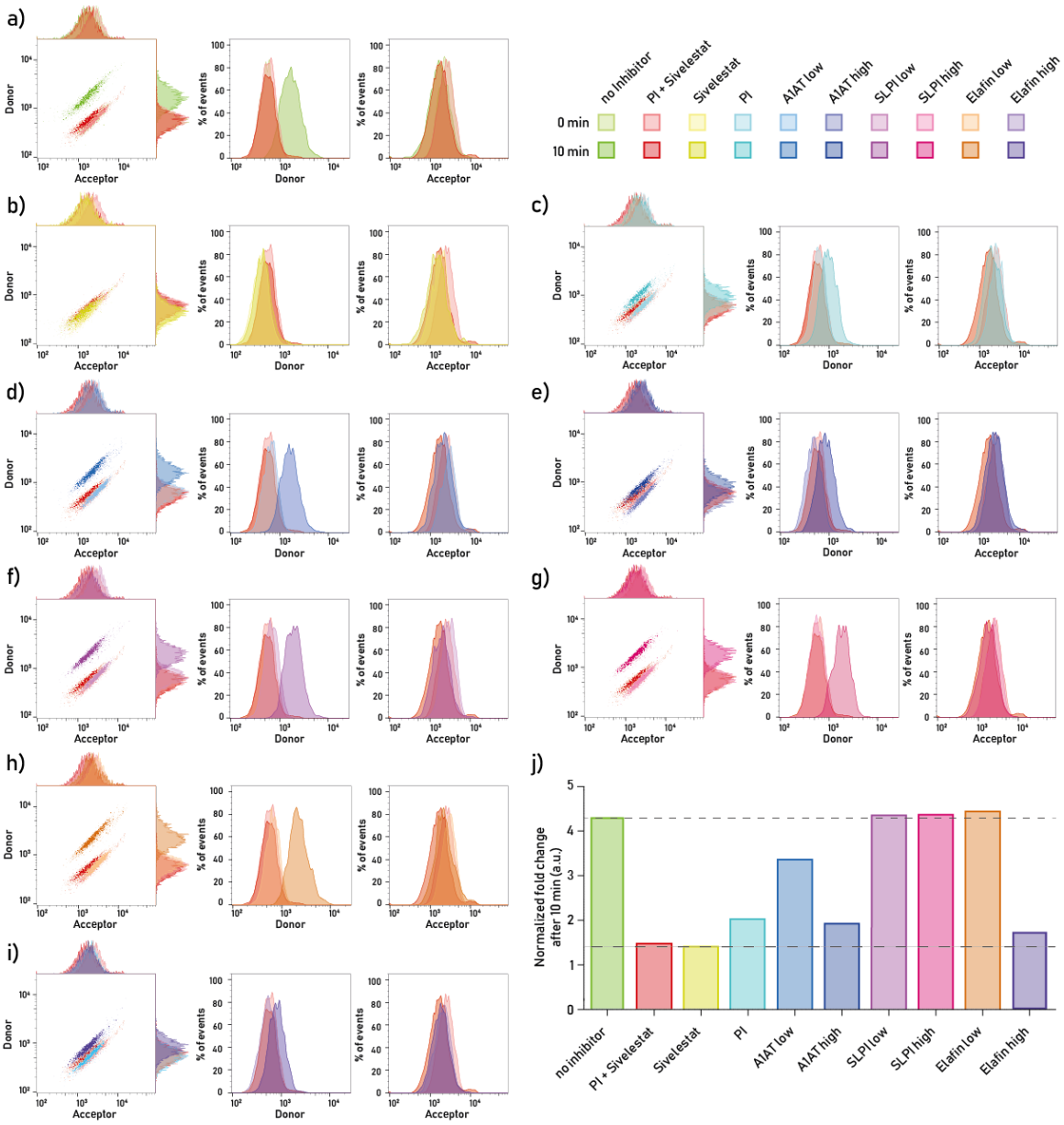

Figure 22: Evaluation of FRET probe selectivity Neutrophils isolated from the same CF patient, were incubated for 10 min with several relevant inhibitors, to evaluate specific inhibition of membrane associated NE activity. Left panel shows dot plot of donor (y-axis) and Acceptor (x-axis) on gated neutrophils measured at the flow cytometer. Lighter colors indicate the 0 min timepoint, darker colors the 10 min time point. A) Non-inhibited sample are shown in bright green, cells inhibited with a mixture of cOmplete proteinase Inhibitor (7.58-fold final concentration) and sivelestat (0.427 mM) as used during routine measurements are shown in red. B) Cells inhibited with sivelestat only (0.427 mM) are shown in lime yellow-green. C) Cells inhibited with cOmplete proteinase Inhibitor (7.58-fold final concentration) are depicted in light aquamarine. D) Cells inhibited with low concentration of A1AT (0.5 µM) are represented in cobalt blue. E) Cells inhibited with high concentration of A1AT (5.08 µM) are shown in phthalo blue. F) Cells inhibited with low concentrations of secretory leucocyte protease inhibitor (0.32 µM) are represented in magenta. G) Cells inhibited with high concentrations of secretory leucocyte protease inhibitor (2.98 µM) are represented in orchid. H) Cells inhibited with low concentrations of elafin (0.16 µM) are shown in orange brown. I) Cells inhibited with high concentrations of elafin (1.55 µM) are shown in violet. J) Box plot of the normalized fold change measured after 10 min of incubation with the different inhibitors shown in panel A-I are given. Dashed line indicates D/A ratio without inhibitor addition (bright green) and dotted line marks for D/A ratio of the most effective inhibitor sivelestat

(yellow-green).To proof the consistency of these results the inhibitor supplementation was repeated in four independent experiments for as many conditions as cells were available (Figure 23). Different conditions were compared by applying a one-way ANOVA with a Dunnett's Multiple Comparison correction. Statistically significant differences to the sample without inhibitor supplementation were reached with sivelestat in combination with PI, sivelestat only as well as with the high concentrated A1AT. Samples supplemented with PI, the low A1AT concentration as well as the high elafin concentration were partially inhibited without reaching significance. The inhibitory efficiency for the individual conditions is comparable among the four different patients (Figure 23).

In summary, NE activity measured with NEmo-2E could be completely abolished upon addition of specific small molecule NE-inhibitors, suggesting selective NE activity quantification in highly complex sputum samples.

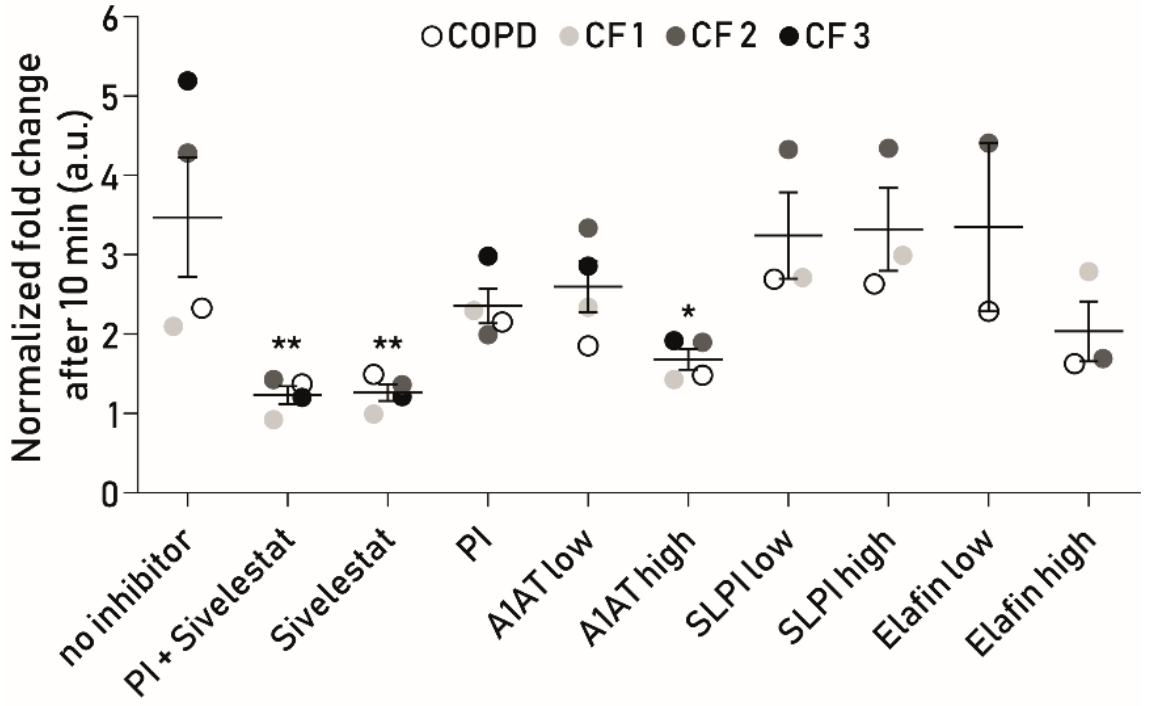

Figure 23: Comparison of inhibitory capacity of several relevant inhibitors after 10 min of inhibition, measured on neutrophils isolated from one COPD and three CF patients. Inhibitors are given at the x-axis and were used with the following concentrations: PI: 7.58-fold; sivelestat: 0.427 mM; A1AT low: 0.5 µM; A1AT high: 5.08 µM; SLPI low: 0.32 µM; SLPI high: 2.98 µM; elafin low: 0.16 µM and elafin high: 1.55 µM. Mean with standard error of the mean are shown. P-values between the different inhibitors to the non-inhibited sample were calculated with a one-way ANOVA with a Dunnett's Multiple Comparison posttest and are given as: *: $p < 0.05$ and **: $p < 0.01$. Measurements belonging to the same patient are depicted in the same color among the different inhibitors tested.

3.2.4 In depth characterization of the airway secretions of CF, COPD patients and controls

In this chapter it was assessed if there is a difference in sputum samples of CF and COPD patients. Therefore, free and membrane associated NE activity, established inflammatory markers, anti-proteases, microbiome structure, and clinical data were measured and correlated to each other. Further, a secretomics analysis was included allowing to evaluate more molecules in an unbiased approach. Healthy control samples were evaluated accordingly. The cross-sectional study included 38 CF patients which were compared to 18 COPD patients and 10 healthy controls, detailed cohort characteristics are described in Table 11.

Table 11: Clinical characteristics of CF, COPD patients and healthy controls.

		CF	COPD	HC
Subjects	n	38	18	10
Age (years)	Median (range)	28.85 (19.77-73.83)	66.82 (50.81-78.20)	30.68 (26.59-49.04)
Sex	n, females/ males	18/20	11/9	5/5
BMI (kg/m²)	Median (range)	20.96 (15.79-30-96)	21.96 (18.59-44.46)	-
FEV_1 % predicted*	Median (range)	57.19 (16.93-92.88)	32.95 (18.28-49.61)	-
CFTR genotype				
F508del/F508del	n (percentage)	14 (36.84)	-	-
F508del/other	n (percentage)	20 (52.63)	-	-
Other/other	n (percentage)	4 (10.53)	-	-
Pancreatic insufficiency	n (percentage)	35 (92.11)	-	-
Clinical Status				
Stable	n (percentage)	34 (89.47)	-	-
Exacerbation	n (percentage)	4 (10.53)	-	-
GOLD stage (3/4)	n (percentage)	-	11(61.11)/7(38.89)	-

*FEV_1 % predicted only available from 32 CF patients

Investigation of cell-type distribution, absolute cell numbers and neutrophil recruitment in sputum samples of healthy controls, CF and COPD patients

Evaluations of the cell type distributions revealed, elevated numbers of neutrophils and eosinophils, but reduced percentages of macrophages in sputum samples from CF and COPD patients, in comparison to healthy controls. The percentage of neutrophils was higher, in CF patients, whereas COPD patients had higher percentage of eosinophils (Figure 24a). Besides, significant elevated cells per gram sputum were found in CF (Figure 24b), however, absolute cell numbers were on a similar level (Figure 24c). Lastly, levels of the secondary chemoattractant for neutrophils during inflammation, Leukotriene B4 (LTB_4), was significantly higher in CF compared to the other two groups (Figure 24d). Thus, in CF increased levels of recruitment factor LTB_4 are present which was less prominent in COPD. As a consequence, an increased number of neutrophils was found in CF, which implies a higher release of NE in CF.

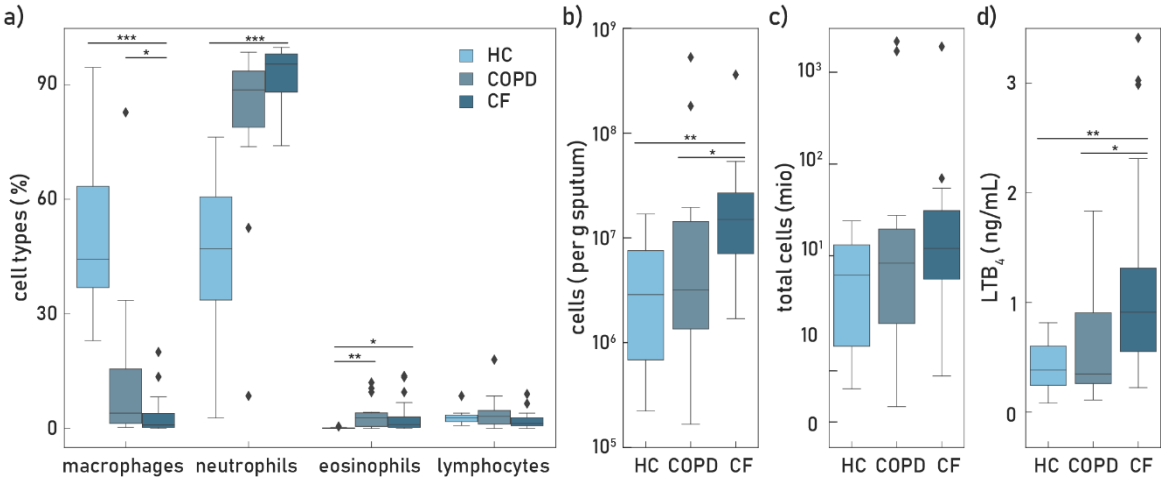

Figure 24: Assessment of cell type percentages, cell numbers and cell recruitment factor LTB_4 in CF and COPD patients and healthy controls. Boxplot of **A)** different cell types in percentages (HC n=7; CF n=36; COPD n=14), **B)** cells per gram sputum (HC n=8, COPD n=15; CF n=36), **C)** total cells in millions (HC n=8; COPD n=15; CF n=36) and **D)** levels of LTB_4 (HC n=10; COPD n=18; CF n=31). P-values between the different groups were calculated with a Kruskal-Wallis ANOVA with a Dunnett's multiple comparison posttest and are given as follows: *: p <0.05, **: p <0.01 and ***: p <0.001. Outliers are shown as diamonds (♦).

Investigation of microbiome composition of sputum samples of healthy controls, CF and COPD patients

In the next step the microbiome structure of healthy controls as well as COPD and CF patients (HC: n=10; COPD: n=16 & CF: n=38) was compared, by 16S RNA sequencing with a subsequent PCoA based on the Unifrac weighted distance (Figure 25). Samples were clustered by kmean into three cluster, based on the result of the gap statistics (Figure S1). All healthy control samples were assigned to cluster 1 (n=10), COPD samples to cluster 1 (n=10) and 2 (n=6) and CF samples to all three clusters (CF 1: n=7; CF 2: n=10 & CF 3: n=21). The distribution of the most common ASVs revealed, that samples of cluster 1 had the most diverse microbiome, whereas samples assigned to cluster 2 and 3 harbored a monospecific infection of different pathogens. Of these, a *Pseudomonas* dominated microbiome, was exclusively found in samples of cluster 3 which contrained only CF patient samples. Next, the three kmean cluster were split in six sub clusters based on the disease pattern (HC 1, COPD 1, COPD 2, CF 1, CF 2 and CF 3).

The highest α-diversity (Shannon index), richness and evenness were found in cluster 1, followed by cluster 2 and 3 (Figure 26). For the dominance the inverse order was found, with cluster 3 being highest and cluster 1 being lowest. Richness and α-diversity of cluster HC 1 was highest followed by cluster COPD 1 and CF 1. Regarding the evenness HC 1 was also highest or lowest in terms of dominance, but there was no significant difference between cluster COPD 1 and CF 1. Analysis of the 3-sub clusters of kmean cluster 1 (HC 1, COPD 1 and CF 1) revealed that the richness of the microbiome from HC 1 to CF 1 was reduced by almost half, suggesting that a “healthy-like” CF microbiome is quite different from the structure of a healthy control.

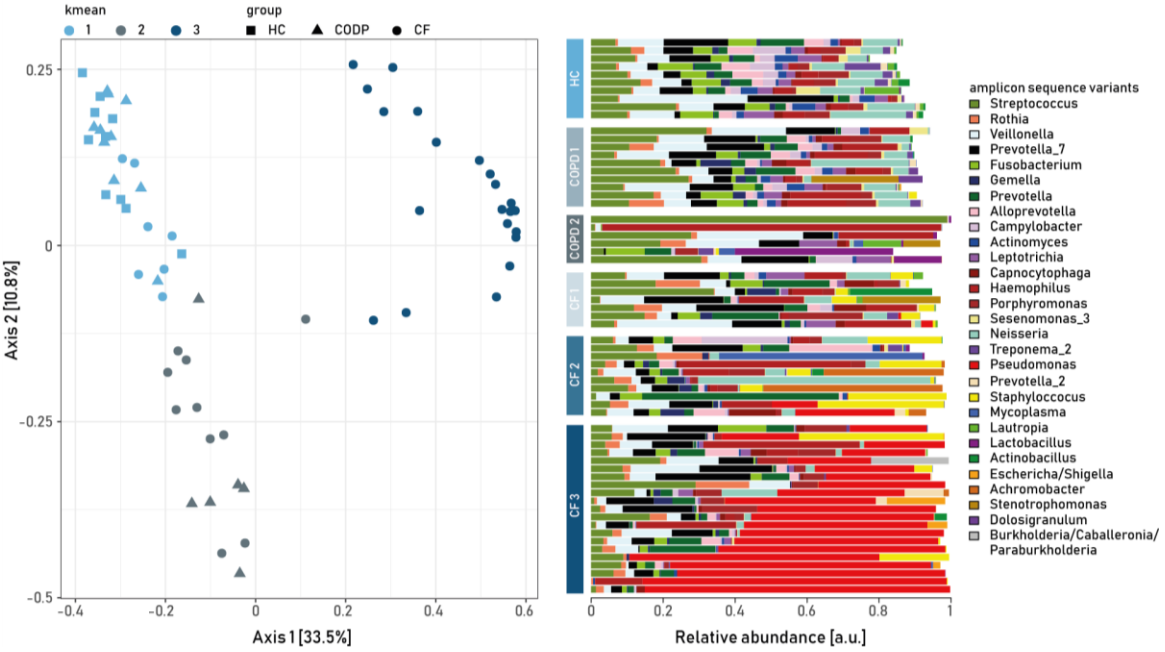

Figure 25: Principal Coordinate Analysis based on Unifrac weighted distances with kmean clustering as well as relative abundances of top 29 ASVs based on the identified cluster. The left panel shows a principal coordinate analysis (PCoA) based on a Unifrac weighted distance matrix, with the kmean cluster indicated by color whereas the shapes indicate the groups. The right panel depicts the relative abundance of the 29 most common ASVs grouped by the respective sub cluster (indicated by colored bars on the side)

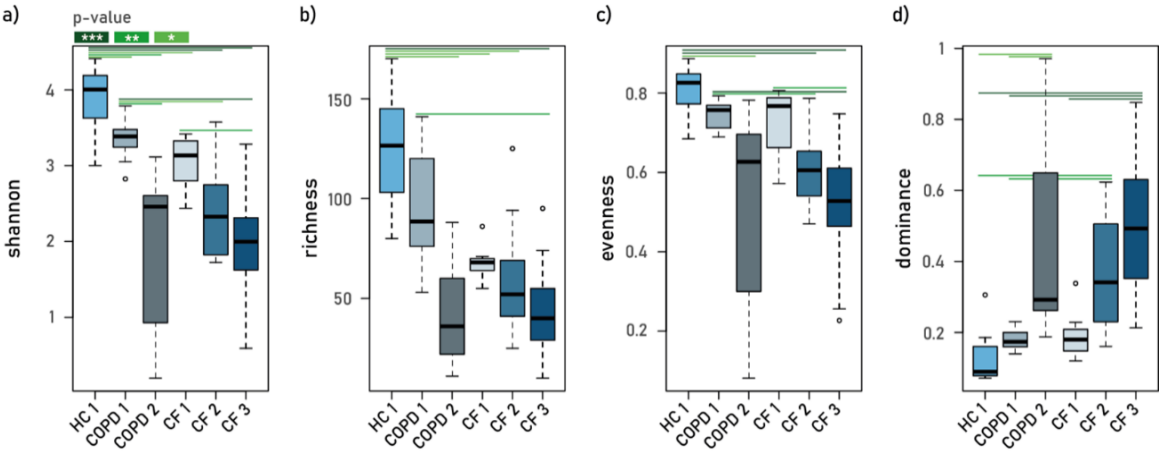

Figure 26: Comparison of microbiome parameters based on kmean clustering. Boxplots of microbiome parameters, **A)** Shannon index, **B)** richness, **C)** evenness and **D)** dominance for each cluster. Cluster were compared by Wilcoxon rank sum test with Bonferroni-Holm correction for multiple comparisons, if significance was reached this is indicated by colored lines which are indicating the p-values: lime green: p <0.05, green: p <0.01 and dark green: p <0.001.

Investigation of inflammatory markers of sputum samples of healthy controls, CF and COPD patients

In the next step, a broad panel of pro- and anti-inflammatory cytokines was evaluated for each of the 6-sub clusters. Levels of IL-1β, TGF-β1 and TNF-α increased by cluster, with 1 being lowest and 3 being highest and further tend to be elevated within the CF group

(Figure 27a-c). Levels of IL-8 were significantly elevated in the cluster of the disease groups, being highest in cluster CF 3 (Figure 27d). IL-5 was significantly higher in COPD 1 & 2, besides IL-6 and IL-10 tend to be increased within the COPD cluster without reaching significance for all comparisons, given the small numbers of samples per cluster (n=6 for COPD 2) and the high variability within the cluster (Figure 27e-g). IL-1α, IFN-γ and the protein content were not significantly different among the clusters (Figure 27h-j). Taken together, these results show a disease specific cytokine panel for some cytokines as for example TNF-α, TGF-β1, IL-5 and IL-6 which are rather independent of the microbiome structure. Whereas other cytokines for example IL-8 were elevated in all disease clusters.

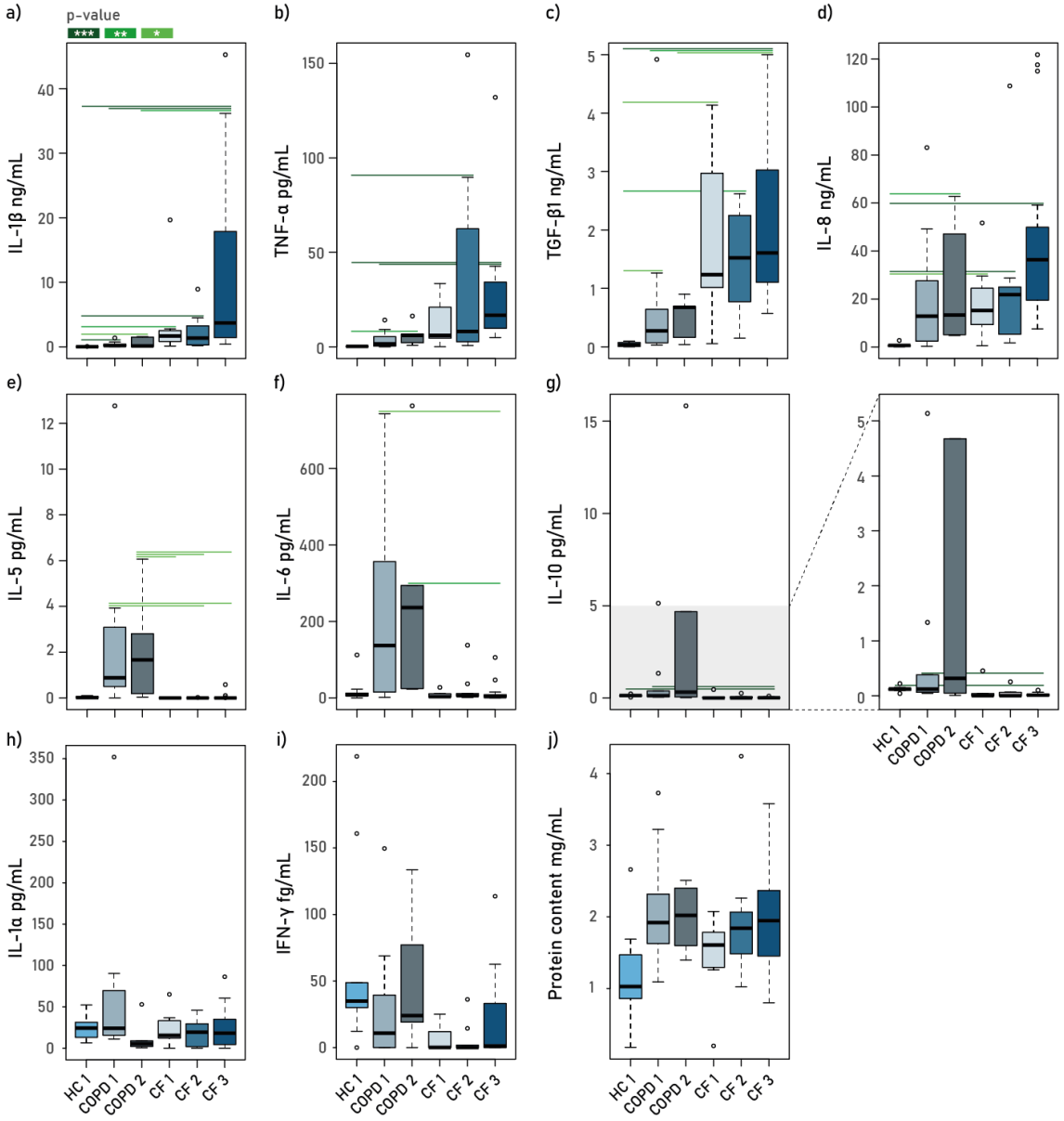

Figure 27: Comparison of significantly different inflammatory markers of the PCoA clusters. Boxplots of **A)** IL-1β **B)** TNF-α, **C)** TGF-β1, **D)** IL-8, **E)** IL-5, **F)** IL-6 and **G)** IL-10 full scale and enlarged plot of grey shaded, **H)** IL-1α **I)** IFN-γ, **J)** Protein content area given. Cluster were compared by Wilcoxon rank sum test with Bonferroni-Holm correction for multiple comparisons, if significance was reached this is indicated by colored lines according to their p-values: lime green: p <0.05, green: p <0.01 and dark green: p <0.001. Outliers are shown as circles (○).

Investigation of protease activity and anti-proteases of sputum samples of healthy controls, CF and COPD patients

Interestingly, the analysis of the free as well as membrane associated NE activity along with the relevant endogenous anti-proteases SLPI, A1AT and the complex of NE and A1AT showed a disease specific inflammatory pattern within the lung, independent of the microbiome structure. Free NE was found elevated in all CF sub-clusters, with the highest activity in cluster CF 3, followed by CF 2 & CF 1 and the COPD 1 & 2 clusters, see Figure 28a. In contrast, the membrane associated NE activity was elevated in both disease groups with significant differences between the three CF cluster and cluster HC 1 only (Figure 28b). This indicates, that the amount of free NE secreted by neutrophils of COPD patients is sufficient to saturate the cell surface. Of note, the closer inspection of the three CF sub-cluster revealed that free NE was slightly higher in CF 1 compared to CF 2&3, the opposite trend was observed regarding the membrane associated NE. Further, for the anti-proteases SLPI and A1AT as well as the complex of NE and A1AT disease specific pattern which was most pronounced for SLPI being significantly elevated in the two COPD sub-cluster. Levels of TIMP1 were comparable between the CF and the COPD cluster with a higher variability found in clusters of COPD patients.

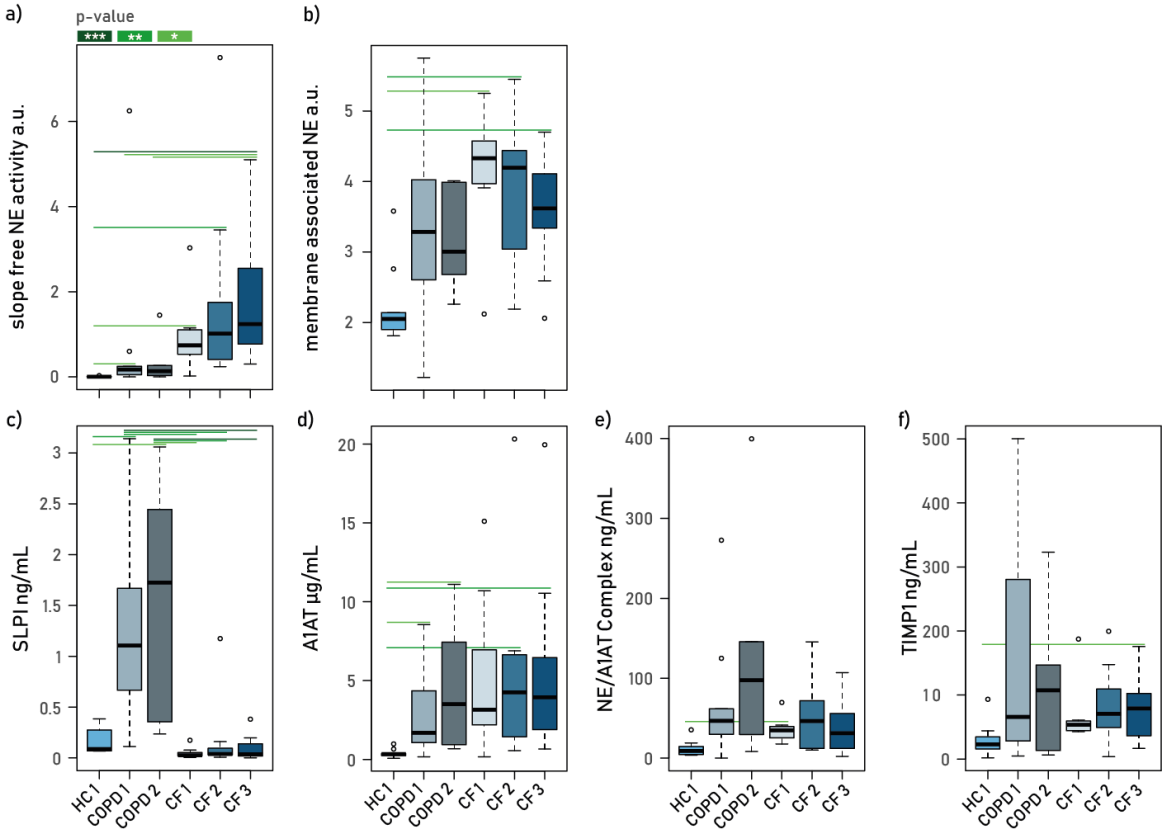

Figure 28: Comparison of free and membrane associated NE activity, as well as relevant endogenous anti-protease levels of all cluster. Boxplots of **A)** slope of free NE activity, **B)** membrane associated NE, **C)** SLPI, **D)** A1AT, **E)** NE/A1AT complex and **F)** TIMP1 given for each cluster. Cluster were compared by Wilcoxon rank sum test with Bonferroni-Holm correction for multiple comparisons, if significance was reached this is indicated by colored lines according to their p-values: lime green: p <0.05, green: p <0.01 and dark green: p <0.001.

Investigation of surface markers of neutrophils isolated from sputum and clinical parameters of healthy controls, CF and COPD patients

Together with the membrane associated NE measurement, cell surface markers of neutrophils were recorded. A down regulation of CD16 in the diseased groups could be observed reaching significant for the cluster CF 2 & 3 in comparison to cluster HC 1 (Figure 29a). For CD63 minor non-significant upregulation within the CF and COPD clusters was detected (Figure 29b). Expression of CD66b was identical among all clusters (Figure 29c). Clinical parameters were only available for CF and COPD patients. Mean lung function was lowest in cluster COPD 1 and highest in cluster CF 1 (Figure 30a). This could be explained by the tremendous age difference between the two groups, with an average age of ~29 years for the CF patients in comparison to ~67 years for the COPD patients which is part of the equation to calculate the FEV_1 % predicted. In case of COPD and CF an age matched cohort is impossible, due to the fact that an inherited an acquired disease are compared. Levels of c-reactive protein (CRP) in the blood and BMI were not significantly different among the groups (Figure 30b-c).

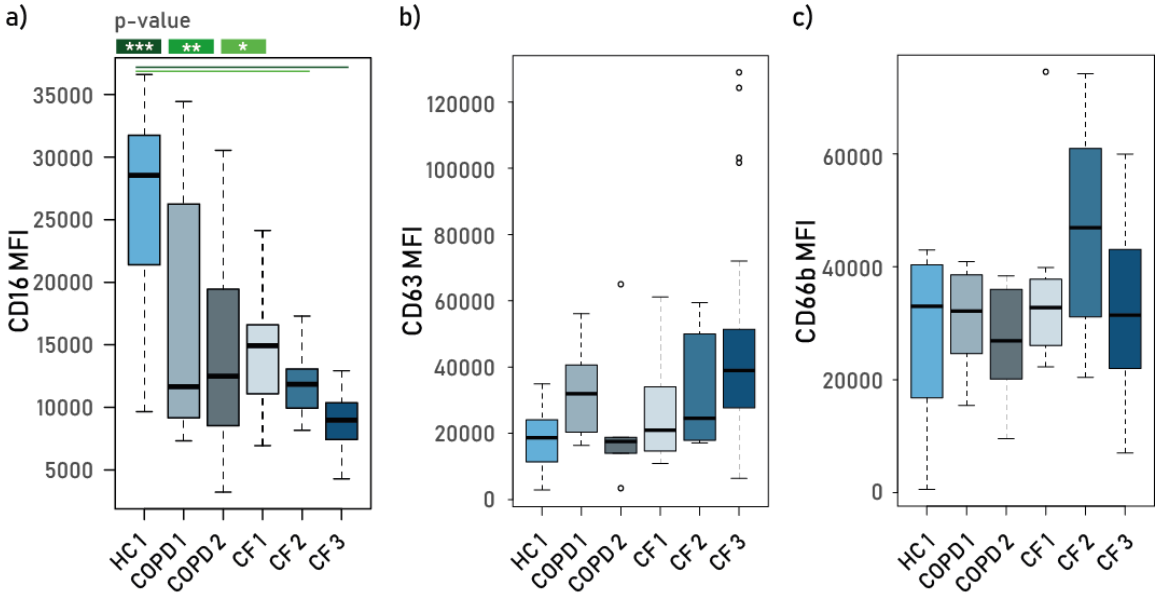

Figure 29: Comparison of surface-markers CD16. CF63 and CD66b of the clusters. Boxplots of **A)** CD16 and **B)** CD63 and **C)** CD66b MFI ordered by cluster. Cluster were compared by Wilcoxon rank sum test with Bonferroni-Holm correction for multiple comparisons, if significance was reached this is indicated by colored lines indicating the p-values: lime green: p <0.05, green: p <0.01 and dark green: p <0.001. Outliers are shown as circles (○).

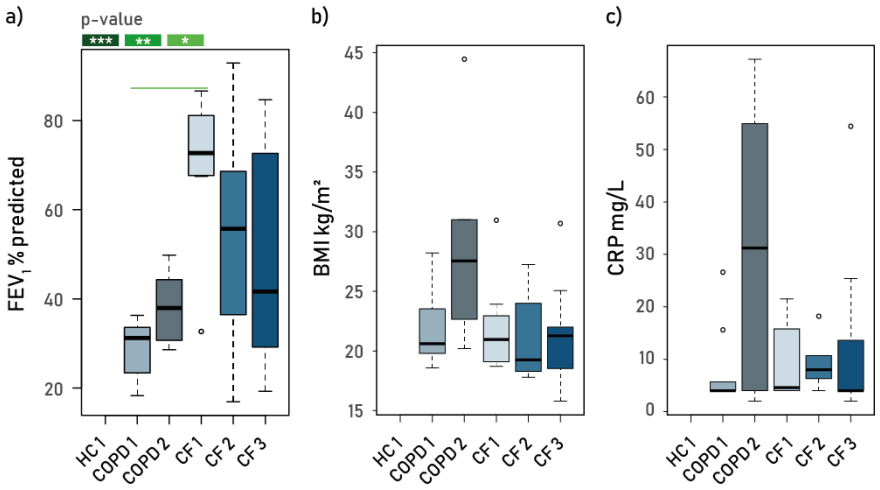

Figure 30: Comparison of clinical markers from the PCoA measured for COPD and CF patients only. Boxplots of **A)** lung function **B)** BMI and **C)** CRP ordered by cluster. Cluster were compared by Wilcoxon rank sum test with Bonferroni-Holm correction for multiple comparisons, if significance was reached this is indicated by colored lines indicating the p-values: lime green: p <0.05, green: p <0.01 and dark green: p <0.001. Outliers are shown as circles (○).

Multiparameter correlation between microbiome indices and individual ASVs in sputum samples of healthy controls, CF and COPD patients

Hierarchical clustering of the correlations between microbiome indices and the other 29 parameters analyzed reveled strong interdependencies. Dominance showed the inverse of richness, α-diversity and evenness. High levels of IL-5, IL-10, CD16 and a high percentage of macrophages were linked to a more diverse microbiome (Figure 31a). High percentage of neutrophils, TNF-α, TGF-β1, IL-8, free and membrane associated NE activity were in contrast linked to a less diverse microbiome (Figure 31a). Of note, the cutoff for the correlation is with 0.01 rather strict. Taken together, these results showed that parameters which are assigned to the COPD or healthy cluster are associated with a less dominated, more diverse, richer and more even microbiome structure. Whereas parameter assigned to the CF cluster show the opposite effect.

The hierarchical clustering on level on individual identified ASVs revealed, that a decline of most of the ASVs is associated inversely with markers of inflammation. Parameter wise, IL-1β was associated with the most ASVs followed by free NE, TNF-α and IL-8 which are all pro-inflammatory markers (Figure 31b). The same ASVs were positively linked to percentages of macrophages levels of CD16 or IL-10. From the considered 29 ASV the abundance of 5 was associated to higher levels of inflammation, with *Pseudomonas* being the most significant one, followed by *Staphylococcus*, *Rothia*, *Achromobacter* and *Escherichia*/*Shigella*. Concerning the ASVs, the abundance of *Pseudomonas* had the most tremendous effect regarding inflammation, followed by *Leptotrichia*, *Actinomyces*, *Selenomonas*_3, *Fusobacterium* and *Treponema*_2 which all showed the inverse correlation compared to *Pseudomonas*.

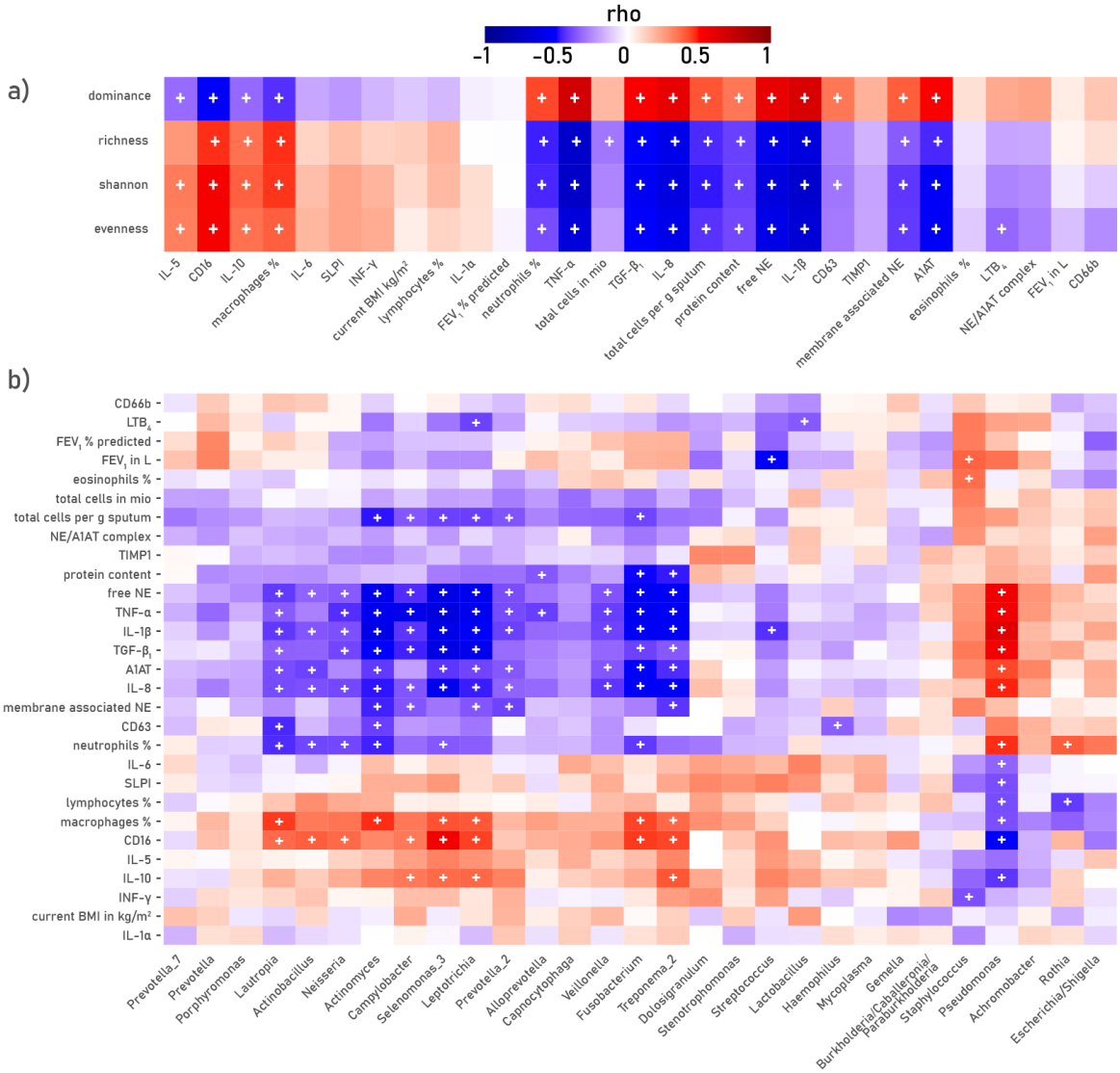

Figure 31: Hierarchical clustering of the correlation between microbiome indices or individual ASVs and all other markers analyzed.. Correlation with a p-value ≤ 0.01 are indicated with a plus (**+**).

Secretomics characterization by mass spectroscopy of sputum sample supernatants of healthy controls, CF and COPD patients

Besides, sputum supernatants were examined via mass spectroscopy (MS) to get an unbiased picture regarding secreted proteins. The PCA of the identified proteins did not show a significant difference between sub-cluster of the disease (Figure 32a), especially the samples belonging to the CF cluster were homogenously clustered, for that reason the secretomic analysis are based on the disease groups and not the cluster of the microbiome PCoA. The three disease groups were compared pairwise, resulting volcano plots of the label-free quantitation (LFQ) intensities. The volcano plot comparing CF and COPD secretomes can be found in Figure 32a, the full panel of volcano plots is shown in Figure S2. The comparison of CF and COPD revealed that 51 proteins are either unique or significantly up regulated in CF, whereas the number of proteins assigned to COPD is only 23. The number of identified proteins might seem to be low for a MS approach but it has to be taken into consideration, that only secreted proteins were evaluated and the analysis

was based on label-free quantitation values, due to the lack of structural proteins as for example actin which could be used for normalization. The proteins S100A8 (protein S100-A8) and S100A9 (protein S100-A9) are for example both Ca^{2+} depended proteins which form the protein complex calprotectin, further proteins as MPO and CTSG were significantly higher expressed in CF. In contrast proteins as MUC5AC which protects mucosa from infections, CFH (complement factor H) which mediates neutrophil adhesion to pathogens as for example *S. aureus* and SERPINB3 (Serpin B3) a papain-like cysteine protease inhibitor were elevated in COPD, see Figure 32b. Highest fold changes were observed in the CF healthy comparison. This was also the comparison where the most unique proteins were identified, in the CF samples. Among the top ten upregulated proteins (which are labeled in Figure 32 with the gene names) many are found in the neutrophil granules as for example ELANE, MPO, MMP9 or CTSG, another group contains calcium depended proteins as ANXA3 (Annexin A3) and S100A9 (Figure S2). For each group and comparison, the significant upregulated and unique proteins were combined and analyzed regarding the gene ontology (GO) to identify up- or downregulated biological processes and the responsible cellular compartments using the GO enrichment analysis combined with the PANTHER classification system (chapter 2.12.3). Which are depicted as balloon plot ordered by their p-value for easier readability. The comparison between CF and COPD revelated that the most significant upregulated cellular compartments are mainly linked to vesicles in form of granules or exosomes released by cells, especially neutrophils. In both diseases extracellular exosomes and ancillary compartments showed the strongest upregulation, with different proteins involved. Within CF samples, secretory granules or vesicles were most significantly upregulated. The only cellular compartment exclusively identified in COPD is the blood microparticle which was almost 60-fold enriched see Figure 32c. On level of the biological processes, four of the top five processes are directly linked to neutrophils, all assigned to the CF samples (Figure S3). The only shared processes are related to the immune response, immune system and immune effector processes. There were no biological processes identified which were exclusively assigned to COPD (Figure S3).

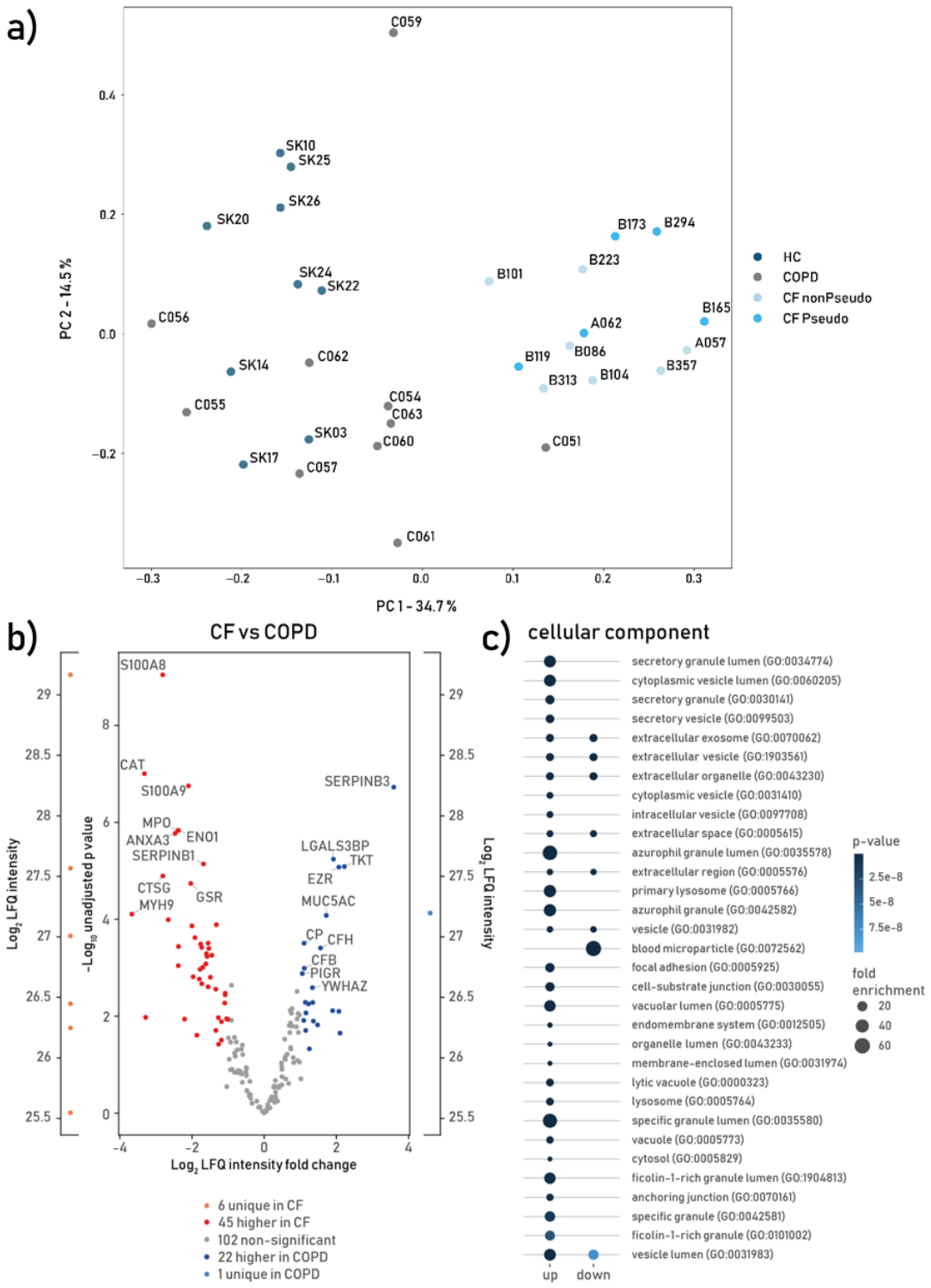

Figure 32: PCA of the Log_2 LFQ intensities of identified proteins, and volcano plots of the secretome comparisons between CF and COPD as well as the corresponding GO analysis of the up and down regulated cellular compartments. A) PCA based on all identified proteins. **B)** Volcano plot comparing CF (red) and COPD (blue). Significantly upregulated proteins are represented in darker shades, unique identified proteins are found to the left and right of the volcano plot in dimmer shades. Protein which are not significant different are shown in grey. Top ten protein for each group and comparison are labeled. Exact number of the non-significant, upregulated and unique proteins are given below the graph. **C)** Gene Ontology analysis for up and down regulated cellular compartments based on unique and significantly upregulated proteins which were grouped and analyzed together for each disease. Name of the cellular compartment and GO id are given. Cutoff value was a 2-fold enrichment which is indicated by color, enrichment by size of the dot.

3.2.5 Validation of enzyme quantities by western blot and mass spectroscopy

NEmo reporters allow only an indirect measurement of enzymatic activity by the analysis of substrate cleavage over time. Thus, high concentrations of endogenous anti-proteases could, antagonize enzyme activities even though the enzyme itself is present in high abundance. Therefore, enzyme amounts of nine randomly selected supernatant fractions of sputum samples of healthy controls, CF and COPD patients were quantified via sodium dodecyl sulfate polyacrylamide gel electrophoresis followed by western blots of ELANE, CTSG and MMP9 (Figure 33). This reveled highest ELANE and CTSG concentrations in CF samples, followed by COPD and controls according the results obtained from the activity measurements. For MMP9 only a trend for higher concentrations in COPD compared to CF and controls was measured with the quantitative setup. To compare NE activity and NE quantity, same samples were assessed for their NE activity via FRET measurement using the NEmo-1 probe alongside with NE quantification via western blot and via mass spectroscopy (Figure 34). All three methods showed the same pattern, in which CF had the highest quantity and activity of NE, followed by COPD and healthy controls. In summary, results obtained by the measurement of NE activity are comparable with those obtained with western blot analysis or mass spectrometry. However, mass spectrometry offers the highest resolution and plate reader set up a fast and simple quantification.

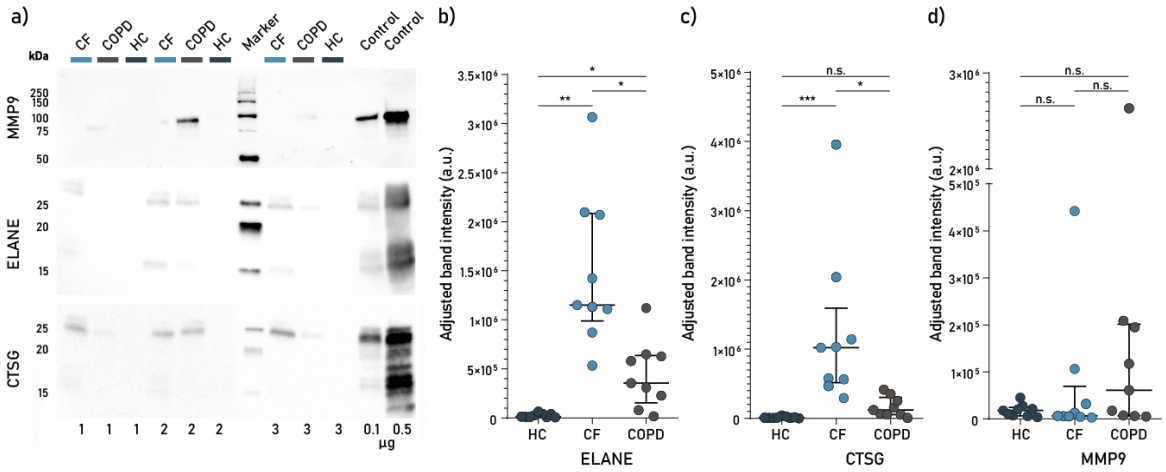

Figure 33: Western blot of MMP9, ELANE and CTSG. A) Representative Image of western blots for MMP9 (1st) ELANE (2nd) and CTSG (3rd) are show. The sizes of the marker bands are given in kDa. On each gel two controls (low and high) of the corresponding enzyme with a concentration of 0.1 µg and 0.5 µg were included. An absolute protein amount of 10 µg of each sample were loaded. Groups; HC (●), CF (●) and COPD (●) and are given above the western blots. Dot plots of the adjusted band intensity of the ELANE (**B**), CTSG (**C**) and MMP9 (**D**) western blots, of all three experiments are depicted. Streaks show median, error bars indicate inter quartile range (IQR) and stars depict the significance level of unpaired nonparametric t-test. P-values are given as: *: p <0.05, **: p <0.01 and ***: p <0.001 and n.s.: not significant

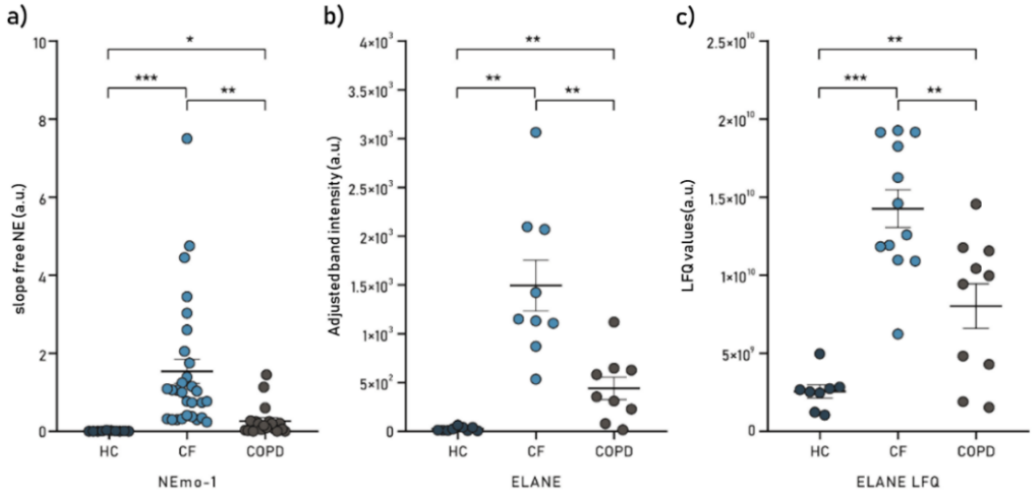

Figure 34: Comparison of the slope of the activity, quantification via western blot as well as the LFQ values measured by mass spectroscopy of NE in the soluble fraction. A) Slopes of free NE activities of healthy controls (HC, n=10, dark blue), CF (n=29, light blue) and COPD patients (n=19, dark grey). **B)** Adjusted band intensity of ELANE of three independent western blots of HC, CF and COPD samples (n=9 per group). **C)** LFQ values of ELANE measured by mass spectroscopy (HC: n=8, CF: n=12 and COPD n=10). Median and inter quartile range (IQR) are shown. Asterisks depict the significance level of Brown-Forsythe and Welch ANOVA test with Tamhane's T2 correction for multiple comparison: *: p <0.05, **: p <0.01, ***: p <0.001.

4 Discussion

4.1 Association of inflammatory markers with airway dysbiosis and lung function in patients with CF

With the cross-sectional study a relation of airway inflammatory load, microbiome structure and lung function impairment was demonstrated by applying linear regression in combination with hierarchical clustering. By focusing on largely clinically stable patients with CF, baseline characteristics and interdependencies of inflammation, microbiome composition, and FEV_1 % predicted can now be understood. These relationships were further elaborated on the individual patient level within the longitudinal follow-up study, spanning over one (short-term) or at least 3 years (long-term). While the microbiome showed a dynamic change only in the short-term study, while inflammatory parameters, anti-proteases and lung function showed gradual changes only in the long-term study. Moreover, serious changes in the microbiome composition were linked to a severe decline in lung function and drastic changes in inflammation.

4.1.1 Identification of interdependencies of airway dysbiosis, inflammation and lung function utilizing a cross-sectional study design

Major findings of the cross-sectional study in CF were the links between the level of inflammation, dysbiosis of the airway microbiome as well as the degree of lung function decline. The inclusion of several statistical aspects of the α-diversity, representing the biodiversity as richness, evenness and dominance, allowed the evaluation of the contribution of individual parameter in more detail. The evenness and dominance were more important than the raw richness, regarding the correlation of increased α-diversity with elevated levels of several inflammatory parameters as IL-1β, IL-8, free NE activity and TNF-α (Figure 8). These parameters were also the highest in the Psae cluster and the lowest in the OF cluster and had the lowest and highest α-diversity, respectively (Figure 10). The receptor of IL-8, CXC chemokine receptor type 1 (CXCR1, also known as CD181), which is important for host defense, can be degraded by NE (Carevic et al. 2016). A lack in CXCR1, expressed mainly on neutrophils, has been linked to an enhanced vulnerability against infections with *P. aeruginosa* which is one of the key pathogens regarding CF lung disease (Carevic et al. 2016). A study with CXCR1 knockout mice has shown that neutrophil recruitment is not affected, but rather interferes with certain neutrophil effector functions via pathways which include reactive oxygen species and Toll-like receptor 5, an important pattern recognition receptor for *P. aeruginosa* (Carevic et al. 2016; Morris et al. 2009). Further, the transcription of flagellin of *P. aeruginosa* is downregulate as consequence of high levels of NE activity, favoring the switch to a mucoid phenotype which leads to biofilm formation (Sonawane et al. 2006).

In contrast to the inflammatory parameters, FEV_1 % predicted was the highest in patients of the OF cluster and the lowest in patients being assigned to the Psae cluster (Figure 10). Further, FEV_1 % predicted and α-diversity were negatively associated (Figure 8), meaning that patients with a monospecific colonization showed a significant decline in lung function and elevated levels of inflammation, which is consistent with the findings of other cross-sectional studies (O'Neill et al. 2015; Cox et al. 2010; Boutin et al. 2017a). The moment a pathogen outcompetes the commensal bacteria, even though they were adults, had a rather diverse microbiome, which was usually during infancy and childhood of Cf patients (Muhlebach et al. 2018b). Moreover, some patients even though they were adults had a rather diverse microbiome, which is usually predominately found during infancy and childhood of CF patients However, those individuals showed elevated inflammatory parameters compared to healthy individuals, even though they harbored a diverse microbiome. This may be explained by hypoxia, release of IL-1 and mucus plugging as described before (Fritzsching et al. 2015; Montgomery et al. 2017; Balázs und Mall 2019; Montgomery et al. 2020). In a recent of bronchiectasis patients, an inverse correlation of NE activity with α-diversity as well as a positive link to relative abundance of *P. aeruginosa* was described (Oriano et al. 2020). A decline in lung function could be directly linked to dominance, whereas richness was linked likewise to reduced FEV_1 % predicted (Figure 8). Hence, there is a direct relation of the overall number of species to lung function. The modified airway secretions, together with the impaired MCC, forester the outgrowth of low abundant species by the most ambitious pathogen (Dickson et al. 2016).

Dominance and richness of the microbiome correlate stronger to inflammatory markers and lung function than biomass

Many studies that assessed the microbiome focused on diversity as key index (Cuthbertson et al. 2020; Hahn et al. 2020). Instead, in this study hierarchical clustering was used to get a more detailed picture of the relationship between the microbiome, lung function and inflammation. The microbiome of different patients can vary widely. Hence, the interrelationship of microbiome structure and clinical outcome were evaluated. However, associations of individual species of commensals with clinical parameters were less pronounced. The structure-based clustering of the microbiome, has been described before as useful regarding the description of the associations between microbiome and disease progression (Boutin et al. 2017a; Muhlebach et al. 2018b; Schmitt et al. 2019; Boutin et al. 2017b). In contrast to previous publications, patients assigned to the OF cluster showed a more even and richer microbiome (Figure 9) (Zemanick et al. 2017; Boutin et al. 2017a; Boutin et al. 2015; Muhlebach et al. 2018b). The hierarchical clustering resulted in seven different clusters, which were only observed in samples assigned to the OF cluster, whereas the other clusters showed a decreased α-diversity conditioned by the

dominance of individual pathogens. Patients assigned to the Psae cluster showed by far the lowest level of lung function and the highest level of inflammation (Figure 10), those findings are in accordance to previously published data (Pienkowska et al. 2019; Boutin et al. 2017a; Boutin et al. 2018). The identified clusters of the cross-sectional study are in accordance to the study of preschool children (Muhlebach et al. 2018b). The cluster OF is equivalent to their cluster C2 whereas the clusters Achro, Psae and Staph correspond to their cluster C3. However, the inclusion of adult CF patients explains the age discrepancy between the studies and besides the lack of the cluster including all the pathogens which is presumably caused by a higher resolution in the older patient cohort. Further, this also explains why the cluster which consists of low biomass samples (C1) could here not identified, this can be found in children, due to their low bacterial abundancies, but not in adults with CF (Muhlebach et al. 2018b). Furthermore, the two studies utilized different clustering approaches, Muhlebach based the clustering on the PCoA of only the most abundant taxa (Muhlebach et al. 2018b) whereas here the full dendrogram including all taxa was used.

Ribosomal sequence variants provide a higher resolution compared to operational taxonomic units

Through the use of ribosomal sequence variants (RSVs) instead of operational taxonomic units a higher resolution could be achieved. However, the level of individual species could not be reached, given the 16S rRNA approach. Further no functional hypothesis can be made, this would require whole genome sequencing (Sherrard et al. 2016; Lamoureux et al. 2019). Besides, the cluster Achro and Staph are limited in their statistical power, compared to the OF and Psae cluster. Important, the correlations of the cross-sectional study are single time points of different patients, which means that correlations regarding timing and causality are not valid. However, certain findings have been described before as for example the lower levels of pro-inflammatory parameters of patients of the OF cluster and the decline in FEV_1 % predicted as well as increased inflammation as result of the dysbiosis. Lately, the elevated levels of amino acids in the sputum were described to favor the dominance of certain bacteria, a fact that has to be taken into consideration (Quinn et al. 2019). Overall, the most likely mechanism favoring the growth of pathogens is that the initial infection causing an elevated inflammation, with increased neutrophil elastase activity as important factor.

4.1.2 Longitudinal changes and dependencies of inflammatory markers with airway dysbiosis and lung function on an individual CF patient basis

Within the longitudinal study the cohort was split in a short- and a long-term study arm. Evaluating a time frame of one year in the short-term, and of at least three years in the long-term, regarding the associations between inflammation, microbiome structure and lung function in CF patients. The key aim of the short-term study was to evaluate the temporary intra-patient variability. Whereas within the long-term study it was intended, to focus on the relevance of those effects over time. For this purpose, samples were collected over an extended period of time by collecting at least one sample per year, for several consecutive years.

Microbiome parameters temporally declined in the short-term study, whereas inflammatory markers and lung function temporally declined in the long-term study

A strong decrease over time of the α-diversity was found, which hints towards a dynamic advancement in the short-term, which is less pronounced in the long-term study. This observation can be explained by the processes which lead to the acquisition of the microbiome in the lower airways. The establishment of the microbiome of the lower respiratory tract by microbes from the oropharyngeal cavity is an iterative process of colonization and elimination, leading to a certain variability within a short period of time (Dickson et al. 2015). Given that and the fact that within the short-term, ~3 samples per year, whereas, in the long-term only one sample a year was analyzed, a correlation with more samples in less time is more likely. Hence, the microbiome of the long-term is more variable but still has an influence over a longer period of time. Besides, pro-inflammatory parameters as IL-1β and free NE rose, alongside with a decrease of anti-protease as TIMP1, SLPI as well as FEV_1 % predicted. Those were only significant in the long-term, suggesting that these changes are more uniform and evolve slowly. The fact that there were more and stronger associations of those measures with the microbiome in the long-term is caused by a lack of progression over time of those parameters during the shorter study period.

Relationships between lung function and microbiome parameters were apperent in the long-term study only

The association between the declines in FEV_1 % predicted and dominance as parameter of the α-diversity, is in accordance to earlier publications of cross-sectional studies (Raghuvanshi et al. 2020; Whelan et al. 2017). Moreover, strong negative associations of changes in FEV_1 % predicted and inflammation with the intra-patient variability were found. These findings suggest that more extreme shifts in the microbiome are linked to a steeper, more rapid decline in FEV_1 % predicted and a more severe inflammation. This relationship has been suggested in an earlier cross-sectional study (Zemanick et al. 2017), but for the

first time the association of periodic dysbiosis and establishment of the microbiome dysbiosis could be proved to be linked to a higher decline in FEV_1 % predicted and more severe inflammation in a longitudinal study layout. The next major challenge is now to find an approach how this could be addressed by therapy.

Increasing Proteobacteria abundance is the main driver for the microbiome diversity decay and subsequent lung function decline

The microbiome parameter which changed the most was the dominance which increased, caused by a higher abundance of Proteobacteria, mainly *P. aeruginosa* alongside with a reduction of Firmicutes and Bacteroidetes. The development of inflammation and FEV_1 % predicted was linked to changes of the abundance of the phyla Firmicutes and Bacteroidetes. Patients in whom the abundance of Proteobacteria increased steadily over time did more often show a drastically reduction of FEV_1 % predicted, together with a significant enhanced inflammation during the long-term period. This is according to what Hahn and colleagues (Hahn et al. 2020) found, that patients with a more diverse microbiome showed a better FEV_1 % predicted and further reinforces the hypothesis of cross-sectional studies (Zemanick et al. 2017; Cox et al. 2010; Boutin et al. 2017a; Jorth et al. 2019). They stated that the substitution of a microbiome abundant in commensals with Firmicutes and Bacteroidetes as predominant members, by a microbiome rich in Proteobacteria hints towards an infection (Zemanick et al. 2017; Cox et al. 2010; Boutin et al. 2017a; Jorth et al. 2019). Besides this strengthens the accordance of the described findings with several cross-sectional studies, comparing for example patients with a rich microbiome to patients which have a chronic infection with *P. aeruginosa* to mimic the changes from onset of infection toward a more end stage like situation.

Antibiotic treatment is a strong driver of microbiome diversity reduction

Lately, a study described that the high persistent variants of *P. aeruginosa* are less likely to be eradicated by antibiotic treatment and dominate in the long-term (Bartell et al. 2020a). In a second study, Bartell and colleagues analyzed the phenotypic and phylogenetic features of isolates from the same patients before and after an eradication period (Bartell et al. 2020b). Within this study they found considerable similarities regarding phenotypic and phylogenetic features pre- and post-antibiotic treatment, in almost half of their cohort (Bartell et al. 2020b). From a treatment point of view this is problematic, as persistent infected patients receive, in most cases a different, more aggressive antibiotic treatment regime as “intermittently colonized” patients, which is therefore rather counterproductive (Bartell et al. 2020b). Within the longitudinal assessment, the deleterious effect of infection by Proteobacteria was strengthened, especially with *P. aeruginosa* in the development of chronic inflammation and decline in FEV_1 % predicted in the context of CF. It has been shown that CFTR is located in neutrophil phagolysosomes and solely located in secretory

vesicles (Painter et al. 2006). Further, neutrophils of CF patients lack the ability to phagocytose bacterial proteins due to faulty chlorination, although extracellular hypochlorous acid secretion is normal (Painter et al. 2006). This can partially explain why CF patients are more prone to chronic infections. Zhao et al. found that antibiotic treatment shifted composition of microbial communities but also resulted in microbial resilience (Zhao et al. 2012). Nevertheless, right before initiation of antibiotic treatment due to exacerbation, a significant lower α-diversity was observed (Zhao et al. 2012). However, a clear signature in the microbiome which hinted towards an upcoming exacerbation could not be identified (Zhao et al. 2012). This study concluded that there are no specific changes in the microbiome structure, only a few or very slight changes in some operational taxonomic units occur, which are rather caused by a change in the magnitude of the host inflammatory response, which could not be identified yet (Zhao et al. 2012). Further, they concluded that antibiotic therapy is one, if not the strongest, driver leading to a reduction in microbiome diversity, an effect which was not observed during exacerbations (Zhao et al. 2012).

Baseline conditions of CF patients impact disease progression

The design of the longitudinal study has certain limitations. A time frame of one year as in the short-term study arm is quite short, for an informed statement regarding the relationships between clinical outcome and microbiome indices in the long run. Given the missing significant changes in FEV_1 % predicted and inflammation together with the dynamic of the microbiome in the short-term, even though the comparable high number of samples (≥ 3) within the study period. Further, the results of the study were profoundly affected by the patient's condition at the baseline visit. Patients which already at the beginning harbored a chronic infection, paired with a low FEV_1 % predicted do not show any significant changes within those parameters over time, given their end-stage like disease status. A patient cohort with a comparably good lung function together with a highly diverse microbiome at the beginning of the study is therefore preferable if the time related progression of the disease should be assessed. This implies focusing on a younger cohort, within a reliable sample acquisition can be problematic. The relationship of microbiome structure and lung function seems to be non-linear, given the fact that the influence of the microbiome within patients whose FEV_1 % predicted declined from high to mid is less pronounced, than within patients whose FEV_1 % predicted declines from mid to low. A finding which Zhao and colleagues had described earlier (Zhao et al. 2012). They observed six patients over a period of 8-9 years, within that time, half of the patients with a mild lung disease (FEV_1 % predicted > 70) showed a stable α-diversity throughout, with two of the three patients having a low but stable α-diversity (Zhao et al. 2012). Hence, to measure the α-diversity alone is not enough for a conclusion concerning the disease status (Zhao et al. 2012).

Spontaneous sputum samples are noninvasive, though sufficient for longitudinal studies

Compared to BALf or brushes, sputum sampling is less invasive, however it has a larger geographical variability which could explain the temporal variations described (Raghuvanshi et al. 2020). The FEV_1 % predicted is more general and therefore a good parameter to assess the whole lung integrity. Nevertheless, with both parameters' significant associations over the long-term study interval were found. Hence, for a longitudinal examination spontaneous sputum is the preferred sample type which is besides more tolerable for the patients, allowing iterative sampling and is sufficient to evaluate the lung microbiome structure. Spontaneously expectorated sputum of CF patients has been described being contaminated only in a small extend, making it superior compared to other sample acquisition techniques (Cuthbertson et al. 2020; Hogan et al. 2016).

4.2 Small molecule FRET flow cytometry

NE secretion is a major hallmark for obstructive lung diseases and has been associated with lung damage severity in CF (Dittrich et al. 2018; Hagner et al. 2020). However, NE is a highly cationic protein, wherefore a substantial proportion binds via electrostatic interactions to the neutrophil surface (Owen et al. 1997; Campbell und Owen 2007). This surface-bound fraction of NE has been shown to have proteolytic activity and is not antagonized by endogenous anti-proteases (Owen et al. 1997, 1995; Korkmaz et al. 2008b). Moreover, long before free NE activity becomes detectable, surface bound NE can be detected and accordingly has is has been shown to be elevated already in young children with CF (Margaroli et al. 2019; Gehrig et al. 2014). Accordingly, surface-bound NE activity plays a key role in pathogenesis and may be used as a potential novel biomarker of CF lung.

In this work, a new flow cytometric based method for the quantification of the FRET probe NEmo-2E cleavage was established to allow direct, rapid and dynamic measurement of membrane associated NE activity on viable airway neutrophils. In contrast to the previously used confocal set up, the new approach offers several advantages. It is less time-consuming and allows to analyze more cells in less time, compared to the tedious and time consuming microscopy based procedure (Korkmaz et al. 2008a). Further, microscopic neutrophil evaluation is often difficult or impossible as sputum samples, especially induced sputum, is often contaminated by epithelial cells from the oral cavity (Kelly et al. 2001; Amado et al. 2019) which overlay the neutrophils. At the flow cytometer, however, neutrophils could be specifically selected by a gating strategy, which was based on their surface marker expression. Moreover, the information from surface markers allowed phenotyping of the cells and revealed extra information about the neutrophil

activation status. Additionally, implementation of a live/dead marker ensured that only viable neutrophils were selected as they are highly fragile and are prone to get apoptotic or die rapidly during or after their isolation from the bio-sample. In the last step, it has been shown, for the first time, that samples from healthy controls as well as sputum from CF and COPD patients can be analyzed using the new method; further studies must now demonstrate the practicability. To make the assay attractive for a clinical application, an important next step would be to evaluate if the FRET probe could be fixed to tolerate a short-term storage. This would allow to collect samples for several days and to analysis them all together. Moreover, the new approach might be of interest to monitor pulmonary inflammation in lung diseases to better understand the short-term response to antibiotics in clinical studies. This would be particularly useful in the context of the new modulator therapy.

4.2.1 The redefined methodology allows a faster and more robust quantification of membrane associated NE activity

When membrane associated NE activity was measured with NEmo-2E with the flow cytometer, a correlation with FEV_1 % predicted could be found, which was, however, not apparent when samples were analyzed with confocal microscopy. This might be explained by the huge spread among samples in the microscopic analysis (Figure 19f-g). Furthermore, some of the microscopic samples were even below the D/A ratio of the negative control (< 1), although, excessive amounts of inhibitor were added. This can, to some extent, be explained since the inhibitor stock contains dimethyl sulfoxide which is a cytotoxic solvent. Accordingly, a marginal higher percentage of dead cells was observed in samples with inhibitor in contrast to those without inhibitor. These apoptotic cells are influencing the result of the confocal measurement, whereas at the flow cytometer these cells can be excluded by gating. Currently, the sm FRET flow cytometry procedure is set up in a way that the same sample is measured twice, at the 0 min and 10 min time point. However, also kinetics profiles can be established, by an increased number of measurements over time as shown in Figure 19c. This may be of interest, when characterizing novel inhibitors.

The plate reader-based characterization on HL-60 cells of the two NEmo-2 variants yielded comparable results (Figure 16). However, during experiments on sputum neutrophils of CF patients, the NEmo-2G variant showed a reduced dynamic range (Figure 16). To some degree, this may be explained by the additional negative charge of the glutamic acid which could lead to a slightly different folding or three-dimensional assembly of the probe in a native sputum environment, resulting in a decreased accessibility for the target enzyme. Although the NEmo reporter was only modified in off target regions, this can still have a tremendous effect on its sensitivity and specificity. Thus, several NE inhibitors were added

to prove, that the reporter was specifically cleaved by NE. Out of the tested inhibitors, sivelestat led to the greatest reduction in reporter cleavage (Figure 23). Intriguingly, application of protease inhibitor cocktail tablets which antagonize of a wide-ranging spectrum of serine, cysteine and metalloproteases as well as calpains, no complete inhibition was although a concentration, several times higher as the one recommended, was used (Roche Diagnostics 2020). Within this study, NEmo reporters were specific regarding NE activity detection. However, an important factor for FRET probe specificity and selectivity is the context in which the probe is used (Lentz 2020), this should be considered if other sample types are investigated, NEmo sensitivity and specificity needs to be revalidated. Regarding smaller probe concentration differences, between samples or replicates, this is a minor issue in context of the NEmo reporters given the ratiometric properties leading to an concentration independent signal (Gehrig et al. 2012).

Besides of expectorated sputum samples a series of experiments based on BALf samples was performed. Analysis of cells derived from BALf are possible per se, however, for the flushing of the airways, prewarmed NaCl solution has to be used, which is not well tolerated by the neutrophils regarding their survival. Second, caused by the suction, which is necessary to remove the flushing solution from the airways, cells encounter shear forces which are rather prejudicial for cell survival. Third, the quality of these samples varied considerably (Hetzel et al. 2021). Therefore, during BALf sample preparation, storage time should be reduced to the minimum and the storage temperature has to be monitored closely.

4.2.2 Characterization of airway secretions of CF and COPD patients alongside with healthy controls

The cause for COPD and CF are different however, there they share certain similarities in their symptoms, such as mucus accumulation, chronic inflammation and chronic infection (Eickmeier et al. 2010). For this reason, microbiome structure, NE activity, inflammatory markers and clinical parameters were examined more closely and compared among the two diseases.

Neutrophil and eosinophil counts are significantly different in CF and COPD sputum samples

First, cytological preparations were evaluated regarding the cell type distributions as well as the total cell number. As expected, for healthy controls, macrophages were the major cell type, whereas in CF the percentage of neutrophils was elevated and in advanced COPD (GOLD III-IV) COPD the percentages of eosinophils. These findings are in agreement with published data (Byrne et al. 2015; Downey et al. 2009; Tashkin und Wechsler 2018). The increased abundance of eosinophils in airway secretions of COPD

patients has been linked to an elevated risk of exacerbations and better responsiveness to therapy with inhaled corticoids (Tashkin und Wechsler 2018). Total cell numbers were comparable in both diseases, but regarding the cells per gram of sputum, CF patients showed a higher cell density. However, this should be considered as a quality parameter rather than a conclusive finding. The divergence in cells per gram sputum may be the result of the sputum rheology, with samples of healthy controls having the lowest viscoelasticity followed by COPD and CF (Patarin et al. 2020). The levels of LTB_4 were significantly elevated in CF, which is accordance with the higher neutrophil recruitment observed. Earlier publications, stated a diminished chemotaxis of CF derived neutrophils compared to non-CF neutrophils after stimulation with LTB_4 (Lawrence und Sorrelli 1992). Further, an accumulation of LTB_4 in the lung has been shown to be inducible by intranasal challenge with elastase causing gradually worsening of emphysema (Shim et al. 2010). Therefore, the crucial role of LTB_4 in context of the structural lung damage progression, especially in form of bronchiectasis in CF has been related to neutrophilic inflammation in a mouse model (Shim et al. 2010).

***P. aeruginosa* dominated microbiota are associated with CF**

The cohort was separated in three cluster, given the result of the Gap statistics (Figure S1), by kmean clustering of the Unifrac weighted distances of the ASVs. All healthy samples gathered in cluster 1, COPD samples in clusters 1 & 2 and CF samples were spread among all three clusters. Cluster 1 was characterized by microbes from the oropharyngeal cavity, while samples in cluster 2 harbored a dominant pathogen, such as *Haemophilus*, *Streptococcus*, *Lactobacillus* or *Veillonella* as well as *Staphylococcus*, *Achromobacter* and *Neisseria* for COPD and CF samples respectively. Samples in cluster 3 showed an increased relative abundance of *P. aeruginosa*. The presence of S. auerus was in the COPD samples lower compared to the CF samples assigned to the same cluster. This may be explained by the age discrepancy between the CF and COPD patients, given that *S. aureus* infections are more common in young CF patients (Hurley und Smyth 2018). *S. aureus* is one of the first pathogens acquired by CF patients during childhood or adolescence, presumable due to the high abundance on skin and the upper respiratory tract (Fenker et al. 2018). With a progressing disease, *S. aureus* is often outgrown by *P. aeruginosa* a pathogen that significantly accelerates disease progression and is more difficult to treat. (Høiby 1993). In contrast to CF, in COPD patients infections with *P. aeruginosa* are less common but if they occur they lead to a substantial loss of the lung function (Crull et al. 2016).

Healthy-like microbiota of CF and COPD patients are less divers compared to the microbiota of healthy controls

A closer look regarding the parameters of the microbiome indicated, that the healthy-like CF and COPD samples assigned to cluster 1 were not healthy but showed a significant reduction in α-diversity. Along the increase in α-diversity also richness and evenness of the microbiome declined while the dominance increased. This change in the parameter become more evident with increasing cluster number. The imbalance of the microbiome went along with changes in the levels of inflammatory parameters. IL-1β and TGF-β1 were significantly higher within cluster 1, or showing strong trends in almost all disease related clusters. For IL-8, strong trends towards an upregulation throughout the five patient clusters was observed. In accordance with the inflammatory parameter findings, free NE was, except for cluster COPD 2, significantly higher in all disease related clusters. The constant release of IL-8 may mobilize more neutrophils to the site of infection whereas the excessive amounts of NE may harm the surrounding tissue (Giacalone et al. 2020b). Regarding membrane associated NE, increased levels were observed for the COPD clusters and significance was reached for the CF clusters. These findings have been confirmed in the correlations of the whole cohort, where several bacteria showed a beneficial effect regarding inflammation and microbiome indices.

Some cytokines are disease specific and microbiome independent

There were certain discrepancies between COPD and CF clusters independent of the microbiome structure. Levels of TGF-β1 tended to be higher in CF clusters compared to those of COPD. TGF-β1 is a key mediator of fibrosis, which can inhibit the CFTR mRNA in human bronchial epithelial cells of patients with various kind of chronic airway disease including idiopathic pulmonary fibrosis, CF and COPD (Mitash et al. 2019). Further IL-10 was found to be downregulated in CF and was also lower than in healthy controls. In contrast, IL-5 and IL-6 were elevated in COPD. The comparison of the NE fractions between CF and COPD patients showed, that the average free NE activity in samples of CF patients was in comparison to COPD patients almost 3 times higher, but the membrane associated NE activity was not significantly different (Figure 28). Hence, a significant decrease of free NE is beneficial for the patient, but this is not necessarily accompanied by a reduction in the considerably more harmful membrane associated NE fraction (Owen 2008). Given the discrepancy between the soluble fraction, levels of healthy individuals were >65-fold and >200-fold lower in comparison to COPD and CF patients, respectively. The membrane associated NE was in the two disease groups >1.5-fold higher, compared to healthy controls. However, with a p-value of 0.04 significance could have been reached if all CF and COPD clusters would be pooled (Figure S4). Endogenous anti-proteases were comparable between CF and COPD with exception of SLPI which was significantly higher in COPD. This can be explained with the higher levels of free NE in CF samples

which can cleave SLPI (Weldon et al. 2009). Important, the assay chosen, only detects the intact molecule, not the cleaved form. The lower levels of CD16 indicate a higher activation of neutrophils with increasing cluster number, with neutrophils of *P. aeruginosa* positive patients being most activated and prone towards apoptosis (Moulding et al. 1999). Further, *P. aeruginosa* secretes several proteases, of which pseudolysin also known as zinc metalloproteinase elastase B, is the most abundant one (Galdino et al. 2019). Pseudolysin has been linked to disease progression of chronic lung disease as it was found in airway secretions of COPD patients during pulmonary exacerbations and of CF patients (Murphy et al. 2008; Storey et al. 1992). In excessive concentrations, pseudolysin has the capability to truncate SLPI, which is locally secreted (Johnson et al. 1982). Besides, pseudolysin was associated with reduced expression and activity of CFTR in epithelial cells, shown to interfere with the immune response leading to tissue injury (Bastaert et al. 2018; Ruffin und Brochiero 2019; Saint-Criq et al. 2018). Thus, pseudolysin is probably one reason for a compromised immune response within the lung, which foresters a persistent infection with *P. aeruginosa*, especially for CF patients (Cigana et al. 2020).

Markers assigned to CF have a negative effect on microbiome composition and lung function

In CF, levels of FEV_1 % predicted were higher compared to COPD which can to a certain extent be explained by the tremendous age difference as well as the GOLD stages of the COPD cohort. Interestingly, there was a trend that patients of the COPD 2 cluster showed a better lung function than patients of the COPD 1 cluster which have a healthier microbiome. However, the inverse trend was observed regarding the CF clusters, with individuals assigned to cluster CF 3 having the most severe lung function decline. The hierarchical clustering of the correlation between microbiome indices to other parameters evaluated revealed that higher levels of IL-5, IL-10 and CD16 as well as a higher abundance of macrophages significantly correlated to a more diverse microbiome structure. Furthermore, elevated pro-inflammatory markers as TNF-α, IL-8 and free NE were inversely associated with microbiome diversity. All of the pro-inflammatory markers mentioned could be directly linked to the abundance of *Pseudomonas*, which further highlights the importance to closely monitor the key pathogens regarding the disease progression.

16S rRNA gene-based metagenomics are sufficient to prove correlations between ASVs to airway inflammation and lung function in sputum samples

In the study of Wang at al. the microbiome structure of COPD patients was not only investigated at a species level but also at the level of strains (Wang et al. 2020). They describe two specific clusters of interactions between inflammatory parameters of the host and bacterial species, related to two inflammatory phenotypes which are specific for

COPD, the eosinophilic and neutrophilic inflammation (Balzano et al. 1999; Saha und Brightling 2006). They found that species of the same taxonomic group can lead to a misinterpretation given the “low” resolution (Zander 2001; Wang et al. 2020). Hence, *Neisseria mucosa* as example was increased in COPD whereas *Neisseria subflava* was significantly decreased (Wang et al. 2020). According to the results, they found a decreased α-diversity in the COPD patients compared to healthy controls (Wang et al. 2020). However, there is a difference in GOLD status between the two studies, Wang et al. included patients of all GOLD stages, whereas in this study only patients with GOLD stage III-IV were included. By applying unsupervised clustering they identified four clusters, a pro-inflammatory, neutrophilic, anti-inflammatory and eosinophilic (Wang et al. 2020). In accordance to this, *P. aeruginosa* was assigned to the neutrophilic group and correlated significantly to IL-1β and IL-8 whereas IL-5 was linked to the eosinophilic cluster. By comparing the fold change regarding specific RSVs certain species could be directly associated with specific disease groups, such as *Alloprevotella* sp. (rsv200) and *Neisseria oralis* (rsv657), *Dolosigranulum pigrum* (rsv716) and *Oceanivirga* sp. (rsv657) as well as *P. aeruginosa* (rsv101), *Staphylococcus* sp. (722), *Prevotella melaninogenica* & *nanceiensis* (rsv165 & 183) to healthy controls, COPD and CF, respectively (Figure 35). The correlations of Wang et al. were based on a cohort of 59 patients of COPD patients only whereas here 66 patients including CF, COPD and healthy controls were included. Nevertheless, the correlations of inflammatory key parameters to pathogens assigned to a neutrophilic or eosinophilic inflammation were consistent independent of the study and sequencing depth, interestingly the spearman’s rho of this study were more profound.

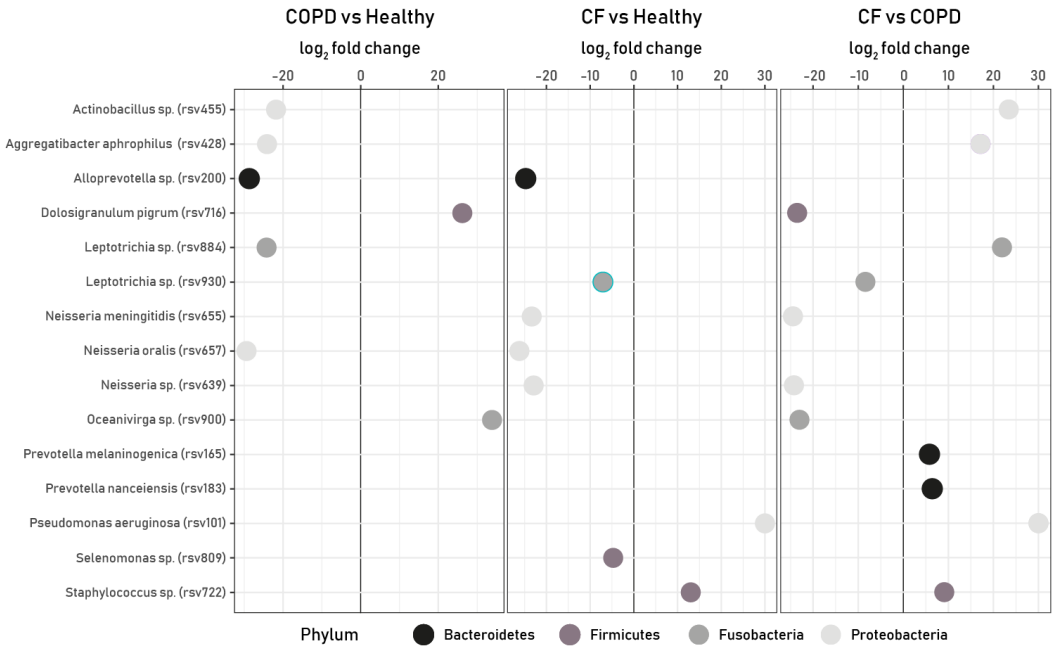

Figure 35: Comparison of the RSV abundance of the three pairwise comparisons between healthy, COPD and CF. Log_2 fold change difference of the top 15 RSVs. A positive fold change belongs to the first group mentioned. The color of the dots represents the phylum of the RSVs.

Neutrophil activation and degranulation pathways are upregulated in CF and COPD sputum sample supernatants

With four of the top five biological processes being directly liked to neutrophils, the results of the secretomics experiments, further strengthen the importance to regulate neutrophil recruitment and granule release. S100A8 and S100A9, together forming the calprotectin complex, have been identified in serum of CF patients as predictor of pulmonary exacerbations (Jung et al. 2020). Besides, calprotectin can starve *P. aeruginosa* and *S. aureus* from iron, which in case of *P. aeruginosa* limits its ability to fight *S. aureus* which is a highly iron depending mechanism (Nguyen et al. 2015). Hence, the starvation of iron leads to a utilization of heme and has been correlated negatively to FEV_1 % predicted (Glasser et al. 2019).

Moreover, the eosinophilic cationic protein (ECP) an eosinophilic granule protein, which exhibits antimicrobial activity against Gram-positive and Gram-negative bacteria can disrupt the membrane and can be expressed by neutrophils to a certain extent (Torrent et al. 2009). ECP has been described to be elevated in CF sputum compared to patient's asthma and healthy controls, even though the eosinophil abundance is relatively low (Koller et al. 1995; Koller et al. 1994). This hints towards an upregulation of granule release in CF potentially due to a common priming mechanism (Giacalone et al. 2020a).

The release of granules by neutrophils was targeted a couple of years ago, in an interesting study characterizing neutrophil exocytosis inhibitors (Johnson et al. 2016). The described molecules blocked the interaction of the small GTPase Rab27a and its effector JFC1, which are both master regulators of neutrophil exocytosis. Of note, the described molecules were capable of preventing the primary granule release, whereas microbial killing, phagocytosis as well as NETosis were not affected. Further, the upregulation of markers as CD66b and CD11b were inhibited, whereas the number of neutrophils released from the bone marrow was not affected (Johnson et al. 2016). This is in accordance to the suggestion of Margaroli et al. to rather regulate the functionality of neutrophils than hindering neutrophil recruitment (Margaroli und Tirouvanziam 2016). Considering the potential adverse effects within the lung environment and the different fraction of NE found either in the soluble or membrane associated fraction or associated to DNA filaments such as in NETs, this is difficult (Margaroli und Tirouvanziam 2016). However, this could be an attractive approach to tackle the overwhelming inflammation within the airways. The major challenge will most likely be to get the inhibitor to the side of inflammation, given the fact that other tissues should not be affected. This means a systemic use as for example intravenous application is not an option, whereas inhalation-based therapy's has shown to not always reach a sufficient concentration in the lungs, as revealed by several A1AT studies (Gaggar et al. 2016; McElvaney et al. 1991).

4.2.3 Potential applications for NE activity evaluation

So far the NEmo reporters have mainly been applied within the context of CF (Dittrich et al. 2018; Frey et al. 2021a; Graeber et al. 2021). As described in section 3.2.4 it has been demonstrated for the first time that an application in another disease as for example COPD is feasible.

Taking the results of previous studies (Margaroli et al. 2019; Dittrich et al. 2018) and the findings of CF and COPD patients into consideration, it was shown, that the membrane associated NE activity reaches a plateau before soluble NE activity, hence, a drastically reduction in soluble NE activity is not necessarily associated with a decrease of membrane associated NE activity. Accordingly, future assessments on NE should also implement measurements on the more harmful membrane associated NE activity.

Further potential applications of NE activity measurements is in studies which evaluate the effect of novel drugs. Anakinra is an IL-1R antagonist that blocks IL-1α/β activity and is currently prescribed to patients with cryopyrin-associated periodic syndromes and rheumatoid arthritis (Cavalli und Dinarello 2018) but has also shown promising results in treatment of COVID19 (Huet et al. 2020; Cavalli et al. 2020). A study to evaluate safety and efficacy of subcutaneous administration of anakinra in patients with CF (ANAKIN; NCT03925194) had to be put on hold due to the coronavirus pandemic. Within this study, evaluation of free and membrane associated NE activities utilizing the here established NEmo reporters was planned as secondary endpoint.

Moreover, NE and pro-inflammatory measurements were included to assess effects of Ivacaftor/Lumacaftor on airway inflammation (Graeber et al. 2021). A similar approach may be of high interest to study neutrophilic inflammation and activity during medication with the very recently approved triple combination Ivacaftor/Tezacaftor/Elexacaftor. However, in a planned large study on the effects of the new treatment, membrane associated NE is not among the parameters which will be evaluated (Nichols et al. 2021). Lately, NE activity was investigated in an case report, which compared in a 1.5-year lasting longitudinal study two siblings with one-year age difference, both homozygous for F508del (Zhang et al. 2021). Even though they were exposed to the same environment, they differed in CF severity. The more sick sibling was treated with Ivacaftor/Lumacaftor during the study period, nevertheless it experience a higher decline in lung function alongside with elevated inflammatory markers as free NE (> 2-fold between the siblings) and IL-8 measured in sputum samples (Zhang et al. 2021).

Coronavirus disease 2019 (COVID-19) is associated with a cytokine storm consisting among others of IL-1β and TNF-α, which are also key parameters of CF (Huet et al. 2020).

Further, it has been reported, that in COVID-19 NE is linked to host cell invasion, lung tissue damage and pathogenesis. Moreover, NE-activity was assessed among other inflammatory markers to show a promising effect upon treatment with the intravenously applied A1AT inflammatory mediator in a CF patient who got infected with COVID-19 (McElvaney et al. 2021).

Phol and collegues found that a functional CFTR is crucial for an intact ion balance of neutrophils (Pohl et al. 2014). Thus, it may be of interest to study if this could modify NE association to neutrophil surface.

4.2.4 NE quantity can be measured by multiple assay formats, while NEmo reporters can provide further information regarding NE activity

Detection of NE in the soluble fraction demonstrated that, regardless whether the NE activity was measured with the FRET reporter NEmo-1 or the enzyme was quantified using western blot or mass spectroscopy (MS), findings were in accordance. Compared to western blot and MS, FRET measurement is significantly faster. Equipment wise western blot and the plate reader-based NEmo-1 measurement are the cheapest options, but MS has the highest resolution (Figure 34). With the plate reader set up, up to 20 samples duplicates can be analyzed in parallel and a minimal hands-on time is required. Further, instead of the enzyme quantity the activity can be detected. The plate reader set up is probably the best approach to perform screening experiments regarding treatments with novel molecules or to perform titrations. The MS based approach offers an unbiased analysis of various proteins. In summary, via NEmo-1 the NE activity can be quantified, which is especially in a clinical setting the more informative measure in contrast NE quantification alone where no information concerning the enzymatically active proportion of NE can be derived.

4.2.5 Is it enough to monitor NE activity alone or are there probes for NSPs available?

Besides free and membrane associated NE, a third “fraction” of NE is associated to NETs which occur as a specific defense strategy of neutrophils, in which they secrete web like structures consisting of their chromatin (Fuchs et al. 2007; Brinkmann et al. 2004). NETs have also been described to be involved in abnormal rheology of the mucus in CF patients (Patarin et al. 2020), to damage the synovial tissue of the joints from rheumatic patients, endorse thrombosis in vessels of atherosclerosis patients and as initiators for gallstone formation (Porto und Stein 2016; Döring et al. 2020; Corsiero et al. 2016; Muñoz et al. 2019). Moreover, enzymatically active CTSG has been found associated to the surface of neutrophils and has been related to an elevated risk of COPD (Guerra et al. 2019). Chronic inflammatory diseases are orchestrated by several enzymes or factors (Chen et al. 2018;

Bennett et al. 2018) wherefore a probe detecting several enzymes or factors at once would allow a more detailed understanding of highly complex processes (Wu et al. 2020). Yang et al. and Wysocka et al. described FRET probes which allows the measurement of three different enzymes in parallel (Yang et al. 2015; Wysocka et al. 2012). Wysocka compared levels of NE, PR3 and GTSG simultaneously in patients suffering from granulomatosis with polyangiitis (GPD), that have inflamed kidneys and blood vessel with healthy individuals (Wysocka et al. 2012). Levels of CTSG were almost identical, NE was 2-fold increased whereas levels of PR3 showed a 10-fold increase compared to healthy individuals (Wysocka et al. 2012). For CF and COPD, especially probes paired with a lipid anchor and perhaps to detect the inflammatory enzymes NE, CTSG and MMP12 could be a promising approach. With this approach different enzymes such as trypsin- and chymotrypsin serine proteases and a matrix metalloproteinase could be assessed in parallel.

The latest version of the probe designed by Craven and colleagues that depending on its localization can detect several processes which are unique during neutrophil activation. These include, phagosomal alkalinisation, pinocytosis and NE activity (Craven et al. 2021). This reporter can even be used during bronchoscopy via optical endomicroscopy (Craven et al. 2021).

Activity based probes such as NEmo-2E which can be analyzed by flow cytometric approaches which are highly effective tools to differentiate immune cell sub-populations (Burster et al. 2021). Further, the activity measurement of the individual enzymes and efficacy of administered inhibitors can be assessed rapidly and easily (Burster et al. 2021).

5 Conclusions and further perspectives

This study revealed, that patients with chronic obstructive lung diseases such as CF and COPD have an alternated airway microbiome, an increased inflammatory response and a decline in lung function. For an adequate treatment of these patients, it is therefore crucial to understand the relations and interdependencies of these factors. According the results of the cross-sectional study, CF patients with a diverse microbiome, containing a high prevalence but low abundance of commensals, showed the best FEV_1 % predicted and the lowest level of inflammation. In contrast, patients with a microbiome dominated by *P. aeruginosa* showed a low α-diversity which was linked to a lower FEV_1 % predicted and increased levels of inflammatory markers. The knowledge of this interplay may be a first step towards the development of improved diagnostics and more targeted therapeutic interventions for the polymicrobial airway infection in patients with CF. Moreover, results of this study suggest that both, correlation analyses and hierarchical clustering should be performed to provide a clearer and more precise understanding of the relation between microbiome and clinical parameters.

The longitudinal study, provided an extensive time-resolved, detailed evaluation including the evaluation of the microbiome structure, various relevant cytokines, major anti-proteases, free NE activity, BMI, and FEV_1 % predicted, which has not been described before in a comparably cohort size. Assessment of the results revealed that changes in lung function and inflammation correlated strongly to the intra-patient variability. This implies that a rapid decline in lung function and a serious increase of inflammatory markers are caused by a massive change in the microbiome. The long-term evolution of the microbiome correlates with the host factors indicating that microbiome changes occurred over a longer time interval, which can be obscured by short-term variability of the microbiome. Thus, it might be of interest to investigate in future studies whether the short-term fluctuations are associated with exacerbations or whether these can be even predicted.

With the novel approach based on flow cytometry, an additional methodology to detect membrane associated NE activity has been described. By including various relevant highly specific inhibitors, a predominately cleavage of NEmo-2E by NE in the context of highly complex samples was evidently confirmed. The observed discrepancies between the soluble and membrane associated NE activity within CF and COPD patients highlights the necessity to not exclusively rely on the activity measured within the sputum supernatants, but rather include the membrane associated NE activity on the surface of airway neutrophils in the assessment of the inflammatory situation. Accordingly, the routine measurement of membrane associated NE may allows an earlier detection of a pulmonary exacerbation and therefore an earlier intervention to prevent tissue damage. As smokers are at risk to acquire COPD, it may be of interest if they have elevated NE levels and if

measurements of NE activity may be a useful parameter at routine checks to predict risk to develop COPD.

With NEmo-1 and NEmo-2E the NE activity of two important compartments in airway secretions can be measured with several assay formats allowing a high level of flexibility to address a wide spectrum of scientific questions, especially at early stages of airway inflammation. In addition, the procedures are applied to non-invasive samples which allows repetitive sampling of the same patient with a low risk for adverse events. The novel methodology can be easily transferred to other labs or even a clinical environment, thereby, allowing more comprehensive studies of membrane associated NE and the relationship to lung disease progression and severity. As a versatile translational research tool, it could be further helpful to monitor responses regarding neutrophil activation and NE activity upon therapy. This could be of special interest for the treatment of CF patients with the triple combination of Ivacaftor/Tezacaftor/Elexacaftor since ~90 % of CF patients are eligible for this therapy. Moreover, the novel set up maybe used to investigate if a treatment with anakinra leads to decreased membrane associated NE activity as it has been already demonstrated for free NE activity.

6 References

Abdullah, L. H.; Coakley, R.; Webster, M. J.; Zhu, Y.; Tarran, R.; Radicioni, G. et al. (2018): Mucin Production and Hydration Responses to Mucopurulent Materials in Normal versus Cystic Fibrosis Airway Epithelia. In: *American journal of respiratory and critical care medicine* 197 (4), S. 481–491.

Adlerova, L.; Bartoskova, A.; Faldyna, M. (2008): Lactoferrin: a review. In: *Veterinarni Medicina* 53 (9), S. 457–468.

Al Alam D.; Danopoulos, S.; Grubbs, B.; Ali, N. A. B. M.; MacAogain, M.; Chotirmall, S. H. et al. (2020): Human Fetal Lungs Harbor a Microbiome Signature. In: *American journal of respiratory and critical care medicine*.

Amado, F.; Calheiros-Lobo, M. J.; Ferreira, R.; Vitorino, R. (2019): Sample Treatment for Saliva Proteomics. In: *Advances in experimental medicine and biology* 1073, S. 23–56.

Anderson, M. P.; Gregory, R. J.; Thompson, S.; Souza, D. W.; Paul, S.; Mulligan, R. C. et al. (1991): Demonstration that CFTR is a chloride channel by alteration of its anion selectivity. In: *Science (New York, N.Y.)* 253 (5016), S. 202–205.

Arkwright, P. D.; Laurie, S.; Super, M.; Pravica, V.; Schwarz, M. J.; Webb, A. K.; Hutchinson, I. V. (2000): TGF-beta(1) genotype and accelerated decline in lung function of patients with cystic fibrosis. In: *Thorax* 55 (6), S. 459–462.

Armbruster, C. R.; Wolter, D. J.; Mishra, M.; Hayden, H. S.; Radey, M. C.; Merrihew, G. et al. (2016): Staphylococcus aureus Protein A Mediates Interspecies Interactions at the Cell Surface of Pseudomonas aeruginosa. In: *mBio* 7 (3).

Aronsen, K. F.; Ekelund, G.; Kindmark, C. O.; Laurell, C. B. (1972): Sequential changes of plasma proteins after surgical trauma. In: *Scandinavian journal of clinical and laboratory investigation. Supplementum* 124, S. 127–136.

Baggiolini, M.; Dewald, B.; Moser, B. (1993): Interleukin-8 and Related Chemotactic Cytokines—CXC and CC Chemokines. In: Frank J. Dixon (Hg.): Advances in Immunology, Bd. 55. 1. Aufl. s.l.: Elsevier textbooks (Advances in Immunology, v.55), S. 97–179.

Balázs, A.; Mall, M. A. (2019): Mucus obstruction and inflammation in early cystic fibrosis lung disease: Emerging role of the IL-1 signaling pathway. In: *Pediatric pulmonology* 54 Suppl 3, S5-S12.

Balmes, J.; Becklake, M.; Blanc, P.; Henneberger, P.; Kreiss, K.; Mapp, C. et al. (2003): American Thoracic Society Statement: Occupational contribution to the burden of airway disease. In: *American journal of respiratory and critical care medicine* 167 (5), S. 787–797.

Balzano, G.; Stefanelli, F.; Iorio, C.; Felice, A. de; Melillo, E. M.; Martucci, M.; Melillo, G. (1999): Eosinophilic inflammation in stable chronic obstructive pulmonary disease. Relationship with neutrophils and airway function. In: *American journal of respiratory and critical care medicine* 160 (5 Pt 1), S. 1486–1492.

Bartell, J. A.; Cameron, D. R.; Mojsoska, B.; Haagensen, J. A. J.; Pressler, T.; Sommer, L. M. et al. (2020a): Bacterial persisters in long-term infection: Emergence and fitness in a complex host environment. In: *PLoS pathogens* 16 (12), e1009112.

Bartell, J. A.; Sommer, L. M.; Marvig, R. L.; Skov, M.; Pressler, T.; Molin, S.; Johansen, H. K. (2020b): Omics-based tracking of Pseudomonas aeruginosa persistence in "eradicated" CF patients. In: *The European respiratory journal*.

Bartoli, M. L.; Di Franco, A.; Vagaggini, B.; Bacci, E.; Cianchetti, S.; Dente, F. L. et al. (2009): Biological markers in induced sputum of patients with different phenotypes of chronic airway obstruction. In: *Respiration; international review of thoracic diseases* 77 (3), S. 265–272.

Bastaert, F.; Kheir, S.; Saint-Criq, V.; Villeret, B.; Dang, P. M.-C.; El-Benna, J. et al. (2018): Pseudomonas aeruginosa LasB Subverts Alveolar Macrophage Activity by Interfering with Bacterial Killing Through Downregulation of Innate Immune Defense, Reactive Oxygen Species Generation, and Complement Activation. In: *Frontiers in Immunology* 9, S. 1675.

Bates, D.; Mächler, M.; Bolker, B.; Walker, S. (2015): Fitting Linear Mixed-Effects Models Using lme4. In: *Journal of Statistical Software* 67 (1).

Bear, C. E. (2020): A Therapy for Most with Cystic Fibrosis. In: *Cell* 180 (2), S. 211.

Belaaouaj, A.; Kim, K. S.; Shapiro, S. D. (2000): Degradation of outer membrane protein A in Escherichia coli killing by neutrophil elastase. In: *Science (New York, N.Y.)* 289 (5482), S. 1185–1188.

Bell, S. C.; Mall, M. A.; Gutierrez, H.; Macek, M.; Madge, S.; Davies, J. C. et al. (2020): The future of cystic fibrosis care: a global perspective. In: *The Lancet Respiratory Medicine* 8 (1), S. 65–124.

Bennett, J. M.; Reeves, G.; Billman, G. E.; Sturmberg, J. P. (2018): Inflammation-Nature's Way to Efficiently Respond to All Types of Challenges: Implications for Understanding and Managing "the Epidemic" of Chronic Diseases. In: *Frontiers in Medicine* 5, S. 316.

Birrer, P.; McElvaney, N. G.; Rüdeberg, A.; Sommer, C. W.; Liechti-Gallati, S.; Kraemer, R. et al. (1994): Protease-antiprotease imbalance in the lungs of children with cystic fibrosis. In: *American journal of respiratory and critical care medicine* 150 (1), S. 207–213.

Black, R. A.; Rauch, C. T.; Kozlosky, C. J.; Peschon, J. J.; Slack, J. L.; Wolfson, M. F. et al. (1997): A metalloproteinase disintegrin that releases tumour-necrosis factor-alpha from cells. In: *Nature* 385 (6618), S. 729–733.

Blobe, G. C.; Schiemann, W. P.; Lodish, H. F.; Epstein, F. H. (2000): Role of Transforming Growth Factor β in Human Disease. In: *New England Journal of Medicine* 342 (18), S. 1350–1358.

Bode, W.; Wei, A. Z.; Huber, R.; Meyer, E.; Travis, J.; Neumann, S. (1986): X-ray crystal structure of the complex of human leukocyte elastase (PMN elastase) and the third domain of the turkey ovomucoid inhibitor. In: *The EMBO journal* 5 (10), S. 2453–2458.

Boeck, K. de (2020): Cystic fibrosis in the year 2020: A disease with a new face. In: *Acta paediatrica*.

Boeck, K. de; Derichs, N.; Fajac, I.; Jonge, H. R. de; Bronsveld, I.; Sermet, I. et al. (2011): New clinical diagnostic procedures for cystic fibrosis in Europe. In: *Journal of Cystic Fibrosis* 10, S53-S66.

Böhm, B.; Aigner, T.; Kinne, R.; Burkhardt, H. (1992): The serine-protease inhibitor of cartilage matrix is not a chondrocytic gene product. In: *European journal of biochemistry* 207 (2), S. 773–779.

Boutin, S.; Dalpke, A. H. (2017): Acquisition and adaptation of the airway microbiota in the early life of cystic fibrosis patients. In: *Molecular and cellular pediatrics* 4 (1), S. 1.

Boutin, S.; Graeber, S. Y.; Stahl, M.; Dittrich, A. S.; Mall, M. A.; Dalpke, A. H. (2017a): Chronic but not intermittent infection with Pseudomonas aeruginosa is associated with global changes of the lung microbiome in cystic fibrosis. In: *The European respiratory journal* 50 (4).

Boutin, S.; Graeber, S. Y.; Weitnauer, M.; Panitz, J.; Stahl, M.; Clausznitzer, D. et al. (2015): Comparison of microbiomes from different niches of upper and lower airways in children and adolescents with cystic fibrosis. In: *PLOS One* 10 (1), e0116029.

Boutin, S.; Hagenfeld, D.; Zimmermann, H.; El Sayed, N.; Höpker, T.; Greiser, H. K. et al. (2017b): Clustering of Subgingival Microbiota Reveals Microbial Disease Ecotypes Associated with Clinical Stages of Periodontitis in a Cross-Sectional Study. In: *Frontiers in Microbiology* 8, S. 340.

Boutin, S.; Weitnauer, M.; Hassel, S.; Graeber, S. Y.; Stahl, M.; Dittrich, A. S. et al. (2018): One time quantitative PCR detection of Pseudomonas aeruginosa to discriminate intermittent from chronic infection in cystic fibrosis. In: *Journal of Cystic Fibrosis* 17 (3), S. 348–355.

Boxio, R.; Wartelle, J.; Nawrocki-Raby, B.; Lagrange, B.; Malleret, L.; Hirche, T. et al. (2016): Neutrophil elastase cleaves epithelial cadherin in acutely injured lung epithelium. In: *Respiratory research* 17 (1), S. 129.

Branzk, N.; Papayannopoulos, V. (2013): Molecular mechanisms regulating NETosis in infection and disease. In: *Seminars in Immunopathology* 35 (4), S. 513–530.

Brinkmann, V.; Reichard, U.; Goosmann, C.; Fauler, B.; Uhlemann, Y.; Weiss, D. S. et al. (2004): Neutrophil extracellular traps kill bacteria. In: *Science (New York, N.Y.)* 303 (5663), S. 1532–1535.

Brinkmann, V.; Zychlinsky, A. (2007): Beneficial suicide: why neutrophils die to make NETs. In: *Nature Reviews Microbiology* 5 (8), S. 577–582.

Brooks, M. E.; Kristensen, K.; van Benthem, K. J.; Magnusson, A.; Berg, C. W.; Nielsen, A. et al. (2017): glmmTMB balances speed and flexibility among packages for zero-inflated generalized linear mixed modeling. In: *The R journal* 9 (2), 378-400.

Bruzzese, E.; Callegari, M. L.; Raia, V.; Viscovo, S.; Scotto, R.; Ferrari, S. et al. (2014): Disrupted intestinal microbiota and intestinal inflammation in children with cystic fibrosis and its restoration with Lactobacillus GG: a randomised clinical trial. In: *PLOS One* 9 (2), e87796.

Bruzzese, E.; Raia, V.; Spagnuolo, M. I.; Volpicelli, M.; Marco, G. de; Maiuri, L.; Guarino, A. (2007): Effect of Lactobacillus GG supplementation on pulmonary exacerbations in patients with cystic fibrosis: a pilot study. In: *Clinical nutrition (Edinburgh, Scotland)* 26 (3), S. 322–328.

Burster, T.; Gärtner, F.; Knippschild, U.; Zhanapiya, A. (2021): Activity-Based Probes to Utilize the Proteolytic Activity of Cathepsin G in Biological Samples. In: *Frontiers in Chemistry* 9, S. 628295.

Butler, M. W.; Robertson, I.; Greene, C. M.; O'Neill, S. J.; Taggart, C. C.; McElvaney, N. G. (2006): Elafin prevents lipopolysaccharide-induced AP-1 and NF-κB activation via an effect on the ubiquitin-proteasome pathway. In: *Journal of Biological Chemistry* 281 (46), S. 34730–34735.

Byrne, A. J.; Mathie, S. A.; Gregory, L. G.; Lloyd, C. M. (2015): Pulmonary macrophages: key players in the innate defence of the airways. In: *Thorax* 70 (12), S. 1189–1196.

Callahan, B. J.; McMurdieE, P. J.; Rosen, M. J.; Han, A. W.; Johnson, A. J. A.; Holmes, S. P. (2016): DADA2: High-resolution sample inference from Illumina amplicon data. In: *Nature methods* 13 (7), S. 581–583.

Campbell, E. J.; Campbell, M. A.; Owen, C. A. (2000): Bioactive Proteinase 3 on the Cell Surface of Human Neutrophils: Quantification, Catalytic Activity, and Susceptibility to Inhibition. In: *The Journal of Immunology* 165 (6), S. 3366–3374.

Campbell, E. J.; Owen, C. A. (2007): The sulfate groups of chondroitin sulfate- and heparan sulfate-containing proteoglycans in neutrophil plasma membranes are novel binding sites for human leukocyte elastase and cathepsin G. In: *Journal of Biological Chemistry* 282 (19), S. 14645–14654.

Carbon, S.; Mungall, C. (2018): Gene Ontology Data Archive.

Carevic, M.; Öz, H.; Fuchs, K.; Laval, J.; Schroth, C.; Frey, N. et al. (2016): CXCR1 Regulates Pulmonary Anti-Pseudomonas Host Defense. In: *Journal of innate immunity* 8 (4), S. 362–373.

Carmody, L. A.; Caverly, L. J.; Foster, B. K.; Rogers, M. A. M.; Kalikin, L. M.; Simon, R. H. et al. (2018): Fluctuations in airway bacterial communities associated with clinical states and disease stages in cystic fibrosis. In: *PLOS One* 13 (3), e0194060.

Castillo, M. J.; Nakajima, K.; Zimmerman, M.; Powers, J. C. (1979): Sensitive substrates for human leukocyte and porcine pancreatic elastase: A study of the merits of various chromophoric and fluorogenic leaving groups in assays for serine proteases. In: *Analytical Biochemistry* 99 (1), S. 53–64.

Cavalli, G.; Dinarello, C. A. (2018): Anakinra Therapy for Non-cancer Inflammatory Diseases. In: *Frontiers in Pharmacology* 9, S. 1157.

Cavalli, G.; Luca, G. de; Campochiaro, C.; Della-Torre, E.; Ripa, M.; Canetti, D. et al. (2020): Interleukin-1 blockade with high-dose anakinra in patients with COVID-19, acute respiratory distress syndrome, and hyperinflammation: a retrospective cohort study. In: *The Lancet Rheumatology* 0 (0).

Centers for Disease Control and Prevention (CDC) (2008): Smoking-attributable mortality, years of potential life lost, and productivity losses--United States, 2000-2004. In: *Morbidity and mortality weekly report* 57 (45), S. 1226–1228.

Chakrabarti, S.; Patel, K. D. (2005): Regulation of matrix metalloproteinase-9 release from IL-8-stimulated human neutrophils. In: *Journal of leukocyte biology* 78 (1), S. 279–288.

Chalmers, J. D.; Moffitt, K. L.; Suarez-Cuartin, G.; Sibila, O.; Finch, S.; Furrie, E. et al. (2017): Neutrophil Elastase Activity Is Associated with Exacerbations and Lung Function Decline in Bronchiectasis. In: *American journal of respiratory and critical care medicine* 195 (10), S. 1384–1393.

Charlson, E. S.; Bittinger, K.; Haas, A. R.; Fitzgerald, A. S.; Frank, I.; Yadav, A. et al. (2011): Topographical continuity of bacterial populations in the healthy human respiratory tract. In: *American journal of respiratory and critical care medicine* 184 (8), S. 957–963.

Chen, L.; Deng, H.; Cui, H.; Fang, J.; Zuo, Z.; Deng, J. et al. (2018): Inflammatory responses and inflammation-associated diseases in organs. In: *Oncotarget* 9 (6), S. 7204–7218.

Chen, P.; Abacherli, L. E.; Nadler, S. T.; Wang, Y.; Li, Q.; Parks, W. C. (2009): MMP7 shedding of syndecan-1 facilitates re-epithelialization by affecting alpha(2)beta(1) integrin activation. In: *PLOS One* 4 (8), e6565.

Chhuon, C.; Pranke, I.; Borot, F.; Tondelier, D.; Lipecka, J.; Fritsch, J. et al. (2016): Changes in lipid raft proteome upon TNF-α stimulation of cystic fibrosis cells. In: *Journal of proteomics* 145, S. 246–253.

Cieutat, A. M.; Lobel, P.; August, J. T.; Kjeldsen, L.; Sengeløv, H.; Borregaard, N.; Bainton, D. F. (1998): Azurophilic granules of human neutrophilic leukocytes are deficient in lysosome-associated membrane proteins but retain the mannose 6-phosphate recognition marker. In: *Blood* 91 (3), S. 1044–1058.

Cigana, C.; Castandet, J.; Sprynski, N.; Melessike, M.; Beyria, L.; Ranucci, S. et al. (2020): Pseudomonas aeruginosa Elastase Contributes to the Establishment of Chronic Lung Colonization and Modulates the Immune Response in a Murine Model. In: *Frontiers in Microbiology* 11, S. 620819.

Clark, J. M.; Vaughan, D. W.; Aiken, B. M.; Kagan, H. M. (1980): Elastase-like enzymes in human neutrophils localized by ultrastructural cytochemistry. In: *The Journal of cell biology* 84 (1), S. 102–119.

Coburn, B.; Wang, P. W.; Diaz Caballero, J.; Clark, S. T.; Brahma, V.; Donaldson, S. et al. (2015): Lung microbiota across age and disease stage in cystic fibrosis. In: *Scientific Reports* 5, S. 10241.

Conese, M.; Copreni, E.; Di Gioia, S.; Rinaldis, P. de; Fumarulo, R. (2003): Neutrophil recruitment and airway epithelial cell involvement in chronic cystic fibrosis lung disease. In: *Journal of Cystic Fibrosis* 2 (3), S. 129–135.

Corsiero, E.; Pratesi, F.; Prediletto, E.; Bombardieri, M.; Migliorini, P. (2016): NETosis as Source of Autoantigens in Rheumatoid Arthritis. In: *Frontiers in Immunology* 7.

Cossarizza, A.; Chang, H.-D.; Radbruch, A.; Acs, A.; Adam, D.; Adam-Klages, S. et al. (2019): Guidelines for the use of flow cytometry and cell sorting in immunological studies (second edition). In: *European journal of immunology* 49 (10), S. 1457–1973.

Cox, J.; Hein, M. Y.; Luber, C. A.; Paron, I.; Nagaraj, N.; Mann, M. (2014): Accurate proteome-wide label-free quantification by delayed normalization and maximal peptide ratio extraction, termed MaxLFQ. In: *Molecular & cellular proteomics: MCP* 13 (9), S. 2513–2526.

Cox, M. J.; Allgaier, M.; Taylor, B.; Baek, M. S.; Huang, Y. J.; Daly, R. A. et al. (2010): Airway microbiota and pathogen abundance in age-stratified cystic fibrosis patients. In: *PLOS One* 5 (6), e11044.

Craven, T. H.; Walton, T.; Akram, A. R.; Scholefield, E.; McDonald, N.; Marshall, A. D. L. et al. (2021): Activated neutrophil fluorescent imaging technique for human lungs. In: *Scientific Reports* 11 (1), S. 976.

Crull, M. R.; Ramos, K. J.; Caldwell, E.; Mayer-Hamblett, N.; Aitken, M. L.; Goss, C. H. (2016): Change in Pseudomonas aeruginosa prevalence in cystic fibrosis adults over time. In: *BMC pulmonary medicine* 16 (1), S. 176.

Csardi G; Nepusz T (2006): The igraph software package for complex network research. In: *International Journal Complex Systems* 1695 (5).

Cuthbertson, L.; Rogers, G. B.; Walker, A. W.; Oliver, A.; Green, L. E.; Daniels, T. W. V. et al. (2016): Respiratory microbiota resistance and resilience to pulmonary exacerbation and subsequent antimicrobial intervention. In: *The ISME Journal* 10 (5), S. 1081–1091.

Cuthbertson, L.; Walker, A. W.; Oliver, A. E.; Rogers, G. B.; Rivett, D. W.; Hampton, T. H. et al. (2020): Lung function and microbiota diversity in cystic fibrosis. In: *Microbiome* 8 (1), S. 45.

Dean, R. A.; Overall, C. M. (2007): Proteomics discovery of metalloproteinase substrates in the cellular context by iTRAQ labeling reveals a diverse MMP-2 substrate degradome. In: *Molecular & cellular proteomics: MCP* 6 (4), S. 611–623.

Desrochers, P. E.; Mookhtiar, K.; van Wart, H. E.; Hasty, K. A.; Weiss, S. J. (1992): Proteolytic inactivation of alpha 1-proteinase inhibitor and alpha 1-antichymotrypsin by oxidatively activated human neutrophil metalloproteinases. In: *Journal of Biological Chemistry* 267 (7), S. 5005–5012.

Devaney, J. M.; Greene, C. M.; Taggart, C. C.; Carroll, T. P.; O'Neill, S. J.; McElvaney, N. G. (2003): Neutrophil elastase up-regulates interleukin-8 via toll-like receptor 4. In: *FEBS Letters* 544 (1-3), S. 129–132.

Dickson, R. P.; Erb-Downward, J. R.; Freeman, C. M.; McCloskey, L.; Beck, J. M.; Huffnagle, G. B.; Curtis, J. L. (2015): Spatial Variation in the Healthy Human Lung Microbiome and the Adapted Island Model of Lung Biogeography. In: *Annals of the American Thoracic Society* 12 (6), S. 821–830.

Dickson, R. P.; Erb-Downward, J. R.; Martinez, F. J.; Huffnagle, G. B. (2016): The Microbiome and the Respiratory Tract. In: *Annual review of physiology* 78, S. 481–504.

Dittrich, A. S.; Kühbandner, I.; Gehrig, S.; Rickert-Zacharias, V.; Twigg, M.; Wege, S. et al. (2018): Elastase activity on sputum neutrophils correlates with severity of lung disease in cystic fibrosis. In: *The European respiratory journal* 51 (3).

Döring, G.; Frank, F.; Boudier, C.; Herbert, S.; Fleischer, B.; Bellon, G. (1995): Cleavage of lymphocyte surface antigens CD2, CD4, and CD8 by polymorphonuclear leukocyte elastase and cathepsin G in patients with cystic fibrosis. In: *The Journal of Immunology* 154 (9), S. 4842–4850.

Döring, Y.; Libby, P.; Soehnlein, O. (2020): Neutrophil Extracellular Traps Participate in Cardiovascular Diseases: Recent Experimental and Clinical Insights. In: *Circulation research* 126 (9), S. 1228–1241.

Downey, D. G.; Bell, S. C.; Elborn, J. S. (2009): Neutrophils in cystic fibrosis. In: *Thorax* 64 (1), S. 81–88.

Dunsmore, S. E.; Saarialho-Kere, U. K.; Roby, J. D.; Wilson, C. L.; Matrisian, L. M.; Welgus, H. G.; Parks, W. C. (1998): Matrilysin expression and function in airway epithelium. In: *The Journal of clinical investigation* 102 (7), S. 1321–1331.

Eickmeier, O.; Huebner, M.; Herrmann, E.; Zissler, U.; Rosewich, M.; Baer, P. C. et al. (2010): Sputum biomarker profiles in cystic fibrosis (CF) and chronic obstructive pulmonary disease (COPD) and association between pulmonary function. In: *Cytokine* 50 (2), S. 152–157.

Eisenberg, S. P.; Hale, K. K.; Heimdal, P.; Thompson, R. C. (1990): Location of the protease-inhibitory region of secretory leukocyte protease inhibitor. In: *Journal of Biological Chemistry* 265 (14), S. 7976–7981.

Eisner, M. D.; Anthonisen, N.; Coultas, D.; Kuenzli, N.; Perez-Padilla, R.; Postma, D. et al. (2010): An official American Thoracic Society public policy statement: Novel risk factors and the global burden of chronic obstructive pulmonary disease. In: *American journal of respiratory and critical care medicine* 182 (5), S. 693–718.

Erb-Downward, J. R.; Thompson, D. L.; Han, M. K.; Freeman, C. M.; McCloskey, L.; Schmidt, L. A. et al. (2011): Analysis of the lung microbiome in the "healthy" smoker and in COPD. In: *PLOS One* 6 (2), e16384.

Fahy, J. V.; Dickey, B. F. (2010): Airway mucus function and dysfunction. In: *The New England journal of medicine* 363 (23), S. 2233–2247.

Faure, E.; Kwong, K.; Nguyen, D. (2018): Pseudomonas aeruginosa in Chronic Lung Infections: How to Adapt Within the Host? In: *Frontiers in Immunology* 9, S. 2416.

Fenker, D. E.; McDaniel, C. T.; Panmanee, W.; Panos, R. J.; Sorscher, E. J.; Sabusap, C. et al. (2018): A Comparison between Two Pathophysiologically Different yet Microbiologically Similar Lung Diseases: Cystic Fibrosis and Chronic Obstructive Pulmonary Disease. In: *International journal of respiratory and pulmonary medicine* 5 (2).

Ferry, G.; Lonchampt, M.; Pennel, L.; Nanteuil, G. de; Canet, E.; Tucker, G. C. (1997): Activation of MMP-9 by neutrophil elastase in an in vivo model of acute lung injury. In: *FEBS Letters* 402 (2-3), S. 111–115.

Finlay, G. A.; Russell, K. J.; McMahon, K. J.; D'arcy, E. M.; Masterson, J. B.; FitzGerald, M. X.; O'Connor, C. M. (1997): Elevated levels of matrix metalloproteinases in bronchoalveolar lavage fluid of emphysematous patients. In: *Thorax* 52 (6), S. 502–506.

Fodor, A. A.; Klem, E. R.; Gilpin, D. F.; Elborn, J. S.; Boucher, R. C.; Tunney, M. M.; Wolfgang, M. C. (2012): The adult cystic fibrosis airway microbiota is stable over time and infection type, and highly resilient to antibiotic treatment of exacerbations. In: *PLOS One* 7 (9), e45001.

Folkesson, A.; Jelsbak, L.; Yang, L.; Johansen, H. K.; Ciofu, O.; Høiby, N.; Molin, S. (2012): Adaptation of Pseudomonas aeruginosa to the cystic fibrosis airway: an evolutionary perspective. In: *Nature Reviews Microbiology* 10 (12), S. 841–851.

Forrest, O. A.; Ingersoll, S. A.; Preininger, M. K.; Laval, J.; Limoli, D. H.; Brown, M. R. et al. (2018): Frontline Science: Pathological conditioning of human neutrophils recruited to the airway milieu in cystic fibrosis. In: *Journal of leukocyte biology* 104 (4), S. 665–675.

Frenette, G.; Deperthes, D.; Tremblay, R. R.; Lazure, C.; Dubé, J. Y. (1997): Purification of enzymatically active kallikrein hK2 from human seminal plasma. In: *Biochimica et Biophysica Acta (BBA) - General Subjects* 1334 (1), S. 109–115.

Frey, D. L.; Boutin, S.; Dittrich, S. A.; Graeber, S. Y.; Stahl, M.; Wege, S. et al. (2021a): Relationship between airway dysbiosis, inflammation and lung function in adults with cystic fibrosis. In: *Journal of Cystic Fibrosis*.

Frey, D. L.; Guerra, M.; Mall, M. A.; Schultz, C. (2021b): Monitoring Neutrophil Elastase and Cathepsin G Activity in Human Sputum Samples. In: *Journal of Visualized Experiments*, e62193.

Fritzsching, B.; Zhou-Suckow, Z.; Trojanek, J. B.; Schubert, S. C.; Schatterny, J.; Hirtz, S. et al. (2015): Hypoxic epithelial necrosis triggers neutrophilic inflammation via IL-1 receptor signaling in cystic fibrosis lung disease. In: *American journal of respiratory and critical care medicine* 191 (8), S. 902–913.

Fuchs, T. A.; Abed, U.; Goosmann, C.; Hurwitz, R.; Schulze, I.; Wahn, V. et al. (2007): Novel cell death program leads to neutrophil extracellular traps. In: *The Journal of cell biology* 176 (2), S. 231–241.

Fujii, M.; Bessho, R. (2019): Neutrophil Elastase Inhibitor Sivelestat Attenuates Myocardial Injury after Cardioplegic Arrest in Rat Hearts. In: *Annals of thoracic and cardiovascular surgery: official journal of the Association of Thoracic and Cardiovascular Surgeons of Asia*.

Gaggar, A.; Chen, J.; Chmiel, J. F.; Dorkin, H. L.; Flume, P. A.; Griffin, R. et al. (2016): Inhaled alpha1-proteinase inhibitor therapy in patients with cystic fibrosis. In: *Journal of Cystic Fibrosis* 15 (2), S. 227–233.

Gaggar, A.; Hector, A.; Bratcher, P. E.; Mall, M. A.; Griese, M.; Hartl, D. (2011): The role of matrix metalloproteinases in cystic fibrosis lung disease. In: *The European respiratory journal* 38 (3), S. 721–727.

Gaggar, A.; Jackson, P. L.; Noerager, B. D.; O'Reilly, P. J.; McQuaid, D. B.; Rowe, S. M. et al. (2008): A novel proteolytic cascade generates an extracellular matrix-derived chemoattractant in chronic neutrophilic inflammation. In: *The Journal of Immunology* 180 (8), S. 5662–5669.

Gaggar, A.; Li, Y.; Weathington, N.; Winkler, M.; Kong, M.; Jackson, P. et al. (2007): Matrix metalloprotease-9 dysregulation in lower airway secretions of cystic fibrosis patients. In: *American journal of physiology. Lung cellular and molecular physiology* 293 (1), L96-L104.

Galdino, A. C. M.; Viganor, L.; Castro, A. A. de; da Cunha, E. F. F.; Mello, T. P.; Mattos, L. M. et al. (2019): Disarming Pseudomonas aeruginosa Virulence by the Inhibitory Action of 1,10-Phenanthroline-5,6-Dione-Based Compounds: Elastase B (LasB) as a Chemotherapeutic Target. In: *Frontiers in Microbiology* 10, S. 1701.

Gehrig, S.; Duerr, J.; Weitnauer, M.; Wagner, C. J.; Graeber, S. Y.; Schatterny, J. et al. (2014): Lack of neutrophil elastase reduces inflammation, mucus hypersecretion, and emphysema, but not mucus obstruction, in mice with cystic fibrosis-like lung disease. In: *American journal of respiratory and critical care medicine* 189 (9), S. 1082–1092.

Gehrig, S.; Mall, M. A.; Schultz, C. (2012): Spatially resolved monitoring of neutrophil elastase activity with ratiometric fluorescent reporters. In: *Angewandte Chemie (International ed. in English)* 51 (25), S. 6258–6261.

Genschmer, K. R.; Russell, D. W.; Lal, C.; Szul, T.; Bratcher, P. E.; Noerager, B. D. et al. (2019): Activated PMN Exosomes: Pathogenic Entities Causing Matrix Destruction and Disease in the Lung. In: *Cell* 176 (1-2), 113-126.e15.

Giacalone, V. D.; Dobosh, B. S.; Gaggar, A.; Tirouvanziam, R.; Margaroli, C. (2020a): Immunomodulation in Cystic Fibrosis: Why and How? In: *International Journal of Molecular Sciences* 21 (9), S. 3331.

Giacalone, V. D.; Margaroli, C.; Mall, M. A.; Tirouvanziam, R. (2020b): Neutrophil Adaptations upon Recruitment to the Lung: New Concepts and Implications for Homeostasis and Disease. In: *International journal of molecular sciences* 21 (3).

Glasser, N. R.; Hunter, R. C.; Liou, T. G.; Newman, D. K. (2019): Refinement of metabolite detection in cystic fibrosis sputum reveals heme correlates with lung function decline. In: *PLOS One* 14 (12), e0226578.

Global Initiative for Chronic Obstructive Lung Disease, Inc. (2020): Global Strategy for the Diagnosis, Management, and Prevention of Chronic Obstructive Lung Disease (2020 Report). Online verfügbar unter https://goldcopd.org/wp-content/uploads/2019/12/GOLD-2020-FINAL-ver1.2-03Dec19_WMV.pdf.

Gloor, G. B.; Hummelen, R.; Macklaim, J. M.; Dickson, R. J.; Fernandes, A. D.; MacPhee, R.; Reid, G. (2010): Microbiome profiling by illumina sequencing of combinatorial sequence-tagged PCR products. In: *PLOS One* 5 (10), e15406.

Goldschmeding, R.; van der Schoot, C. E.; Bokkel Huinink, D. ten; Hack, C. E.; van den Ende, M. E.; Kallenberg, C. G.; Borne, A. E. von dem (1989): Wegener's granulomatosis autoantibodies identify a novel diisopropylfluorophosphate-binding protein in the lysosomes of normal human neutrophils. In: *The Journal of clinical investigation* 84 (5), S. 1577–1587.

Gordon, S.; Yifang, H.; Matthew, R.; Jeremy, S.; James, W.; Davis, M. et al. (2017): limma: Bioconductor.

Graeber, S. Y.; Boutin, S.; Wielpütz, M. O.; Joachim, C.; Frey, D. L.; Wege, S. et al. (2021): Effects of Lumacaftor-Ivacaftor on Lung Clearance Index, Magnetic Resonance Imaging and Airway Microbiome in Phe508del Homozygous Patients with Cystic Fibrosis. In: *Annals of the American Thoracic Society*.

Greally, P.; Hussein, M. J.; Cook, A. J.; Sampson, A. P.; Piper, P. J.; Price, J. F. (1993): Sputum tumour necrosis factor-alpha and leukotriene concentrations in cystic fibrosis. In: *Archives of disease in childhood* 68 (3), S. 389–392.

Greene, C. M.; McElvaney, N. G. (2009): Proteases and antiproteases in chronic neutrophilic lung disease - relevance to drug discovery. In: *British journal of pharmacology* 158 (4), S. 1048–1058.

Greenlee, K. J.; Werb, Z.; Kheradmand, F. (2007): Matrix metalloproteinases in lung: multiple, multifarious, and multifaceted. In: *Physiological reviews* 87 (1), S. 69–98.

Griffin, S.; Taggart, C. C.; Greene, C. M.; O'Neill, S.; McElvaney, N. G. (2003): Neutrophil elastase up-regulates human β-defensin-2 expression in human bronchial epithelial cells. In: *FEBS Letters* 546 (2-3), S. 233–236.

Groutas, W. C.; Dou, D.; Alliston, K. R. (2011): Neutrophil elastase inhibitors. In: *Expert opinion on therapeutic patents* 21 (3), S. 339–354.

Guerra, M.; Frey, D. L.; Hagner, M.; Dittrich, S.; Paulsen, M.; Mall, M. A.; Schultz, C. (2019): Cathepsin G Activity as a New Marker for Detecting Airway Inflammation by Microscopy and Flow Cytometry. In: *ACS Central Science*.

Guerra, M.; Halls, V. S.; Schatterny, J.; Hagner, M.; Mall, M. A.; Schultz, C. (2020): Protease FRET Reporters Targeting Neutrophil Extracellular Traps. In: *Journal of the American Chemical Society*.

Guyot, N.; Bergsson, G.; Butler, M. W.; Greene, C. M.; Weldon, S.; Kessler, E. et al. (2010): Functional study of elafin cleaved by Pseudomonas aeruginosa metalloproteinases. In: *Biological chemistry* 391 (6), S. 705–716.

Guyot, N.; Butler, M. W.; McNally, P.; Weldon, S.; Greene, C. M.; Levine, R. L. et al. (2008): Elafin, an elastase-specific inhibitor, is cleaved by its cognate enzyme neutrophil elastase in sputum from individuals with cystic fibrosis. In: *Journal of Biological Chemistry* 283 (47), S. 32377–32385.

Hagner, M.; Frey, D. L.; Guerra, M.; Dittrich, A. S.; Halls, V. S.; Wege, S. et al. (2020): New method for rapid and dynamic quantification of elastase activity on sputum neutrophils from patients with cystic fibrosis using flow cytometry. In: *The European respiratory journal* 55 (4).

Hahn, A.; Burrell, A.; Ansusinha, E.; Peng, D.; Chaney, H.; Sami, I. et al. (2020): Airway microbial diversity is decreased in young children with cystic fibrosis compared to healthy controls but improved with CFTR modulation. In: *Heliyon* 6 (6), e04104.

Hamano, N.; Murata, M.; Kawano, T.; Piao, J. S.; Narahara, S.; Nakata, R. et al. (2016): Förster Resonance Energy Transfer-Based Self-Assembled Nanoprobe for Rapid and Sensitive Detection of Postoperative Pancreatic Fistula. In: *ACS applied materials & interfaces* 8 (8), S. 5114–5123.

Haslett, C. (1999): Granulocyte apoptosis and its role in the resolution and control of lung inflammation. In: *American journal of respiratory and critical care medicine* 160 (5 Pt 2), S5-11.

Heijerman, H. (2005): Infection and inflammation in cystic fibrosis: a short review. In: *Journal of Cystic Fibrosis* 4 Suppl 2, S. 3–5.

Heijerman, H. G. M.; McKone, E. F.; Downey, D. G.; van Braeckel, E.; Rowe, S. M.; Tullis, E. et al. (2019): Efficacy and safety of the elexacaftor plus tezacaftor plus ivacaftor combination regimen in people with cystic fibrosis homozygous for the F508del mutation: a double-blind, randomised, phase 3 trial. In: *The Lancet* 394 (10212), S. 1940–1948.

Hetzel, J.; Kreuter, M.; Kähler, C. M.; Kabitz, H.-J.; Gschwendtner, A.; Eberhardt, R. et al. (2021): Bronchoscopic performance of bronchoalveolar lavage in germany - a call for standardization. In: *Sarcoidosis, vasculitis, and diffuse lung diseases : official journal of WASOG* 38 (1), e2021003.

Hobbs, C. A.; Da Tan, C.; Tarran, R. (2013): Does epithelial sodium channel hyperactivity contribute to cystic fibrosis lung disease? In: *The Journal of physiology* 591 (18), S. 4377–4387.

Hogan, D. A.; Willger, S. D.; Dolben, E. L.; Hampton, T. H.; Stanton, B. A.; Morrison, H. G. et al. (2016): Analysis of Lung Microbiota in Bronchoalveolar Lavage, Protected Brush and Sputum Samples from Subjects with Mild-To-Moderate Cystic Fibrosis Lung Disease. In: *PLOS One* 11 (3), e0149998.

Høiby, N. (1993): Antibiotic therapy for chronic infection of pseudomonas in the lung. In: *Annual review of medicine* 44, S. 1–10.

Hou, H.-H.; Wang, H.-C.; Cheng, S.-L.; Chen, Y.-F.; Lu, K.-Z.; Yu, C.-J. (2018): MMP-12 activates protease-activated receptor-1, upregulates placenta growth factor, and leads to pulmonary emphysema. In: *American journal of physiology. Lung cellular and molecular physiology* 315 (3), L432-L442.

Hsieh, T. C.; Ma, K. H.; Chao, A. (2016): iNEXT: an R package for rarefaction and extrapolation of species diversity (Hill numbers). In: *Methods in Ecology and Evolution* 7 (12), S. 1451–1456.

Huet, T.; Beaussier, H.; Voisin, O.; Jouveshomme, S.; Dauriat, G.; Lazareth, I. et al. (2020): Anakinra for severe forms of COVID-19: a cohort study. In: *The Lancet Rheumatology*.

Hughes, C. S.; Sorensen, P. H.; Morin, G. B. (2019): A Standardized and Reproducible Proteomics Protocol for Bottom-Up Quantitative Analysis of Protein Samples Using SP3 and Mass Spectrometry. In: *Methods in molecular biology (Clifton, N.J.)* 1959, S. 65–87.

Hurley, M. N.; Smyth, A. R. (2018): Staphylococcus aureus in cystic fibrosis: pivotal role or bit part actor? In: *Current opinion in pulmonary medicine* 24 (6), S. 586–591.

Ingersoll, S. A.; Laval, J.; Forrest, O. A.; Preininger, M.; Brown, M. R.; Arafat, D. et al. (2015): Mature cystic fibrosis airway neutrophils suppress T cell function: evidence for a role of arginase 1 but not programmed death-ligand 1. In: *Journal of immunology (Baltimore, Md. : 1950)* 194 (11), S. 5520–5528.

Jackson, P. L.; Xu, X.; Wilson, L.; Weathington, N. M.; Clancy, J. P.; Blalock, J. E.; Gaggar, A. (2010): Human neutrophil elastase-mediated cleavage sites of MMP-9 and TIMP-1: implications to cystic fibrosis proteolytic dysfunction. In: *Molecular medicine (Cambridge, Mass.)* 16 (5-6), S. 159–166.

Janciauskiene, S. (2001): Conformational properties of serine proteinase inhibitors (serpins) confer multiple pathophysiological roles. In: *Biochimica et Biophysica Acta (BBA) - Molecular Basis of Disease* 1535 (3), S. 221–235.

Janoff, A. (1985): Elastase in tissue injury. In: *Annual review of medicine* 36 (1), S. 207–216.

Jin, F.-y.; Nathan, C.; Radzioch, D.; Ding, A. (1997): Secretory Leukocyte Protease Inhibitor: A Macrophage Product Induced by and Antagonistic to Bacterial Lipopolysaccharide. In: *Cell* 88 (3), S. 417–426.

Johnson, D. A.; Carter-Hamm, B.; Dralle, W. M. (1982): Inactivation of human bronchial mucosal proteinase inhibitor by Pseudomonas aeruginosa elastase. In: *The American review of respiratory disease* 126 (6), S. 1070–1073.

Johnson, J. L.; Ramadass, M.; He, J.; Brown, S. J.; Zhang, J.; Abgaryan, L. et al. (2016): Identification of Neutrophil Exocytosis Inhibitors (Nexinhibs), Small Molecule Inhibitors of Neutrophil Exocytosis and Inflammation. DRUGGABILITY OF THE SMALL GTPase Rab27a. In: *The Journal of biological chemistry* 291 (50), S. 25965–25982.

Jorth, P.; Ehsan, Z.; Rezayat, A.; Caldwell, E.; Pope, C.; Brewington, J. J. et al. (2019): Direct Lung Sampling Indicates That Established Pathogens Dominate Early Infections in Children with Cystic Fibrosis. In: *Cell reports* 27 (4), 1190-1204.e3.

Jung, D.; Dong, K.; Jang, J.; Lam, G. Y.; Wilcox, P. G.; Quon, B. S. (2020): Circulating CRP and calprotectin to diagnose CF pulmonary exacerbations. In: *Journal of Cystic Fibrosis*.

Kawabata, K.; Suzuki, M.; Sugitani, M.; Imaki, K.; Toda, M.; Miyamoto, T. (1991): ONO-5046, a novel inhibitor of human neutrophil elastase. In: *Biochemical and Biophysical Research Communications* 177 (2), S. 814–820.

Kelly, E.; Greene, C. M.; McElvaney, N. G. (2008): Targeting neutrophil elastase in cystic fibrosis. In: *Expert opinion on therapeutic targets* 12 (2), S. 145–157.

Kelly, M. M.; Efthimiadis, A.; Hargreave, F. E. (2001): Induced sputum : selection method. In: *Methods in molecular medicine* 56, S. 77–91.

Kettritz, R. (2016): Neutral serine proteases of neutrophils. In: *Immunological reviews* 273 (1), S. 232–248.

Khan, M. A.; Farahvash, A.; Douda, D. N.; Licht, J.-C.; Grasemann, H.; Sweezey, N.; Palaniyar, N. (2017): JNK Activation Turns on LPS- and Gram-Negative Bacteria-Induced NADPH Oxidase-Dependent Suicidal NETosis. In: *Scientific Reports* 7 (1), S. 3409.

Khan, T. Z.; Wagener, J. S.; Bost, T.; Martinez, J.; Accurso, F. J.; Riches, D. W. (1995): Early pulmonary inflammation in infants with cystic fibrosis. In: *American journal of respiratory and critical care medicine* 151 (4), S. 1075–1082.

Kishimoto, M.; Yamana, H.; Inoue, S.; Noda, T.; Myojin, T.; Matsui, H. et al. (2017): Sivelestat sodium and mortality in pneumonia patients requiring mechanical ventilation: propensity score analysis of a Japanese nationwide database. In: *Journal of anesthesia* 31 (3), S. 405–412.

Knäuper, V.; Reinke, H.; Tschesche, H. (1990): Inactivation of human plasma α 1 - proteinase inhibitor by human PMN leucocyte collagenase. In: *FEBS Letters* 263 (2), S. 355–357.

Koller, D. Y.; Götz, M.; Eichler, I.; Urbanek, R. (1994): Eosinophilic activation in cystic fibrosis. In: *Thorax* 49 (5), S. 496–499.

Koller, D. Y.; Urbanek, R.; Götz, M. (1995): Increased degranulation of eosinophil and neutrophil granulocytes in cystic fibrosis. In: *American journal of respiratory and critical care medicine* 152 (2), S. 629–633.

Konstan, M. W.; Hilliard, K. A.; Norvell, T. M.; Berger, M. (1994): Bronchoalveolar lavage findings in cystic fibrosis patients with stable, clinically mild lung disease suggest ongoing infection and inflammation. In: *American journal of respiratory and critical care medicine* 150 (2), S. 448–454.

Korkmaz, B.; Attucci, S.; Jourdan, M.-L.; Juliano, L.; Gauthier, F. (2005a): Inhibition of Neutrophil Elastase by 1-Protease Inhibitor at the Surface of Human Polymorphonuclear Neutrophils. In: *The Journal of Immunology* 175 (5), S. 3329–3338.

Korkmaz, B.; Attucci, S.; Juliano, M. A.; Kalupov, T.; Jourdan, M.-L.; Juliano, L.; Gauthier, F. (2008a): Measuring elastase, proteinase 3 and cathepsin G activities at the surface of human neutrophils with fluorescence resonance energy transfer substrates. In: *Nature Protocols* 3 (6), S. 991–1001.

Korkmaz, B.; Horwitz, M. S.; Jenne, D. E.; Gauthier, F. (2010): Neutrophil elastase, proteinase 3, and cathepsin G as therapeutic targets in human diseases. In: *Pharmacological reviews* 62 (4), S. 726–759.

Korkmaz, B.; Moreau, T.; Gauthier, F. (2008b): Neutrophil elastase, proteinase 3 and cathepsin G: Physicochemical properties, activity and physiopathological functions. In: *Biochimie* 90 (2), S. 227–242.

Korkmaz, B.; Poutrain, P.; Hazouard, E.; Monte, M. d.; Attucci, S.; Gauthier, F. L. (2005b): Competition between elastase and related proteases from human neutrophil for binding to alpha1-protease inhibitor. In: *American journal of respiratory cell and molecular biology* 32 (6), S. 553–559.

Kreda, S. M.; Davis, C. W.; Rose, M. C. (2012): CFTR, mucins, and mucus obstruction in cystic fibrosis. In: *Cold Spring Harbor perspectives in medicine* 2 (9), a009589.

Kress, L. F. (1983): Inactivation of human plasma alpha 1-antichymotrypsin by microbial proteinases. In: *Acta biochimica Polonica* 30 (2), S. 159–164.

Kube, D.; Sontich, U.; Fletcher, D.; Davis, P. B. (2001): Proinflammatory cytokine responses to P. aeruginosa infection in human airway epithelial cell lines. In: *American journal of physiology. Lung cellular and molecular physiology* 280 (3), L493-502.

Kuznetsova, A.; Brockhoff, P. B.; Christensen, R. H. B. (2017): lmerTest Package: Tests in Linear Mixed Effects Models. In: *Journal of Statistical Software* 82 (13).

Lahti, L.; Shetty, S.; Salojarvi, J. (2012-2017): microbiome: Bioconductor.

Lamoureux, C.; Guilloux, C.-A.; Beauruelle, C.; Jolivet-Gougeon, A.; Héry-Arnaud, G. (2019): Anaerobes in cystic fibrosis patients' airways. In: *Critical reviews in microbiology* 45 (1), S. 103–117.

Lawrence, R. H.; Sorrelli, T. C. (1992): Decreased polymorphonuclear leucocyte chemotactic response to leukotriene B4 in cystic fibrosis. In: *Clinical and experimental immunology* 89 (2), S. 321–324.

Lay, J. C.; Peden, D. B.; Alexis, N. E. (2011): Flow cytometry of sputum: assessing inflammation and immune response elements in the bronchial airways. In: *Inhalation toxicology* 23 (7), S. 392–406.

Le-Barillec, K.; Si-Tahar, M.; Balloy, V.; Chignard, M. (1999): Proteolysis of monocyte CD14 by human leukocyte elastase inhibits lipopolysaccharide-mediated cell activation. In: *The Journal of clinical investigation* 103 (7), S. 1039–1046.

Lentsch, A. B.; Jordan, J. A.; Czermak, B. J.; Diehl, K. M.; Younkin, E. M.; Sarma, V.; Ward, P. A. (1999): Inhibition of NF-κB Activation and Augmentation of IκBβ by Secretory Leukocyte Protease Inhibitor during Lung Inflammation. In: *The American journal of pathology* 154 (1), S. 239–247.

Lentz, C. S. (2020): What you see is what you get: activity-based probes in single-cell analysis of enzymatic activities. In: *Biological chemistry* 401 (2), S. 233–248.

Limoli, D. H.; Yang, J.; Khansaheb, M. K.; Helfman, B.; Peng, L.; Stecenko, A. A.; Goldberg, J. B. (2016): Staphylococcus aureus and Pseudomonas aeruginosa co-infection is associated with cystic fibrosis-related diabetes and poor clinical outcomes. In: *European journal of clinical microbiology & infectious diseases : official publication of the European Society of Clinical Microbiology* 35 (6), S. 947–953.

Lin, S. J.; Dong, K. C.; Eigenbrot, C.; van Lookeren Campagne, M.; Kirchhofer, D. (2014): Structures of neutrophil serine protease 4 reveal an unusual mechanism of substrate recognition by a trypsin-fold protease. In: *Structure (London, England : 1993)* 22 (9), S. 1333–1340.

Liu, S.-Y.; Yan, A.-M.; Guo, W. Y.-Z.; Fang, Y.-Y.; Dong, Q.-J.; Li, R.-R. et al. (2020): Human Neutrophil Elastase Activated Fluorescent Probe for Pulmonary Diseases Based on Fluorescence Resonance Energy Transfer Using CdSe/ZnS Quantum Dots. In: *ACS nano*.

López-Boado, Y. S.; Espinola, M.; Bahr, S.; Belaaouaj, A. (2004): Neutrophil serine proteinases cleave bacterial flagellin, abrogating its host response-inducing activity. In: *The Journal of Immunology* 172 (1), S. 509–515.

Lowrey, G. E.; Henderson, N.; Blakey, J. D.; Corne, J. M.; Johnson, S. R. (2008): MMP-9 protein level does not reflect overall MMP activity in the airways of patients with COPD. In: *Respiratory medicine* 102 (6), S. 845–851.

Lozupone, C.; Knight, R. (2005): UniFrac: A new phylogenetic method for comparing microbial communities. In: *Applied and Environmental Microbiology* 71 (12), S. 8228–8235.

Lyczak, J. B.; Cannon, C. L.; Pier, G. B. (2000): Establishment of Pseudomonas aeruginosa infection: lessons from a versatile opportunist1*Address for correspondence: Channing Laboratory, 181 Longwood Avenue, Boston, MA 02115, USA. In: *Microbes and Infection* 2 (9), S. 1051–1060.

Madan, J. C.; Koestler, D. C.; Stanton, B. A.; Davidson, L.; Moulton, L. A.; Housman, M. L. et al. (2012): Serial analysis of the gut and respiratory microbiome in cystic fibrosis in infancy: interaction between intestinal and respiratory tracts and impact of nutritional exposures. In: *mBio* 3 (4).

Mahadeva, R.; Sharples, L.; Ross-Russell, R. I.; Webb, A. K.; Bilton, D.; Lomas, D. A. (2001): Association of alpha(1)-antichymotrypsin deficiency with milder lung disease in patients with cystic fibrosis. In: *Thorax* 56 (1), S. 53–58.

Makam, M.; Diaz, D.; Laval, J.; Gernez, Y.; Conrad, C. K.; Dunn, C. E. et al. (2009): Activation of critical, host-induced, metabolic and stress pathways marks neutrophil entry into cystic fibrosis lungs. In: *Proceedings of the National Academy of Sciences of the United States of America* 106 (14), S. 5779–5783.

Malhotra, S.; Hayes, D.; Wozniak, D. J. (2019): Cystic Fibrosis and Pseudomonas aeruginosa: the Host-Microbe Interface. In: *Clinical microbiology reviews* 32 (3).

Mall, M.; Grubb, B. R.; Harkema, J. R.; O'Neal, W. K.; Boucher, R. C. (2004): Increased airway epithelial Na+ absorption produces cystic fibrosis-like lung disease in mice. In: *Nature Medicine* 10 (5), S. 487–493.

Mall, M. A. (2008): Role of cilia, mucus, and airway surface liquid in mucociliary dysfunction: lessons from mouse models. In: *Journal of aerosol medicine and pulmonary drug delivery* 21 (1), S. 13–24.

Mall, M. A.; Hartl, D. (2014): CFTR: cystic fibrosis and beyond. In: *The European respiratory journal* 44 (4), S. 1042–1054.

Margaroli, C.; Garratt, L. W.; Horati, H.; Dittrich, A. S.; Rosenow, T.; Montgomery, S. T. et al. (2019): Elastase Exocytosis by Airway Neutrophils Associates with Early Lung Damage in Cystic Fibrosis Children. In: *American journal of respiratory and critical care medicine*.

Margaroli, C.; Tirouvanziam, R. (2016): Neutrophil plasticity enables the development of pathological microenvironments: implications for cystic fibrosis airway disease. In: *Molecular and cellular pediatrics* 3 (1), S. 38.

Marshall, B.; Faro, A.; Fink, A. K. (2018): Cystic fibrosis patient registry: 2017 annual data report. In: *Bethesda, MD: Cystic Fibrosis Foundation*.

Mayer-Hamblett, N.; Aitken, M. L.; Accurso, F. J.; Kronmal, R. A.; Konstan, M. W.; Burns, J. L. et al. (2007): Association between pulmonary function and sputum biomarkers in cystic fibrosis. In: *American journal of respiratory and critical care medicine* 175 (8), S. 822–828.

McCawley, L. J.; O'Brien, P.; Hudson, L. G. (1998): Epidermal growth factor (EGF)- and scatter factor/hepatocyte growth factor (SF/HGF)-mediated keratinocyte migration is coincident with induction of matrix metalloproteinase (MMP)-9. In: *Journal of Cellular Physiology* 176 (2), S. 255–265.

McElvaney, N. G.; Hubbard, R. C.; Birrer, P.; Crystal, R. G.; Chernick, M. S.; Frank, M. M.; Caplan, D. B. (1991): Aerosol α1 -antitrypsin treatment for cystic fibrosis. In: *The Lancet* 337 (8738), S. 392–394.

McElvaney, O. J.; Gunaratnam, C.; Reeves, E. P.; McElvaney, N. G. (2018): A specialized method of sputum collection and processing for therapeutic interventions in cystic fibrosis. In: *Journal of Cystic Fibrosis*.

McElvaney, O. J.; O'Connor, E.; McEvoy, N. L.; Fraughan, D. D.; Clarke, J.; McElvaney, O. F. et al. (2021): Alpha-1 antitrypsin for cystic fibrosis complicated by severe cytokinemic COVID-19. In: *Journal of Cystic Fibrosis* 20 (1), S. 31–35.

McElvaney, O. J.; Wade, P.; Murphy, M.; Reeves, E. P.; McElvaney, N. G. (2019): Targeting airway inflammation in cystic fibrosis. In: *Expert review of respiratory medicine* 13 (11), S. 1041–1055.

McKelvey, M. C.; Weldon, S.; McAuley, D. F.; Mall, M. A.; Taggart, C. C. (2019): Targeting Proteases in Cystic Fibrosis Lung Disease: Paradigms, Progress, and Potential. In: *American journal of respiratory and critical care medicine*.

McMurdie, P. J.; Holmes, S. (2012): Phyloseq: a bioconductor package for handling and analysis of high-throughput phylogenetic sequence data. In: Biocomputing 2012: WORLD SCIENTIFIC, S. 235–246.

Michaelis, J.; Vissers, M. C.; Winterbourn, C. C. (1990): Human neutrophil collagenase cleaves alpha 1-antitrypsin. In: *The Biochemical journal* 270 (3), S. 809–814.

Middleton, P. G.; Mall, M. A.; Dřevínek, P.; Lands, L. C.; McKone, E. F.; Polineni, D. et al. (2019): Elexacaftor-Tezacaftor-Ivacaftor for Cystic Fibrosis with a Single Phe508del Allele. In: *The New England journal of medicine* 381 (19), S. 1809–1819.

Miller, M. R.; Hankinson, J.; Brusasco, V.; Burgos, F.; Casaburi, R.; Coates, A. et al. (2005): Standardisation of spirometry. In: *The European respiratory journal* 26 (2), S. 319–338.

Mitash, N.; Mu, F.; Donovan, J. E.; Myerburg, M. M.; Ranganathan, S.; Greene, C. M.; Swiatecka-Urban, A. (2019): Transforming Growth Factor-β1 Selectively Recruits microRNAs to the RNA-Induced Silencing Complex and Degrades CFTR mRNA under Permissive Conditions in Human Bronchial Epithelial Cells. In: *International journal of molecular sciences* 20 (19).

Mitchell, T. C. (2018): A GRIM fate for human neutrophils in airway disease. In: *Journal of leukocyte biology* 104 (4), S. 657–659.

Montgomery, S. T.; Frey, D. L.; Mall, M. A.; Stick, S. M.; Kicic, A. (2020): Rhinovirus Infection Is Associated With Airway Epithelial Cell Necrosis and Inflammation via

Interleukin-1 in Young Children With Cystic Fibrosis. In: *Frontiers in Immunology* 11, S. 146.

Montgomery, S. T.; Mall, M. A.; Kicic, A.; Stick, S. M. (2017): Hypoxia and sterile inflammation in cystic fibrosis airways: mechanisms and potential therapies. In: *The European respiratory journal* 49 (1).

Morihara, K.; Tsuzuki, H.; Harada, M.; Iwata, T. (1984): Purification of human plasma alpha 1-proteinase inhibitor and its inactivation by Pseudomonas aeruginosa elastase. In: *Journal of biochemistry* 95 (3), S. 795–804.

Morris, A. E.; Liggitt, H. D.; Hawn, T. R.; Skerrett, S. J. (2009): Role of Toll-like receptor 5 in the innate immune response to acute P. aeruginosa pneumonia. In: *American journal of physiology. Lung cellular and molecular physiology* 297 (6), L1112-9.

Moulding, D. A.; Hart, C. A.; Edwards, S. W. (1999): Regulation of neutrophil FcgammaRIIIb (CD16) surface expression following delayed apoptosis in response to GM-CSF and sodium butyrate. In: *Journal of leukocyte biology* 65 (6), S. 875–882.

Muhlebach, M. S.; Hatch, J. E.; Einarsson, G. G.; McGrath, S. J.; Gilipin, D. F.; Lavelle, G. et al. (2018a): Anaerobic bacteria cultured from cystic fibrosis airways correlate to milder disease: a multisite study. In: *The European respiratory journal* 52 (1).

Muhlebach, M. S.; Zorn, B. T.; Esther, C. R.; Hatch, J. E.; Murray, C. P.; Turkovic, L. et al. (2018b): Initial acquisition and succession of the cystic fibrosis lung microbiome is associated with disease progression in infants and preschool children. In: *PLoS pathogens* 14 (1), e1006798.

Muñoz, L. E.; Boeltz, S.; Bilyy, R.; Schauer, C.; Mahajan, A.; Widulin, N. et al. (2019): Neutrophil Extracellular Traps Initiate Gallstone Formation. In: *Immunity* 51 (3), 443-450.e4.

Murphy, T. F.; Brauer, A. L.; Eschberger, K.; Lobbins, P.; Grove, L.; Cai, X.; Sethi, S. (2008): Pseudomonas aeruginosa in chronic obstructive pulmonary disease. In: *American journal of respiratory and critical care medicine* 177 (8), S. 853–860.

Murtagh, F.; Legendre, P. (2014): Ward's Hierarchical Agglomerative Clustering Method: Which Algorithms Implement Ward's Criterion? In: *Journal of Classification* 31 (3), S. 274–295.

Naegelen, I.; Beaume, N.; Plançon, S.; Schenten, V.; Tschirhart, E. J.; Bréchard, S. (2015): Regulation of Neutrophil Degranulation and Cytokine Secretion: A Novel Model Approach Based on Linear Fitting. In: *Journal of immunology research* 2015, S. 817038.

Naidoo, N.; Cooperman, B. S.; Wang, Z. M.; Liu, X. Z.; Rubin, H. (1995): Identification of lysines within alpha 1-antichymotrypsin important for DNA binding. An unusual combination of DNA-binding elements. In: *Journal of Biological Chemistry* 270 (24), S. 14548–14555.

Nakajima, K.; Powers, J. C.; Ashe, B. M.; Zimmerman, M. (1979): Mapping the extended substrate binding site of cathepsin G and human leukocyte elastase. In: *J Biol Chem* 254 (10), S. 4027–4032.

Nguyen, A. T.; Jones, J. W.; Ruge, M. A.; Kane, M. A.; Oglesby-Sherrouse, A. G. (2015): Iron Depletion Enhances Production of Antimicrobials by Pseudomonas aeruginosa. In: *Journal of bacteriology* 197 (14), S. 2265–2275.

Nichols, D. P.; Donaldson, S. H.; Frederick, C. A.; Freedman, S. D.; Gelfond, D.; Hoffman, L. R. et al. (2021): PROMISE: Working with the CF community to understand emerging clinical and research needs for those treated with highly effective CFTR modulator therapy. In: *Journal of Cystic Fibrosis*.

Nonnenmacher, C.; Dalpke, A.; Mutters, R.; Heeg, K. (2004): Quantitative detection of periodontopathogens by real-time PCR. In: *Journal of microbiological methods* 59 (1), S. 117–125.

Oksanen J; Blanchet FG; Friendly M; Kindt R; Legendre P; Mcglinn D et al.: vegan: Community Ecology Package 2018. Online verfügbar unter https://CRAN.Rproject.org/package=vegan.

O'Neill, K.; Bradley, J. M.; Johnston, E.; McGrath, S.; McIlreavey, L.; Rowan, S. et al. (2015): Reduced bacterial colony count of anaerobic bacteria is associated with a worsening in lung clearance index and inflammation in cystic fibrosis. In: *PLOS One* 10 (5), e0126980.

Oriano, M.; Gramegna, A.; Terranova, L.; Sotgiu, G.; Sulaiman, I.; Ruggiero, L. et al. (2020): Sputum Neutrophil Elastase associates with microbiota and P. aeruginosa in bronchiectasis. In: *The European respiratory journal*.

Owen, C. A. (1995): Cell surface-bound elastase and cathepsin G on human neutrophils: A novel, non-oxidative mechanism by which neutrophils focus and preserve catalytic activity of serine proteinases. In: *The Journal of cell biology* 131 (3), S. 775–789.

Owen, C. A. (2008): Leukocyte cell surface proteinases: Regulation of expression, functions, and mechanisms of surface localization. In: *The international journal of biochemistry & cell biology* 40 (6-7), S. 1246–1272.

Owen, C. A.; Campbell, M. A.; Boukedes, S. S.; Campbell, E. J. (1995): Inducible binding of bioactive cathepsin G to the cell surface of neutrophils. A novel mechanism for mediating extracellular catalytic activity of cathepsin G. In: *The Journal of Immunology* 155 (12), S. 5803–5810. Online verfügbar unter https://www.jimmunol.org/content/155/12/5803.short.

Owen, C. A.; Campbell, M. A.; Boukedes, S. S.; Campbell, E. J. (1997): Cytokines regulate membrane-bound leukocyte elastase on neutrophils: a novel mechanism for effector activity. In: *The American journal of physiology* 272 (3 Pt 1), L385-93.

Padrines, M.; Wolf, M.; Walz, A.; Baggiolini, M. (1994): Interleukin-8 processing by neutrophil elastase, cathepsin G and proteinase-3. In: *FEBS Letters* 352 (2), S. 231–235.

Painter, R. G.; Valentine, V. G.; Lanson, N. A.; Leidal, K.; Zhang, Q.; Lombard, G. et al. (2006): CFTR Expression in human neutrophils and the phagolysosomal chlorination defect in cystic fibrosis. In: *Biochemistry* 45 (34), S. 10260–10269.

Papayannopoulos, V.; Metzler, K. D.; Hakkim, A.; Zychlinsky, A. (2010): Neutrophil elastase and myeloperoxidase regulate the formation of neutrophil extracellular traps. In: *Journal of Cell Biology* 191 (3), S. 677–691.

Park, J.-A.; He, F.; Martin, L. D.; Li, Y.; Chorley, B. N.; Adler, K. B. (2005): Human Neutrophil Elastase Induces Hypersecretion of Mucin from Well-Differentiated Human Bronchial Epithelial Cells in Vitro via a Protein Kinase Cδ-Mediated Mechanism. In: *The American journal of pathology* 167 (3), S. 651–661.

Parks, W. C.; Wilson, C. L.; López-Boado, Y. S. (2004): Matrix metalloproteinases as modulators of inflammation and innate immunity. In: *Nature reviews. Immunology* 4 (8), S. 617–629.

Patarin, J.; Ghiringhelli, É.; Darsy, G.; Obamba, M.; Bochu, P.; Camara, B. et al. (2020): Rheological analysis of sputum from patients with chronic bronchial diseases. In: *Scientific Reports* 10 (1), S. 15685.

Pedersen, T. L. (2020): ggraph: An implementation of grammar of graphics for graphs and networks. Online verfügbar unter https://CRAN.R-project.org/package=ggraph.

Perera, N. C.; Schilling, O.; Kittel, H.; Back, W.; Kremmer, E.; Jenne, D. E. (2012): NSP4, an elastase-related protease in human neutrophils with arginine specificity. In: *Proceedings of the National Academy of Sciences of the United States of America* 109 (16), S. 6229–6234.

Pernet, E.; Guillemot, L.; Burgel, P.-R.; Martin, C.; Lambeau, G.; Sermet-Gaudelus, I. et al. (2014): Pseudomonas aeruginosa eradicates Staphylococcus aureus by manipulating the host immunity. In: *Nature communications* 5, S. 5105.

Pienkowska, K.; Wiehlmann, L.; Tümmler, B. (2019): Metagenome - Inferred bacterial replication rates in cystic fibrosis airways. In: *Journal of Cystic Fibrosis* 18 (5), S. 653–656.

Pinto-Plata, V.; Toso, J.; Lee, K.; Park, D.; Bilello, J.; Mullerova, H. et al. (2007): Profiling serum biomarkers in patients with COPD: associations with clinical parameters. In: *Thorax* 62 (7), S. 595–601.

Pohl, K.; Hayes, E.; Keenan, J.; Henry, M.; Meleady, P.; Molloy, K. et al. (2014): A neutrophil intrinsic impairment affecting Rab27a and degranulation in cystic fibrosis is corrected by CFTR potentiator therapy. In: *Blood* 124 (7), S. 999–1009.

Poller, W.; Faber, J. P.; Weidinger, S.; Tief, K.; Scholz, S.; Fischer, M. et al. (1993): A leucine-to-proline substitution causes a defective alpha 1-antichymotrypsin allele associated with familial obstructive lung disease. In: *Genomics* 17 (3), S. 740–743.

Porto, B. N.; Stein, R. T. (2016): Neutrophil Extracellular Traps in Pulmonary Diseases: Too Much of a Good Thing? In: *Frontiers in Immunology* 7, S. 311.

Quaderi, S. A.; Hurst, J. R. (2018): The unmet global burden of COPD. In: *Global health, epidemiology and genomics* 3, e4.

Quanjer, P. H.; Stanojevic, S.; Cole, T. J.; Baur, X.; Hall, G. L.; Culver, B. H. et al. (2012): Multi-ethnic reference values for spirometry for the 3-95-yr age range: The global lung function 2012 equations. In: *The European respiratory journal* 40 (6), S. 1324–1343.

Quinn, R. A.; Adem, S.; Mills, R. H.; Comstock, W.; DeRight Goldasich, L.; Humphrey, G. et al. (2019): Neutrophilic proteolysis in the cystic fibrosis lung correlates with a pathogenic microbiome. In: *Microbiome* 7 (1), S. 23.

R Core Team (2017): A language and environment for statistical computing. Vienna, Austria: R Foundation for Statistical Computing. Online verfügbar unter https://www.R-project.org/, zuletzt geprüft am 21.05.2121.

Raghuvanshi, R.; Vasco, K.; Vázquez-Baeza, Y.; Jiang, L.; Morton, J. T.; Li, D. et al. (2020): High-Resolution Longitudinal Dynamics of the Cystic Fibrosis Sputum Microbiome and Metabolome through Antibiotic Therapy. In: *mSystems* 5 (3).

Rahman, S.; Gadjeva, M. (2014): Does NETosis Contribute to the Bacterial Pathoadaptation in Cystic Fibrosis? In: *Frontiers in Immunology* 5, S. 378.

Ramsey, B. W. (1996): Management of pulmonary disease in patients with cystic fibrosis. In: *The New England journal of medicine* 335 (3), S. 179–188.

Rapala-Kozik, M.; Potempa, J.; Nelson, D.; Kozik, A.; Travis, J. (1999): Comparative cleavage sites within the reactive-site loop of native and oxidized alpha1-proteinase inhibitor by selected bacterial proteinases. In: *Biological chemistry* 380 (10), S. 1211–1216.

Ratjen, F.; Hartog, C.-M.; Paul, K.; Wermelt, J.; Braun, J. (2002): Matrix metalloproteases in BAL fluid of patients with cystic fibrosis and their modulation by treatment with dornase alpha. In: *Thorax* 57 (11), S. 930–934.

Ratjen, F.; Waters, V.; Klingel, M.; McDonald, N.; Dell, S.; Leahy, T. R. et al. (2016): Changes in airway inflammation during pulmonary exacerbations in patients with cystic fibrosis and primary ciliary dyskinesia. In: *The European respiratory journal* 47 (3), S. 829–836.

Revell, L. J. (2012): phytools: An R package for phylogenetic comparative biology (and other things). In: *Methods in Ecology and Evolution* 3 (2), S. 217–223.

Revelle W (2019): psych: Procedures for Psychological, Psychometric, and Personality Research. R package version 1.9.12.31. Online verfügbar unter https://CRAN.R-project.org/package=psych.

Roche Diagnostics (2020): cOmplete™ Protease Inhibitor Cocktail Tablets Bulletin. Online verfügbar unter https://www.sigmaaldrich.com/content/dam/sigma-aldrich/docs/Roche/Bulletin/1/corobul.pdf, zuletzt geprüft am 21.05.2121.

Roderfeld, M.; Rath, T.; Schulz, R.; Seeger, W.; Tschuschner, A.; Graf, J.; Roeb, E. (2009): Serum matrix metalloproteinases in adult CF patients: Relation to pulmonary exacerbation. In: *Journal of Cystic Fibrosis* 8 (5), S. 338–347.

Rodríguez, D.; Morrison, C. J.; Overall, C. M. (2010): Matrix metalloproteinases: what do they not do? New substrates and biological roles identified by murine models and proteomics. In: *Biochimica et biophysica acta* 1803 (1), S. 39–54.

Rogan, M. P.; Taggart, C. C.; Greene, C. M.; Murphy, P. G.; O'Neill, S. J.; McElvaney, N. G. (2004): Loss of microbicidal activity and increased formation of biofilm due to decreased lactoferrin activity in patients with cystic fibrosis. In: *The Journal of infectious diseases* 190 (7), S. 1245–1253.

Rørvig, S.; Østergaard, O.; Heegaard, N. H. H.; Borregaard, N. (2013): Proteome profiling of human neutrophil granule subsets, secretory vesicles, and cell membrane: correlation with transcriptome profiling of neutrophil precursors. In: *Journal of leukocyte biology* 94 (4), S. 711–721.

Rosenfeld, M.; Emerson, J.; McNamara, S.; Thompson, V.; Ramsey, B. W.; Morgan, W.; Gibson, R. L. (2012): Risk factors for age at initial Pseudomonas acquisition in the cystic fibrosis epic observational cohort. In: *Journal of Cystic Fibrosis* 11 (5), S. 446–453.

Rosenfeld, M. A.; Yoshimura, K.; Trapnell, B. C.; Yoneyama, K.; Rosenthal, E. R.; Dalemans, W. et al. (1992): In vivo transfer of the human cystic fibrosis transmembrane conductance regulator gene to the airway epithelium. In: *Cell* 68 (1), S. 143–155.

Rubio, F.; Cooley, J.; Accurso, F. J.; Remold-O'Donnell, E. (2004): Linkage of neutrophil serine proteases and decreased surfactant protein-A (SP-A) levels in inflammatory lung disease. In: *Thorax* 59 (4), S. 318–323.

Ruffin, M.; Brochiero, E. (2019): Repair Process Impairment by Pseudomonas aeruginosa in Epithelial Tissues: Major Features and Potential Therapeutic Avenues. In: *Frontiers in Cellular and Infection Microbiology* 9, S. 182.

Ruivo, E. F. P.; Gonçalves, L. M.; Carvalho, L. A. R.; Guedes, R. C.; Hofbauer, S.; Brito, J. A. et al. (2016): Clickable 4-Oxo-β-lactam-Based Selective Probing for Human Neutrophil Elastase Related Proteomes. In: *ChemMedChem* 11 (18), S. 2037–2042.

Saeki, K.; Yagisawa, M.; Kitagawa, S.; Yuo, A. (2001): Diverse effects of cytochalasin B on priming and triggering the respiratory burst activity in human neutrophils and monocytes. In: *International journal of hematology* 74 (4).

Sagel, S. D.; Wagner, B. D.; Anthony, M. M.; Emmett, P.; Zemanick, E. T. (2012): Sputum biomarkers of inflammation and lung function decline in children with cystic fibrosis. In: *American journal of respiratory and critical care medicine* 186 (9), S. 857–865.

Saha, S.; Brightling, C. E. (2006): Eosinophilic airway inflammation in COPD. In: *International journal of chronic obstructive pulmonary disease* 1 (1), S. 39–47.

Saint-Criq, V.; Gray, M. A. (2017): Role of CFTR in epithelial physiology. In: *Cellular and Molecular Life Sciences* 74 (1), S. 93–115.

Saint-Criq, V.; Villeret, B.; Bastaert, F.; Kheir, S.; Hatton, A.; Cazes, A. et al. (2018): Pseudomonas aeruginosa LasB protease impairs innate immunity in mice and humans by targeting a lung epithelial cystic fibrosis transmembrane regulator-IL-6-antimicrobial-repair pathway. In: *Thorax* 73 (1), S. 49–61.

Saitoh, H.; Masuda, T.; Shimura, S.; Fushimi, T.; Shirato, K. (2001): Secretion and gene expression of secretory leukocyte protease inhibitor by human airway submucosal glands. In: *American journal of physiology. Lung cellular and molecular physiology* 280 (1), L79-87.

Sallenave, J. M. (2000): The role of secretory leukocyte proteinase inhibitor and elafin (elastase-specific inhibitor/skin-derived antileukoprotease) as alarm antiproteinases in inflammatory lung disease. In: *Respiratory research* 1 (2), S. 87–92.

Salvesen, G.; Enghild, J. J. (1991): Zymogen activation specificity and genomic structures of human neutrophil elastase and cathepsin G reveal a new branch of the chymotrypsinogen superfamily of serine proteinases. In: *Biomedica biochimica acta* 50 (4-6), S. 665–671.

Schindelin, J.; Arganda-Carreras, I.; Frise, E.; Kaynig, V.; Longair, M.; Pietzsch, T. et al. (2012): Fiji: an open-source platform for biological-image analysis. In: *Nature methods* 9 (7), S. 676–682.

Schliep, K. P. (2011): phangorn: phylogenetic analysis in R. In: *Bioinformatics* 27 (4), S. 592–593.

Schmitt, F. C. F.; Brenner, T.; Uhle, F.; Loesch, S.; Hackert, T.; Ulrich, A. et al. (2019): Gut microbiome patterns correlate with higher postoperative complication rates after pancreatic surgery. In: *BMC microbiology* 19 (1), S. 42.

Schulenburg, C.; Faccio, G.; Jankowska, D.; Maniura-Weber, K.; Richter, M. (2016): A FRET-based biosensor for the detection of neutrophil elastase. In: *The Analyst* 141 (5), S. 1645–1648.

Schulz-Fincke, A.-C.; Blaut, M.; Braune, A.; Gütschow, M. (2018a): A BODIPY-Tagged Phosphono Peptide as Activity-Based Probe for Human Leukocyte Elastase. In: *ACS medicinal chemistry letters* 9 (4), S. 345–350.

Schulz-Fincke, A.-C.; Tikhomirov, A. S.; Braune, A.; Girbl, T.; Gilberg, E.; Bajorath, J. et al. (2018b): Design of an Activity-Based Probe for Human Neutrophil Elastase: Implementation of the Lossen Rearrangement To Induce Förster Resonance Energy Transfers. In: *Biochemistry* 57 (5), S. 742–752.

Schwiebert, E. M.; Benos, D. J.; Egan, M. E.; Stutts, M. J.; Guggino, W. B. (1999): CFTR is a conductance regulator as well as a chloride channel. In: *Physiological reviews* 79 (1 Suppl), S145-66.

Scott, A.; Weldon, S.; Taggart, C. C. (2011): SLPI and elafin: multifunctional antiproteases of the WFDC family. In: *Biochemical Society transactions* 39 (5), S. 1437–1440.

Segata, N.; Haake, S. K.; Mannon, P.; Lemon, K. P.; Waldron, L.; Gevers, D. et al. (2012): Composition of the adult digestive tract bacterial microbiome based on seven mouth surfaces, tonsils, throat and stool samples. In: *Genome biology* 13 (6), R42.

Senior, R. M.; Tegner, H.; Kuhn, C.; Ohlsson, K.; Starcher, B. C.; Pierce, J. A. (1977): The induction of pulmonary emphysema with human leukocyte elastase. In: *The American review of respiratory disease* 116 (3), S. 469–475.

Shannon, C. E. (1948): A Mathematical Theory of Communication. In: *Bell System Technical Journal* 27 (4), S. 623–656.

Shanthikumar, S.; Stick, S. M.; Ranganathan, S. C. (2020): Minimal structural lung disease in early life represents significant pathology. In: *Journal of Cystic Fibrosis*.

Shao, M. X. G.; Nadel, J. A. (2005): Neutrophil elastase induces MUC5AC mucin production in human airway epithelial cells via a cascade involving protein kinase C, reactive oxygen species, and TNF-alpha-converting enzyme. In: *The Journal of Immunology* 175 (6), S. 4009–4016.

Shapiro, S. D.; Goldstein, N. M.; Houghton, A. M.; Kobayashi, D. K.; Kelley, D.; Belaaouaj, A. (2003): Neutrophil Elastase Contributes to Cigarette Smoke-Induced Emphysema in Mice. In: *The American journal of pathology* 163 (6), S. 2329–2335.

Sherrard, L. J.; Bell, S. C.; Tunney, M. M. (2016): The role of anaerobic bacteria in the cystic fibrosis airway. In: *Current opinion in pulmonary medicine* 22 (6), S. 637–643.

Sherrard, L. J.; Graham, K. A.; McGrath, S. J.; McIlreavey, L.; Hatch, J.; Muhlebach, M. S. et al. (2013): Antibiotic resistance in Prevotella species isolated from patients with cystic fibrosis. In: *The Journal of antimicrobial chemotherapy* 68 (10), S. 2369–2374.

Shim, Y. M.; Paige, M.; Hanna, H.; Kim, S. H.; Burdick, M. D.; Strieter, R. M. (2010): Role of LTB_4 in the pathogenesis of elastase-induced murine pulmonary emphysema. In: *American journal of physiology. Lung cellular and molecular physiology* 299 (6), L749-59.

Singh, D.; Agusti, A.; Anzueto, A.; Barnes, P. J.; Bourbeau, J.; Celli, B. R. et al. (2019): Global Strategy for the Diagnosis, Management, and Prevention of Chronic Obstructive

Lung Disease: the GOLD science committee report 2019. In: *The European respiratory journal* 53 (5).

Singh, D.; Edwards, L.; Tal-Singer, R.; Rennard, S. (2010): Sputum neutrophils as a biomarker in COPD: findings from the ECLIPSE study. In: *Respiratory research* 11, S. 77.

Sly, P. D.; Brennan, S.; Gangell, C.; Klerk, N. d.; Murray, C.; Mott, L. et al. (2009): Lung Disease at Diagnosis in Infants with Cystic Fibrosis Detected by Newborn Screening. In: *American journal of respiratory and critical care medicine* 180 (2), S. 146–152.

Sly, P. D.; Gangell, C. L.; Chen, L.; Ware, R. S.; Ranganathan, S.; Mott, L. S. et al. (2013): Risk factors for bronchiectasis in children with cystic fibrosis. In: *The New England journal of medicine* 368 (21), S. 1963–1970.

Smith, J. J.; Welsh, M. J. (1992): cAMP stimulates bicarbonate secretion across normal, but not cystic fibrosis airway epithelia. In: *The Journal of clinical investigation* 89 (4), S. 1148–1153.

Somayaji, R.; Nichols, D.; Bell, S. C. (2020): Cystic fibrosis - Ten promising therapeutic approaches in the current era of care. In: *Expert opinion on investigational drugs*.

Sonawane, A.; Jyot, J.; During, R.; Ramphal, R. (2006): Neutrophil elastase, an innate immunity effector molecule, represses flagellin transcription in Pseudomonas aeruginosa. In: *Infection and Immunity* 74 (12), S. 6682–6689.

Stamenkovic, I. (2003): Extracellular matrix remodelling: the role of matrix metalloproteinases. In: *The Journal of pathology* 200 (4), S. 448–464.

Stein, F.; Kress, M.; Reither, S.; Piljić, A.; Schultz, C. (2013): FluoQ: a tool for rapid analysis of multiparameter fluorescence imaging data applied to oscillatory events. In: *ACS chemical biology* 8 (9), S. 1862–1868.

Sternlicht, M. D.; Werb, Z. (2001): How matrix metalloproteinases regulate cell behavior. In: *Annual review of cell and developmental biology* 17, S. 463–516.

Stöcker, W.; Bode, W. (1995): Structural features of a superfamily of zinc-endopeptidases: the metzincins. In: *Current Opinion in Structural Biology* 5 (3), S. 383–390.

Storey, D. G.; Ujack, E. E.; Rabin, H. R. (1992): Population transcript accumulation of Pseudomonas aeruginosa exotoxin A and elastase in sputa from patients with cystic fibrosis. In: *Infection and Immunity* 60 (11).

Sturrock, A. B.; Espinosa, R.; Hoidal, J. R.; Le Beau, M. M. (1993): Localization of the gene encoding proteinase-3 (the Wegener's granulomatosis autoantigen) to human chromosome band 19p13.3. In: *Cytogenetics and cell genetics* 64 (1), S. 33–34.

Sun, Q.; Li, J.; Liu, W.-N.; Dong, Q.-J.; Yang, W.-C.; Yang, G.-F. (2013): Non-peptide-based fluorogenic small-molecule probe for elastase. In: *Analytical chemistry* 85 (23), S. 11304–11311.

Taggart, C.; Coakley, R. J.; Greally, P.; Canny, G.; O'Neill, S. J.; McElvaney, N. G. (2000): Increased elastase release by CF neutrophils is mediated by tumor necrosis factor-alpha and interleukin-8. In: *American journal of physiology. Lung cellular and molecular physiology* 278 (1), L33-41.

Taggart, C.; Mall, M. A.; Lalmanach, G.; Cataldo, D.; Ludwig, A.; Janciauskiene, S. et al. (2017): Protean proteases: At the cutting edge of lung diseases. In: *The European respiratory journal* 49 (2).

Taggart, C. C.; Cryan, S.-A.; Weldon, S.; Gibbons, A.; Greene, C. M.; Kelly, E. et al. (2005): Secretory leucoprotease inhibitor binds to NF-kappaB binding sites in monocytes and inhibits p65 binding. In: *The Journal of experimental medicine* 202 (12), S. 1659–1668.

Taggart, C. C.; Greene, C. M.; McElvaney, N. G.; O'Neill, S. (2002): Secretory leucoprotease inhibitor prevents lipopolysaccharide-induced IkappaBalpha degradation without affecting phosphorylation or ubiquitination. In: *Journal of Biological Chemistry* 277 (37), S. 33648–33653.

Tanaka, H.; Miyazaki, N.; Oashi, K.; Tanaka, S.; Ohmichi, M.; Abe, S. (2000): Sputum matrix metalloproteinase-9: tissue inhibitor of metalloproteinase-1 ratio in acute asthma. In: *The Journal of allergy and clinical immunology* 105 (5), S. 900–905.

Tashkin, D. P.; Wechsler, M. E. (2018): Role of eosinophils in airway inflammation of chronic obstructive pulmonary disease. In: *International journal of chronic obstructive pulmonary disease* 13, S. 335–349.

Tibshirani, R.; Walther, G.; Hastie, T. (2001): Estimating the number of clusters in a data set via the gap statistic. In: *Journal of the Royal Statistical Society: Series B (Statistical Methodology)* 63 (2), S. 411–423.

Tirouvanziam, R.; Gernez, Y.; Conrad, C. K.; Moss, R. B.; Schrijver, I.; Dunn, C. E. et al. (2008): Profound functional and signaling changes in viable inflammatory neutrophils homing to cystic fibrosis airways. In: *Proceedings of the National Academy of Sciences of the United States of America* 105 (11), S. 4335–4339.

Torrent, M.; La Torre, B. G. de; Nogués, V. M.; Andreu, D.; Boix, E. (2009): Bactericidal and membrane disruption activities of the eosinophil cationic protein are largely retained in an N-terminal fragment. In: *The Biochemical journal* 421 (3), S. 425–434.

Tosi, M. F.; Zakem, H.; Berger, M. (1990): Neutrophil elastase cleaves C3bi on opsonized pseudomonas as well as CR1 on neutrophils to create a functionally important opsonin receptor mismatch. In: *The Journal of clinical investigation* 86 (1), S. 300–308.

Travis, J.; Bowen, J.; Baugh, R. (1978): Human alpha-1-antichymotrypsin: interaction with chymotrypsin-like proteinases. In: *Biochemistry* 17 (26), S. 5651–5656.

Trivedi, R.; Barve, K. (2020): Gut microbiome a promising target for management of respiratory diseases. In: *The Biochemical journal* 477 (14), S. 2679–2696.

Trojanek, J. B.; Cobos-Correa, A.; Diemer, S.; Kormann, M.; Schubert, S. C.; Zhou-Suckow, Z. et al. (2014): Airway mucus obstruction triggers macrophage activation and matrix metalloproteinase 12-dependent emphysema. In: *American journal of respiratory cell and molecular biology* 51 (5), S. 709–720.

Tsai, C. C.; McArthur, W. P.; Baehni, P. C.; Hammond, B. F.; Taichman, N. S. (1979): Extraction and partial characterization of a leukotoxin from a plaque-derived Gram-negative microorganism. In: *Infection and Immunity* 25 (1), S. 427–439.

Tunney, M. M.; Klem, E. R.; Fodor, A. A.; Gilpin, D. F.; Moriarty, T. F.; McGrath, S. J. et al. (2011): Use of culture and molecular analysis to determine the effect of antibiotic treatment on microbial community diversity and abundance during exacerbation in patients with cystic fibrosis. In: *Thorax* 66 (7), S. 579–584.

Turk, V.; Stoka, V.; Vasiljeva, O.; Renko, M.; Sun, T.; Turk, B.; Turk, D. (2012): Cysteine cathepsins: from structure, function and regulation to new frontiers. In: *Biochimica et biophysica acta* 1824 (1), S. 68–88.

Twigg, M. S.; Brockbank, S.; Lowry, P.; FitzGerald, S. P.; Taggart, C.; Weldon, S. (2015): The Role of Serine Proteases and Antiproteases in the Cystic Fibrosis Lung. In: *Mediators of inflammation* 2015, S. 293053.

Uriarte, S. M.; Powell, D. W.; Luerman, G. C.; Merchant, M. L.; Cummins, T. D.; Jog, N. R. et al. (2008): Comparison of proteins expressed on secretory vesicle membranes and plasma membranes of human neutrophils. In: *The Journal of Immunology* 180 (8), S. 5575–5581.

Ute Bank; Siegfried Ansorge (2001): More than destructive: neutrophil-derived serine proteases in cytokine bioactivity control. In: *Journal of leukocyte biology* 69 (2), S. 197–206.

van den Steen, P. E.; Proost, P.; Wuyts, A.; van Damme, J.; Opdenakker, G. (2000): Neutrophil gelatinase B potentiates interleukin-8 tenfold by aminoterminal processing, whereas it degrades CTAP-III, PF-4, and GRO-α and leaves RANTES and MCP-2 intact. In: *Blood* 96 (8), S. 2673–2681.

van Wetering, S.; van der Linden, A. C.; van Sterkenburg, M. A.; Boer, W. I. de; Kuijpers, A. L.; Schalkwijk, J.; Hiemstra, P. S. (2000): Regulation of SLPI and elafin release from bronchial epithelial cells by neutrophil defensins. In: *American journal of physiology. Lung cellular and molecular physiology* 278 (1), L51-8.

Vandivier, R. W.; Fadok, V. A.; Hoffmann, P. R.; Bratton, D. L.; Penvari, C.; Brown, K. K. et al. (2002): Elastase-mediated phosphatidylserine receptor cleavage impairs apoptotic cell clearance in cystic fibrosis and bronchiectasis. In: *The Journal of clinical investigation* 109 (5), S. 661–670.

Vertex Pharmaceuticals (Europe) Ltd. (2018a): Orkambi (lumacaftor/ivacaftor). Summary of product characteristics. Online verfügbar unter https://www.ema.europa.eu/en/documents/product-information/orkambi-epar-product-information_en.pdf, zuletzt geprüft am 28.08.2020.

Vertex Pharmaceuticals (Europe) Ltd. (2018b): Symkevi (tezacaftor/ivacaftor). Summary of product characteristics. Online verfügbar unter https://www.ema.europa.eu/en/documents/product-information/symkevi-epar-product-information_en.pdf, zuletzt geprüft am 28.08.2020.

Voynow, J. A.; Fischer, B. M.; Zheng, S. (2008): Proteases and cystic fibrosis. In: *The international journal of biochemistry & cell biology* 40 (6-7), S. 1238–1245.

Wang, Z.; Liu, H.; Wang, F.; Yang, Y.; Wang, X.; Chen, B. et al. (2020): A Refined View of Airway Microbiome in Chronic Obstructive Pulmonary Disease at Species and Strain-Levels. In: *Frontiers in Microbiology* 11, S. 1758.

Wanger, J.; Clausen, J. L.; Coates, A.; Pedersen, O. F.; Brusasco, V.; Burgos, F. et al. (2005): Standardisation of the measurement of lung volumes. In: *The European respiratory journal* 26 (3), S. 511–522.

Watt, A. P.; Courtney, J.; Moore, J.; Ennis, M.; Elborn, J. S. (2005): Neutrophil cell death, activation and bacterial infection in cystic fibrosis. In: *Thorax* 60 (8), S. 659–664.

Weldon, S.; McNally, P.; McElvaney, N. G.; Elborn, J. S.; McAuley, D. F.; Wartelle, J. et al. (2009): Decreased levels of secretory leucoprotease inhibitor in the Pseudomonas-infected cystic fibrosis lung are due to neutrophil elastase degradation. In: *Journal of immunology (Baltimore, Md. : 1950)* 183 (12), S. 8148–8156.

Welp, A. L.; Bomberger, J. M. (2020): Bacterial Community Interactions During Chronic Respiratory Disease. In: *Frontiers in Cellular and Infection Microbiology* 10, S. 213.

Whelan, F. J.; Heirali, A. A.; Rossi, L.; Rabin, H. R.; Parkins, M. D.; Surette, M. G. (2017): Longitudinal sampling of the lung microbiota in individuals with cystic fibrosis. In: *PLOS One* 12 (3), e0172811.

Wiedow, O.; Schröder, J. M.; Gregory, H.; Young, J. A.; Christophers, E. (1990): Elafin: an elastase-specific inhibitor of human skin. Purification, characterization, and complete amino acid sequence. In: *Journal of Biological Chemistry* 265 (25), S. 14791–14795.

William T. Harris; Marianne S. Muhlebach; Robert A. Oster; Michael R. Knowles; Terry L. Noah (2009): Transforming growth factor-β1 in bronchoalveolar lavage fluid from children with cystic fibrosis. In: *Pediatric pulmonology* 44 (11), S. 1057–1064.

Witko-Sarsat, V.; Cramer, E. M.; Hieblot, C.; Guichard, J.; Nusbaum, P.; Lopez, S. et al. (1999): Presence of Proteinase 3 in Secretory Vesicles: Evidence of a Novel, Highly Mobilizable Intracellular Pool Distinct From Azurophil Granules. In: *Blood* 94 (7), S. 2487–2496.

World Health Organization (2017): Chronic obstructive pulmonary disease (COPD). key facts. Hg. v. World Health Organization. Geneva, Switzerland. Online verfügbar unter https://www.who.int/news-room/fact-sheets/detail/chronic-obstructive-pulmonary-disease-(copd), zuletzt geprüft am 06.04.2021.

Worlitzsch, D.; Rintelen, C.; Böhm, K.; Wollschläger, B.; Merkel, N.; Borneff-Lipp, M.; Döring, G. (2009): Antibiotic-resistant obligate anaerobes during exacerbations of cystic fibrosis patients. In: *Clinical microbiology and infection: the official publication of the European Society of Clinical Microbiology and Infectious Diseases* 15 (5), S. 454–460.

Wysocka, M.; Lesner, A.; Gruba, N.; Korkmaz, B.; Gauthier, F.; Kitamatsu, M. et al. (2012): Three wavelength substrate system of neutrophil serine proteinases. In: *Analytical chemistry* 84 (16), S. 7241–7248.

Xinyan Zhang; Nengjun Yi (2020): NBZIMM: negative binomial and zero-inflated mixed models, with application to microbiome/metagenomics data analysis. In: *BMC Bioinformatics* 21 (1), S. 1–19.

Yang, G.-Y.; Li, C.; Fischer, M.; Cairo, C. W.; Feng, Y.; Withers, S. G. (2015): A FRET probe for cell-based imaging of ganglioside-processing enzyme activity and high-throughput screening. In: *Angewandte Chemie (International ed. in English)* 54 (18), S. 5389–5393.

Yuan, L.; Lin, W.; Zheng, K.; Zhu, S. (2013): FRET-based small-molecule fluorescent probes: rational design and bioimaging applications. In: *Accounts of chemical research* 46 (7), S. 1462–1473.

Zander, C. D. (2001): The guild as a concept and a means in ecological parasitology. In: *Parasitology research* 87 (6), S. 484–488.

Zemanick, E. T.; Wagner, B. D.; Robertson, C. E.; Ahrens, R. C.; Chmiel, J. F.; Clancy, J. P. et al. (2017): Airway microbiota across age and disease spectrum in cystic fibrosis. In: *The European respiratory journal* 50 (5).

Zhang, Z.; Wang, J.; Zhang, Y. H.; Gardner, T. E.; Fitzpatrick, E. A.; Zhang, W. (2021): Two Siblings Homozygous for F508del-CFTR Have Varied Disease Phenotypes and Protein Biomarkers. In: *International Journal of Molecular Sciences* 22 (5), S. 2631.

Zhang, Z.; Winyard, P. G.; Chidwick, K.; Murphy, G.; Wardell, M.; Robin W., C.; Blake, D. R. (1994): Proteolysis of human native and oxidised α1-proteinase inhibitor by matrulysin and stromelysin. In: *Biochimica et Biophysica Acta (BBA) - General Subjects* 1199 (2), S. 224–228.

Zhao, J.; Schloss, P. D.; Kalikin, L. M.; Carmody, L. A.; Foster, B. K.; Petrosino, J. F. et al. (2012): Decade-long bacterial community dynamics in cystic fibrosis airways. In: *Proceedings of the National Academy of Sciences of the United States of America* 109 (15), S. 5809–5814.

Zimmer, M.; Medcalf, R. L.; Fink, T. M.; Mattmann, C.; Lichter, P.; Jenne, D. E. (1992): Three human elastase-like genes coordinately expressed in the myelomonocyte lineage are organized as a single genetic locus on 19pter. In: *Proceedings of the National Academy of Sciences of the United States of America* 89 (17), S. 8215–8219.

Publications, Talks and Posters during PhD studies

Published original articles:

Frey, D.L., Guerra, M., *Schultz, C., Mall, M.A. (2021) A guide for monitoring neutrophil serine protease activity in human sputum. J. Vis. Exp. e62193*

Frey, D.L., Boutin, S., Dittrich, A.S., *Graeber, S.Y., Stahl, M., Wege, S., Herth, F.J.F., Sommerburg, O., Schultz, C., Mall, M.A. Dalpke, A.H. (2021) Relationship between airway dysbiosis, inflammation and lung function in adolescents and adults with cystic fibrosis. J. Cyst. Fibros., S1569-1993(20)30954-1*

Hagner, M., Frey, D.L., Guerra, M.*, Dittrich, A.S., Halls, V.S., Wege, S., Herth, F.J.F., Schultz, C., Mall, M.A. (2020) New method for rapid and dynamic quantification of elastase activity on sputum neutrophils from patients with cystic fibrosis using flow cytometry. Eur. Respir; 55: 1902355*

Graeber, S.Y., Boutin, S., *Wielpütz, M.O., Joachim, C., Frey, D.L., Wege, S., Olaf Sommerburg, O., Kauczor, H.U., Stahl, M., Dalpke, A.H., Mall, M.A. (2021) Effects of Lumacaftor-Ivacaftor Therapy on Lung Clearance Index, Magnetic Resonance Imaging and Airway Microbiome in Phe508del Homozygous Patients with Cystic Fibrosis. Ann. Am. Thorac. Soc.*

Montgomery, S.T., *Frey, D.L., Mall, M.A., Stick, S.M., Kicic, A., WAERP & AREST CF. Rhinovirus infection is associated with airway epithelial cell necrosis and inflammation via interleukin-1 in young children with cystic fibrosis. (2020) Front. Immunol.*

Guerra, M., *Frey, D.L., Hagner, M., Dittrich, A.S., Paulsen, M., Mall, M.A., Schultz, C. (2019) Cathepsin G Activity as a New Marker for Detecting Airway Inflammation by Microscopy and Flow Cytometry. ACS Cent. Sci. 5, 3, 539-548.*

Margaroli, C., Garratt, L.W., Horati, H., Dittrich, A.S., Rosenow, T.*, Montgomery, S.T., Frey, D.L., Brown, M.R., Schultz, C., Guglani, L., Kicic, A., Peng, L., Scholte, B.J., Mall, M.A., Janssens, H.M., Stick, S.M., Tirouvanziam, R. (2018) Elastase Exocytosis by Airway Neutrophils Associates with Early Lung Damage in Cystic Fibrosis Children. Am. J. Respir. Crit. Care Med., 199(7):873-81.*

Montgomery, S.T., Dittrich, A.S.*, Garratt, L.W., Turkovic, L., Frey, D.L., Stick, S.M., Mall, M.A., Kicic, A., CF AREST. (2018) Interleukin-1 is associated with inflammation and structural lung disease in young children with cystic fibrosis. J. Cyst. Fibros., 17(6):715-22.*

Original articles in preparation:

Frey, D.L., Bridson, C., *Dittrich, A.S., Graeber, S.Y., Stahl, M., Wege, S., Herth, F.J.F., Sommerburg, O., Schultz, C., Mall, M.A. Dalpke, A.H., Boutin, S. Longitudinal characterization of airway dysbiosis and inflammation in the lung of CF patients*

Frey, D.L., Guerra, M, *Helm, B., Dittrich, A.S., Wege, S., Eberhardt, R., Herth, F.J.F., Sommerburg, O., Klingmüller, U., Schultz, C., Mall, M.A. Dalpke, A.H., Boutin, S. Comparison of the inflammatory niches of CF and COPD and the differences to healthy controls*

Margaroli, C., Horati, H., Garratt, L.W., *Giacalone, V., Dittrich, A.S., Rosenow, T., Dobosh, B.S., Lim, H.S., Frey, D.L., Veltman, M., Silva, G.L., Brown, M.R., Schultz, C., Tiddens, H.A.W.M., Ranganathan, S., Chandler, J.D., Qiu, P., Peng, L., Scholte, B.J., Mall, M.A., Kicic, A., Guglani, L., Stick, S.M., Tirouvanziam. R., Janssens, H.M. Macrophage exhaustion signals early neutrophil takeover and lung damage in cystic fibrosis.*

Poster abstracts:

***Frey, D.L**., Hagner, M., Guerra, M., Uselmann, T., Wege, S., Eberhardt, R., Herth, F.J.F., Schultz, C., Mall, M.A.* (2020). Relationship between microbiome dysbiosis, inflammation neutrophil recruitment and lung function in CF patients. DZL Annual Meeting, Lübeck-Travemünde, Germany.

***Frey, D.L**., Boutin, S., Dittrich, A.S., Wege, S., Herth, F.J.F., Sommerburg, O., Schultz, C., Dalpke, A.H., Mall, M.A*. (2020). A distinct inflammatory profile characterizes Chronic Obstructive Pulmonary Disease and Cystic Fibrosis lung disease. DZL Annual Meeting, Lübeck-Travemünde, Germany.

***Frey D.L.**, Dittrich A.S., Kühbandner I., Halavatyi A., Hagner M., Guerra M., Wege S., Halls V.S., Herth F., Schultz C., Mall M.A.* (2019) P219 Small-molecule FRET flow cytometry: A novel technique to monitor surface-associated protease activity in CF. *J. Cyst. Fibros.* Jun 1;18: S119.

***Frey, D.L.**, Dittrich, A.S., Kühbandner, I., Halavatyi, A., Hagner, M., Guerra, M., Wege, S., Halls, V.S., Herth, F., Schultz, C., Mall, M.A.* (2019) Small-molecule FRET flow cytometry: A novel technique to monitor surface-associated protease activity in CF. *Pediatr. Pulmonol.* 54, S357-S358.

***Frey, D.L.**, Dittrich, A.S., Kühbandner, I., Halavatyi, A., Hagner, M., Guerra, M., Wege, S., Halls, V.S., Schultz, C., Herth, F., Mall, M.A.* (2019) Small-molecule FRET flow cytometry: A novel technique to monitor surface-associated protease activity in CF. DZL Annual Meeting, Mannheim, Germany.

***Frey, D.L.,** Dittrich, A.S., Kühbandner, I., Halavatyi, A., Herth, F., Schultz, C., Mall, M.A.* (2018). Monitoring of protease activity in airway inflammatory cells of Cystic Fibrosis patients using FRET sensors. DZL Annual Meeting, Bad Nauheim, Germany.

Oral presentations:

Relationship between microbiome dysbiosis, inflammation neutrophil recruitment and lung function in CF patients. Scientific Meeting, Muko e.V., Montabaur, 19th – 20th September 2019.

The role of Neutrophil Serine Proteases in Cystic Fibrosis lung disease. International Symposium on Cathepsin C, Tours, France, 17th – 18th April 2019.

Flow cytometric FRET: An advanced technique to measure surface- associated protease activity in CF. European Young Investigator Meeting, Paris, France, 27th February – 1st March 2019.

Longitudinal monitoring of protease activity in airway inflammatory cells of Cystic Fibrosis patients using FRET sensors. Scientific Meeting, Muko e.V., Bad Salzschlirf, 27th – 28th September 2018.

Statement on copyright and self-plagiarism

Parts of the presented data of the thesis have been published in Frey et al. 2021a, Frey et al. 2021b and Hagner et al. 2020. The text was restructured in accordance to the author copyright and reuse rights of the journals, but the wording has been modified.

The protocols that have been applied and/or developed within this work (chapters: 2.3.2, 2.4.2 and 2.4.3) are summarized in the publication with the title: Monitoring neutrophil elastase and cathepsin G activity in human sputum samples, this was published as collaborative work from Dario L. Frey, Matteo Guerra, Carsten Schultz and Marcus A. Mall. The contribution of the individual authors is given in Table SP1. I, D. L. Frey was involved in the conceptualization, development of the methodology, visualization, investigation, writing of the original draft as well as review & editing.

The data of section 3.1.1 Cross-sectional Study as well as parts of the corresponding section of the discussion was published as collaborative work from Dario L. Frey, Sébastien Boutin, Susanne A. Dittrich, Simon Y. Graeber, Mirjam Stahl, Sabine Wege, Felix J.F. Herth, Olaf Sommerburg, Carsten Schultz, Marcus A. Mall and Alexander H. Dalpke. The contribution of the individual authors is given in Table SP2. I, D. L. Frey was involved in the conceptualization, development of the methodology, analysis via software, formal analysis, investigation, writing of the original draft as well as review & editing.

The data of section 3.1.2 Longitudinal Study as well as parts of the corresponding section of the discussion is close to submission as collaborative work from Dario L. Frey, Calum Bridson, Susanne A. Dittrich, Simon Y. Graeber, Mirjam Stahl, Sabine Wege, Felix J.F. Herth, Olaf Sommerburg, Carsten Schultz, Marcus A. Mall, Alexander H. Dalpke and Sébastien Boutin. The contribution of the individual authors is given in Table SP3. I, D. L. Frey was involved in the conceptualization, development of the methodology, analysis via software, formal analysis, investigation, writing of the original draft as well as review & editing.

The core data of section 3.2.2 Change in technology, transforming the assay from microscopy to flow cytometry as well as parts of the corresponding section of the discussion was published as collaborative work from Dario L. Frey, Matthias Hagner, Matteo Guerra, A. Susanne Dittrich, Victoria S. Halls, Sabine Wege, Felix J.F. Herth, Carsten Schultz and Marcus A. Mall. The contribution of the individual authors is given in Table SP4. I, D. L. Frey was involved in conceptualization, data collection as well as manuscript writing & review and editing.

Table SP1: Overview of author contributions Frey et al. 2021b. First authors are given in bold, senior authors are indicated with an asterisk.

Participation	Authors involved
Conceptualization	**D. L. Frey and M. Guerra**
Methodology	**D. L. Frey and M. Guerra**
Manuscript writing	**D. L. Frey and M. Guerra**
Review and editing	**D. L. Frey, M. Guerra,** C. Schultz* and M. Mall*
Visualization	**D. L. Frey and, M. Guerra**
Supervision	C. Schultz* and M. Mall*

Table SP2: Overview of author contributions Frey et al. 2021a. First authors are given in bold, senior authors are indicated with an asterisk.

Participation	Authors involved
Conceptualization	**D. L. Frey, S. Boutin, A. S. Dittrich,** M. A. Mall*, A. H. Dalpke*
Methodology	**D. L. Frey, S. Boutin, A. S. Dittrich**
Software	**D. L. Frey, S. Boutin**
Formal analysis	**D. L. Frey, S. Boutin**
Investigation	**D. L. Frey, S. Boutin**
Manuscript writing	**D. L. Frey, S. Boutin**
Review & Editing	**D. L. Frey, S. Boutin, A. S. Dittrich,** S. Y. Graeber, M. Stahl, S. Wege, F. J. F. Herth, O. Sommerburg, C. Schultz, M. A. Mall*, A. H. Dalpke*
Supervision	**A. S. Dittrich,** M. A. Mall*, A. H. Dalpke*

Table SP3: Overview of author contributions longitudinal CF study. First authors are given in bold, senior authors are indicated with an asterisk.

Participation	Authors involved
Conceptualization	**D. L. Frey, C. Bridson,** M. A. Mall*, A. H. Dalpke*, S. Boutin*
Methodology	**D. L. Frey,** S. Boutin*
Software	**D. L. Frey, C. Bridson,** S. Boutin*
Formal analysis	**D. L. Frey, C. Bridson,** S. Boutin*
Investigation	**D. L. Frey, C. Bridson,** S. Boutin*
Manuscript writing	**D. L. Frey, C Bridson,** S. Boutin*
Review & Editing	**D. L. Frey, C Bridson,** A. S. Dittrich, S. Y. Graeber, M. Stahl, S. Wege, F. J. F. Herth, O. Sommerburg, C. Schultz**,** S. Boutin*, M. A. Mall*, A. H. Dalpke*
Supervision	M. A. Mall*, A. H. Dalpke*

Table SP4: Overview of author contributions Hagner et al. 2020. First authors are given in bold, senior authors are indicated with an asterisk.

Participation	Authors involved
Conceptualization	**D. L. Frey, M. Hagner, M. Guerra**
Data collection	**D. L. Frey, M. Hagner, M. Guerra**
Manuscript writing	**D. L. Frey, M. Hagner, M. Guerra**
Review and editing	**D. L. Frey, M. Hagner, M. Guerra,** A. S. Dittrich, V. S. Halls, F. J. F. Herth, C. Schultz* and M. Mall*
Supervision	A. S. Dittrich, C. Schultz* and M. Mall*

Acknowledgements

I want to thank,

Prof. Dr. Marcus Mall for giving me the opportunity to work on this highly interesting project under his supervision; for his expertise, his critical thinking and discussions about the results, the chance to present parts of my project at several international conferences and most of all for being an exceptional doctoral thesis supervisor.

Dr. Rainer Pepperkok and Prof. Dr. Alexander Dalpke for their interest in my work and their helpful suggestions and in-depth discussions during the TAC meetings.

Prof. Dr. Stefan Wölfl and Prof. Dr. Ana Martin-Villalba for reviewing of my thesis.

Dr. A. Susanne Dittrich for her initial introduction in the project, supervision and her assistance regarding the patient recruitment.

Prof. Dr. Hans-Ulrich Kauczor and Prof. Dr. Rory Morty for all of their support and for giving me the opportunity to finalize my PhD studies.

Dr. Matthias Hagner and Dr. Matteo Guerra for their collaboration, help and their expertise in the lab to push the project further.

Dr. Aliaksandr Halavatyi and Dr. Marco Lampe for their support regarding confocal microscopy and image processing.

Dr. Sebastien Boutin and his lab members for all the effort they put in the microbiome experiments and analysis.

Dr. Ursula Klingmüller and her lab members for the collaboration to explore the secretome of the samples.

Dr. Olaf Sommerburg, Prof. Dr. Felix Herth, Dr. Sabine Wege and Prof. Dr. Ralf Eberhardt for the collaboration and willingness to support and facilitate the clinical part of the translational studies.

All lab members of the Department of Translational Pulmonology for having a nice working atmosphere and motivating lunch discussions.

Dr. Simon Graeber, Dr. Mirjam Stahl, Tatjana Uselmann, Yvonne Koch, Annegret Hövel, Cornelia Joachim, Ines Kirsch, Iris Kühbandner and Christiane Labitzke for their assistance regarding sample acquisition, as well as for providing clinical data.
Simone Butz, Jolanthe Schatterny, Angela Frank, Heike Scheuermann and Stephanie Hirtz for their training in methods and their experimental help.

Elena for always cheering me up no matter how crazy and busy the times were, without your support things would have evolved differently. Thank you for sharing this journey.

Especially, my parents Gabi and Hartmut, for their endless support during my studies and my sister Alissa for always listening to my boring statements about latest set-backs or achievements.

Appendix

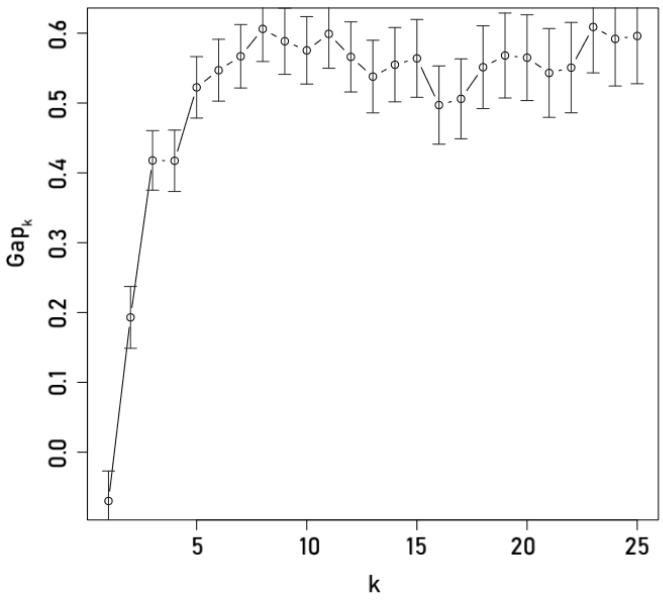

Figure S1: Graph of the Gap statistics. Based on the function clusGap(x=x[, 1:2], FUNcluster=kmeans, K.max=25, B=1000, nstart=20, according to Tibshirani et al. 2001.

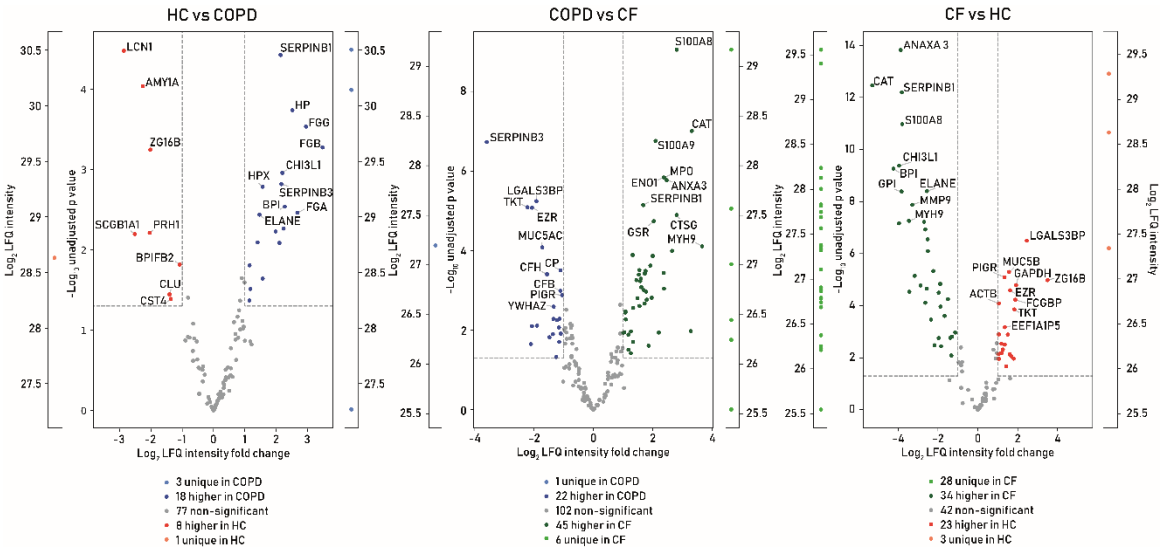

Figure S2: Volcano plots of the proteome comparisons between Healthy, CF and COPD. Healthy are represented in red, COPD in blue and CF are shown in green. Significantly upregulated proteins are represented in darker shades, unique identified proteins are found to the left and right of the central plots in dimmer shades. Protein those are not significant different are shown in grey. Top ten protein for each group and comparison are labeled. Exact number of the non-significant, upregulated and unique proteins are given below each graph.

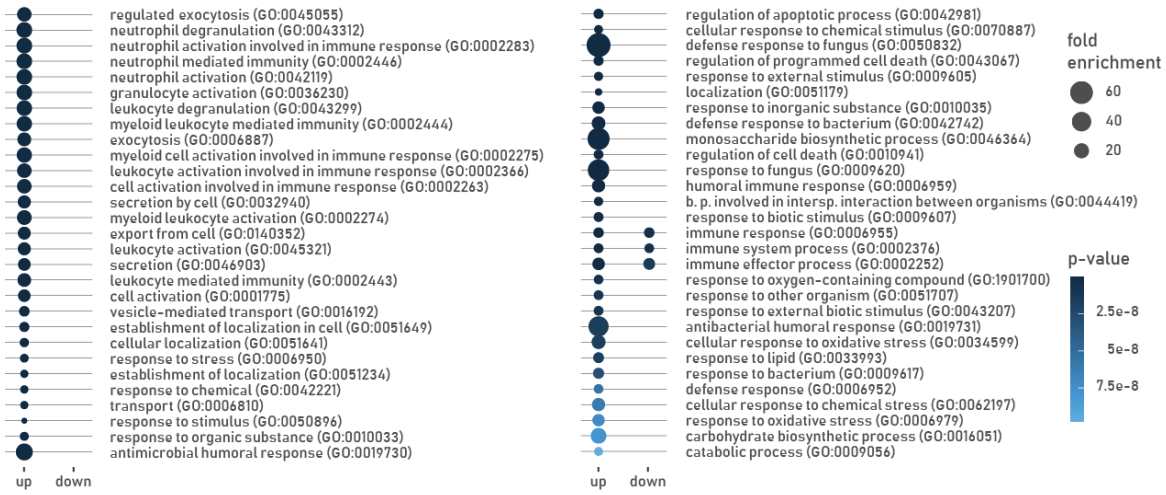

Figure S3: Biological processes identified by gene ontology analysis. All processes being either 2-fold up or downregulated are shown, ordered by their p-value. Names of the processes and GO id are given. Up regulated processes are dominant in CF down regulated processes are rather dominant in COPD.

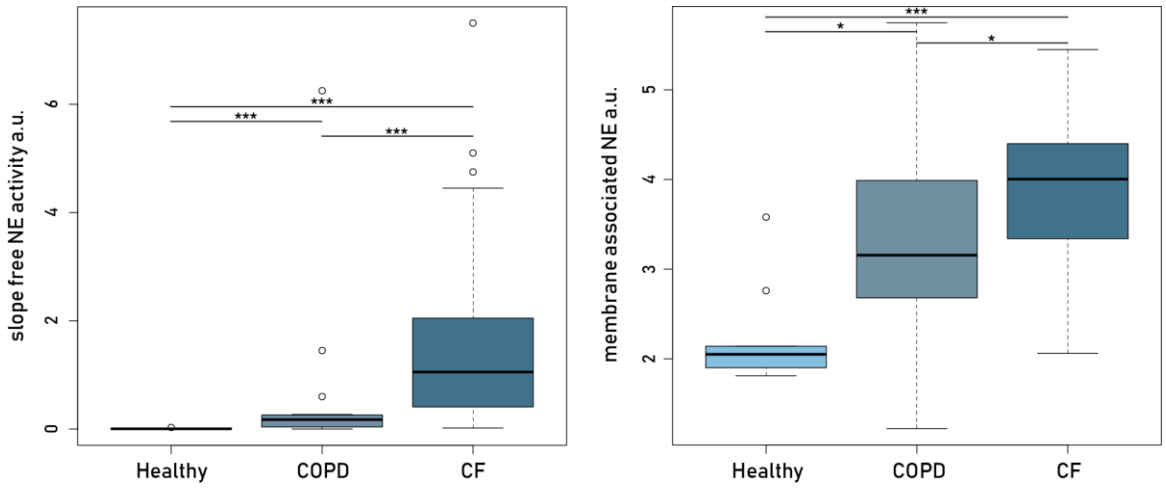

Figure S4: Comparison of free and membrane associated NE activity. Left: Boxplots of slope of free NE activity. **Right:** membrane associated NE given for each disease group. Groups were compared by Wilcoxon rank sum test with Bonferroni-Holm correction for multiple comparisons, if significance was reached this is indicated by asterisks according to their p-values: *: p <0.05 and ***: p <0.001. Outliers are shown as circles (○)